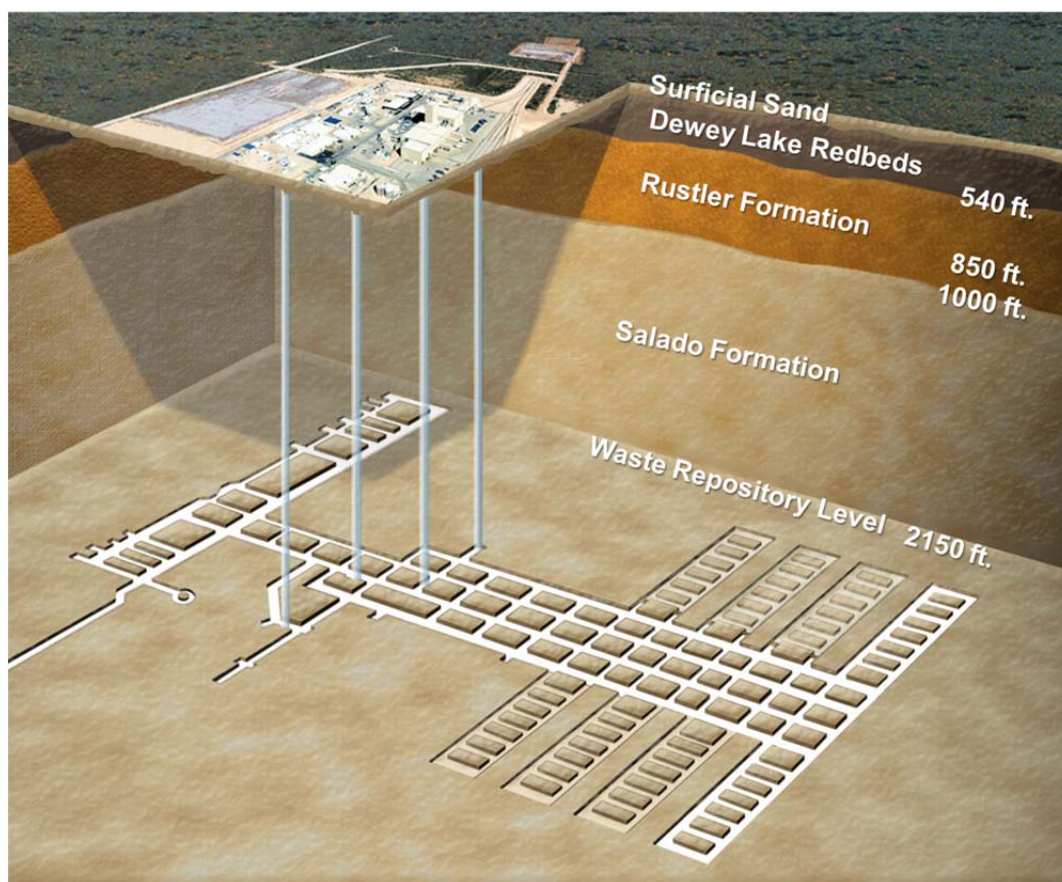# Proceedings of the Third International Workshop on Actinide and Brine Chemistry in a Salt-Based Repository (ABC-Salt III)

WIPP Facility and Stratigraphic Sequence

Los Alamos
NATIONAL LABORATORY
— EST.1943 —

Cover illustration:
WIPP TRU Repository

Proceedings of the Third International Workshop on Actinide and Brine Chemistry in a Salt-Based Repository (ABC-Salt III) *

April 15-17, 2013

Santa Fe, NM, USA.

Edited by:

Donald Reed

       Actinide Chemistry and Repository Science Team
       Repository Science & Operations Program
       Los Alamos National Laboratory
       Carlsbad, NM, USA

Marcus Altmaier

       Karlsruhe Institute for Technology
       Institute for Nuclear Waste Disposal
       Karlsruhe, Germany

*ABC-Salt (III) was co-organized by D. Reed and M. Altmaier as an activity of the NEA Salt Club

(http://www.oecd-nea.org/rwm/saltclub)

This page intentionally left blank.

ABC-Salt III Workshop

FOREWORD

The Actinide and Brine Chemistry in a Salt Repository (ABC-Salt III) workshop was held in April 2013 in Santa Fe at a time when there was a clear record of success in the Waste Isolation Pilot Plant (WIPP) project and there was much talk and optimism about building towards future expanded nuclear repository options in salt. This workshop, which is the third of a workshop series we started in Carlsbad in 2010, provided an international forum to present and discuss recent scientific results that provide insight into the actinide and brine chemistry that are key to supporting the safety case for the permanent geologic isolation of nuclear waste in salt. It was supported by our Carlsbad Department of Energy (DOE) office and jointly organized by Los Alamos-Carlsbad Office WIPP researchers and researchers from the German Institute for Nuclear Waste Disposal (KIT/INE).

It was good to see that there were many new scientific results relevant to a radioactive waste repository in deep rock salt presented at this workshop. The over 50 presentations made re-affirmed the need and importance of having a strong scientific basis to support the safety case for the permanent isolation of nuclear waste in salt. The DOE remains committed to a continuing process to strengthen the scientific foundation for a salt repository concept and workshops like these that bring together the key researchers in high ionic-strength actinide chemistry are an important part of this scientific process.

I am especially pleased to note, with over 20 international researchers representing seven countries in attendance, the significant participation of international scientists in this workshop. A special thank-you goes to the German Federal Ministry of Economics and Technology (BMWi) for the support they provided and the KIT/INE researchers for helping organize this international participation. It is important that we continue to strengthen international scientific ties through workshops like this and the long-term disposal of nuclear waste is truly an international problem that only benefits from international cooperation.

Since this workshop, we have had some operational setbacks at our WIPP transuranic (TRU) repository that have raised concerns about the viability of a radioactive waste repository in deep rock salt and the nuclear repository concept that was best exemplified by the WIPP. Although these operational issues are serious and need to be addressed, they do not impact the core safety case of the WIPP or the attributes of salt repositories that links to the science presented and discussed at this workshop. We remain committed to the concept of a nuclear salt repository. It is critical that even during this time of reassessment that international and scientific progress continues forward.

Jose R. Franco, Manager
Department of Energy – Carlsbad Field Office

This page intentionally left blank.

Table of Contents

This page intentionally left blank.

Actinide and Brine Chemistry in a Salt-Based Repository (ABC-Salt III) Workshop

Proceedings Summary

Historical Perspective and Importance

ABC-Salt Workshop Series

This is the third international workshop in the ABC-Salt series and was held at the La Fonda Hotel in the Santa Fe, New Mexico (USA) downtown Plaza area on April 15-17, 2013. The goals of this workshop series, organized as an activity of the Nuclear Energy Agency (NEA) Salt Club, has been to status the state-of-the-art of actinide and brine chemistry experimental and modeling results and continue an international dialog to coordinate and prioritize research in this field. This workshop series evolved out of a collaborative dialog between the Los Alamos Actinide Chemistry and Repository Science Program (ACRSP) team investigating actinide/brine chemistry for the U.S. Waste Isolation Pilot Plant (WIPP) and the German Karlsruhe Institute for Technology Institute for Nuclear Waste Disposal (KIT/INE) researchers who were also investigating potential applications of a salt repository concept for nuclear waste.

The ABC-Salt III workshop was comprised of forty six presentations and sixteen posters on the topics of international program updates, brine chemistry, microbial effects, actinide chemistry in brine, and the modeling of high ionic-strength solutions. There were over fifty attendees (twenty one of which were international) representing seven countries (United States, Germany, Canada, United Kingdom, France, Australia and Spain). The majority of the participants, as expected, were from Germany and the United States as these are the two countries that are most active in research to support salt repository concepts. The abstracts for many of these presentations and posters (see list of abstracts on page 9) are provided in this proceedings report. In all there was a very good international dialog established in this workshop and this key aspect of the ABC-Salt workshop series was well met.

The first ABC-Salt workshop was held in Carlsbad New Mexico (USA) on September 8 and 9, 2010. This was well attended with forty five scientists from four countries, but mostly from the United States and German repository programs. The technical agenda, extended abstracts, and attendees list can be found in the published workshop proceedings [Proceedings of the International Workshop on Actinide and Brine Chemistry in a Salt –Based Repository (ABC-Salt), Donald Reed and Marcus Altmaier (Eds.), Los Alamos Report LAUR-14-28463, Los Alamos, NM, USA]. A tour of the WIPP facility was also given to the international visitors and was an important feature of the workshop.

The second workshop was held in Karlsruhe Germany on November 7 and 8, 2011 and was hosted by the KIT/INE. This was again a well-attended workshop with over 80 participants from several countries and was coupled to a workshop on High Temperature Aqueous Chemistry (HITAC 2011). The abstracts and summary of these workshops are published in the proceedings [Proceedings of the Interantional Workshops ABC-Salt (II) and HiTAC 2011, Marcus Altmaier, Christiane Bube, Bernhard Kienzler, Volker Metz, Donald Reed (Eds.), KIT Scientific Reports 7625, KIT Scientific Publishing].

Further workshops are planned and the ABC-Salt IV workshop will be held on the 14th and 15th of April 2015 in Heidelberg, Germany.

Importance of High Ionic-Strength Actinide Chemistry to the Salt Repository Safety Case

The safety case for the use of a bedded salt or salt dome for the permanent geologic isolation of nuclear waste is centered on the self-sealing properties of salt that lead to geologic isolation. This, under ideal conditions, will lead to a "dry" site that can geologically isolate the nuclear waste for millions of years. The salt formations being considered or used for geologic isolation are hundreds of millions of years old and have remained unsaturated with no interconnected groundwater for much of this time. In many respects this disposal concept is somewhat independent of the nature of the wasteform since it relies on geologic isolation and not on container material and wasteform properties under the expected repository conditions. There are also significant cost advantages to a salt repository approach since the technology for the mining of salt is well established and we have a 12-year operational history and experience at the WIPP site, which is the best working example and application of this repository concept.

It is critically important that a repository concept, and its associated safety case, has a sound scientific basis to assure the public that the repository will perform as predicted. For a salt-based nuclear repository, although primary safety reliance is on the self-sealing of its geology, there are low probability scenarios where brine intrusion can solubilize actinides/ radionuclides in high ionic-strength brines leading to their subsequent release to the accessible environment. It is this low-probability scenario that justifies the actinide and brine chemistry research that is the subject of this workshop. In this context, it is critical to show that even if the worse-case scenario of brine intrusion and release occurs, the repository will still perform and regulatory release limits are not exceeded. The dissolved actinide/ radionuclide concentration, in this low-probability scenario, is defined by the multitude of subsurface processes that impact actinide/radionuclide speciation and the associated modeling of actinide chemistry in high ionic-strength brine systems.

Summary of Key ABC-Salt III Workshop Results

A general summary of each of the key presentation areas is given in the following sections. In all, this workshop provided a very comprehensive discussion of the programmatic and technical issues that pertain to brine and actinide chemistry in a salt repository.

International Program Updates

Detailed program updates from the United States and German salt repository programs were provided. For the German programs, an overview of German repository activities was provided along with results of a recently completed preliminary safety assessment of the Gorleben site (VSG). The preliminary safety assessment was favorable and confirmed that salt is a viable option as the host rock for a high-level waste (HLW) repository in Germany.

In the United States, the WIPP project continued towards its third recertification and there was much discussion of the possibility of an alternative salt repository concept for thermally-hot nuclear waste (e.g., defense HLW) in salt. Strong support was expressed within the United States repository program for continued international dialog on nuclear waste applications of the salt repository concept.

There were also program overviews and updates provided by the Canadian and British nuclear waste programs where intermediate and even some high ionic-strength issues are discussed. There are scenarios at depth in granite where transient high ionic-strength brine systems may be present. In the UK, these are mostly linked to waste storage concerns rather than a repository concept. There is also significant research in Australia on brine systems to support mining operations. All of this was put in the context of ongoing Nuclear Energy Agency (NEA) activities to support salt repository research within the NEA international Salt Club and within the thermodynamic database activity to produce a state-of-the-art report on high ionic-strength systems.

Brine Chemistry

Approximately ten presentations and posters were given on various aspects of brine chemistry.   These were focused on high pH brine chemistry, the development of new Pitzer parameters for organic complexants and iron, and new insights on borate chemistry.   These data continue to extend and challenge the "oceanic" salt Pitzer data sets currently used in the modeling of the brine chemistry. A broader pH range is needed in many cases to account for the interactions of waste forms and barrier materials (e.g., MgO and cement). Data on the potential contribution of mineral colloids show that these are not likely to contribute significantly to dissolved actinide concentrations. The complexation of borate by actinides continues to be investigated and the interpretation of these data are complicated by the fact the underlying borate chemistry is not well understood at pH>8.

A key focus of these presentations was on recent results from temperature-variable studies. The effects of increased temperature are identified as key gaps in the extension of the salt repository concept to high-level (thermally hot) nuclear waste applications. Effects of increased radiolysis under these conditions are likewise a topic of concern. New results on the effects of temperature on the movement of brine and associated mineral transformations were presented that show accelerated brine movement above 75°C. Data that extends the solubility of aluminum to above 200°C were summarized. Initial studies on the effects of alpha radiolysis on iron and multivalent actinides speciation were presented. These initial studies are showing significant effects and issues that need further evaluation.

Microbial Effects at High Ionic Strength

There were five presentations and posters given on recent results to establish the microbial ecology in a salt geology and the associated high ionic-strength brines; as well as their effects on actinide speciation. Significant progress is reported in the WIPP project on identifying indigenous microbes from the salt itself. These tend to be archaea that are obligate aerobes and attempts to cultivate anaerobic microorganisms in the salt at I > 5 M have been unsuccessful. A much higher archaeal and bacterial diversity is being seen at somewhat lower ionic strength (I ~ 3 M) which is more typical of the groundwater/brine systems. It has been noted that these microcosms are effective in degrading organic chelators and there is initial evidence that iron reduction is occurring. Preliminary data was presented on two key microbial effects on actinides: Some bioreduction of actinides is observed and, in many cases, significant sorption is noted at moderately high pH. These latter data are being used to define the potential formation of bio-colloids in brine.

Initial results were also presented within the German program on some of the biodiversity present in the Asse salt mine and the microorganisms generally being observed in saline environments. The biodiversity noted in Gorleben salt and saline samples from Israel were also presented. There is significant overlap between the results from the WIPP site and those from Israel with further work planned on the Gorleben site.

Microbial effects remain a key and dominant factor when the salt repository concept is approached from a regulatory point of view due to the high uncertainty and relative lack of understanding of microbial effects. This area of research, and particularly the potential impacts of microbial processes on the speciation and mobile concentration of actinides, as well as their viability at elevated temperature and increased radiation exposure, remains a key research need.

Actinide Chemistry at High Ionic Strength

There were approximately twenty presentations and posters on a variety of experimental results on actinide systems at high ionic-strength. This ranged from process chemistry, to near-

neutral high ionic-strength systems, to cement-dominated very high pH brine systems. Processes being investigated include colloid formation, redox chemistry, sorption, and solubility.

There has been a recent emphasis on the role of colloidal species in defining the mobile concentration of actinides in the WIPP project. Intrinsic colloid contributions are reported in the thorium and neodymium solubility studies. Biocolloid formation is conservatively accounted for in performance assessment (PA) models as an additional contribution to the mobile actinide concentration although, realistically, the bio-association of actinides is expected to decrease their mobility in brine systems. Intrinsic colloids are relatively small (<10 nm) and appear to be highly structured, something that certainly is true for the uranyl peroxide system. The need to account for these kinds of colloidal contributions remains high and accounting for these species is critical to the proper evaluation of solubility data.

Extensive results were presented on the solubility of actinides in the presence of borate and simplified brines systems over a wide range of pH and elevated temperature. Detailed studies on actinide solubility and speciation are required for the development of reliable thermodynamic data and chemical models. Spectroscopic methods are being widely used and time resolved laser fluorescence spectroscopy (TRLS), in particular, is providing key and detailed insight into the speciation of trivalent actinides in a variety of systems. Specific results on the complexation of actinides with oxalate, borate, nitrate, chloride and carbonate were presented. These data reflect the complexity that is typically present in brine systems, but also show that significant progress is being made to identify solubility-controlling phases and measure Pitzer parameters to support modeling activities. A few temperature-variable results were presented and small elevations in temperature (~50-100°C) do not have a large effect on the observed actinide solubilities and show generally favorable trends toward immobilization.

Lastly, experimental results on the sorption of actinide species on clays and clay minerals were presented. Many of the lower-valent actinides are highly sorptive and this process is predicted to significantly contribute to their immobilization when these minerals are present.

Modeling High Ionic Strength Solutions

The modeling of actinide and brine systems in the salt repository concept requires the use of the Pitzer approach due to the very high ionic-strengths (typically > 5 M) involved. There were approximately ten presentations and posters that provided a very good update on the state-of-the-art in the development and application of Pitzer data bases.

A very detailed description of the German THEREDA database project was presented. This is an ongoing project by several leading German research organizations that aims to provide a well-designed platform for a self-consistent Pitzer model. Although extensive data exist, there are a number of gaps, and in particular, there is a need for more actinide data. There are also relatively few reliable data at variable temperature.

Overall assessments of the various Pitzer databases were presented along with new concepts for modeling multicomponent electrolyte systems. There are many self-consistency problems in the various databases that are in use and there was extensive discussion on ways to reconcile this problem and the idea of trying to move towards a unified database was proposed. A second issue identified was that the regulatory process necessarily invokes a literature assessment of solubility data to determine the range of uncertainties in the data. This is also needed to account for and reconcile non project-specific data. The neglection of available chemical process understanding and the tendency to treat solubility data from different studies as mere "statistical numbers", can lead to extremely high ranges of "apparent" uncertainty for some actinides, particularly when there are colloidal contributions that cannot be easily defined. There are no formalized or automated ways to screen the literature solubility data without having a detailed analysis that is supported by expert interpretation of the several known parameters influencing the solubility processes. Unless the available chemical process understanding is included in a systematic data evaluation (as is being done within the NEA thermodynamic database project) and reflected in the determination of uncertainties, the calculated "apparent" uncertainties often are unreasonably high. The importance of considering realistic uncertainties when comparing and assessing solubility data and agreeing on a common approach for this process within the context of regulatory requirements was identified as a key future need.

Summary of Overall Observations, Key Gaps/Issues, and Path Forward

The actinide and brine chemistry systems and the many processes that define this chemistry, which were the focus of this workshop, are reasonably well understood and much progress is being reported. These continue to support the salt repository concept and provide a needed understanding to address the low-probability scenarios of brine inundation/intrusion that are driven by the regulatory process to define a comprehensive and sufficient safety case. This does not mean that there are no gaps in the available data or unresolved issues in the modeling of dissolved actinide concentrations. In this regard, however, a robust assessment of radionuclide solubility continues to be possible through the use of conservative assumptions and modeling strategies.

Key data gaps that address needs or can significantly minimize the degree of conservatism in the modeling approach are:

- Additional scientific investigations of the solubility and speciation of actinides in simplified brine systems are needed to increase the reliability of chemical models and develop a more extensive thermodynamic database. This is especially needed for less-investigated systems where no reliable data are available; e.g. certain organic ligands, and future research is required. If geochemical modeling is to be used as a key tool in PA, the availability of transparent, consistent and correct thermodynamic data and databases are essential.

- There is a need for more actinide and especially transuranic solubility data, rather than a reliance on solubility data obtained through the use of chemical analogs. This will improve (i.e. lessen) the extent of the conservatisms currently being used and lead to more realism in the models. This is especially true in the case of plutonium species.

- There are too many inconsistencies in the literature Pitzer databases. This gap can be addressed by a unified and internationally coordinated effort to strengthen and improve the Pitzer database for actinides that are important to the safety case. As a follow-up to several focused discussions on this topic during the ABC-Salt workshops, an activity to form a working group to start this process was initiated within the NEA Salt Club.

- There are relatively few studies that have investigated the effects of temperature on actinide speciation, solubility and redox. These studies are needed to extend the salt safety case to the HLW or spent fuel waste form where higher temperatures and radiation levels will be present. The investigation of temperature effects is challenging and is best tackled within the framework of strong international cooperation.

- Continued improvement in the understanding of the microbial ecology and the associated impacts of microbial activity on actinide solubility and speciation is needed. The high uncertainty associated with microbial effects that are simply caused by, in many cases, the lack of reliable data continues to drive costly engineering decisions and overly conservative assumptions. This high uncertainty is best mitigated by an improved understanding of these effects that is gained through laboratory studies.

- There is a critical need for a more widely accepted and peer-friendly process to evaluate the many literature uncertainties that are used to derive the overall range of uncertainties for the actinide solubilities used in performance assessment. In particular, this process should be based on an adequate understanding of the underlying chemical processes that define the solubility. This approach would help to greatly improve the relevance and realism of the uncertainty ranges used to assess performance to meet the requirements of the regulatory process.

Donald Reed

Repository Science and Operations
Los Alamos National Laboratory

Marcus Altmaier

Institute for Nuclear Waste Disposal (INE)
Karlsruhe Institute of Technology

This page intentionally left blank.

ACKNOWLEDGEMENTS

The organizers of this workshop wish to acknowledge the following contributions:

This page intentionally left blank.

ABC Salt III Workshop
April 15-17, 2013
Santa Fe, NM, USA

ABC Salt III Workshop Attendees
Outside the Cathedral Basilica of St. Francis of Assisi
in Santa Fe NM, USA

This page intentionally left blank.

Actinide and Brine Chemistry in a Salt Repository
ABC Salt III
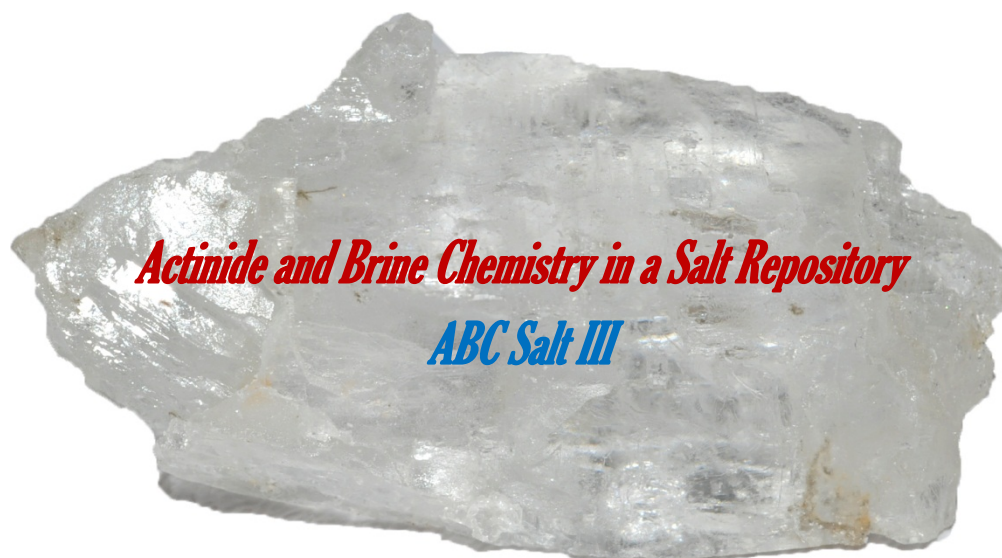
Technical Program

Monday, April 15	**8:30 AM – 12:30 PM**	**Welcome and Program Overviews**
	1:40 PM – 5:30 PM	**Brine Chemistry**
	6:30 – 8:00 PM	**Poster Session: All workshop topics** **Refreshments courtesy of BMWi**
Tuesday, April 16	**8:30 AM – 9:50 AM**	**Microbial Effects**
	10:20 AM to 5:20 PM	**Actinides in High Ionic Strength Media**
	6:30 PM – 9:00 PM	**Dinner: La Fonda Hotel** **Plenary Talk by Horst Geckeis entitled "Nuclear waste disposal – a technically resolved problem or a scientific challenge"**
Wednesday, April 17	**8:30 AM – 12:30 PM**	**Modeling in High Ionic Strength Systems**

This page intentionally left blank.

Monday, April 15:: ABC Salt III Workshop, La Fonda Hotel, New Mexico Room		
8:30 – 8:40	Workshops Logistics and Updates	Don Reed (LANL) and Marcus Altmaier (KIT/INE)
8:40 – 9:00	LANL Welcome	Nan Sauer (LANL-AD)
Program Overviews and General Directions: Repository Science in a Salt Geology **Co-Chairs: Russ Patterson and Marcus Altmaier**		
9:00 – 9:20	Overview of Repository Science in the US	Bruce Robinson (LANL)
9:20 – 9:50	Activities of the Department "Safety of nuclear waste management" at the Federal Office for Radiation Protection	Ingo Böttcher (Federal Office of Radiation Protection, Germany)
9:50 – 10:10	OECD/NEA Salt Club and Perspectives on Repository Science	Michael Siemann (NEA, France)
10:10 – 10:30	The Role of In-Situ Testing In Support of a Salt Repository Safety Case	Abe Van Luik (DOE-CBFO)
10:30 – 10:50	**Break**	
10:50 – 11:10	DOE Welcome: WIPP TRU Repository: Operational Success that Builds towards Future Salt Repository Options	Joe Franco (DOE-CBFO Manager)
11:10 – 11:30	Status of Operational and Recertification Activities in the WIPP	Russ Patterson (DOE-CBFO)
11:30 – 11:50	Preliminary Safety Assessment of the Gorleben Site	Guido Bracke (GRS, Germany)
11:50 – 12:10	Canadian Repository Program Overview	Tammy Yang (NMWO, Canada)
12:10 – 12:30	An integrated research programme in support of the safe disposal of nuclear waste in the UK	Rebecca Beard (NDA RWMD, UK)
12:30 – 1:40	**Lunch – Provided by the La Fonda Hotel**	
Brine Chemistry and Microbial Effects **Co-Chairs: Greg Roselle and Daniela Freyer**		
1:40 – 2:00	Summary of US/German workshops on salt repository research, design and operations	Christi Leigh and Frank Hansen (SNL)
2:00 – 2:20	WIPP Hydrous mineral phase transformations at elevated temperatures	Florie A. Caporuscio, Michael C. Cheshire, and Hakim Boukhalfa (LANL)
2:20 – 2:40	Applying Neutron Techniques to Investigation of the Salt-Brine System: Capabilities and Perspectives	Hongwu Xu (LANL)
2:40 – 3:00	Constraints on parameters for mineral fragment colloids and humic substance colloids at WIPP	Paul Mariner and Dave Sassani (SNL)
3:00 – 3:30	**Break**	
3:30 – 3:50	Borate Chemistry at alkaline pH	M. Borkowski, Mike Richmann, J-F Lucchini, Julie Swanson, Danielle Cleveland and Donald Reed (LANL)
3:50 – 4:10	Chemistry of the Fe(II)-System in Brines	Andrés G. Muñoz, Barbara P. Bischofer, Helge C. Moog (GRS)
4:10 – 4:30	Speciation and Solubility of Aluminum in High Ionic Strength Solutions at Elevated Temperatures to 250 $^{\circ}$C	Yongliang Xiong (SNL)
4:30 – 4:50	WIPP brine chemistry at high pC_{H+}	J.F. Lucchini, M. Borkowski, M.K. Richmann, J. S. Swanson, K. Simmons, D. Cleveland, and D.T. Reed (LANL)
4:50 – 5:10	α-Radiolysis under alkaline conditions in 0.5 and 5.0 molar NaCl	Martínez-Torrents, Albert; Gonzalez-Robles, Ernesto; Bohnert, Elke; Casas, Ignasi; De Pablo, Joan and Metz, Volker (UPC Barcelona, Spain)
5:10 – 5:30	Derivation of Pitzer Interaction Parameters for an Aqueous Species Pair of $FeEDTA^{2-}$ and Na^{+}	Je-Hun Jang, Taya Olivas, and Martin Nemer (SNL)

Poster Session: Monday, 6:30 to 8:00 PM, La Fonda Hotel, New Mexico Room	
Refreshments provided by BMWi **Co-chairs: Jef Lucchini and Danielle Cleveland**	
Anoxic Corrosion of Steel and Lead in Na-Cl±Mg Dominated Brines	Gregory Roselle (SNL)
Br distribution between halite and parent brine as an example for a natural analogue for the incorporation of radiogenic components in evaporites	Michael Schramm (BGR)
Brine migration in intact salt crystals under variable temperature gradients	H. Boukhalfa and F. Caporuscio (LANL)
C-14 as carbon dioxide and saline solutions of a HLW repository	Guido Bracke (GRS)
Microbial Diversity Associated with Halite within the Waste Isolation Pilot Plant	Juliet Swanson and Karen Simmons (LANL)
Comparison of bacterial populations in briny groundwaters of different ionic strengths under a variety of incubation conditions	Karen A. Simmons and Juliet S. Swanson (LANL)
Complexation of Np(IV) with gluconate in dilute to concentrated $CaCl_2$ solutions: solubility and NMR studies	X. Gaona, C. Adam, H. Rojo, M. Böttle, P. Kaden, M. Altmaier (KIT-INE)
Experimental and Thermodynamic Modeling Solubility of Lead in the Carbonate System to High Ionic Strengths: Part One, Solubility of Cerussite ($PbCO_3$) in $NaHCO_3$ + NaCl Solutions	Yongliang Xiong, Leslie Kirkes and Terry Westfall (SNL)
Experimental data establish low uranium (VI) solubility in the WIPP	J.F. Lucchini, M. Borkowski, M.K. Richmann, J. S. Swanson, K. Simmons, D. Cleveland, and D.T. Reed (LANL)
Long-term Plutonium speciation in WIPP Brines	D. T. Reed, M.K. Richmann, J. F. Lucchini and M. Borkowski (LANL)
Preliminary Safety Assessment of the Gorleben Site	Guido Bracke (GRS)
Redox chemistry and solubility of ^{99}Tc in saline NaCl and $MgCl_2$ solutions	E. Yalcintas, X. Gaona, T. Kobayashi, M. Altmaier, H. Geckeis (KIT-INE)
Retention of trivalent Cm and Eu on Stable Solid Phases in the System Mg-Na-Cl-H_2O at Room Temperature	M. Wiedemann, V. Metz, T. Rabung, H. Geckeis (KIT-INE)
Solid-liquid equilibria in the system $Mg(OH)_2$-$MgCl_2$-H_2O at elevated temperatures (60°C-100°C)	Melanie Pannach, Daniela Freyer and Wolfgang Voigt (Freiberg University, Germany)
Thermodynamic Interaction of Carbonate to Fe Ion Species in Brine Solutions	Sungtae Kim, Taya Olivas, Leslie Kirkes and Terry Westfall (SNL)
WIPP Monitoring Program	Punam Thakur (CEMRC/NMSU)

Tuesday, April 16, La Fonda Hotel, New Mexico Room		
Brine Chemistry and Microbial Effects – Continued **Chair: Rebecca Beard**		
8:30 – 8:50	Microorganisms in saline environments	<u>Andrea Geissler</u>, Velina Bachvarova, Katrin Flemming, Sonja Selenska-Pobell (HZDR, Germany)
8:50 – 9:10	`Insights into the Biodiversity of salt sumps in the Asse II salt mine, Germany`	Isabel Zirnstein, <u>Thuro Arnold</u> (HZDR, Germany)
9:10 – 9:30	Update on Microbiology Research at the Waste Isolation Pilot Plant	<u>Julie Swanson</u>, K. Simmons, D. Ams, J. F. Lucchini, and D. Reed (LANL)
9:30 – 9:50	Wrap-up discussion – brine chemistry and microbial issues	Organizers
9:50 – 10:20	**Break**	
Actinide Interactions in High Ionic Strength Brine Systems **Co-Chairs: Thomas Rabung and Michael Richmann (morning sessions)** **Co-Chairs: Horst Geckeis and Marian Borkowski (afternoon sessions)**		
10:20 – 10:40	Solubility of thorium WIPP brine	<u>Marian Borkowski</u>, Mike Richmann, J-F Lucchini, Julie Swanson, Danielle Cleveland and Donald Reed (LANL)
10:40 – 11:00	Actinide Chemistry in Alkaline High Ionic-Strength Solutions	<u>D.T. Hobbs</u>, L.N. Oji, K.M.L. Taylor-Pashow, W.R. Wilmarth (SRL, USA)
11:00 – 11:20	WIPP actinide colloid model update	<u>D.T. Reed</u>, J.S. Swanson, J.F. Lucchini, M.K. Richmann, M. Borkowski, and D. Cleveland (LANL)
11:20 – 11:40	Actinide Materials: Uranyl Peroxide Cage Clusters	<u>Ginger E. Sigmon</u>, Christine M. Wallace, Ernest M. Wylie, Kristi L. Pellegrini, Brendan McGrail, Peter C. Burns (Notre Dame University)
11:40 – 12:00	Recent activities on HLW and Spent Nuclear Fuel related research at KIT-INE	<u>M. Altmaier</u> for B. Kienzler, V. Metz, E. González-Robles, E. Bohnert, A. Loida, N. Müller (KIT-INE, Germany)
12:00 – 1:30	**Lunch – Provided at the La Fonda Hotel**	
1:30 – 1:50	Aquatic chemistry of actinides at elevated temperatures: solubility and spectroscopic studies at KIT–INE	<u>Xavi Gaona</u>, A. Skerencak-Frech, M. Marques, D. R. Fröhlich, J. Rothe, K. Dardenne, P. J. Panak, M. Altmaier (KIT-INE, Germany)
1:50 – 2:10	Complexation of Actinides with Oxalate at High Temperature and Ionic Strength	Punam Thakur (NMSU, CEMRC)
2:10 – 2:30	Np(V) Interactions and Speciation at High Ionic Strength	<u>Michael Richmann</u>, J-F Lucchini, M. Borkowski, J. S. Swanson, K. Simmons, D. Cleveland, and D.T. Reed (LANL)
2:30 – 2:50	Investigations of Actinide and Lanthanide Sorption on Clay Minerals under Saline Conditions	A. Schnurr, R. Marsac, <u>Th. Rabung</u>, J. Lützenkirchen, H. Geckeis (KIT-INE, Germany)
2:50 – 3:10	Uranium(VI) sorption on montmorillonite in high ionic strength media	<u>Katharina Fritsch</u>, Katja Schmeide (HZDR, Germany)
3:10-3:30	**Break**	
3:30 – 3:50	Complexation of An(III/IV) with borate in dilute to concentrated alkaline NaCl, $CaCl_2$ and $MgCl_2$ solutions	K. Hinz, <u>M. Altmaier</u>, Th. Rabung, M. Richmann, H. Geckeis (KIT-INE, Germany)
3:50 – 4:10	Investigations to the Eu(III)-B(OH)$_3$-Organic System at increased salt concentrations	<u>J. Schott</u>, M. Acker, J. Kretzschmar, A. Barkleit, S. Taut, V. Brendler, G. Bernhard (HZDR, Germany)
4:10 – 4:30	Nd Solubility in Brine Systems	<u>J. Icenhower</u> and D. Shuh (LBL)
4:30 – 4:50	Coordination of hexavalent actinides in chloride brines	Wolfgang Runde (LANL)
4:50 – 5:10	The effect of nitrate on trivalent actinide and lanthanide solubility in dilute to concentrated brine solutions	M. Herm, <u>Xavi Gaona</u>, Th. Rabung, C. Crepin, V. Metz, M. Altmaier, H. Geckeis (KIT-INE, Germany)
5:10 – 5:30	Wrap up session – actinides at high ionic strength	Organizers

Wednesday April 17, La Fonda Hotel, New Mexico Room		
Modeling in High Ionic Strength Systems **Co-chairs: Tammy Yang and Yongliang Xiong**		
8:30 – 8:50	Geochemical Process Modeling for the Waste Isolation Pilot Plant (WIPP) 2014 Compliance Recertification Application (CRA-2014) Performance Assessment (PA) Calculations	Larry Brush (SNL) and Paul Domski (Stoller)
8:50 – 9:10	The Effect of Laboratory Studies on the WIPP Actinide Solubility Uncertainty Model	Paul Domski (Stoller) and Larry Brush (SNL)
9:10 – 9:30	Geochemical modeling in highly saline conditions	L. Duro, D. García, E. Colàs, V. Montoya (AMPHOS21, Spain)
9:30 – 9:50	Pitzer equations and alternative methods of modeling multicomponent electrolyte solutions	Darren Rowland and Peter May (Murdoch University, Australia)
9:50 – 10:20	**Break**	
10:20 – 10:40	Advanced Simulation Capability for Environmental Management – Current Status and Phase II Demonstration Highlights	Paul Dixon (LANL), Mark D. Freshley (PNNL), Susan S. Hubbard (LBL), Tim Scheibe (PNNL), Stefan Finsterle (LBL), J. David Moulton (LANL), Carl I. Steefel (LBL), Roger R. Seitz (SRNL), and Justin Marble (DOE)
10:40 – 11:00	THEREDA Database Project	Helge C. Moog (GRS, Germany)
11:00 – 11:20	A Brief Comparison of Pitzer Databases for Nuclear Waste Disposal Modeling	Frank Bok, Wolfgang Voigt, Christiane Bube, Stefan Wilhelm and Helge Moog (GRS, Germany)
11:20 – 11:40	THEREDA Database Project: Extensions of the Pitzer database with respect to phosphate, alkaline earth metal sulfates, heavy metals, and fission products – first results	Helge C. Moog (GRS, Germany)
11:40 – 12:30	Wrap-up Session and Coordination Meeting: Modeling in High Ionic Strength Systems	Organizers
12:30 – 1:30	**Lunch – Provided by the La Fonda Hotel**	

ABC-Salt III Workshop

Abstracts

- 8 -

This page intentionally left blank.

List of Abstracts

Tuesday, April 16th, Workshop Presentation Abstracts

Wednesday, April 17th, Workshop Presentation Abstracts

This page intentionally left blank.

ABC-Salt III Workshop

Monday, April 15th
Presentation
Abstracts

This page intentionally left blank.

The Role of In-Situ Testing In Support of a Salt Repository Safety Case

Abraham Van Luik[1]

[1]FU.S. Department of Energy, Carlsbad Field Office, 4021 National Parks Highway, Carlsbad, New Mexico, USA
email: abraham.vanluik@wipp.ws

INTRODUCTION

Actinide brine chemistry (ABC) work done to define thermodynamic properties of actinides in brines is useful in terms of allowing performance assessment calculations to make less uncertain estimates of actinide solubility when encountering brine. Questions remain, however, on when the radioactive contaminants will encounter brine, how much brine they will encounter, and what the chemical composition and physical properties of that brine may be. Only in-situ testing can help narrow the possibilities in terms of the nature and volume of brine to be expected over time.

Theoretical and laboratory experimental work, coupled with limited field work, has sought to define expected natural system behavior foe repositories in salt. This work has resulted in ranges of likely brine compositions, physical properties, and volumes, all as a function of time. Repositories in deep crystalline rock may encounter Ca-Na-Cl brines, and deep formation brines can be found in some deep sedimentary rock basins. Although proposed crystalline or sedimentary rock formation repositories may also benefit from ABC work, the focus of this paper will be on salt repositories.

BACKGROUND

Work performed in the US in the 1980s, in cooperation with work done elsewhere, especially in Germany, provided conservative estimates of likely brine characteristics and volumes to be encountered by waste packages in a salt repository. Assumptions made at that time included the movement of all brine within a certain radius from a hot waste package toward that heat source. Other assumption cases were even more conservative and suggested that all open space at the time of final closure would become brine filled over time. These assumptions made calculations simple, but resulting brine volumes contacting waste were so conservative as to, arguably, be wrong.

The US is currently disposing of radioactive waste with negligible heat output in a salt repository. Even if some brine is assumed to migrate toward the mined openings and contact waste, it cannot go anywhere and the repository remains fully functional. The only way to remove materials from the repository is via human

intrusion scenarios involving brines introduced by drilling, or by striking a pressurized brine pocket that sends brine up along the drill-hole into and through the repository. Brines in contact with the waste, with a loading of actinides in solution or carried on particulates, may be removed by such a brine flow. Although the scenarios are unlikely, several occur in every 10,000-year system performance calculation. Reducing actinide solubility in brine would help further reduce the relatively benign calculated consequences from these scenarios.

INVESTIGATION NEEDS

The US may decide to dispose of heat-bearing wastes in salt. Whether from research or defense activities by the government or from civilian sources, analyzing the performance of these waste forms in a salt repository requires an analytical capability that was partially developed several decades ago. That capability is now being improved upon by the Department of Energy's (DOE's) Office of Nuclear Energy (DOE-NE).

The DOE Office of Environmental Management (DOE-EM) is investigating the possibility of the Department making a decision to dispose of defense-related wastes in salt, separating the defense and civilian waste streams. To inform such a decision, a heater test is being proposed, to be conducted in the Waste Isolation Pilot Plant (WIPP), that will (1) address the processes induced by using a new horizontal emplacement scheme with blown-in crushed-salt shielding, (2) address the relatively low wattage of the vast majority of defense wastes ("old, cold, and useless"), and (3) address the movement of moisture in response to the heat source in both the crushed salt backfill and the intact surrounding rock salt formation.

INVESTIGATION GOALS

Prior to the start of the testing, the temperature profiles and physical properties of the salt will be predicted as a function of time and temperature. These predictions will utilize the existing constitutive models based on information gained through the testing and modeling programs of the 1980s and 1990s. If the parameters that are measured match what was predicted, the adequacy of

the prior knowledge base is confirmed with respect to the physical response of the repository to heat, and a safety case can be written.

With respect to moisture movement, it is hoped that there can be observation and quantification of the rates of moisture movement within the salt, brine volumes coming into contact with waste as a function of time, the physical and chemical properties of that brine, and the role of vapor transport in this process.

If the proposed testing does not provide information on brine migration and brine chemistry, the salt disposal safety case will need to continue to make conservative assumptions respecting brine volumes encountering the waste over time, and the aggressiveness of these brines in terms of corroding waste package and waste form materials.

It is a considerable challenge to instrument the proposed test to provide hydrologic data on brine- and vapor-movement, and to allow very small amounts of brine at the heater surface to be sampled for analysis. Of course a null result, no observed or detected brine migration toward the heat source, is also quite valuable since it likely indicates that predictions made based on previous knowledge were much too conservative.

PREDICTIONS BASED ON PREVIOUS KNOWLEDGE

The temperature fields and salt reconsolidation predictions made prior to the testing will be based on the experimental and modeling work done in the 1980s and 1990s, and refined since that time to an extent allowed by new experience and testing results. The expectation is that these results will closely match results to be observed in the planned tests.

With respect to brine inflow volumes, previous tests at WIPP showed these were very dependent on the nearness of higher water content anhydrite-clay interbeds. Where there were such interbeds nearby, brine inflow was substantial, but were clearly a response to induced pressure gradients, not temperature gradients. Where there were no nearby interbeds the brine inflow was barely detectable.

In terms of brine chemistry, the observed inflow brines at WIPP were high magnesium brines. This makes sense since in the formation of the host rock the sea-water evaporation-sequence dictated the removal of calcium first through anhydrite precipitation, then sodium removal through sodium chloride precipitation, leaving brines still saturated with sodium, but enriched in more soluble magnesium and potassium. That is the nature of the solution that became trapped in growing salt crystals.

By contrast, in domal salts brines are typically sodium dominated. Diapirism succeeds in part through the lubrication provided by the brines in salt crystals that

are broken under the pressures that are causing the salt to be deformed and to rise. In that physical process the salt is actually purified since it is the sodium chloride that is plastically deformable, not some of its harder impurities, and much of its brine is lost in the deformation process due to the deformation-causing pressure gradients, assuring that domes are typically purer and have considerably less water in them compared with bedded salt formations.

These chemical and volume differences between typical bedded and domal salt bodies may make some of the brine-movement and chemistry related results from the proposed tests at WIPP quite specific to bedded salt bodies. That does not mean there are no lessons to be learned that have qualitative implications for domal salt bodies, however. If the brine inflow observed does not meet expectations based on previous knowledge, it is likely that the temperature-gradient driving mechanism for brine inflow have in the past been much too conservatively estimated, and that is a generic result.

OPPORTUNITY FOR COLLABORATION

Collaboration is already occurring between the two Offices in DOE with repository responsibilities, DOE-NE and DOE-EM. This collaboration has to this point involved DOE-NE addressing clearly 'generic,' but necessary, supporting research in terms of laboratory and modeling work. DOE-EM has contributed coordinated research to this effort, and is in charge of the site-specific aspects of the in-situ testing program it has proposed.

Wider collaboration now becomes possible as the field testing phase is beginning to be defined in detail. As the detailed test plans are written, there is opportunity for our fellow Salt Club members, as well as others, to review these plans and make suggestions for their improvement based on their own testing results. This collaboration may result in the avoidance of approaches that, based on test results obtained elsewhere, are not likely to result in the data desired. It could also result, and this is to be hoped, in suggestions for using more effective instruments for measuring the physical, chemical, and thermal conditions in and around the test. A major challenge is to measure the response of moisture to the introduced heat source.

The Salt Club is the ideal forum for conduction such reviews, and the resulting recommendations can be internationally shared for the benefit of other programs dealing with the introduction of heat into high ionic strength solutions.

WIPP Environmental Compliance and the Chemistry Program

Russell Patterson
Department of Energy
4021 National Parks Hwy.
Carlsbad, NM 88220
Phone- 575-234-7457
russ.patterson@wipp.ws

The Department of Energy/Carlsbad Field Office (DOE/CBFO) is responsible for managing, planning, integrating and implementing the National Transuranic Waste Program (NTWP) activities. CBFO directs all activities related to the disposal of Transuranic (TRU) and TRU-mixed waste at the Waste Isolation Pilot Plant (WIPP). The WIPP, a deep geologic repository, is mined 655m below the land surface in a deep underground salt formation, and is a government-owned and contractor-operated facility that is constructed on DOE property near Carlsbad, New Mexico.

Radioactive waste disposal at WIPP is regulated by the Environmental Protection Agency (EPA) to meet requirements in 40 Code of Federal Regulations Parts 191(40 CFR Part 191) Subpart A (operations) and Subparts B and C (long-term performance), and 40 CFR Part 194 and the WIPP Land Withdrawal Act. WIPP is further regulated by the New Mexico Environment Department (NMED) to meet the requirements of the Resource Conservation and Recovery Act (RCRA) under the WIPP Hazardous Waste Facility Permit (HWFP) for mixed waste. Radioactive waste was first received at WIPP on March 26, 1999.

In the Compliance Certification Application (CCA), the 2004 and 2009 Compliance Recertification Applications (CRA-2004 and CRA-2009), as well as the most recent NMED permit renewal, the repository chemistry plays a role in convincing the regulators that the repository will contain waste for the next 10, 000 years and beyond. WIPP continues to study actinide chemistry to support previous conservative assumptions used in performance assessment and to allow for potential changes in repository operations that may save taxpayer money through efficiencies.

This presentation will provide an overview of the regulatory chronology of WIPP, discuss actinide chemistry's role in compliance, and list potential future activities.

This page intentionally left blank.

Preliminary Safety Assessment of the Gorleben Site

Guido Bracke

Department of Final Disposal, GRS mbH, Schwertnergasse 1, 50667 Cologne, Germany
email: guido.bracke@grs.de

INTRODUCTION

The safety requirements governing the final disposal of heat-generating radioactive waste (HLW) in Germany implemented by the federal ministry of environment, natural conservation and nuclear safety (BMU) from 2010 consider the fundamental objective to protect man and environment against the hazard from radioactive waste [1]. Unreasonable burdens and obligation for future generations shall be avoided. The main safety principles are concentration and inclusion of radioactive and other pollutants in a containment providing rock zone. Any release of radioactive nuclides may increase the risk for men and the environment only negligibly compared with natural radiation exposure. No intervention or maintenance work shall be required during the post-closure phase. The retrieval / recovering of the waste shall be possible.

The objective of the project preliminary safety analysis (VSG) was to compile and assess the available data on exploration of the Gorleben site and research on disposal in salt rock. An important objective is also to identify the needs for future R&D-work and further Gorleben site investigations. In addition the feasibility of the methodology for use with a future site selection procedure shall be assessed.

RESULTS

The VSG is composed of four main working topics:

1.   The safety assessment is based on the description of the geological site [2] and its geological evolution over the next million years [3]. The waste that could presumably be emplaced in a repository at the Gorleben site according to the current situation in Germany with its phase out of nuclear energy (June 2011) is compiled and classified [4]. A safety and demonstration concept based on the safety requirements was developed [5] which is currently under revision.

2.   Based on these data repository concepts are developed considering operational safety, long-term safety and retrieval / recovering of the waste. Several alternatives, such as storage in drifts or boreholes and different types of canisters, are projected. The retrieval of disposed waste from boreholes during the operational phase was projected for the first time [6].

3.   The system analysis is based on these concepts. The features, events and processes are described, compiled and used to derive scenarios for the evolution of the systems and their probability [7]. Geomechanical analyses show that integrity of the geological barrier (containment providing rock zone) can be demonstrated for 1 million years [8], This applies for external (e.g. glaciation) and for internal events and processes such as decay heat or gas generation. Similarly, the seals for shafts and drifts were designed and analysed as a concept [9, 10]. The radiological consequences were analysed by numerical models for the transport of the liquid and gas phase (two phase transport) in the long-term safety analysis [11].

4.   The synthesis of the results is currently finalized. The feasibility to assess the repository system as containment system for radionuclides according to the safety requirements will be shown. The uncertainties and additional R&D will be shown, which are resulting from the partial geological exploration of the Gorleben site [12].

SUMMARY

The safety and demonstration concept, which was generated during the course of the project, is suitable to show the compatibility of the repository designs with the safety requirements. The generated design of the repository system is technically feasible and complies with the safety requirements. Nevertheless some assumptions are necessary. The assumptions refer to the status of geological exploration, the reliability of construction and some inherent uncertainties, which cannot further minimized presently. If these assumptions are met, the designed repository systems are assessed to be robust with regards to radiological consequences and a long term safety assessment.

Optimizing strategies regarding the repository design are conceivable. A repository layout such as placing the structural components farther away from the drift seals would likely result in a lower C-14 flow through the drift seals. Furthermore, implementing a void volume as a sink (like an infrastructure area backfilled with gravel) might hinder gas flow through the shaft seals. The use of gas tight casks for the structural components (like POLLUX®) could confine volatile radionuclides for

decades to centuries. The option of retrieval / recovering of the emplaced waste need further technical R&D for the concept of borehole disposal.

Some lessons learnt are:

The possible release of gaseous radionuclides, the two phase-flow processes and the subsequent model for radiation exposure require additional research and development.

The containment providing rock zone can be minimized by an iterative process but has to be assessed preliminary as an initial guess.

The handling of combinations of less probable but interdependent FEP has to be improved.

Requirements concerning the mobilization of other pollutants and groundwater flow were missing.

SUMMARY

The preliminary safety analysis for the Gorleben site identified important tasks for research and development. This would have not been possible by a generic safety analysis. A safety analysis should be repeated in time intervals and for different geological conditions.

OUTLOOK

There is still a strong political discussion on the suitability of the Gorleben site for disposal of HLW. A law is drafted to initiate a site selection process for a HLW repository. Therefore the methodology of a preliminary safety assessment may be applied to find or evaluate criteria for a site selection process.

REFERENCES

1. BMU (2010): Sicherheitsanforderungen an die Endlagerung wärmeentwickelnder radioaktiver Abfälle (Stand: 30.09.2010). Bundesministerium für Umwelt, Naturschutz und Reaktorsicherheit (BMU), Bonn, Germany.

2. Bornemann O., Behlau J., Fischbeck R., Hammer J., Jaritz W., Keller S., Mingerzahn G. & Schramm M.: Description of the Gorleben Site, part 3: Results of the geological surface and underground exploration of the salt formation. Bundesanstalt für Geowissenschaften und Rohstoffe (2011), 223 pp., 50 fig., 7 tab., 5 app., Hannover, ISBN 978-3-9813373-6-5.

3. Mrugalla S., Geowissenschaftliche Langzeit-prognose, Bericht zum Arbeitspaket 2, GRS-275, ISBN 978-3-939355-51-9, 2011.

4. Peiffer F., McStocker B., Gründler D., Ewig F., Thomauske B., Havenith A., Kettler J., Abfall-spezifikation und Mengengerüst, Bericht zum Arbeitspaket 3, GRS-278, ISBN 978-3-939355-54-0, 2011.

5. Mönig J., Buhmann D., Wolf J., Baltes B., Peiffer F, Fischer-Appelt K., VSG: Grundzüge des Sicherheits-und Nachweiskonzepts – AP 4, GRS-271, ISBN 978-3-939355-47-2.

6. Bollingerfehr W., Filbert W., Dörr S., Herold P., Lerch C., Burgwinkel P., Charlier F., Thomauske B., Bracke G., Kilger R., Endlagerauslegung und – optimierung, Bericht zum Arbeitspaket 6, GRS-281, ISBN 978-3-939355-57-1.

7. Beuth T., Bracke G., Buhmann D., Dresbach C., Keller S., Krone J., Lommerzheim A., Mönig J., Mrugalla S., Rübel A, Wolf J., Szenarien-entwicklung: Methodik und Anwendung, Bericht zum Arbeitspaket 8, GRS-284; ISBN 978-3-939355-60-1, to be published.

8. Kock I., Eickemeier R, Frieling G., Heusermann S., Knauth M., Minkley W., Navarro M., Nipp H.-K., Vogel P., Integritätsanalyse der geologischen Barriere, Bericht zum Arbeitspaket 9.1, GRS-286, ISBN xx, to be published.

9. Müller-Höppe N., Engelhardt H.-J., Lerch C., Linkamp M., Buhmann D., Czaikowski O., Herbert H.-J., Wieczorek K., Xie M., Integrität geotechnischer Barrieren, Teil 1: Vorbemessung, Bericht zum Arbeitspaket 9.2, GRS-287, ISBN xx, to be published.

10. Müller-Höppe N., Breustedt M., Wolf J., Czaikowski O., Wieczorek K., Integrität geotechnischer Barrieren, Teil 2: Vertiefte Nachweisführung, Bericht zum Arbeitspaket 9.2, GRS-288, ISBN xx, to be published.

11. Larue J., Baltes B., Fischer H., Frieling G., Kock I., Navarro M., Seher H., Radiologische Konsequenzenanalyse, Bericht zum Arbeitspaket 10, GRS-289, ISBN 978-3-939355-65-6, in preparation.

12. Fischer-Appelt K., Baltes B., Buhmann D., Larue J., Mönig J.: Synthesebericht für die VSG, Bericht zum Arbeitspaket 13, Vorläufige Sicherheitsanalyse für den Standort Gorleben, GRS 290, ISBN 978-3-939355-66-3, in preparation.

An integrated research programme in support of the safe disposal of nuclear waste in the UK

Dr Rebecca Beard [1]

[1] *Nuclear Decommissioning Authority Radioactive Waste Management Directorate, Harwell, UK, OX11 0RH*
email: *rebecca.beard@nda.gov.uk*

INTRODUCTION

This presentation will provide an update on the geological disposal process within the UK, an overview of NDA RWMDs research programme and highlight some of the technical challenges currently being addressed in the UK.

DISCUSSION

UK Government policy is that geological disposal is the way higher activity radioactive wastes will be managed in the long term: this will be preceded by safe and secure interim storage until a geological disposal facility (GDF) is available and can receive waste [1]. Currently the UK has no site identified for a GDF and so the UK has a series of illustrative concepts which are considered in the generic Disposal System Safety Case (DSSC) [2]. The generic DSSC proposes approaches for the disposal of high level waste (HLW) and spent fuel as well as intermediate level waste (ILW) and longer-lived low level waste (LLW). This generic safety case enables the optimisation of disposal concepts and underpins existing and future assessments of waste packaging proposals developed by the nuclear industry.

Our use of a series of disposal concepts appropriate to a range of geological settings and wasteforms has enabled the industry to make significant progress in addressing the historical waste liability whilst not foreclosing options for disposal in a variety of geological formations. The development of these concepts will enable well developed technical solutions for the safe disposal of Higher Activity Wastes, and the associated facility designs, to be integrated into the geological setting of Potential Candidate Sites for the UK GDF once volunteer sites are available, characterised and assessed as suitable. We term this combination of a concept and its geological setting as a Disposal System.

The generic safety case has enabled us to identify specific knowledge gaps and our extensive research programme is driven by these needs in a range of technical areas which are broken down into the following research topics relevant to multi-barrier concepts for geological disposal (as shown in Figure 1):

- Waste package evolution;
- Near field evolution;
- Radionuclide behaviour;
- Release by the gas pathway;
- Geosphere and its evolution;
- Biosphere;
- Waste package accident performance;
- Criticality safety.

The technical integrity and transparency of our research programme will be critical in underpinning regulatory and public confidence in the safe disposal of these wastes. All available research is published on our on-line bibliography under our policy of transparency and openness.

Knowledge gaps or 'information needs' in the scientific evidence base are identified in a document which describes the R&D programme for the preparatory studies phase of implementation of geological disposal [3]. This document provides the foundation on which the future R&D programme is built.

Early research is often targeted at specific processes at a laboratory scale; however as our programme matures we complement this approach through underground large-scale experiments and studies of natural analogues of disposal systems and their components. In this way we are able to model the performance of disposal systems, providing appropriate underpinning against fundamental research-based parameters whilst validating this understanding against the 'real world'. This approach both furthers our scientific understanding and delivers confidence to stakeholders.
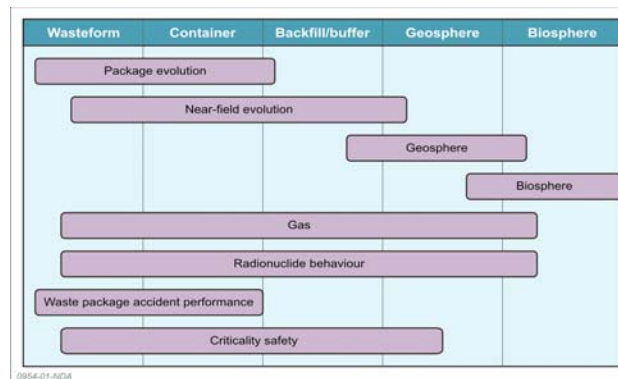
Fig. 1: RWMD Research topics.

REFERENCES

1. Managing Radioactive Waste Safely: A Framework for Implementing Geological Disposal, June 2008, Cm

7386   http://mrws.decc.gov.uk/assets/decc/mrws/white-paper-final.pdf

2. Geological Disposal. An overview of the generic Disposal System Safety Case, December 2010, NDA Report no.NDA/RWMD/010.

3. Nuclear Decommissioning Authority (2011) Geological Disposal: R&D Programme Overview, Research and Development Needs in the Preparatory Studies Phase. NDA Report NDA/RWMD/073.

Summary of US/German Workshop on Salt Repository Research, Design and Operation

Christi Leigh and Frank Hansen

Sandia National Laboratories, Defense Waste Management Programs,
4100 National Parks Highway, Carlsbad, NM 88220, USA
(email): *cdleigh@sandia.gov*

ABSTRACT

The 3rd US/German Workshop on Salt Repository Research, Design and Operation was held in Albuquerque and Carlsbad New Mexico October 8-11, 2012.[1] Thirty salt research scientists from Germany and an approximately equal number from the US met to discuss repository science state of the art. The main workshop topics were: 1. Readiness for the safety case for high-level waste disposal in salt, 2. Joint Project on the Comparison of Constitutive Models for Rock Salt, which involves benchmark modeling of thermo-mechanical field-scale tests, and 3. Reconsolidation of granular salt. Effort was focused on building new collaborations and researcher-to-researcher relationships.

The Joint Project meeting occurred the day before the 3rd US/German Workshop on Salt Repository Research, Design and Operation (day one of the agenda). A summary of the Joint Project in the context of benchmark modeling within the 3rd Workshop is contained here, but abstracts or presentations from the Joint Project are not included because it is being conducted under a Memorandum of Understanding agreement and has its own schedules and deliverables. The coincidence of the Joint Project meeting and the 3rd US/German Workshop on Salt Repository Research, Design and Operation allowed a larger number of salt scientists to attend and participate.

This document follows the workshop in chronological order. Both the agenda and these Proceedings are organized topically as follows:

1. <u>Safety case for heat-generating waste disposal in salt.</u> The international salt research community has a solid foundation for a safety case and the associated performance assessment. Workshop material covered Germany's preliminary safety analysis for the Gorleben site (Vorläufige Sicherheit-sanalyse Gorleben or VSG). Consistent with German progress, the US has the technical basis and ability to make a safety case for salt disposal of high level waste in the immediate future—if the nation adopts this strategy.

2. <u>Benchmark modeling.</u> The Joint Project has been extremely timely and helpful in assessing the salt science community's ability to model salt coupled thermal and mechanical behavior using appropriate, yet different, constitutive models. Progress made to date guides formulation of a strategy for generic modeling of thermomechanical field-scale tests.

3. <u>Reconsolidation of granular salt.</u> Salt repository scientists benefit from significant existing information on granular salt consolidation. It is essential to understand granular salt reconsolidation under a wide range of conditions to establish certain performance bases for heat-generating waste salt repositories (borehole and drift emplacement concepts). Mechanical and hydrological crushed salt properties depend strongly on porosity, which decreases as the surrounding salt creeps inward and compresses granular salt within the rooms, drifts, or shafts.

Significant effort was focused on laying grounds for future collaborations and building relationships among the many newer and younger members of the salt research community to facilitate knowledge transfer and succession planning. Exchanges were renewed

regarding exploiting our respective underground resources through new field-scale collaborative projects. A dialogue of this progress is included in the Section IV of these Proceedings. As with previous US/German salt repository workshops, these Proceedings are posted on our Salt Repository Website (http://www.sandia.gov/SALT/SALT_Home.html). The 4th US/German salt repository workshop is planned for Berlin Germany in September 2013. The main topics will include repository research on granular salt reconsolidation, the safety case for salt disposal of heat-generating waste, confidence and data supporting plugging/sealing/barriers, and an introduction of hydrology collaborations.

The US/German workshop series concerned with salt repository research, design and operation is a significant part of US/German salt repository collaboration. Contemporary developments in both countries have given rise to renewed interest and collaborations in salt repository investigations and related studies. A recent paper for Waste Management authored by the US and German collaboration leadership summarizes the various ways in which salt repository research is unfolding. This Waste Management paper's development directly reflects achievement of collaboration goals as laid out in our prospectus for our US/German Workshops on Salt Repository Research, Design and Operation.

Both the German rock salt repository program and the US waste management program grapple with challenges in terms of maintaining and honing their respective current state-of-the-art core capabilities in rock salt repository science and technology. The following sections describe several venues of constructive international collaborations being pursued by US and German salt repository researchers.

REFERENCES

[1] HANSEN, F., KUHLMAN, K., BIURRUN, E. Proceedings for 3rd US/German Workshop on Salt Repository Research, Design and Operation." SAND2013-1231P.

[2] STEININGER, W., F.D. HANSEN, E. BIURRUN and W. BOLLINGERFEHR. *US/German Collaboration in Salt Repository Research, Design and Operation*. WM2013 Conference, February 24-28, 2013, Phoenix, Arizona, USA.

———————————————————————————

WIPP Hydrous Mineral Phase Transformations at Elevated Temperatures

Florie A. Caporuscio, Michael C. Cheshire, and Hakim Boukhalfa.

Earth and Environmental Sciences Division, EES-14 MS-J966,
Los Alamos National Laboratory, Los Alamos NM 87505 USA
email:floriec@lanl.gov

INTRODUCTION

Salt rocks contain a significant amount of water associated with hydrated minerals contained in the salt. Minerals most commonly associated with salt include oxyhydroxide minerals, carnallite ($KMgCl_3 \cdot 6(H_2O)$), bischofite ($MgCl_2 \cdot 6H_2O$), kieserite ($MgSO_4 \cdot H_2O$), gypsum($CaSO_4 \cdot 2H_2O$),polyhalite ($K_2Ca_2Mg(SO_4)_4 \cdot 2H_2O$) and clay minerals. The distribution of these various hydrated minerals and the water associated with them is highly variable and varies significantly within samples from the same location [1-3]. At the WIPP site, the dominant clay mineral is corrensite, and the sulfate minerals are bassanite, anhydrite and polyhalite.

Polyhalite contains up to 6 wt. % water, clay minerals can contain between 5 and 18 wt. % water and gypsum contains up to 20.9 wt. % water. The first and second dehydration temperature domains for polyhalite are 150-160 ^{o}C and 340 – 360 ^{o}C respectively. Clay minerals undergo dehydration between 100 and 800 ^{o}C. Gypsum undergoes dehydration between 75 to 175 ^{o}C. Bassanite is a persistant metastable phase during the gypsum-anhydrite phase transformation. These sulfate phase transformations are influenced by the amount of water present, the temperature, pressure, and amount of dissolved electrolytes or organics [4].

Clay minerals present as minor mineral phases in salt rocks can play a critical role in the performance of the repository. They can influence the performance of the repository though their chemical interaction with radionuclides, retention and release of water, and influence mechanical behavior of the salt (porosity). Clays can undergo dehydration processes and change physical structure and chemical composition under heat and pressure loads [5]. These changes in turn can influence their capacity to retain water, and their sorption/desorption capacity and concomitant retention of radionuclides.

Sulfate minerals associated with salt have been examined to determine their ability to retain and release significant amounts of water through hydration /dehydration processes as a function of heat and pressure loads. The gypsum ($CaSO_4 \cdot 2H_2O$) to anhydrite transformation creates a large water release (up to 21% wt. loss) and volume reduction (of up to 40%) [6]. Volume loss results in contraction, which can affect salt porosity by creation of fractures. Such water losses and volume changes may have significant effects on salt

repository performance at high heat loads. Therefore, we undertook this study characterize the hydrous minerals at WIPP.

DESCRIPTION OF THE WORK

The two experimental studies we undertook were: 1) XRD mineral characterization using a heated stage (Figure 1), with temperatures ranging from 25 to 250 ^{o}C and 20% RH, and, 2) experimental mineral runs of 6 weeks at 300°C and 150 bar using Dickson rocking autoclaves (Figure 2)

FIGURE 1. XRD cell used for in situ XRD examination under controlled temperature and relative humidity.

FIGURE 2. Bridgeman seal-type pressure vessel for 300°C, 150 bar hydrothermal experiment.

RESULTS

Experiments performed on WIPP corrensite (clay) Naica Mexico gypsum, and WIPP bassanite, anhydrite (sulfates) provided informative data. The clay run on the heated XRD stage showed a water dehydration step at < 100 ^{o}C (Figure 3). The experiments at 300 ^{o}C, 150 bar indicated no further water release occurred.
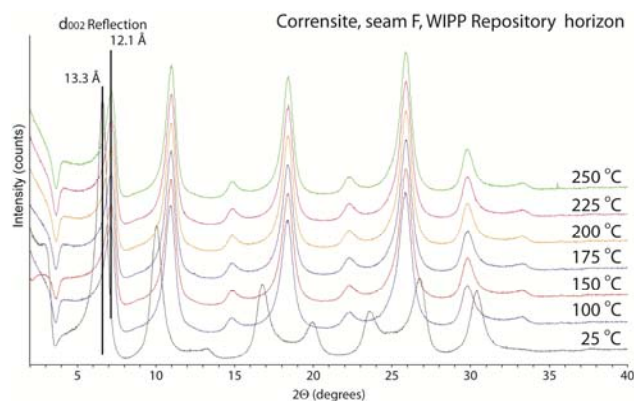
Figure 3. Corrensite XRD patterns 25 -250 ^{o}C. Note d_{002} reflection shift from13.3 Å to 12.1 Å indicating a structure change at < 100 ^{o}C

Determination of WIPP salt minor phases by powder XRD indicate bassanite, anhydrite, and polyhalite. A "polyhalite" bed examined by XRD reveals that in fact anhydrite exceeded polyhalite by three to one. Low overall sulfate abundances at WIPP necessitated the use of gypsum samples from Mexico for the phase stability studies. The phase transition from gypsum to anhydrite (using a gypsum sample from Naica, Mexico) reveals that bassanite forms at approximately 75 ^{o}C, 1 bar. Bassanite phase stability at higher temperatures is not yet determined, but experiments are ongoing. In very recent work bassanite exists at 275 ^{o}C, 1 bar, with slow in-growth of anhydrite. Anhydrite abundance increases with time.

Experiments run at 300 ^{o}C and 150 bar show that anhydrite is stable, bassanite no longer occurs, and remnant gypsum is still present. These experiments were run both "dry" (ie, gypsum powder starting material) and saturated with DI. The remnant gypsum may be just a kinetic artifact. Both types of experiments (1 bar and 150 bar, with various liquid water contents) indicate differing phase stabilities. Time, temperature and pressure all seem to be controlling factors on the "stability" of metastable bassanite [4]. This two step reaction involving a metastable phase results in researchers deterimng wide stability differences. Reasonable boundaries may be (1) gypsum to bassanite transformation at 76 ^{o}C [7] and (2) bassanite to anhydrite at 100 to 140 ^{o}C [8]. Determining the metastable bassanite field would be critical to

understanding the water release timing and amounts in a high temperature repository setting.

REFERENCES

[1] Braitsch, O, "Salt deposits their origin and composition" Springer-Verlag, New York, 297pp. (1971)

[2] Stewart, F. H. "Marine evaporites: U.S. Geological Survey Professional Paper 440Y, 52 p. (1963)

[3] Kopp, O. C., and Combs, D. W. "Mineral sources of water in evaporite sequences (Salado salt and adjacent beds at the proposed waste disposal facility near Carlsbad in Lea and Eddy Counties, New Mexico)". Oak Ridge National Laboratory, Final Report, ORNL/SUB-3670-3-4, 34 p (1975)

[4] Freyer, D. and Voigt, W. Invited Review: Crystallization and Phase Stability of $CaSO_4$ and $CaSO_4$-Based Salts. Mon. fur Chemie 134, pp 693-719. (2003)

[5] Altaner, S.P., and Ylagan, R.F. "Comparison of Structural Models of Mixed-Layer Illite-Smectite and Reaction Mechanisms of Smectite Illitization." Clays and Clay Min., Vol. 45, p. 517-533. (1997)

[6] Smyth, J.R., and Bish, D. "*Crystal Structures and Cation Sites f the Rock-Forming Minerals*" Allen & Unwin. (1988)

[7] Freyer,D. Zur Phasenbildung und stabilitat im System $Na_2SO_4 – CaSO_4 – H_2O$. Dissertation , TU Bergakademie, Feiburg. (2000)

[8] Shcherban, J.P., and Shirokikh, I.N. Thermodynamic and experimental data on Stability of gypsum, hennhydrate, and anhydrite under hydrothermal conditions. Int. Geology Review, 13: 11, pp 1671-1673. (1971)

Constraints on Parameters for Mineral Fragment Colloids and Humic Substance Colloids at WIPP

Paul E. Mariner[1] and David C. Sassani[1]

[1]*Sandia National Laboratories, P.O. Box 5800, MS 0747,*
Albuquerque, NM 87123, U.S.A
email: pmarine@sandia.gov

INTRODUCTION

In 2010, U.S. Environmental Protection Agency (EPA) review[1] of the 2009 Waste Isolation Pilot Plant (WIPP) recertification application CRA-2009[2] resulted in requests that the U.S. Department of Energy (DOE), prior to the next recertification (CRA-2014), re-evaluate thorium intrinsic colloids and Mg-Cl-OH mineral-fragment colloids under WIPP-relevant conditions. In response, DOE initiated a concerted effort to update and reanalyze the technical bases for all colloid parameters. This paper summarizes recent work that addresses parameter constraints on mineral fragment colloids and humic substance colloids.

DESCRIPTION OF THE WORK

Sandia National Laboratories (SNL) reviewed the literature since the 1996 compliance certification application[3] for studies relevant to colloid stability and migration under WIPP conditions, performed experimental work on Mg-Cl-OH colloid formation, and reviewed the colloid parameter values. This paper addresses (1) the potential impact of recent data regarding constraints on mineral-fragment and humic substance colloid parameters and (2) conservatisms included in these constraints.

RESULTS

Mineral Fragment Colloids

In early 2010, EPA noted that Mg-Cl-OH mineral fragment colloids may form in $MgCl_2$ solutions and requested that DOE address whether these colloids could form in the WIPP repository[4]. EPA's request was based on research by Altmaier et al.[5] in which Mg-Cl-OH mineral fragment colloids formed in $MgCl_2$ solutions at high ionic strength (2.5 to 4.5 M). In the response to the EPA comment, Xiong et al.[6] stated why the mineral fragment colloids reported by Altmaier et al.[5] (i.e., $Mg_2Cl(OH)_3 \cdot 4H_2O$, also termed "phase 3") are not relevant to WIPP and concluded that these colloids will not form. EPA in its Chemistry Technical Support Document expressed additional interest[1].

The Xiong et al.[6] conclusion was based in part on SNL testing of MgO hydration/carbonation that indicated

phase 5 ($Mg_3Cl(OH)_5 \cdot 4H_2O$) rather than phase 3 is the stable precipitate under WIPP-relevant conditions[7; 8]. This conclusion is supported by geochemical calculations that include both phases. Further, the rapid precipitation step implemented to form the Mg-Cl-OH mineral fragment colloids in the Altmaier et al.[5] study is believed to be a process that will not occur within WIPP[9]. On-going sampling and analysis of MgO hydration/carbonation tests show no evidence for Mg-Cl-OH colloid formation under WIPP-relevant conditions.

Long-term (~6 year) plutonium-iron experiments at Los Alamos National Laboratory (LANL) support the current representation of mineral fragment colloids in the WIPP performance assessment (PA)[10]. In these experiments, which were conducted in ERDA-6 and GWB brines at pC_{H+} values (negative log of the hydrogen ion concentration) between 7.7 and 9.5, iron coupons actively corroded under anoxic conditions in the presence of plutonium. For the repository-relevant pC_{H+} values, the mineral fragment plutonium concentrations were measured to be 8.6×10^{-9} M and 2.3×10^{-8} M, which are consistent with the value of 2.6×10^{-8} M cautiously chosen for the CONCMIN mineral fragment enhancement parameter used in the WIPP PA.

Though these experiments corroborate a CONCMIN value of 2.6×10^{-8} M, this concentration may far exceed what is sustainable for natural mineral colloids in WIPP brines. If it is assumed that plutonium sorbs at a site density of 10 nm^{-2} and the colloids are spherical and have a representative diameter of 10 nm and a solid density of 3 g mL^{-1}, the implied colloid concentration is approximately 8 μg L^{-1}. In groundwaters around the world, natural mineral colloid concentrations are observed to drop below 0.02 μg L^{-1} when the ionic strength exceeds 0.2 M[11]. The CONCMIN value, therefore, is ~400 times higher than these data (~4,000 times higher if a site density of 1 nm^{-2} or a nominal diameter of 100 nm is assumed). The data from the LANL experiments, which corroborate the CONCMIN value, are thought to be sustained in the experiments by a steady-state condition driven by irreversible iron corrosion coupled with colloid flocculation. Depending on the physical and chemical conditions within the repository and the abundance of brine, similar sustained rates of iron corrosion might also be possible in the repository. Therefore, the current CONCMIN value for mineral fragment colloids is believed to be a reasonably conservative upper bound

value. A more realistic parameter constraint would need to account for the possibility of lower corrosion rates and therefore lower corrosion product concentrations, consistent with a natural brine system.

Solubility experiments have also been recently performed at LANL for Nd(III), Th(IV), and U(VI) using GWB and ERDA-6 brine at pC_{H+} values between 7 and 12 and varying concentrations of carbonate and organic complexants[10]. These experiments were conducted in the absence of corroding iron. The results show negligible Mg-Cl-OH colloid formation under WIPP conditions. Consistent with data for natural systems, this suggests that Pu(III) and Pu(IV) would have negligible mineral fragment components in the absence of iron corrosion product colloids. The potential for active formation of iron corrosion product colloids to enhance various actinide source terms within WIPP over long periods of time is bounded by the CONCMIN parameter.

Humic Substance Colloids

The maximum concentration of an actinide associated with humic substances in the WIPP PA is 1.1×10^{-5} M[3]. This value is based on a site-binding capacity of 5.56 meq g^{-1} and a maximum concentration of humic substances of 2.0 mg L^{-1} observed in systems containing 10 mM or greater Ca^{2+} and Mg^{2+}. Work at SNL has since shown that humic substances are not stable (rapidly flocculate) in ERDA-6 and GWB brines reacted with MgO[12]. Because WIPP waste forms are surrounded by MgO, these results imply that no humic substance colloids should be stable in WIPP source-term brines.

Based on those data, the proportionality constants for the humic substance colloids also appear to be conservative. We have begun to revisit them to assess whether revisions are justified based on recent data and potentially improved understanding of humic complexation under WIPP conditions. For example, the 6.3 value for the +4 oxidation state was taken from a study of the aqueous and colloidal fractions of Th(IV) in seawater[3]. Seawater is much different than the ERDA-6 and GWB brines in the presence of MgO. High concentrations of Mg^{2+} from the MgO at high pH not only appear to cause humic substances to flocculate but are also expected to compete with the actinides for humic complexation sites. In addition, we have discovered a slight miscalculation in the median value of the proportionality constant for Pu(III) in Castile brine that conservatively overestimates the humic colloid component (1.37 instead of 1.15).

ACKNOWLEDGMENT

REFERENCES

[1] U.S. EPA, "Technical Support Document for Section 194.24: Evaluation of the Compliance Recertification Actinide Source Term, Backfill Efficacy and Culebra Dolomite Distribution Coefficient Values (Revision 1)," Docket No. A-98-49, Item II-B1-25. EDOCKET NO: EPA-HQ-OAR-2009-0330. U.S. Environmental Protection Agency (2010).

[2] U.S. DOE, "Title 40 CFR Part 191 Subparts B and C Compliance Recertification Application for the Waste Isolation Pilot Plant," DOE/WIPP 09 3424. U.S. Department of Energy Carlsbad, NM (2009).

[3] U.S. DOE, "Title 40 CFR Part 191 Compliance Certification Application for the Waste Isolation Pilot Plant," DOE/CAO-1994-2184. U.S. Department of Energy, Carlsbad, NM (1996).

[4] KELLY, T., "Untitled letter with enclosure to D.C Moody with fourth set of CRA comments and requests for additional information, February 22, 2010," U.S. Environmental Protection Agency, Washington, DC (2010).

[5] ALTMAIER, M., et al., "Solubility and colloid formation of Th(IV) in concentrated NaCl and MgCl2 solution" *Radiochimica Acta* **92**, 537-543 (2004).

[6] XIONG, Y.-L., et al., "Responses to three EPA comments pertaining to comparisons of measured and predicted dissolved and colloidal Th(IV) and Am(III) concentrations," Analysis report, May 4, 2010. Sandia National Laboratories, Carlsbad, NM (2010).

[7] XIONG, Y.-L., et al., "Experimental investigations of the reaction path in the MgO–CO2–H2O system in solutions with ionic strengths, and their applications to nuclear waste isolation" *Applied Geochemistry* **23**, 1634–1659 (2008).

[8] DENG, H.-R., et al., "Experimental work conducted on MgO long-term hydration," 2008 Milestone Report. Sandia National Laboratories, Carlsbad, NM (2009).

[9] ALTMAIER, M., "Untitled email to D. Sassani, March 29," (2012).

[10] REED, D., et al., "Intrinsic, mineral and microbial colloid enhancement parameters for the WIPP actinide source term," LANL-CO ACRSP/LCO-ACP-18. Los Alamos National Laboratory, Los Alamos, NM (2013).

[11] ALEXANDER, W.R., et al., "Review of colloids in the geosphere and their treatment in performance assessments.," NPO003512. Report to NDA-RWMD. Serco Ltd., Oxfordshire, UK (2011).

[12] WALL, N.A., et al., "Sustainability of humic acids in the presence of magnesium oxide" *Applied Geochemistry* **20**, 1704-1713 (2005).

Borate chemistry at alkaline pH

Marian Borkowski, Mike Richmann, Jean-Francois Lucchini, Julie Swanson, Danielle Cleveland, Donald Reed.

Earth and Environmental Sciences, Los Alamos National Laboratory- Carlsbad Operations, 1400 University Drive, Carlsbad, NM 88220, USA
email: marian@lanl.gov

INTRODUCTION

Borates solutions have many interesting properties for studying metal ion complexation. Borate compounds are soluble in water and the solutions display a wide UV-VIS-NIR spectroscopic window. Naturally occurring isotopes B-10 (19.6%) and B-11 (80.4%) are NMR active. Borate oxy-anions provide a useful Raman-active probe and borate solutions are good solvents for electrochemical studies. Borate provides a wide range of pH buffering capacity from 6 to 12. Borate has been found in Waste Isolation Pilot Plant (WIPP) brines (up to ~160 mM) and is currently present in the simulated brines used to establish actinide solubility.

Borate chemistry, especially in basic media, is still not well understood and its behavior in basic media is the focus of this study.   Recently we reported that neodymium is complexed by tetraborate ion (log K ~4) [1] and that plutonium forms a stronger complexes than that of neodymium [2]. Further investigations of borate chemistry and its complexing properties are discussed.

DESCRIPTION OF THE WORK

Samples of sodium tetraborate and boric acid at pH ranging from 2 to 12 were prepared and an NMR study was conducted. Chemical shift versus pH was measured. These results are supported by XRD analysis of crystallized solids precipitated from similar solutions.

RESULTS

Boron can link either three oxygens to form a triangle (trigonal) or four oxygens to form a tetrahedron. Boric acid is a very weak acid and acts exclusively by hydroxyl-ion acceptance rather than proton donation.

Titration of sodium tetraborate, that is present in WIPP brine, with hydrochloric acid indicated, that tetraboric acid is a diprotic acid with both centers having the same $pK_a = 8.95$, and they behave similarly to monoboric acid.

The solution chemistry of borates is a topic of current interest due to a history of conflicting reports that are not yet totally resolved. A variety of methods unequivocally established the existence of polyborate anions in aqueous solution. Aqueous polyborate equilibria were studied by ^{11}B NMR and by Raman Spectroscopy [3, 4]. On the basis of these data the formation constants for $B(OH)_4^-$, $B_3O_3(OH)_4^-$, $B_4O_5(OH)_4^{2-}$ and $B_5O_6(OH)_4^-$ were reported [3] and the distribution of the expected forms of borate as a function of pH are presented in Figure 1.
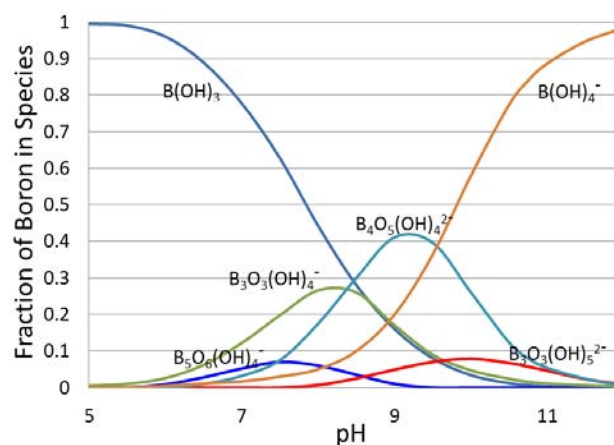
Fig. 1: Abundance of different polyborate species as a function of pH.

This speciation is a function of pH and also boron concentration. The relative importance of the concentrations of various boric acid species over the 5 to 11 pH range and 0.4 M boric acid is presented in the Figure 1. The lengths of vertical line segments between the curves represent the fraction of boron present as a given species.

NMR studies of sodium tetraborate solutions presented in Figure 2 confirmed our earlier observations from the XRD measurements of solids crystallized using sodium tetraborate and boric acid as a function of pH. These data collectively show that the borate speciation in the solution only depends on the pH of the solution and not on the initial form of the borate used for solution preparation.
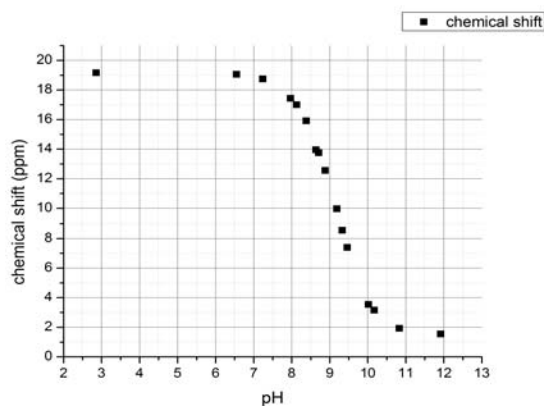
Fig. 2: Chemical shift measured sodium tetraborate solutions as a function of pH at 30°C.

The observed chemical shift with pH is caused by the conversion of trigonal boron atoms into tetrahedral. With increasing pH, newly created borate forms have a higher percent of tetrahedral boron atoms in the molecule that increases up to a 100% conversion. The various equilibria in aqueous solution with increasing pH is presented in Figure 3. This sequence is a simple function of the increased content of tetrahedral boron atoms in the polyborate molecule. On the basis of the data in Figure 1, some of the species will be at a very low concentration and may not affect the overall complexation of borate.
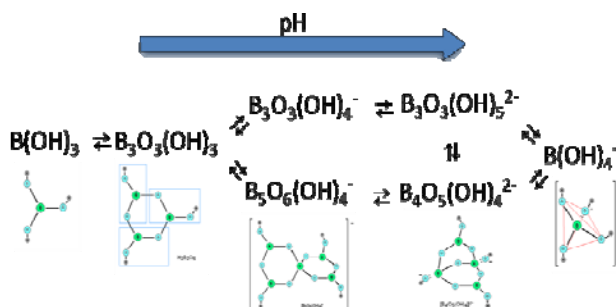
Fig. 3: Expected transitional species of borate as a function of pH.

The complexation strength of different polyborate forms depends on the number of tetrahedral boron atoms in the molecule. According to the NMR and spectral data several forms of borate in solution have one tetrahedral boron atom and only two forms have two tetrahedral boron atoms in the molecule. Only the forms having two tetrahedral boron atoms in molecule are able to form a covalent bond with metal ions. Other forms can only attract cations through weak electrostatic interactions.

The relative concentration of negatively-charged polyborate species (-2 and -1) as a function of pH is presented in Figure 4. The highest affinity of borate ions
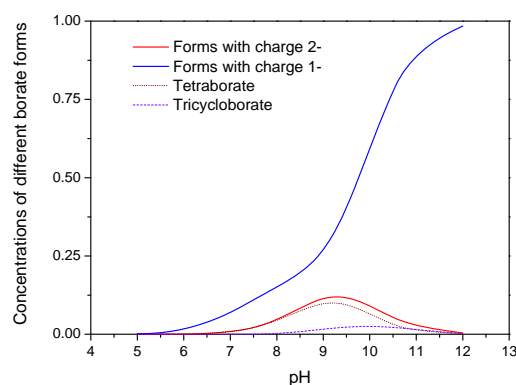
Fig. 4: Relative concentrations of the two-negative and mono-negative forms of polyborates as a function of pH.

to form coordination bonds is at pH ~ 9.3. This tendency decreases with both an increase or decrease in pH. Borate can only form complexes with metals in under moderately alkaline pH conditions. At this pH actinides are strongly hydrolyzed and borate ions will directly compete with hydrolysis. For this reason, the formation of ternary complexes will be the rule. At higher borate concentrations the formation of 1:2 complexes cannot be excluded, however we did not see experimental evidence for the formation of this complex. The interaction of borate with trivalent and hexavalent actinides should be much stronger and experimental data confirm this trend. In this context, the borate complexation of tetravalent cations is overwhelmed by hydrolysis. At pH > 11, the mono-boric anion will only form ion pairs by weak electrostatic interaction with cations.

REFERENCES

1. BORKOWSKI, M. et al., "Complexation of Nd(III) with tetraborate ion and its effect on actinide (III) solubility in WIPP brine" *Radiochimica Acta*, **98**, 577 (2010).

2. BORKOWSKI, M. et al., "Borate Ion Complexation of the Lanthanides and Actinides: Implications for the WIPP Salt Geologic Repository" *Proceedings of the ACTINIDES-2009 Conference*, San Francisco, CA, (2009).

3. ANDERSON JL. et al., "Temperature jump rate studies of polyborate formation in aqueous boric acid", *J. Phys Chem* **68**, 1128-1132 (1964).

4. HERTAM, A. Diplomarbeit "^{11}B-NMR spektroskopische Untersuchungen zum Lösungszustand von Boraten in konzentrierten Salzlösungen", Freiberg, Germany, 2011.

Chemistry of the Fe(II)-System in Brines

Andrés G. Muñoz, Barbara P. Bischofer, Helge C. Moog

Global Research for Safety, GRSmbH, Theodor-Heuss-Str. 4, 38122 Braunschweig, Germany.

INTRODUCTION

The knowledge of thermodynamic properties of Fe(II) in concentrated solutions of the hexary oceanic salt system is essential for the modeling and prediction of corrosion processes in steel-based spent-fuel disposal containers in salt-rock repositories. Corrosion of steel leads to reducing conditions in the disposal room due to the generation of hydrogen [1]. This not only results in the reduction of heavy radionuclides, such as Pu(VI) and U(VI) to lower oxidation states +III and +IV of lower solubility in water but also to considerable mechanical stress accelerating the corrosion process and the formation of fissures. The stability of corrosion products generated upon contact of steel containers with brines may have large influence on the transport and migration of radioactive contaminants. For instance, zero-valent iron was tried for removing of uranium by reductive precipitation of uranyl to less soluble U(IV)-compounds and the adsorption of uranyl on iron corrosion products [2]. The removing rate by reduction of U(VI) to slightly soluble U(IV) species depends greatly on the activity of solution species and the nature of the formed corrosion products in brines under anaerobic conditions. Dissolution and precipitation processes can be modeled by applying the Pitzer formalism [3], formulated from an analogy of the virial concept of real gases, which describes the concentration dependence of the excess free energy of solutions. This requires a consistent set of specific binary and ternary interaction parameters, which have to be determined experimentally from water activity, solubility and potentiometric data.

MODELLING

The Pitzer model describes the thermodynamic behavior of electrolyte solutions at high ionic strengths by adding a term accounting for non-electrostatic ion interactions to the expression extended Debye-Hückel equation for the free excess energy:

$$\frac{G^{ex}}{kg_w RT} = f(I) + \sum_{i,j} \lambda_{ij}(I)\, m_i m_j + \sum_{i,j} \mu_{ijk}\, m_i m_j m_k \quad (1)$$

where m_i is the molality of the species i and $f(I)$ is a function of the ionic strength. λ_{ij} (I) is the ionic-strength dependent interaction parameter of pairs of species and

μ_{ijk} is a concentration independent ternary interaction parameter for ion-triplets. The derivative of function (1) leads to expressions of activity and osmotic coefficients of the form:

$$Y_s = f_s(I) + f_s[\alpha_{ij}^{(1)}, \alpha_{ij}^{(2)}, \beta_{ij}^{(0)}, \beta_{ij}^{(1)}, \beta_{ij}^{(2)}, C_{ij}^{\phi}, \theta_{ii}, \Psi_{ijk}] \quad (2)$$

where Y_s: ϕ, $\ln\gamma_i$ (see ref. [1] for more details). Pitzer equations (2) are linear with respect to the unknown interaction parameters and can be written for each individual data set as:

$$Y_n = \sum_i A_{n,P_i} P_i + C_n \quad (3)$$

where each A_{n,P_i} is the constant prefactor in the nth data set for the Pitzer parameter P_i and C_n is a constant. The adjustment of semi-empirical Pitzer equations (2) to the experimentally accessible quantities was made by minimization of the sum of the relative error:

$$E = \sum_i \left(\sum_j \frac{A_{i,j} P_j}{Y_i} + \frac{C_i}{Y_i} - 1 \right)_i \quad (4)$$

by the generalized reduced gradient method.

Phase diagrams were constructed by using the program The Geochemist´s Workbench with a self-generated parameter file. Interaction Pitzer parameters and solubility constants of minerals belonging to the hexary oceanic salt system were taken from the revision provided by Voigt as available at the THEREDA data base [4]. The temperature dependence of Pitzer parameters and solubility constants was expressed by the generalized function:

$$Y(T) = Y(T_0) + a\left(\frac{1}{T} - \frac{1}{T_0}\right) + b\ln\left(\frac{T}{T_0}\right) + c(T - T_0) \quad (5)$$

where $Y(T)$: $\beta_{ij}^{(0)}(T), \beta_{ij}^{(1)}(T), \beta_{ij}^{(2)}(T), C_{ij}^{\phi}(T), \theta_{ij}(T), \Psi_{ijk}(T); \ln K(T)$. T_0: 298.15 K. This temperature expansion suits very well in the range of investigated temperatures.

RESULTS

A comprehensive set of Pitzer interaction parameters for the system Fe(II)-K-Na-Mg-Ca-Cl-SO4-H2O, valid for the temperature range of 25°C to 90°C was calculated from an extensive revision of reported and measured

solubility and isopiestic data. Solubility and solution activity data reported in the literature were complemented with water activity and solubility data obtained from isopiestic and solubility experiments, respectively, carried out for some particular systems at 25°C and t=40°C, 60°C and 90°C. Details of the measurement set up were reported elsewhere [5]. Water thermostatic baths were used to for 40°C and 60°C. For 90°C, an air based heat case was used.

Binary Systems

Temperature dependent binary interaction Pitzer parameters for the systems Fe-Cl- H_2O and Fe-SO_4-H_2O were obtained by fitting a large set of solubility data reported in the literature. In spite of the large volume of data available for $FeSO_4$ at T > 320°C, no concluding statements about the relative thermodynamic stability of phases $FeSO_4 \cdot 4H_2O$ and $FeSO_4 \cdot 1H_2O$ in sulfate saturated solutions can be drawn. Our solubility experiments have also shown some dispersion in this region in spite of the very long equilibration time (longer than 24 months). This fact is probably related with the meta-stability of the tetrahydrate (see fig.1).
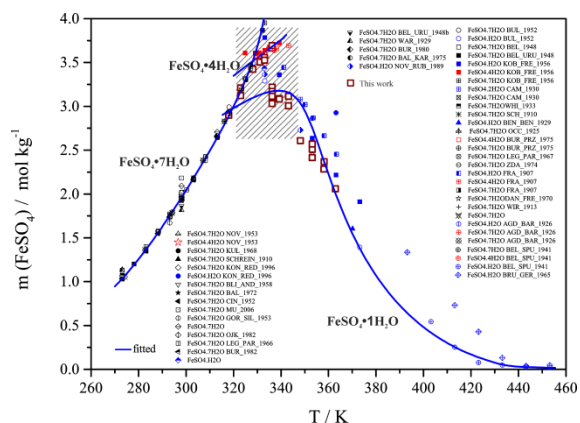
Fig.1: Solubility diagram for the Fe(II)-SO_4-H_2O System.

Ternary Systems

Table 2 Summarizes the availability of data for the different ternary systems. It can be seen, that in contrast with chloride systems, for systems with sulfate water activity data are practically absent in the literature. This does not seem to be unfounded, considering the difficulty of sulfate systems to attain thermodynamic equilibrium in isopiestic experiments.

Based on available experimental data, ternary interaction parameters $\theta_{c\text{-Fe}}$ and $\Psi_{c\text{-Fe-X, Fe-a-X}}$ were calculated; the former one by simultaneous fitting of Cl- and SO_4- systems.

System	a_w(25°)	a_w(t)	log k_w(25°)	log k(t)
Fe-Cl-Na	✓	✓	✓	✓
Fe-Cl-K	✓	✓	✓	✓
Fe-Cl-Mg	✓	✓	✓	
Fe-Cl-Ca	✓	✓	✓	
Fe-SO_4-Na			✓	✓
Fe-SO_4-K			✓	✓
Fe-SO_4-Mg	✓	✓	✓	
Fe-SO_4-Ca			✓	
Fe- SO_4-Cl			✓	✓

Table 1: Resume of availability of thermodynamic data.
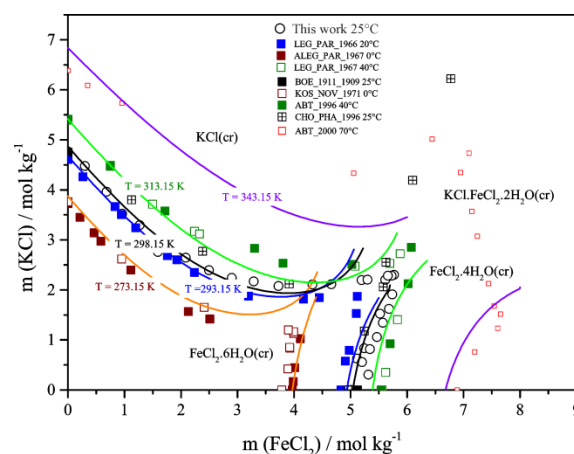
Fig.2: Solubility diagram for the Fe(II)-K-Cl-H_2O System.

Solubility diagrams for systems containing K were particularly difficult to model near the point of coexistence of two solid phases (see fig.2). This feature is tentatively ascribed to the strong influence of chloride complex formation which cannot be accounted for by the speciation model presently in use.

REFERENCES

1. Z. WANG et al., "A study of the corrosion products of mild steel in high ionic strength brines" *Waste Management* **21**, 335 (2001).
2. J. FARREL et al.,"Uranium removal from ground water using zero valent iron media" *Ground Water* **37**, 618 (1999).
3. K.S. PITZER, "Activity coefficients in electrolyte solutions" CRC Press, Boca Raton, FL (1991).
4. W. VOIGT, "THEREDA-Thermodynamische Referenzdatenbasis, GRS-Report. http://thereda.de.
5. A.V. RUMYANTSEV et al., "Isopiestic investigations of the systems $Fe_2(SO_4)_3$-H_2SO_4-H_2O, $FeCl_3$-H_2O and Fe(III)-(Na,K,Mg,Ca)Cl_n-H_2O at 298.15 K. *Z. Phys. Chem.* **218**, 1089 (2004).

Speciation and Solubility of Aluminum in High Ionic Strength Solutions at Elevated Temperatures to 250 °C [A]

Yongliang Xiong[1]

[1]*Repository Performance Dept. 6212, Sandia National Laboratories,*[B]
yxiong@sandia.gov

INTRODUCTION

As one of the most abundant elements in the earth's crust, aluminum forms numerous minerals in hydrothermal systems. In addition, borosilicate glasses in which aluminum is a major component, are strong candidate waste forms for immobilization of high level nuclear waste (HLW). Activity coefficient models valid to high ionic strength are required to describe accurately the aqueous geochemical behavior of aluminum in hydrothermal systems, as hydrothermal fluids are frequently of high ionic strength in nature, and to model geochemical behavior of aluminum in the near-field in geological repositories for HLW, especially in salt formations and deep boreholes.

The often used B dot equation in geochemistry[1] is valid only to an ionic strength of 1.0 mol•kg^{-1} at most[2]. The Pitzer activity coefficient model is valid to high ionic strengths, up to saturation of most salts[3], and is suitable to modeling the aqueous behavior of aluminum in high ionic strength hydrothermal fluids. The aqueous speciation of aluminum depends on pH$_m$. At 25 °C, Al^{3+}, $Al(OH)^{2+}$, and $Al(OH)_2^+$ dominate in the acidic pH$_m$ range[4]. $Al(OH)_3(aq)$ has a narrow dominant field around pH 7[4]. $Al(OH)_4^-$ dominates from pH$_m$~7 to alkaline pH$_m$'s[4]. At 150 °C, the neutral pH is 5.82. At 150 °C, Al^{3+}, $Al(OH)^{2+}$, and $Al(OH)_2^+$ still dominate in the acidic pH$_m$ range[5]. The narrow dominant field of $Al(OH)_3(aq)$ is around pH$_m$~4[5]. In contrast, $Al(OH)_4^-$ dominates from pH$_m$~4 to alkaline pH$_m$'s at 150 °C[5]. Therefore, $Al(OH)_4^-$ is a dominant aqueous aluminum species under the mildly acidic to alkaline conditions in hydrothermal systems. As Na^+ is an important and ubiquitous species in natural hydrothermal systems, especially in salt formations, the interaction between Na^+ and $Al(OH)_4^-$ must be known in modeling geochemical behavior of aluminum in hydrothermal systems.

In the work of Wesolowski[4], the Pitzer parameters for the Na^+—$Al(OH)_4^-$ interaction were obtained. This set of the Pitzer parameters has been successfully applied into the thermodynamic models for the solubility of gibbsite $(Al(OH)_3)$ and boehmite $(AlOOH)$[6] and for the Si-Al speciation and solubility to 100 °C[7].

METHODOLOGY

In the work of Palmer et al.[5], the equilibrium quotients (log Q$_{s4}$) for the following reaction in a NaCl medium,

$$AlOOH(cr) + 2H_2O(l) = Al(OH)_4^- + H^+ \qquad (1)$$

are determined to the ionic strengths up to 5 mol•kg^{-1} and to the temperatures up to 290 °C. In this work, the equilibrium quotients determined by Palmer et al.[5] are modeled to derive the Pitzer parameters to 250 °C for the Na^+—$Al(OH)_4^-$ interaction with the database, DATA0.YPF[8], by using EQ3/6 Version 8.0a[9, 10].

RESULTS

In Figure 1, equilibrium quotients referring to Reaction (1) as a function of ionic strength are displayed. The equilibrium quotients calculated by using the Pitzer parameters for the Na^+—$Al(OH)_4^-$ interaction are also shown. Figure 1 demonstrates that the calculated equilibrium quotients based on the derived Pitzer parameters for the Na^+—$Al(OH)_4^-$ interaction are in excellent agreement with the experimental values.

We are in the process of modeling solubilities of boehmite in various solutions including NaOH to 200 °C using the derived Pitzer parameters the Na^+—$Al(OH)_4^-$ interaction.

REFERENCES

1. Helgeson, H. C., 1969. Thermodynamics of hydrothermal systems at elevated temperatures and pressures: American Journal of Science, 267, 729–804.
2. Wolery, T.J., 1992. "EQ3NR, A Computer Program for Geochemical Aqueous Speciation-Solubility

Calculations: Theoretical Manual, User's Guide, and Related Documentation (Version7.0)". UCRL-MA-110662 PT III. Livermore CA: Lawrence Livermore National Laboratory.

3. Pitzer, K.S., 1991. Ion interaction approach: Theory and data correlation. In *Activity Coefficients in Electrolyte Solutions* 2nd edition. Edited by: Pitzer KS. Boca Raton, Florida, USA: CRC Press, pp. 75–153.

4. Wesolowski, D.J., 1992. Aluminum speciation and equilibrium in aqueous solution: I. The solubility of gibbsite in the system Na-K-Cl-OH-Al(OH)$_4$ from 0 ^{o}C to 100 ^{o}C. Geochimica et Cosmochimica Acta, 56, 1065–1091.

5. Palmer, D.A., Benezeth, P., Wesolowski, D.J., 2001. Aqueous high-temperature solubility studies. I. The solubility of boehmite as functions of ionic strength (to 5 molal, NaCl), temperature (100–290°C), and pH as determined by in situ measurements. Geochimica et Cosmochimica Acta, 65, 2081–2095.

6. Konigsberger, E., May, P.M., and Helfter, G., 2006. Comprehensive model of synthetic Bayer liquors. Part 3. Sodium aluminate solutions and the solubility of gibbsite and boehmite. Monatishefte fur Chemie, 137, 1139–1149.

7. Xiong, Y.-L., 2013. A thermodynamic model for silica and aluminum in alkaline solutions with high ionic strength at elevated temperatures up to 100 °C: Applications to zeolites. American Mineralogist, 98, 141−153.

8. Wolery, T.J., and R.L. Jarek. 2003. "Software User's Manual: EQ3/6, Version 8.0." Doc. No. 10813 UM-8.0-00. Albuquerque, NM: Sandia National Laboratories.

9. Wolery, T.J., Y.-L. Xiong, and J.J. Long. 2010. "Verification and Validation Plan/Validation Document for EQ3/6 Version 8.0a for Actinide Chemistry, Document Ver. 8.10." . ERMS 550239. Carlsbad, NM: Sandia National laboratories.

10. Xiong, Y.-L., 2011. "WIPP Verification and Validation Plan/Validation Document for EQ3/6 Version 8.0a for Actinide Chemistry, Rev. 1." ERMS 555358. Carlsbad, NM. Sandia National Laboratories.
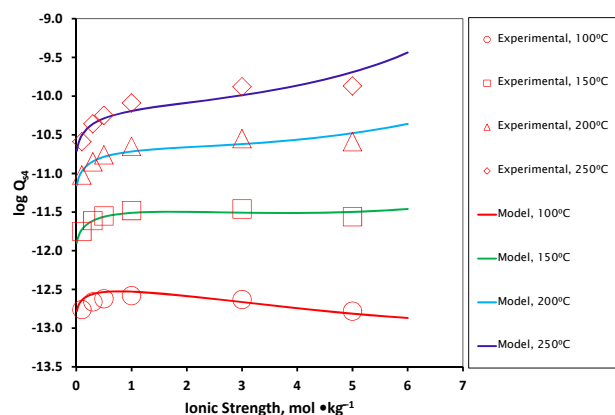
Figure 1. A plot showing equilibrium quotients for boehmite specified by Reaction (1) in the text as a function of ionic strength.

WIPP brine chemistry at high pC$_{H+}$

J.F. Lucchini, M. Borkowski, M.K. Richmann, J. S. Swanson, K. Simmons, D. Cleveland, and D.T. Reed

Los Alamos National Laboratory-Carlsbad Operations, 115 N. Main Street, Carlsbad, NM 88220, U.S.A.
Email: lucchini@lanl.gov

INTRODUCTION

Two synthetic brines that simulate the brine in and around the Waste Isolation Pilot Plant (WIPP) prior to waste emplacement were developed and have been used for WIPP laboratory studies since the initial WIPP Compliance Certification Application (CCA) [1].

These simulated brines are: 1) the Generic Weep Brine (GWB) that simulates intergranular (grain-boundary) brines from the Salado Formation at or near the stratigraphic horizon of the repository [2], and 2) the ERDA-6 (Energy Research and Development Administration Well 6) brine from the ERDA-6 well, typical of fluids in Castile Formation brine reservoirs below the WIPP [3]. These two brines bracket the expected compositional range in WIPP brine.

These brine formulations were shown to be stable only at a certain operational pH range [4]. In both brines, the higher pC$_{H+}$ value corresponded to a "cloud" point (precipitation point) where significant insoluble hydroxide phases were observed. Above these values, the brine composition effectively changed.

The goal of the work that is described herein was to investigate the effect of pC$_{H+}$ on WIPP simulated brines. A complete presentation of this work is given in [5].

DESCRIPTION OF THE WORK

GWB brine (100% saturated formulation - composition in Table 1) was stepwise titrated up to pC$_{H+}$ ~ 13 and the brine component concentrations were determined after 3-week equilibration. These experimental results were compared with the predicted composition of the brine from the current WIPP brine model [6].

RESULTS

The key results of this work were:

1) No changes were found in the concentrations of the main anions (Cl$^-$, SO$_4^{2-}$ and Br$^-$) up to pC$_{H+}$ 13, as it was predicted by the WIPP model.

Table 1: Composition of full strength GWB and ERDA-6 brines (100% saturated formulation) [2, 3].

Elements/Species	Concentrations (mol/L)	
	GWB	ERDA-6
Na$^+$	3.53E+00	4.87E+00
K$^+$	4.67E-01	9.70E-02
Mg^{2+}	1.02E+00	1.90E-02
Ca^{2+}	1.38E-02	1.20E-02
Li$^+$	4.48E-03	Not applicable
B$_4$O$_7^{2-}$	3.95E-02	1.58E-02
Cl$^-$	5.86E+00	4.80E+00
SO$_4^{2-}$	1.77E-01	1.70E-01
Br$^-$	2.66E-02	1.10E-02

2) A good agreement was found between the experimental data and the modeling results at pC$_{H+}$ ≤ 10.5 (including pC$_{H+}$ of interest to the WIPP, i.e. ~9.4), with the exception of tetraborate (Fig. 1). The WIPP model didn't predict a decrease of tetraborate concentrations to ~2×10^{-3}M between 10 and 10.5 (Fig. 1), because the corresponding Pitzer parameters do not exist.

3) Discrepancies between experimental and predicted data were noticed for Mg^{2+}, Ca^{2+} and tetraborate at pC$_{H+}$ ≥10.5 (Fig. 1 and 2). Specifically calcium precipitation is only observed experimentally at pC$_{H+}$ > 10.5 (Fig. 2); magnesium remains in solution above pC$_{H+}$ 10.5 in the experiments performed and does not precipitate to the extent predicted by the modeling (Fig. 1); and the tetraborate concentration goes through a minimum at pC$_{H+}$ 9.75 that is also not captured in the modeling results (Fig. 1). The experimental results were tentatively explained by precipitation of calcium carbonate (as it was observed in [7]) and resolubilization of some magnesium due to a change in the speciation of tetraborate at high pC$_{H+}$ [8], but these assumptions would need to be investigated further. However, these discrepancies occur above the expected pH range in the current WIPP Performance Assessment (PA).

4) GWB and ERDA-6 brines were confirmed as good "bracketing" brines for WIPP-relevant studies, as GWB brine transitions into ERDA-6 at pC$_{H+}$ ~10.5.
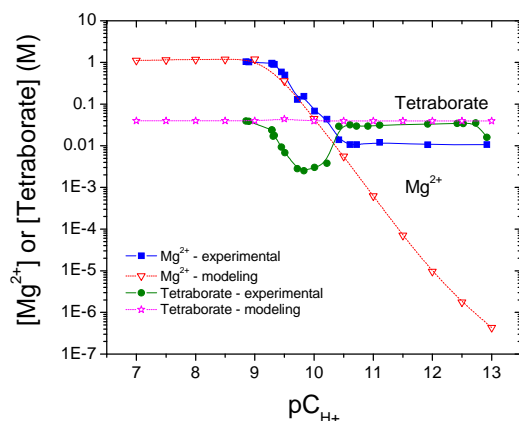
Fig. 1: Concentrations of tetraborate and Mg^{2+} in GWB 100% saturated brine as a function of pC_{H+}. Blue square symbols and green round symbols represent data on Mg^{2+} and tetraborate respectively that were measured experimentally by titration of the brine stepwise [5]. Red triangular symbols and pink star symbols are data on Mg^{2+} and tetraborate respectively that were obtained by modeling [6].
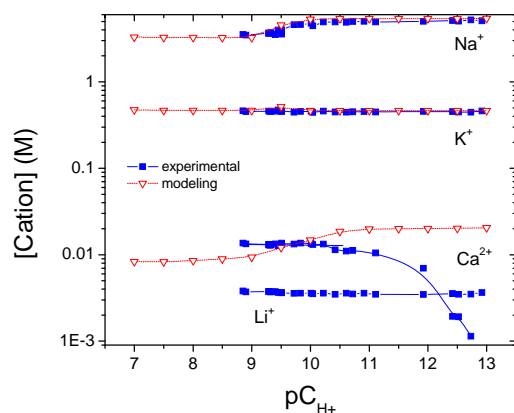
Fig. 2: Concentrations of Na^+, K^+, Ca^{2+} and Li^+ in GWB 100% saturated brine (respectively from the top to the bottom of the graph) as a function of pC_{H+}. Blue square symbols represent data measured experimentally by titration of the brine stepwise [5]. Red triangular symbols are data obtained by modeling [6]. Li^+ was not considered in the numerical simulation.

Based on these experimental data, the compositions of transitional WIPP brines in the pC_{H+} range 9 to 13 were established [5]. These transitional brines will be used for future WIPP-relevant studies.

Overall, this experimental investigation provided a confirmation of past modeling and experimental studies in the WIPP and established a better understanding of the actinide-relevant brine chemistry over a broad pC_{H+} range. The results support an improved understanding of the brine chemistry that defines the actinide solution concentrations used as a source term in brine-inundation scenarios addresses by WIPP PA and will be used as input to the WIPP Compliance Recertification Application (CRA) scheduled for 2014.

REFERENCES

1. U.S. Department of Energy (DOE), "Title 40 CFR Part 191 Compliance Certification Application for the Waste Isolation Pilot Plant (October)" 21vols. DOE/CAO 1996-2184. Carlsbad, NM: Carlsbad Field Office (1996).

2. SNIDER, A.C. "Verification of the Definition of Generic Weep Brine and the Development of a Recipe for this Brine." BOE 1.3.5.1.2. Sandia National Laboratories. Carlsbad, NM. (2003).

3. POPIELAK, R.S., et al. "Brine Reservoirs in the Castile Formation, Waste Isolation Pilot Plant (WIPP) Project, Southeastern New Mexico." TME-3153. ERMS 242085. Carlsbad, NM: U.S. Department of Energy (1983).

4. BORKOWSKI, M., et al. "Actinide (III) Solubility in WIPP Brine: Data Summary and Recommendations." LCO-ACP-08, LANL-CO\ACRSP Report. LA-14360, Los Alamos, NM: Los Alamos National Laboratory (2009).

5. LUCCHINI, J.-F., et al. "WIPP Actinide-Relevant Brine Chemistry". LCO-ACP-15, LANL\ACRSP Report. LA-UR 13-20620. Los Alamos: Los Alamos National Laboratory (2013).

6. BRUSH, L.H., et al. "Predictions of the Compositions of Standard WIPP Brines as a Function of pcH for Laboratory Studies of the Speciation and Solubilities of Actinides". Analysis report, June 23, 2011. Carlsbad, NM: Sandia National Laboratories (2011).

7. KERBER SCHUTZ, M., et al."Effect of Time on the Carbonation Reaction of Saline Aquifers with Controlled pH." *Energy Procedia*, **4**, 4546-51 (2011).

8. SCHWEITZER, G.K., et al. "Chapter 7: The Boron Group." *The Aqueous Chemistry of the Elements*. (pp. 150-154) Oxford University Press, USA, Oxford. (2010).

α-Radiolysis under alkaline conditions in 0.05 and 5.0 molar NaCl

A. Martínez-Torrents[1,2*], E. González-Robles[3], E. Bohnert[3], I. Casas[2], J. de Pablo[1,2], V. Metz[3]

[1] CTM Centre Tecnològic, Avda. Bases de Manresa 1, 08240 Manresa, Spain
[2]Department of Chemical Engineering, Universitat Politècnica de Catalunya, Avda. Diagonal 647, 08028 Barcelona, Spain
[3]Institute for Nuclear Waste Disposal, Karlsruhe Institute of Technology, Hermann-von-Helmholtz-Platz 1, 76344 Eggenstein-Leopoldshafen Germany

*albert.martinez@ctm.com.es

INTRODUCTION

Assessing the performance of spent nuclear fuel (SNF) in a deep geologic disposal system requires a process understanding of the stability of the fuel's UO_2 matrix in contact with aqueous solution potentially intruding into the repository. The corrosion behavior of the UO_2 fuel matrix and the consecutive radionuclide release are influenced by a variety of factors such as radionuclide inventory, resulting α/β/γ-dose rates, availability of oxidizing radiolytic products, and water composition. With respect to the dose rate, several studies focus on effects of α-radiation because any effects of β/γ-radiation will become insignificant after the first 1000 years [1]. The ionic strength of water in granitic, argillaceous and rock salt host formations is in the range of 0.01 mol/L to 15 mol/L [2,3]. In the near field of the waste containers, the pH may increase to medium or strongly alkaline conditions due to interactions of water with cementitious structural and sealing materials (e.g., Portland cement , Sorel cement).

Several works relate to the specific α-activity with the oxidative dissolution-rate and also to the surface-oxidation rate of UO_2 to UO_{2+x} [4 and references therein]. To our knowledge, only the studies carried out by Kelm et al., [5] and Kelm and Bohnert [6] dealt with α−radiolysis of concentrated salt solutions under alkaline conditions. Generally, α−radiolysis of aqueous solutions is accompanied by the formation of redox agents. Regarding the formation of primary radiolysis products, H_2 molecules are the main reductants in groundwater. On the other hand, the main oxidants are H_2O_2 molecules in aqueous solutions of low chloride concentration and OH^- and oxo-halogenides, such as HClO, in saturated NaCl solutions [7].

The enhancement of $UO_2(s)$ dissolution by α−radiolysis in 5.0 mol/L solution at pH 8 and 11 was studied by Kelm and Bohnert [6]. Previous studies on the effect of ionic strength and pH on $UO_2(s)$ dissolution in diluted solutions without irradiation were conducted by different research groups [8,9,10,11,12]. In these experiments, H_2O_2 was added to the system to simulate the main α−radiolysis product in diluted solutions. The radiolytic oxidation of UO_2 pellets doped with alpha-emitters([238/239]Pu) in diluted solutions was studied by Muzeau et al. [13] concluding that the main parameters

that affects radiolytic oxidation in their experiments are the sample α-activity and H_2 concentration.

DESCRIPTION OF THE WORK

A total of ten multisampling and single-point batch experiments were performed in parallel in a glove box under argon atmosphere (see Table 1). Two kind of experiments were carried out in glass vessels, those using $UO_2(s)$ pellets doped with 10% and 0.01% of [238]Pu in NaCl solutions (1a, 1b, 2a, 2b) and those using depleted $UO_2(s)$ pellets in NaCl solutions with dissolved [238]Pu (3a, 3b, 4a, 4b). Additionally, two experiments with depleted UO_2 pellets in NaCl solution (6a, 6b) were carried out as blanks to compare with the previous experiments.

Table 1: Summary of the experiments performed.

Experiment*	Solid	Pu in solution	NaCl
1a	$Pu_{0.10}U_{0.90}O_2$ [10%]	0	5 M
2a	$Pu_{0.001}U_{0.999}O_2$ [0.1%]	0	5 M
3a	Pellet UO_2 depleted	2.7 GBq/l	5 M
4a	Pellet UO_2 depleted	2.7 GBq/l	0.05 M
6a	Pellet UO_2 depleted	0	5 M
1b	$Pu_{0.10}U_{0.90}O_2$ [10%]	0	5 M
2b	$Pu_{0.001}U_{0.999}O_2$ [0.1%]	0	5 M
3b	Pellet UO_2 depleted	2.7 GBq/l	5 M
4b	Pellet UO_2 depleted	2.7 GBq/l	0.05 M
6b	Pellet UO_2 depleted	0	5 M

* a:Single point experiments; b:Multi-sample batch experiments.

Pretreatment of $UO_2(s)$ pellets

$UO_2(s)$ pellets were pretreated prior to the start of the experiments. The doped pellets were immersed in 0.001 M HCl to clean and eliminate possible impurities on the surface. In a second step, the pellets were immersed in a 1mM $NaHCO_3$ solution to ensure that the remaining oxidized layer was completely removed. Pellets with depleted $UO_2(s)$ were annealed at 1100° C under Ar/H_2 atmosphere.

Leachants

All solutions were prepared with ultrapure water (Milli Q, 18.2 MΩ·cm) under Ar atmosphere. The [238]Pu solution, with a specific activity of 2.7GBq/L, was prepared from 10.8 mg of PuO_2 (specific activity of

$6.3 \cdot 10^{11}$ Bq/g). The 5 M and 0.05 M NaCl solutions were prepared from recrystallized NaCl according to the procedure described by [7]. The pH of the experiments was adjusted to pHc = 12, using 0.01 M NaOH.

Analytical procedures

In the multi-sampling batch experiments (1b, 2b, 3b, 4b, 6b), the solution composition was continuously monitored. U and Pu concentrations were analyzed by ICP-MS (ELAN 6100, Perkin Elmer Inc, Waltham, USA) and α-spectroscopy (Canberra 74/01, Canberra Industries Inc, Meriden, USA), and H_2O_2 concentration was measured using a compact photomer PF-12 Macherey-Nagel. The ClO^- concentration in solution was measured by UV-visible spectrometry.

Single point batch experiments were equipped with gas sampling devices, similar to those previously used by Kelm and Bohnert [6]. In addition to solution composition, gas composition was determined by gas mass spectrometry (GAM400, In Process Instruments, Bremen, Germany).

RESULTS

H_2 and O_2 production by α-radiolysis.

As can be seen in Figures 1 and 2 the measured concentrations of rediolytic produced H_2 and O_2 in 5 M NaCl are in well agreement with those obtained by Kelm and Bohnert [6]. In the present study the lower dose range was determined in detail. Furthermore, in the experiments with 0.05 M NaCl the production of H_2 and O_2 is surprisingly similar to those obtained in experiments with an ionic strength of 5M NaCl (Fig. 1 and Fig.2).

H_2O_2 and ClO^- production by α-radiolysis.

In experiments 1a, 1b, 3a and 3b, ClO^- was detected. On the other hand, in experiments 2a, 2b, 6a, 6b, 4a and 4b the presence of ClO^- was not detected due to the low dose rate (2a, 2b, 6a, 6b) and the low Cl^- concentration (4a, 4b), respectively. However in experiments 4a and 4b the presence of H_2O_2 was observed. As expected, in high ionic strength solution mainly ClO^- is produced by α-radiolysis, meanwhile in solutions with a lower chloride concentration H_2O_2 is produced as main oxidative radiolysis product.

Uranium release.

The concentration of different U and Pu isotopes in solution was determined. The dissolved uranium concentration in experiment 3a and 3b is one order of magnitude higher than in experiment 4a and 4b. In these experimental series the uranium concentration is significantly higher than in the blank experiments (6a and 6b). Under the conditions of the present study, a faster U release at 5 M NaCl than at 0.05 M NaCl is observed.

Further studies are on-going to check the effect of ionic strength on α-radiolysis enhanced UO_2 corrosion.
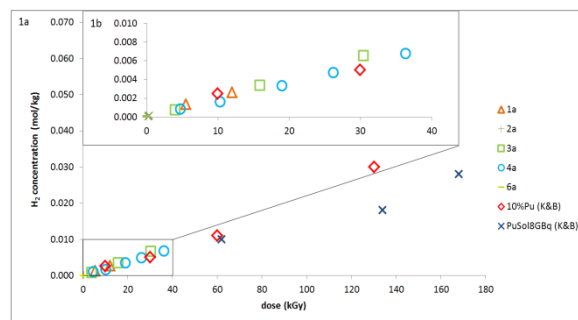
Figure 1: H_2 production. (K&B : Kelm and Bohnert [6]).
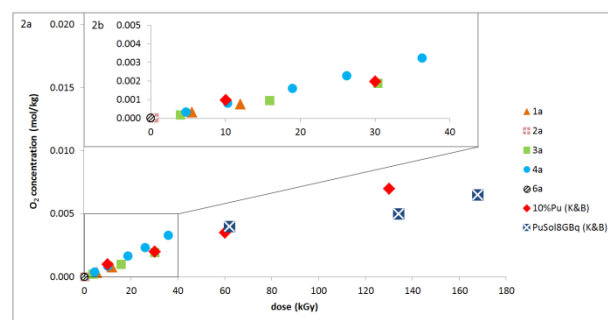
Figure 2: O_2 production. (K&B : Kelm and Bohnert [6]).

REFERENCES

[1] Metz, V. et al., *Radiochimica Acta*, **100**, 699-713 (2012).

[2] Carbol, P. et al., (Konings, R. J. M., ed.) Elsevier, Amsterdam, Netherlands (2012).

[3] Metz, V. et al., *Journal of Contaminant Hydrology*, **61**, 265-279. (2003).

[4] Eriksen, T.E. et al., *Journal of Nuclear Materials*, **420**, 403-423 (2012).

[5] Kelm, M. et al., *Applied Radiation and Isotopes*, **51**, 637-642 (1999).

[6] Kelm, M. and Bohnert, E., *Proc. Indian Acad. Sci. (Chem. Sci.)*, **114**: 697-704 (2002).

[7] Kelm, M. and Bohnert, E., *Forschungszentrum Karlsruhe Wissenschaftliche Berichte FZKA,* 6977, 60 (2004).

[8] Hossain, M. M. and Jonsson, M., Journal of Nuclear Materials, **372**, 190-193. (2008).

[9] Roth, O. et al., *Journal of Nuclear Materials,* **383**, 231-236 (2009).

[10] Giménez, J. et al., *Journal of Nuclear Materials*, **238**, 64-69. (1996).

[11] Clarens, F. et al., *Journal of Nuclear Materials*, **345**, 225-231 (2005).

[12] Casas, I. et al., Radiochimica Acta, **97**, 485-490 (2009).

[13] Muzeau, B. et al., *Journal of Alloys and Compounds,* **467**, 578-589.

Derivation of Pitzer Interaction Parameters for an Aqueous Species Pair of FeEDTA^{2-} and Na$^+$

Je-Hun Jang[1], Taya Olivas[1], and Martin Nemer[2]

[1]*Sandia National Laboratories*[*], *Defense Waste Management Programs, Org. 6212, 4100 National Parks Highway, Carlsbad NM 88220, U.S.A.*
email: jjang@sandia.gov
[2]*Sandia National Laboratories*[*], *Thermal and Fluid Sciences, Org. 1512, 1515 Eubank Blvd SE, Albuquerque, NM 87123, U.S,A.*

INTRODUCTION

The Waste Isolation Pilot Plant (WIPP) is a deep underground repository for the disposal of transuranic (TRU) radioactive waste developed by the U.S. Department of Energy (DOE). The WIPP is located within the bedded salts of the Permian Salado Formation, which consists of interbedded halite and anhydrite layers overlaying the Castile Formation. The waste includes, but is not limited to, the salts of ethylenediaminetetraacetic (EDTA) acid and iron.

To calculate the solution chemistry for brines of WIPP-relevance, WIPP PA employs the Pitzer formulation (1, 2) to determine the activity coefficients for aqueous species in the brines. However, the current WIPP thermodynamic database does not include iron species and their Pitzer parameters, although there will be a large amount of iron in the WIPP. Iron would be emplaced as part of the wastes, as well as the containers for the wastes.

The objective of this analysis is to derive the Pitzer binary interaction parameters for the pair of Na$^+$ and FeEDTA^{2-}.

DESCRIPTION OF THE WORK

Briefly, an aqueous model for dissolution of Fe(OH)$_2$(s) in mixed Na$_2$H$_2$EDTA and NaCl solution was fitted to the experimentally measured solubility data. All of the experiments were performed in the Geochemistry Laboratory in Carlsbad, NM. Anoxic gloveboxes were used to keep the oxygen level low. Fe(OH)$_2$(s) was synthesized in the glovebox, and its solubility was measured over a range of NaCl concentrations in the presence of Na$_2$H$_2$EDTA.

The aqueous model consists of several chemical reactions and related Pitzer interaction parameters (See Tables 1 and 2). The model is implemented within the aqueous speciation code EQ3/6 v.8.0a (3). Specifically, Pitzer binary interaction parameters for the Na$^+$ and FeEDTA^{2-} pair ($\beta^{(0)}$, $\beta^{(1)}$, and C$^\varphi$; Table 2) were fitted to the experimental data.

EQ3NR packaged in EQ3/6 v.8.0a was used to calculate the aqueous speciation and saturation index for a given number of EQ3NR input files. An input file represents one set of measurements from an individual experiment. To calculate the aqueous speciation and saturation index, EQ3NR refers to one of the databases for values of logK's (10-based logarithm of equilibrium constants for reactions) and Pitzer parameters. The saturation index indicates how far the system is from equilibrium with respect to the solid of interest, and can be calculated from the aqueous speciation. The value could be (i) zero if the system is saturated (equilibrated) with the solid of interest, (ii) positive if the system is supersaturated with the solid of interest, or (iii) negative if the system is undersaturated with the solid of interest. Thus, the smaller the sum of squared saturation indices that the aqueous model calculates for the given number of input files, the more closely the model attributes equilibrium to the individual experiment with respect to the solid of interest.

Hence, we seek $\beta^{(0)}$, $\beta^{(1)}$, and C$^\varphi$ (Table 2) that make the sum of squared saturation indices as small as possible. To do so, the calculation of aqueous speciation and saturation index was repeated by adjusting the $\beta^{(0)}$, $\beta^{(1)}$, and C$^\varphi$ in the database until the values of $\beta^{(0)}$, $\beta^{(1)}$, and C$^\varphi$ were found that make the sum of squared saturation indices the least for the given number of input files. The repetition was driven by a script written in the "Python" programming language, *EQ3CodeModule.py* (4).

Table 1: Reactions and 10-based logarithms of their equilibrium constants (logK's) used in this model fitting.

Reactions	logK
Aqueous reactions	
(1) H$^+$ + OH$^-$ = H$_2$O	13.99
(2) H$_4$EDTA(aq) = 4H$^+$ + EDTA$^{4-,\,a}$	-23.03
(3) H$_3$EDTA$^-$ = 3H$^+$ + EDTA^{4-}	-20.53
(4) H$_2$EDTA^{2-} = 2H$^+$ + EDTA^{4-}	-17.45
(5) HEDTA^{3-} = H$^+$ + EDTA^{4-}	-10.57
(6) FeOH$^+$ + H$^+$ = Fe^{2+} + H$_2$O	9.31
(7) FeEDTA^{2-} = Fe^{2+} + EDTA^{4-}	-16.1
Dissolution	
(8) Fe(OH)$_2$(s) + 2H$^+$ = Fe^{2+} + 2H$_2$O	12.95
(9) NaCl(s) = Na$^+$ + Cl$^-$	1.57

[a] EDTA^{4-}: C$_{10}$H$_{12}$O$_8$N$_2{}^{4-}$

Table 2: Pitzer interaction parameters used in this model fitting. Three Pitzer parameters for $FeEDTA^{2-}/Na^+$ pair ($\beta^{(0)}$, $\beta^{(1)}$, and C^{φ}) were fitted to the experimental data.

i	j	$\beta^{(0)}$	$\beta^{(1)}$	C^{φ}
Na^+	Cl^-	0.0765	0.2664	0.00127
Na^+	OH^-	0.0864	0.253	0.0044
Na^+	H_3EDTA^-	-0.2345	0.29	0.059
Na^+	H_2EDTA^{2-}	-0.1262	1.74	0.054
Na^+	$HEDTA^{3-}$	0.5458	5.22	-0.048
Na^+	$EDTA^{4-\ a}$	1.016	11.6	0.001
H^+	Cl^-	0.1775	0.2945	0.0008
Fe^{2+}	Cl^-	0.3359	1.5322	-0.00861
Na^+	$FeEDTA^{2-}$	TBD[b]	TBD[b]	TBD[b]

i	j	$\theta_{cc'}$ or $\theta_{aa'}$
Na^+	H^+	0.036
Na^+	Fe^{2+}	0.08
Cl^-	OH^-	-0.05

i	j	k	$\psi_{cc'a}$ or $\psi_{aa'c}$
Na^+	H^+	Cl^-	-0.004
Cl^-	OH^-	Na^+	-0.006

[a] $EDTA^{4-}$: $C_{10}H_{12}O_8N_2^{4-}$
[b] TBD: To Be Determined

RESULTS

The fitting results are summarized in Table 3 below.

Table 3: Fitting results for the $FeEDTA^{2-}/Na^+$ pair.

Pitzer parameters	value	Residual
$\beta^{(0)}$	-8.43	
$\beta^{(1)}$	52.49	0.854
C^{φ}	3.41	

    The values of saturation indices from 14 experiments are confined within a narrow range of -0.463 to 0.390 over the entire ionic strength investigated (Figure 1). This indicates that the aqueous model (Tables 1 and 2), including newly fitted $\beta^{(0)}$, $\beta^{(1)}$, and C^{φ}, predicts the equilibria with respect to $Fe(OH)_2$(s) for all of the 14 experiments very closely.
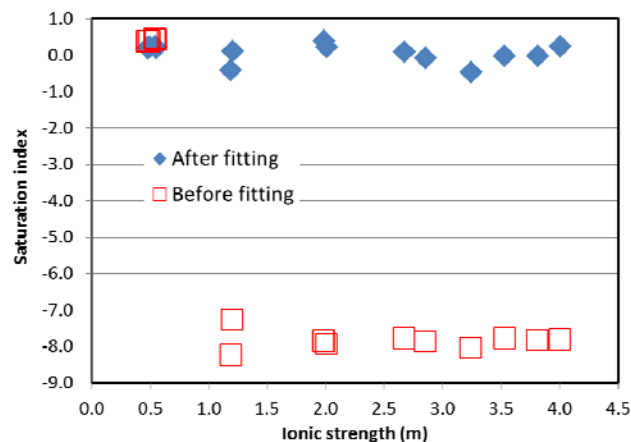
Fig. 1: Plot of saturation indices over ionic strength. Blue solid diamonds aligned around 0.0 (within a range of -0.463 to 0.390) represent the saturation indices calculated with fitting of the Pitzer interaction parameters for $Na^+/FeEDTA^{2-}$ pair to the experimental data. Red open squares represent the saturation indices calculated without considering Pitzer interaction for $Na^+/FeEDTA^{2-}$ pair.

REFERENCES

1. Pitzer, KS, "Ion Interaction Approach: Theory and Data Correlation", in Pitzer, K.S., ed. Activity Coefficients in Electrolyte Solutions, 2nd edition, Chapter 3, p. 75-153, CRC Press, Boca Raton, Florida. (1991)

2. Harvie, CE et al., "The Prediction of Mineral Solubilities in Natural Waters: The Na-K-Mg-Ca-H-Cl-SO4-OH-HCO3-CO3-CO2-H2O System to High Ionic Strength at 25 °C", *Geochimica et Cosmochimica Acta*, 48, 723-751 (1984)

3. Wolery, TJ et al., "Software User's Manual, EQ3/6", Version 8.0. 10813-UM-8.0-00. Albuquerque, NM: Sandia National Laboratories, ERMS 548926. (2003)

4. Kirchner, TB, "User's Manual for the EQ3CodeModule", Sandia National Laboratories, ERMS 557360 (2012)

ABC-Salt III Workshop

Monday, April 15th
Poster
Abstracts

This page intentionally left blank.

Anoxic Corrosion of Steel and Lead in Na-Cl±Mg Dominated Brine

Gregory T. Roselle

Sandia National Laboratories, 4100 National Parks Hwy, Carlsbad, NM 88220, USA
email: gtrosel@sandia.gov

INTRODUCTION

The Waste Isolation Pilot Plant (WIPP) is a deep geologic repository developed by the U.S. Department of Energy (DOE) for disposal of transuranic radioactive waste in bedded salt. The DOE demonstrates compliance with U.S. Environmental Protection Agency containment requirements by means of performance assessment (PA) for a regulatory period of 10,000 years post-closure.

In the PA, steel corrosion rates affect waste material degradation, influencing the long-term properties of the repository. Steel corrosion is a major H_2-generation process. Gas production due to corrosion affects room closure and chemistry. Microbially-produced CO_2 from cellulosic, plastic and rubber materials in the waste may acidify brine and increase actinide solubilities. Thus, the DOE emplaces MgO in the repository to buffer f_{CO2} and pH within ranges favoring lower actinide solubilities. Large quantities of steel and Pb present in the WIPP may also consume CO_2.

DESCRIPTION OF WORK

Experiments were conducted to assess the corrosion behavior of low-carbon steel and Pb under WIPP-relevant conditions. The experiments determined the metal corrosion rates and the nature of the corrosion products. An additional objective is to determine the extent that steel and Pb consume CO_2 via formation of carbonates or other phases, potentially supporting MgO in CO_2 sequestration.

In these experiments steel and Pb coupons are immersed in brines under WIPP-relevant conditions using a continuous gas flow-through system. The experimental apparatus maintains the following conditions: $O_2 < 5$ ppm; temperature of 26°C; relative humidity at 78%±10%; and a range of CO_2 concentrations (0, 350, 1500 and 3500 ppm, balance N_2). Four high-ionic-strength-brines are used: GWB, a Na-Mg-Cl dominated brine; ERDA-6, a predominately Na-Cl brine; GWB with organic ligands (EDTA, acetate, citrate, and oxalate); and ERDA-6 with the same ligands.

RESULTS

Results from multiyear experiments are presented. Steel coupons show formation of several phases dependent on P_{CO2}. SEM analysis with EDS shows the presence of a green Fe (±Mg)-chlori-hydroxide phase at $CO_2 <1500$ ppm. At higher CO_2 the dominant corrosion product is a Fe-Mg-Ca hydroxicarbonate phase. Lead coupons show no corrosion products at lower CO_2 but formation of Pb-Ca hydroxicarbonate phase at $CO_2 > 350$ ppm. Multiple cleaning cycles were used to remove corrosion products from coupons, which were weighed to determine corrosive mass loss. These data are used to calculate corrosion rates for each experiment. The data show steel corrosion rates are a strong function of P_{CO2} for all brine types. ERDA-6 brines appear to be more corrosive than GWB brines. Steel corrosion rates vary from 0.14±0.07 μm/yr at 0 ppm CO_2 to 0.95±0.26 μm/yr at 3500 ppm CO_2. Corrosion rates for Pb coupons show no consistent trend as a function of P_{CO2} or brine type. Lead corrosion rates range from 0.24±0.18 to 0.54±0.45 μm/yr.

ACKNOWLEDGEMENT

This page intentionally left blank.

Br Distribution between Halite and Parent Brine as an Example for a Natural Analogue for the Incorporation of Radiogenic Components in Evaporites

Michael Schramm

[1]*Federal Institute for Geosciences and Natural Resources (BGR), Stilleweg 2, 30655 Hannover, Germany*
email: michael.schramm@bgr.de

INTRODUCTION

The behaviour of Br during evaporation of seawater is a well understood process, especially the distribution of Br between brine and precipitating chlorine minerals. Br is incorporated in successive precipitating chlorine minerals like halite. During this process Br replaces the Cl position in the crystal lattice representing an extreme form of a solid solution system.

Based on this knowledge, Br can be used as a natural analogue for the incorporation of radiogenic components in evaporite minerals.

As shown in previous publications for example by SIEMANN & SCHRAMM (2002), experimental studies have demonstrated that the distribution coefficient (D_{Br}) is not a constant. D_{Br} shifts from higher values in low concentrated solutions to lower D_{Br} values in higher concentrated brines of a single system (NaCl-NaBr) as for example in evaporating seawater. Therefore it is necessary to use a thermodynamic approach to calculate the trace element distribution between solution and precipitate.

Different solid solution models (for example SAXENA 1973) have been used in order to describe the Br distribution between brine and precipitating halite, whereas the trace element solid solution model is the most satisfying model (SIEMANN & SCHRAMM 2000). Based on the fact that the distribution coefficient is dynamic, because it depends on the chemical composition of the brine, only thermodynamic modeling is the consequent approach to solve this problem.

DESCRIPTION OF THE INVESTIGATIONS

Based on experimental data of the NaCl-NaBr system, thermodynamic data have been developed (SIEMANN & SCHRAMM (2000). Afterwards the thermodynamic data of this single system have been fitted using the trace element solid solution model by modifying the exchange parameters (p1, p2 and p3). Moreover, including these exchange parameters the more complex seawater evaporation and its Br distribution was modeled with EQ3/6 in the version 7.2c (WOLERY 1992).

RESULTS

The distribution of Br between precipitating halite and the equilibrium solution in the system NaCl-NaBr was intensively studied for example by BRAITSCH & HERRMANN (1963). They concluded that the distribution coefficient (b_{Br} or D_{Br} = wt.% Br in halite / wt.% Br in solution) is about 0.14. Investigations related to evaporating seawater under laboratory conditions (BRAITSCH 1962) and to a salt study in the Adriatic Sea (HERRMANN et al. 1973, HERRMANN 1980) demonstrated that at least the distribution coefficient varies. In the beginning of the seawater evaporation a value of about 0.14 was observed, and the value decreases over 0.10 to 0.07 in higher concentrated brines. Studies of fluid inclusions have shown a decrease of the distribution coefficient to 0.04 at high Mg concentrations.

The investigations by SIEMANN & SCHRAMM (2000, 2002) have shown that the variation of the distribution coefficient depends on the geochemical composition of the solution, mainly on the concentration of Br but also on the concentration of Mg, K, Ca, Sr, Rb and Li. Together with other components in the brine they have influence on the activity of Na, Cl and Br. This complex geochemical situation in the solution as well as in the solid solution (mixed crystal) can't be calculated with a fixed Br distribution coefficient because of its variability.

Another approach is the thermodynamic calculation with the help of EQ3/6 which enables the calculation of trace component distribution in sense of an extreme form of solid solution.

The experimental studies of SIEMANN & SCHRAMM (2002) demonstrate a wide range of Br concentration in the solution and precipitating halites, reflecting also a spot of a Br content between 0.0015 wt. % up to 0.7 wt.% in the brine. This concentration range represents in the lower values a refreshment / recycling or metamorphic process during sedimentation or a post-sedimentary phase. At about 0.054 wt. % Br in evaporating seawater, the first halite precipitates with a Br concentration of about 0.0075 wt. % (BRAITSCH 1962). The EQ3/6 modeling shows a good correlation with this initial Br value for the first precipitating halite. The further evaporating seawater and the increasing Br content at about 0.18 wt. % corresponds with the precipitation of polyhalite. The Br content in the paragenetic halite should be 0.018 wt. %. The results of

the EQ3/6 modeling demonstrate values nearby 0.018 wt. % Br in the halite. During progressive evaporation, the seawater saturates with respect to carnallite at the invariant point R in the Jänecke-Diagram. The modeling of the Br concentration in the brine and the corresponding halite will be demonstrated in more details.

REFERENCES

1. BRAITSCH O. "Entstehung und Stoffbestand der Salzlagerstätten". *Mineralogie und Petrographie in Einzeldarstellungen* (eds T. H. W. von Engelhardt und J. Zehmann); **3. Band**; 232 p. (1962)

2. BRAITSCH O. & HERRMANN A. G. "Zur Geochemie des Broms in salinaren Sedimenten. Teil 1: Experimentelle Bestimmung der Br-Verteilung in verschiedenen natürlichen Systemen". *Geochim. Cosmochim. Acta* **27**, 361-391 (1963)

3. SAXENA S. K. "Thermodynamics of rock-forming crystalline solution" In *Minerals, Rocks and Inorganic Materials* (eds. T. H. W. von Engelhardt, R. Roy, P. J. Wyllie), **8**, 188 p. (1973)

4. SIEMANN M. G. & SCHRAMM M. "Thermodynamic modeling of the Br partition between aqueous solutions and halite". *Geochim. Cosmochim. Acta.* **64**, 1681-1693 (2000)

5. SIEMANN M. G. & SCHRAMM M. "Henry's and non-Henry's law behavior of Br in simple marine systems." *Geochim. Cosmochim. Acta.* **66**, 1387-1399 (2002)

6. WOLERY T. J. "EQ3/6 software package, version 7.2c". Lawrence Livermore National Laboratory, Livermore, USA (1992)

C-14 as Carbon Dioxide and Saline Solutions of a HLW Repository

Guido Bracke

Department of Final Disposal, GRS mbH, Schwertnergasse 1, 50667 Cologne, Germany
email: guido.bracke@grs.de

INTRODUCTION

The modelling results on radiation exposure in a long term safety assessment of high level radioactive waste disposal can be strongly increased when applying conservative assumptions and omitting chemical processes. C-14 represents such an example when assuming its instantaneous and gaseous release as carbon dioxide or methane. Chemical processes leading to retention are neglected and unrealistic high radiation exposure may be modelled. Recently, the Henry coefficient was used in TOUGH2 [1] to model the 2-phase transport and dissolution of carbon dioxide in salt grit [2].

Alternative approaches have to be tested to improve the modelling capabilities of THM codes beyond the application of Henry coefficients.

A very recent release of PHREEQC 3.0 (March 21th, 2013) [3] can use the Pitzer aqueous model for high-salinity waters that are beyond the range of application of the Debye-Hückel theory. PHREEQC 3.0 is improved for calculating the solubility of gases at high pressure.

DESCRIPTION OF THE WORK

The planned work will apply PHREEQC 3.0 to investigate the retention of C-14 as carbon dioxide species in saline solutions. Also barrier materials which are applied typically in a salt repository for high level waste will be tested for their chemical interactions.

Since the practical experience with this code is quite limited in our institution simple cases will be investigated in the beginning.

RESULTS

There are presently no results available using PHREEQC 3.0.

A recent preliminary safety assessment [4] models a significant fraction of C-14 penetrating at less than 100 years through a seal (Fig. 1), when C-14 is released instantaneously as carbon dioxide. This is a fast transport resulting in a hypothetical radiation exposure. This seems unrealistic considering chemical reactions such as dissolution and precipitation of carbonates.
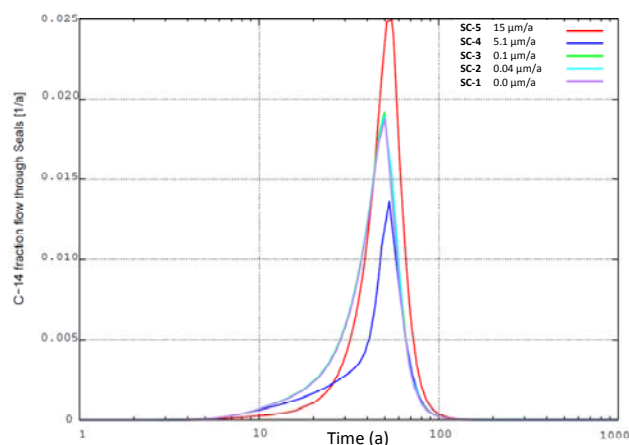
Fig. 1: Release of gaseous C-14 from structural parts for different corrosion rates [2].

REFERENCES

1. Pruess K., TOUGH2: A general purpose numerical simulator for multiphase fluid flow, 1990, Lawrence Berkeley National Laboratory, University of California: Berkeley, California, USA.
2. Larue J., Baltes B., Fischer H., Frieling G., Kock I., Navarro M., Seher H., Radiologische Konsequenzenanalyse, Bericht zum Arbeitspaket 10, GRS-289, ISBN 978-3-939355-65-6, in preparation.
3. Parkhurst D.L., and Appelo C.A.J., 2013, Description of input and examples for PHREEQC version 3—A computer program for speciation, batch-reaction, one-dimensional transport, and inverse geochemical calculations: U.S. Geological Survey Techniques and Methods, book 6, chap. A43, 497 p., available only at http://pubs.usgs.gov/tm/06/a43/.
4. Bracke G., and K. Fischer-Appelt K., "Overview on the Preliminary Safety Analysis of the Gorleben Site", WM2013 Conference, Phoenix, Arizona, USA, Feb. 24 -28, 2013, paper no. 13298.

- 48 -

This page intentionally left blank.

Microbial Diversity Associated with Halite within the Waste Isolation Pilot Plant

Juliet S. Swanson and Karen A. Simmons

Los Alamos National Laboratory—Carlsbad Operations
1400 University Drive/Carlsbad, NM 88220 USA
email: jsswanson@lanl.gov

INTRODUCTION

Microbial activity is considered by many to have potentially deleterious effects on nuclear waste repositories. Due to insufficient knowledge about the microbial communities indigenous to the Waste Isolation Pilot Plant (WIPP) at the time of its inception, those same effects were attributed to these organisms as well. However, significant differences exist between the communities present in low- and high-ionic strength matrices.

Studies have been underway to gain a better understanding of the microbial ecology at the WIPP and the potential effects of microbial activity on the waste therein. Results suggest that the halophilic microorganisms detected in the WIPP will play a much smaller role than that predicted by performance models, thereby supporting the level of conservativism built into the WIPP model. Whether or not these findings will extend to other salt-based repositories needs further investigation.

METHODS

Halite was collected from the WIPP underground and processed without prior sterilization. Halite was used as an inoculum in a generic growth medium designed to enrich for moderately to extremely halophilic organisms. DNA was extracted from these incubations after growth was observed and also directly from raw halite. Small subunit ribosomal DNA from both prokaryotes and eukaryotes was amplified using PCR, cloned, and sequenced.

RESULTS

The microbial ecology within the WIPP repository is limited to halotolerant and halophilic organisms. Haloarchaea (*Halobacterium*, *Halorubrum*, *Natronomonas*, *Halolamina*, unclassified) dominated cultures enriched under high-salt conditions and were found in both pure and argillaceous halite samples. These cultures have been shown to survive in generic growth media, as well as more stringent WIPP brines. Halophilic and halotolerant bacteria and fungi (*Chromohalobacter*, *Nesterenkonia*, *Salinicoccus*; *Cladosporium*,

Engyodontium, *Phoma*) dominated cultures enriched at lower salt concentrations, although some species survived higher concentrations as well. Additional bacterial DNA sequences were detected, but those organisms were not isolated (*Enterobacter, Nevskia, Caulobacter, Pelomonas, Limnobacter*). It is probable that their DNA was preserved although no viable cells were present or that culture conditions were inadequate for their growth. Fungal species were likely introduced from the mine surface on equipment and personnel or via the air-intake shaft.
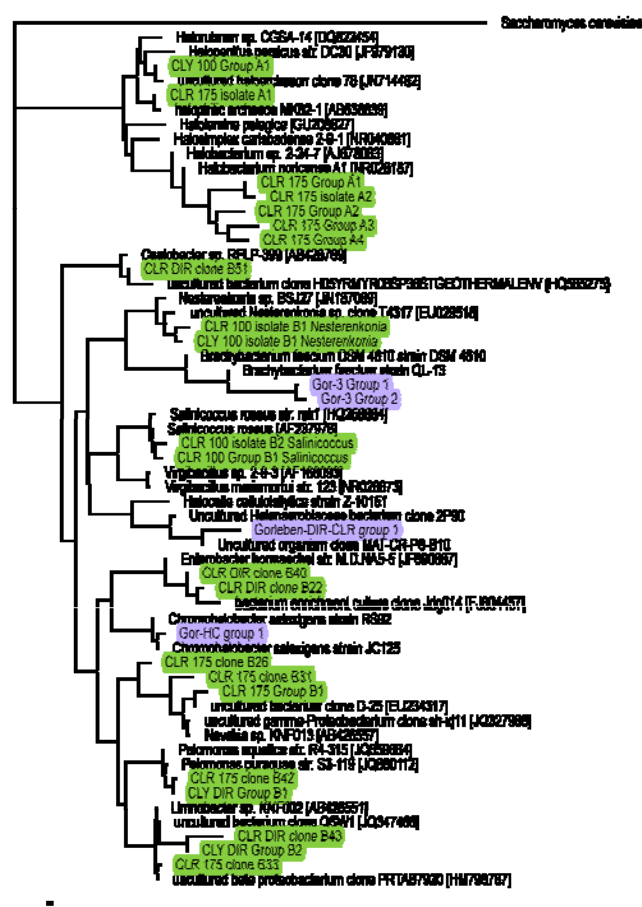

Fig. 1: Phylogenetic tree showing archaeal and bacterial sequences associated with halite, in addition to sequences from halite isolates. Also included are sequences from Gorleben samples enriched in similar media.

Although the haloarchaea are the most adapted to survival at the ionic strength expected in the repository, they are the least capable of utilizing the more complex organic substrates present in the waste (e.g. cellulosics). While some haloarchaea ferment small organics (e.g. amino acids) or reduce nitrate, they are essentially limited to aerobic metabolism [1, 2]. These organisms may function during the repository's oxic phase and degrade organic complexing agents in the waste. Still, the longevity of these organisms in halite crystals is well established; therefore, they are likely to be present throughout repository history [4].
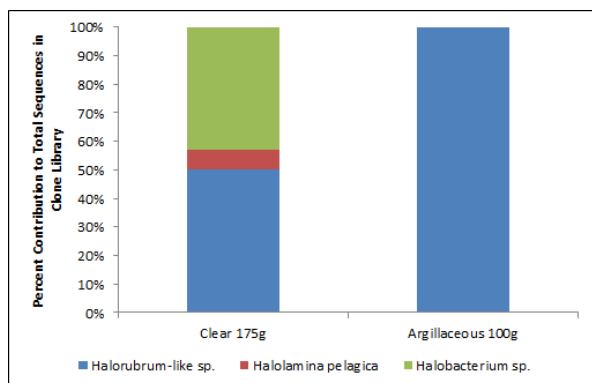

Fig. 2: Archaeal genus distribution within clone libraries of clear and argillaceous halite from the WIPP.

Bacteria detected within the WIPP range from moderately (*Nesterenkonia*, *Salinicoccus*) to extremely halophilic (*Chromohalobacter*). *Nesterenkonia* and *Salinicoccus* spp. exhibit cellulase activity, and *Salinicoccus* and *Chromohalobacter* spp. are capable of citrate utilization [5-7]. However, none have been shown to survive long in WIPP brines and all are aerobic, suggesting their roles will also be limited to the early oxic phase. A *Chromohalobacter* sp. was also detected in enrichment cultures of hydrocarbon-bearing Gorleben halite and has been previously shown to degrade some HCs, suggesting it may play a role in HC transformation during this repository's oxic phase [8].

Two of the fungal isolates, *Cladosporium* and *Phoma*, were found to be cellulolytic and, should they come into contact with waste, may be able to hydrolyze cellulose to smaller compounds for resident *Bacteria*. Still, they are also obligate aerobes whose growth will be limited.

In conclusion, the impact of microbial activity on the WIPP is expected to be far less than that predicted by the performance model, based on limited microbial metabolic capability and survival in WIPP brines, thus affirming the model's conservativism. The extension of this implication to other salt-based repositories is contingent upon their waste contents and expected repository conditions and should be an area of ongoing research. Continued efforts are focused on anaerobic enrichments of halite and the degradation of cellulosics by indigenous organisms.
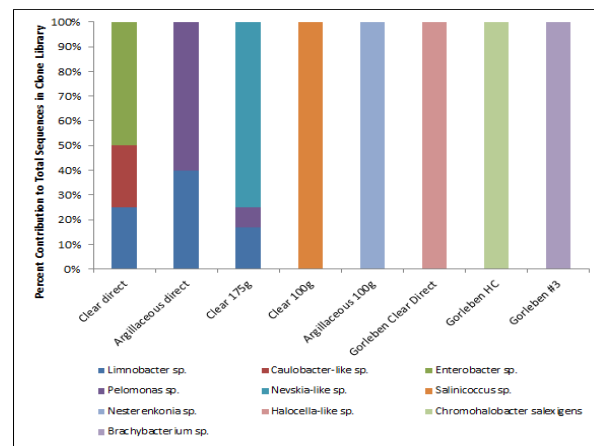
Fig 3: Bacterial genus distribution within clone libraries of clear and argillaceous halite from the WIPP and incubations of Gorleben halite.

REFERENCES

1. OREN A. "The Order Halobacteriales". In *The Prokaryotes*, vol 4, 3rd ed. (2006).
2. OREN A., "Thermodynamic limits to microbial life at high salt concentrations" *Environmental Microbiology*, **13**, 1908-1923 (2011).
3. GUNDE-CIMERMAN N. et al., "Halotolerant and halophilic fungi" *Mycological Research*, **113**, 1231-1241 (2009).
4. MORMILE, M.R. et al., "Isolation of Halobacterium salinarum retrieved directly from halite brine inclusions" *Environmental Microbiology*, **5**, 1094-1102 (2003).
5. ROHBAN, R. et al., "Screening and isolation of halophilic bacteria producing extracellular hydrolyses from Howz Soltan Lake, Iran" *Journal of Industrial Microbiology & Biotechnology*, **36**, 333-340 (2009).
6. VENTOSA, A. et al., "*Salinicoccus roseus* gen. nov., sp. nov., a new moderately halophilic Gram-positive coccus" *Systematic and Applied Microbiology*, **13**, 29-33 (1990).
7. KIM, D. et al., "Molecular cloning and functional characterization of the genes encoding benzoate and p-hydroxybenzoate degradation by the halophilic *Chromohalobacter* sp. strain HS-2" *FEMS Microbiology Letters*, **280**, 235-241 (2008).

Comparison of Bacterial Populations Enriched from Briny Groundwaters of Different Ionic Strengths under a Variety of Incubation Conditions

Karen A. Simmons, Juliet S. Swanson
LA-UR-13-22594
Los Alamos National Laboratory—Carlsbad Operations
1400 University Drive, Carlsbad, NM 88220 USA
ksimmons@lanl.gov

INTRODUCTION

The Waste Isolation Pilot Plant (WIPP) is located within the salt evaporite Salado Formation in southeastern New Mexico. Overlying the Salado Formation is the Culebra Member, a fractured, dolomitic layer bearing saline to brackish water. In the event of a breach into the WIPP horizon, the Culebra is considered to be the most likely pathway for actinide migration from the repository. Thus, it is important to understand the potential for microbial influence on WIPP waste in this far-field environment.

There is considerable variety within the Culebra in terms of ionic strength and constituents in the water. Diverse functional groups of bacteria have previously been observed along salinity gradients, suggesting that there could be considerable variety within the microorganisms inhabiting the different environments in the Culebra as well. The goal of this study was to see how bacterial structural and functional diversity varied between groundwaters taken from two areas of the Culebra with significantly different ionic strengths.

METHODS

Water was sampled from two monitoring wells (W1 and W3) approximately 1.5 miles apart which had a depth difference of about 140 feet. The water from these wells varied considerably in terms of overall ionic strength (1.5 M vs. 3.7 M), especially in terms of magnesium, chloride, and sulfate content (Figure 1).

Parameter	W1	W3	Units
Sampling depth	737	879	feet
pH	7.2	6.8	SU
TOC	0.39*	0.16*	mg/L
Overall ionic strength	1.5	3.7	M
Na^+	346.2	3483	mM
Mg^{2+}	49.78	108.5	mM
K^+	14.14	44.49	mM
B^+	0.955	4.483	mM
Cl^-	1000	3367	mM
SO_4^{2-}	46.48	73.36	mM
Br^-	0.372	0.852	mM

*Indicates value near instrument's limit of detection

Fig. 1: Higher ionic strength and concentration of constituents in W3 water as compared to W1 water

Organisms were enriched under aerobic (Aer), transitional (aerobic → anaerobic; Tr), nitrate-reducing (NR), iron-reducing (IR), and sulfate-reducing (SR) conditions. Bacterial clone libraries were constructed from these enrichments as well as from direct DNA extracts and used to compare the resulting populations under each condition for each groundwater.

RESULTS

Bacterial diversity was much higher in the low-ionic strength groundwater (W1) cultures than in the high-ionic strength cultures (W3) (Figures 2 & 3). This reflects the increase in stress imposed by high salt concentrations and the selection for groups better able to survive.
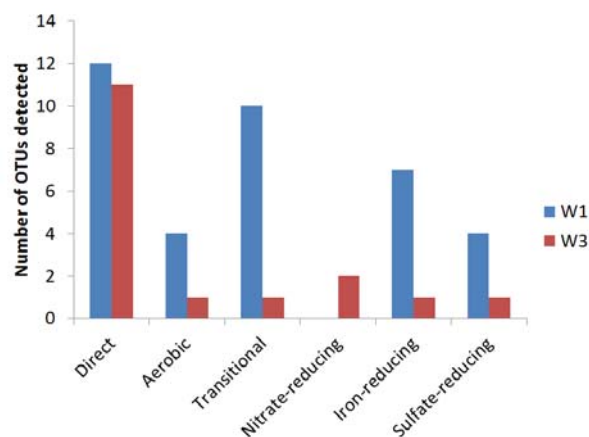

Fig. 2: Higher diversity in W1 as compared to W3, as demonstrated by number of operational taxonomic units (OTUs) detected
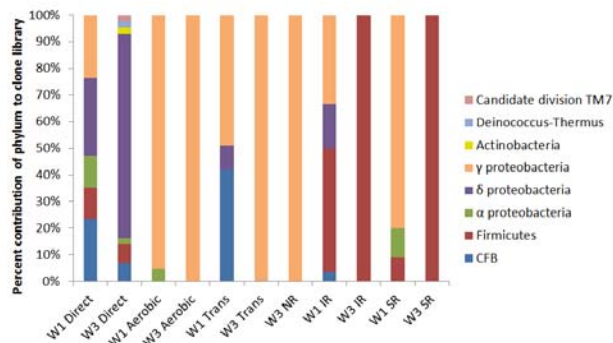

Fig. 3: Comparison of diversity in W1 and W3 through phylum contribution to clone libraries

The direct DNA extract from W1 comprised five phyla—*Cytophaga-Flavobacteria-Bacteroides* (CFB), *Firmicutes*, and α, δ, and γ *Proteobacteria*—all of which were represented in the enrichment cultures. In contrast, the direct DNA extract from W3 comprised seven phyla—CFB, *Firmicutes*, α and δ *Proteobacteria*, *Actinobacteria*, *Deinococcus-Thermus*, and Candidate division TM7; however, enrichment cultures contained only two of these seven (*Firmicutes* and γ *Proteobacteria*). This may reflect culture bias or the detection of DNA preserved at high salt concentrations.

Diversity within each incubation was low (maximum 4 phyla detected), and some incubations yielded monocultures. Aerobic incubations were limited to α and γ *Proteobacteria* while *Firmicutes* dominated anaerobic incubations. Only three OTUs (a *Haloanaerobium* species, a *Cytophaga*-like species, and an *Enterobacter* species) were shared between both groundwaters.

Despite the low structural diversity, the inferred metabolic diversity spans the range of aerobic and anaerobic respiration and fermentation. Although both groundwaters contained no detectable nitrate, nitrate reducers (e.g. *Arhodomonas* sp.) were present in the W3 incubations but not detected in W1.

Both iron and sulfate reducers were detected in W1 IR incubations after metal sulfide precipitates were observed. These precipitates contained both oxidized and reduced iron, suggesting that sulfide complexation may help remove actinides from solution, regardless of oxidation state. The reduction of iron in the W1 IR incubations was likely due to both direct and indirect processes, as both metal and sulfate reducers were detected. In contrast, iron reduction in the W3 IR likely occurred through the creation of a reduced environment by fermentation. This is supported by the presence of a large proportion of *Firmicutes* (e.g. *Clostridium* and *Halanaerobium* spp.) and the fact that lactate, a substrate commonly utilized by *Firmicutes*, was present in the culture media.

The high-ionic strength SR incubation consisted of a single OTU whose closest match was *Halocella cellulolytica*, a halophilic, obligate anaerobe which is capable of cellulose degradation. It is currently unknown if the microorganisms enriched in this incubation will be able to degrade cellulose, but it is potentially significant considering the expected inventory of cellulose in the WIPP.

In summary, higher ionic strength led to a decrease in microbial structural diversity and a shift in metabolic potential. This latter finding, in part, reflects the high energetic cost of survival in hypersaline environments and the ability of limited groups of bacteria, such as *Halanaerobiales*, to function there.

In spite of the considerable differences between the groundwaters, the microorganisms detected in each may play an important role in mitigating actinide migration through the Culebra, should this aquifer be breached.

REFERENCES

1. OREN, A. "The Order Haloanaerobiales" *The Prokaryotes, vol. 4, 3rd ed.*, **3**, 113-164 (2006).
2. OREN, A. "Thermodynamic limits to microbial life at high salt concentrations" *Environmental Microbiology*, **13(8)**, 1908-1923 (2011).
3. SIMANKOVA, M.V. et al., "*Halocella cellulolytica* gen. nov., sp. nov., a new obligately anaerobic, halophilic, cellulolytic bacterium" *Systematic and Applied Microbiology*, **16**, 385-389 (1993).

Complexation of Np(IV) with Gluconate in Dilute to Concentrated CaCl2 Solutions: Solubility and NMR Studies

X. Gaona[1], C. Adam[1], H. Rojo[1,2], M. Böttle[1], P. Kaden[1], M. Altmaier[1]

[1] *Karlsruhe Institute of Technology, Institute for Nuclear Waste Disposal (KIT–INE), Germany*
xavier.gaona@kit.edu
[2] *Paul Scherrer Institut, Laboratory for Waste Disposal (PSI–LES), Switzerland*

INTRODUCTION

Neptunium is a relevant actinide in performance assessment calculations (PA) on the long–term safety of nuclear waste repositories because of its long half–life ($t_{1/2} = 2.14 \times 10^6$ years), radiotoxicity and redox sensitivity. Under the reducing conditions expected for a deep underground repository, neptunium is expected to predominantly form Np(IV) species [1].

Radionuclide sorption and solubility in cementitious and saline systems can be affected by the presence of organic ligands. Gluconic acid (GLU, $C_6H_{12}O_7$) is a poly–hydroxocarboxylic acid expected in repositories for low and intermediate–level radioactive waste (LILW) as component of cementitious materials. GLU is also considered a close analogue of iso-saccharinic acid (ISA), a polyhydroxy carboxylic ligand resulting from the degradation of cellulose under alkaline conditions. The formation of very stable An(IV)–GLU/ISA complexes has been reported in literature. The stability of these complexes can be further increased in the presence of Ca^{2+} due to the formation of ternary Ca–An(IV)-GLU/ISA complexes [2, 3]. To the date, all studies available in literature have focused on low ionic strengths and low Ca^{2+} concentrations. In CaCl2–rich brines, which can be generated by the corrosion of cementitious waste forms in certain MgCl2 dominated saline systems, highly stable binary Ca–GLU/ISA complexes may outcompete the formation of ternary Ca–An(IV)–GLU/ISA complexes.

This study aims at obtaining a complete thermodynamic description of (a) the binary system Ca-GLU, including solubility and complex formation in dilute to concentrated CaCl2 solutions and (b) the ternary system Ca–An(IV)–GLU. The accurate knowledge of $[GLU^-]_{free}$ and $[Ca^{2+}]_{free}$ in solution is required as input parameters in the thermodynamic modeling of (b). This can only be achieved provided the availability of $\log *K°_{s,0}$, $\log *\beta°$ and corresponding ion interaction parameters (SIT, Pitzer) for the solids and aqueous species forming within the binary system Ca-GLU.

DESCRIPTION OF THE WORK

All samples were prepared and stored in inert gas (Ar) gloveboxes under exclusion of oxygen and CO2. A combination glass pH electrode (type ROSS, Orion), calibrated against dilute standard pH buffers (Merck) was used to determine the molal H^+ concentration, m_{H+} (with $pH_m = -\log m_{H+}$). In salt solutions of ionic strength $I \geq 0.1$ mol·kg^{-1}, the measured pH value (pH_{exp}) is an operational apparent value related to m_{H+} by $pH_m = pH_{exp} + A_m$, where A_m is given as function of the NaCl or CaCl2 concentration [4].

The solubility of Ca(GLU)2(s) was investigated within $8 \leq pH_m \leq 12$ following $[Ca]_{tot}$ (ICP-OES) and $[GLU]_{tot}$ (as TOC), and complemented with ^{13}C–NMR measurements of the supernatant solution. The aqueous complexation of calcium with GLU was further studied by ^{13}C–NMR in the absence of solid phase with $[GLU] = 0.02$ M, $pH_m = 10$ and varying $[Ca]_{tot}$. In both approaches, dilute to concentrated NaCl (0.1–5.0 M) and CaCl2 (0.25–4.5 M) solutions were used as background electrolytes. NMR measurements were performed on a Bruker Avance III 400 spectrometer operating at 100.63 MHz for ^{13}C and equipped with a broadband observe probe head (BBFO).

Np(IV) was obtained by chemical reduction of a $^{237}Np(V)$ stock solution with 0.05 M Na2S2O4 at pH= 8, and quantitatively precipitated at $pH_m = 12$ as NpO2(am,hyd). The resulting solid phase was divided in different series (~2 mg ^{237}Np per batch experiment) with 0.1–3.5 M CaCl2 as background electrolyte at $10^{-6} \leq [GLU]_{tot} \leq 10^{-2}$ M and $9 \leq pH_m \leq 12$. The aqueous concentration of Np was measured after 10 kD ultrafiltration (Pall Life Sciences) by LSC. Aliquots for LSC analysis were mixed with 10 mL of LSC–cocktail Ultima Gold XR (Perkin–Elmer), resulting in a detection limit of ~5×10^{-9} M for ^{237}Np (α–radiation measured after α/β–discrimination of the counts from the daughter nuclide ^{233}Pa).

RESULTS

^{13}C–NMR revealed clear shifts of C1–C3 resonance signal positions of gluconate with increasing $[Ca]_{tot}$ (see Figure 1). The observed shifts are consistent with the single formation of CaGLU$^+$ in both NaCl and CaCl2 solutions with $[Ca]_{tot} \leq 0.5$ M. The stability of this complex decreases significantly with increasing ionic strength, consistently with previous observations available

in the literature [5]. Above $[Ca]_{tot} = 0.5$ M, the strong shift in C4 hints towards the formation of a new species, likely a cyclic Ca-GLU structure with certain similarities to the lactone-ring reported to form under acidic conditions. $Ca(GLU)_2(s)$ sets very high solubilities in both NaCl and $CaCl_2$ solutions. At high $CaCl_2$ concentrations (≥ 3.5 M), all the initial solid dissolved resulting in GLU concentrations above 0.5 M. This indicates that gluconate is hardly limited by solubility in concentrated $CaCl_2$ solutions, and that Ca–bearing aqueous species are able to stabilize very high gluconate concentrations in solution.
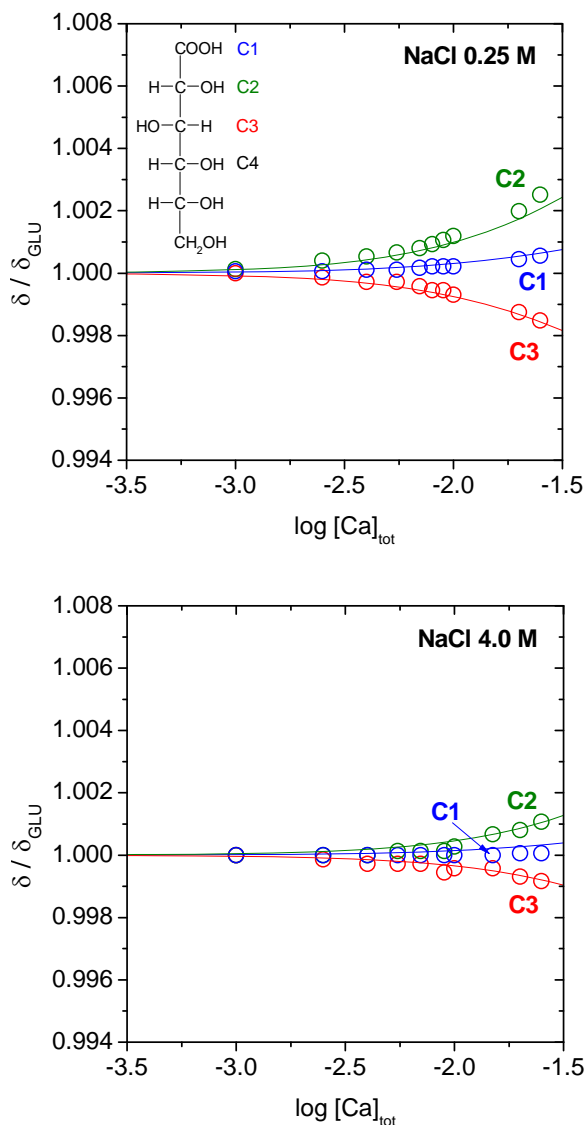
Fig. 1: ^{13}C–NMR chemical shifts of C1, C2 and C3 carbon atoms. Solid lines correspond to the fit assuming the formation of the aqueous species $CaGLU^+$.

The presence of GLU induces a significant increase on $NpO_2(am,hyd)$ solubility in $CaCl_2$ solutions (Fig. 2). This increase is stronger at higher concentrations of Ca^{2+}, thus

indicating the formation of ternary complexes analogous to those described in the literature for Th(IV) $(CaAn^{IV}(OH)_4GLU_2(aq))$ [2, 3]. The system reaches a saturation level at [Np] $\sim10^{-5.5}$ M, independently of $[CaCl_2]$. This observation can be explained by the formation of a new Ca–Np(IV)–GLU solid phase, although this hypothesis remains to be further confirmed by appropriate solid phase characterization (XRD, SEM-EDS, quantitative chemical analysis) which is currently under way.
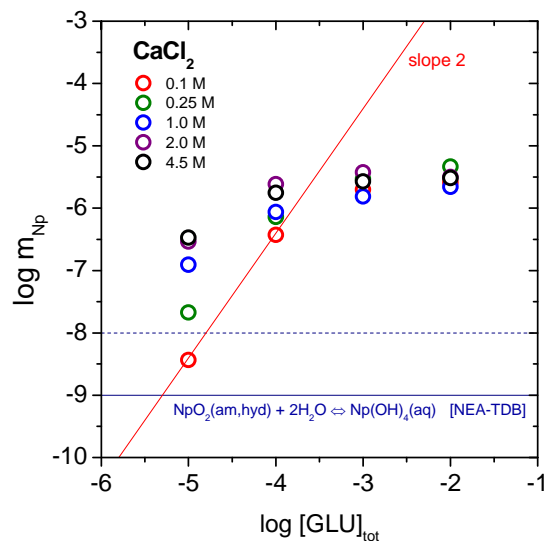
Fig. 2: Solubility of $NpO_2(am,hyd)$ at $pH_m = pH_{max}$ under increasing $[GLU]_{tot}$.

REFERENCES

[1] Guillaumont, R. et al., "Chemical Thermodynamics 5. Update on the Chemical Thermodynamics of Uranium, Neptunium, Plutonium, Americium and Technetium" NEA OECD, Elsevier (2003).

[2] Tits, J. et al., The effect of isosaccharinic acid and gluconic acid on the retention of Eu(III), Am(III) and Th(IV) by calcite. *Appl. Geochem.* **20**, 2082–2096 (2005).

[3] Gaona, X. et al., Review of the complexation of tetravalent actinides by ISA and gluconate under alkaline to hyperalkaline conditions. *J. Contam. Hydrol.* **102**, 217–227 (2008).

[4] Altmaier, M. et al., Solid-liquid equilibria of $Mg(OH)_2(cr)$ and $Mg_2(OH)_3Cl\cdot4H_2O(cr)$ in the system Mg–Na–H–OH–O–Cl–H_2O at 25°C. *Geochim. Cosmochim. Acta* **67**, 3595-3601 (2003).

[5] Pallagi, A. et al., Multinuclear NMR and molecular modelling investigations on the structure and equilibria of complexes that form in aqueous solutions of Ca^{2+} and gluconate. *Carbohyd. Res.* **345**, 1856–1864 (2010).

**Experimental and Thermodynamic Modeling Solubility of Lead in the Carbonate System to High Ionic Strengths:
Part One, Solubility of Cerussite (PbCO$_3$) in NaHCO$_3$ + NaCl Solutions [A]**

Yongliang Xiong[1], Leslie Kirkes[1] and Terry Westfall[1, 2]
[1]Repository Performance Dept. 6212, Sandia National Laboratories,[B]
4100 National Parks Highway, Carlsbad, NM 8822, USA
yxiong@sandia.gov

[2]Retired

INTRODUCTION

Lead is an important heavy metal to many fields. In the automobile industry, lead batteries are widely used. In the environmental science field, contamination caused by lead is of great concern. Lead is also used as a radiation-shielding material for wastes with significant γ-radiation in the field of nuclear waste isolation.

The Waste Isolation Pilot Plant (WIPP) is a U.S. Department of Energy (DOE) repository in southeast New Mexico for defense-related transuranic (TRU) waste. The repository, which opened in March 1999, is located at a subsurface depth of 655 m in the Salado Fm., a Permian bedded-salt formation. It is planned to use a significant amount of lead as a radiation-shielding material for wastes with significant γ-radiation placed in the WIPP.

Carbonate is an important inorganic ligand in the WIPP brines such as Generic Weep Brine (GWB)[1, 2] from the Salado Fm. at the stratigraphic horizon of the repository, and Energy Research and Development Administration (WIPP Well) 6 (ERDA-6)[3] from the underlying Castile Fm. When lead is corroded under anoxic conditions in carbonate-containing brines, lead carbonate, cerussite (PbCO$_3$(cr)), is expected to form. Therefore, the accurate knowledge of solubilities of cerussite in a wide range of ionic strengths has important bearings on the chemical behavior in the repository.

In the review performed by Powell et al. (2009)[4], they recommended a log K_s^0 of –13.18 for the following reaction,
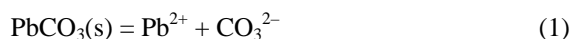
$$PbCO_3(s) = Pb^{2+} + CO_3^{2-} \qquad (1)$$

Their recommendation was based on a few studies with very short experimental time of 2–4 days[5, 6]. We conducted a long-term study on the solubilities of cerussite in NaHCO$_3$ + NaCl solutions.

About 2 grams of the solubility controlling material, crystalline lead carbonate from Alfa Aesar, were weighed out and placed into 150 mL plastic bottles in our solubility experiments. For each experiment, 100 mL of various supporting solutions were added to the bottles. Once filled, the lids of the bottles were sealed with parafilm. The supporting electrolytes are a series of NaHCO$_3$ + NaCl solutions ranging from 0.159 to 1.16 mol•kg^{-1} in total ionic strength. The supporting solutions were prepared with reagent grade NaHCO$_3$ and NaCl from Fisher Scientific. Deionized (DI) water with 18.0 MΩ•cm was produced by a NANOpure Infinity Ultra Pure Water System from Barnstead. Undersaturation experiments were conducted at the laboratory room temperature (295.65 ± 1.0 K). Lead concentrations of solutions were analyzed with a Perkin Elmer dual-view inductively coupled plasma-atomic emission spectrometer (ICP-AES) (Perkin Elmer DV 3300).

Our experimental results seem to indicate that the attainment of equilibrium for solubility of cerussite takes much longer time than previously suggested (Figure 1). Our results suggest that the attainment of equilibrium may require at least 900 days, instead of a few days as suggested before. The equilibrium solubility of cerussite ranges from 10^{-6} to 10^{-5} mol•kg^{-1}, depending on the ionic strengths of supporting solutions.

We are in the process of modeling solubilities of cerussite in NaHCO$_3$ + NaCl solutions using EQ3/6 Version 8.0a[7, 8]. In our modeling, we plan to test and revise the Pitzer parameters related to lead species in a recent publication[9].

REFERENCES

1. Krumhansl, J.L., K.M. Kimball, and C.L. Stein. 1991. *Intergranular Fluid Compositions from the Waste Isolation Pilot Plant (WIPP), Southeastern New Mexico.* SAND90-0584. Albuquerque, NM: Sandia National Laboratories.

2. Snider, A.C. 2003. "Verification of the Definition of Generic Weep Brine and the Development of a Recipe for This Brine." ERMS 527505. Carlsbad, NM: Sandia National Laboratories.

3. Popielak, R.S., R.L. Beauheim, S.R. Black, W.E. Coons, C.T. Ellingson and R.L. Olsen. 1983. *Brine Reservoirs in the Castile Formation, Waste Isolation Pilot Plant Project, Southeastern New Mexico.* TME 3153. Carlsbad, NM: U.S. Department of Energy WIPP Project Office.

4. Powell, K.J., Brown. P.L., Byrne, R.H., Gajda, T., Hefter. G., Luez, A.-K., Sjöberg, S., and Wanner, H., 2009. Chemical speciation of environmentally significant metals with inorganic ligands. Part 3: The Pb^{2+} + OH^-, Cl^-, CO_3^{2-}, SO_4^{2-}, and PO_4^{3-} systems (IUPAC Technical Report). Pure and Applied Chemistry 81 (12), 2425-2476.

5. Nasanen, R., Merilainen, P., and Leppanen, K., 1961. Potentiometric determination of the solubility product of lead carbonate. Acta Chemica Scandinavica 15, 913-918.

6. Bilinski, H., and Schindler, P., 1982. Solubility and equilibrium constants of lead in carbonate solutions (25 ^{o}C, I = 0.3 mol dm^{-3}). Geochimica et Cosmochimica Acta 46, 921-928.

7. Wolery, T.J., Y.-L. Xiong, and J.J. Long. 2010. "Verification and Validation Plan/Validation Document for EQ3/6 Version 8.0a for Actinide Chemistry, Document Ver. 8.10." . ERMS 550239. Carlsbad, NM: Sandia National laboratories.

8. Xiong, Y.-L., 2011. "WIPP Verification and Validation Plan/Validation Document for EQ3/6 Ver. 8.0a for Actinide Chemistry, Rev. 1." ERMS 555358. Carlsbad, NM. Sandia National Laboratories.

9. Woosley, R.J., and Millero, F.J., 2013. Pitzer model for the speciation of lead chloride and carbonate complexes in natural waters. Marine Chemistry 149, 1-7.
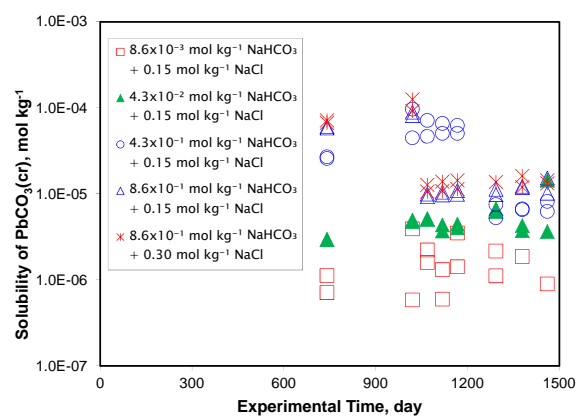
Figure 1. A plot showing solubilities of cerussite as a function of experimental time

Experimental Evidence for Low Uranium (VI) Solubility in the WIPP

J.F. Lucchini, M. Borkowski, M.K. Richmann, J.S. Swanson, K. Simmons, D. Cleveland, and D.T. Reed

Los Alamos National Laboratory-Carlsbad Operations, 115 N. Main Street, Carlsbad, NM 88220, U.S.A.
Email: lucchini@lanl.gov
LA-UR-13-22634

INTRODUCTION

In the performance assessment (PA) for the Waste Isolation Pilot Plant (WIPP), the solubility of uranium (VI) was conservatively set at 10^{-3} M for all expected WIPP conditions, including the potential and likely effects of carbonate complexation [1]. Under WIPP-relevant conditions, long-term experiments were performed to establish the uranium (VI) solubility limits in WIPP-simulated brine over a broad range of pC_{H+} values [7.5-12.5] and to evaluate the contribution of carbonate complexation and hydrolysis to uranium (VI) speciation. Data were reported in earlier publications [2, 3]. They are summarized herein.

DESCRIPTION OF THE WORK

The general experimental approach was to investigate uranium (VI) solubility from over-saturation in the two simulated WIPP brines, GWB and ERDA-6 (95% of initial formulations). Carbonate was first removed from the brines using a two-step process: acidification of the brines, and a slow pump-down process to smoothly remove CO_2 gas from the brines. The hydrogen ion concentration of the brines was then adjusted with low-carbonate sodium hydroxide (50 weight%). The level of carbonate in the experiments was established by the addition of a small volume of an appropriate intermediate carbonate solution to achieve the desired initial concentration of carbonate in solution: 2×10^{-4} M or 2×10^{-3} M. The experiments were initiated by the addition of uranyl-spiked brine into the pC_{H+}-adjusted brine solutions containing no carbonate or a known amount of carbonate. Aliquots were periodically removed, centrifuged and filtered through Microcon® Millipore centrifugal filters (30,000 Daltons). Filtrates were analyzed for uranium content using an inductively-coupled plasma mass spectrometer (ICP-MS).

RESULTS

Fig. 1 shows the uranium concentrations measured in ERDA-6 and GWB brines as a function of pC_{H+}. The data obtained when carbonate was present correspond to 17 samplings performed throughout 994 days of experiments.
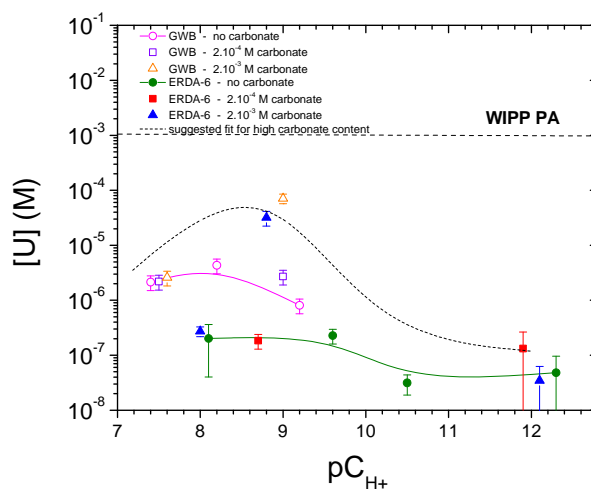
Fig. 1: Uranium concentration in ERDA-6 (filled symbols) and GWB (open symbols) versus pC_{H+} in nitrogen-controlled atmosphere, in the absence of carbonate or in the presence of two concentrations of carbonate (2×10^{-4} M and 2×10^{-3} M) at the beginning of the experiments [3].

In the absence of carbonate, the measured U(VI) solubilities were about 10^{-6} M in GWB brine at $pC_{H+} \geq 7.5$ and about 10^{-8} - 10^{-7} M in ERDA-6 at $pC_{H+} \geq 8$. These results put an upper bound of $\sim 10^{-5}$ M for the solubility of uranyl in the carbonate-free WIPP brines for the investigated range of experimental conditions. At the expected pC_{H+} in the WIPP ($\sim$9.4), the measured uranium solubility was between 10^{-7} M and 10^{-6} M.

In the presence of carbonate, the highest uranium solubility obtained experimentally was $\sim 10^{-4}$ M, under WIPP-related conditions ($pC_{H+} \sim 9$). This is an order of magnitude lower than the uranium (VI) solubility currently assumed by WIPP PA and mandated by the EPA. This high uranium solubility value was obtained at the highest carbonate concentration (2×10^{-3} M) investigated which is $\sim$ 10 times higher than the carbonate concentration predicted by WIPP PA.

In conclusion, the 1 mM value for uranium (VI) solubility used in WIPP PA is confirmed to be conservative, by over

a factor of 50, relative to the experimental results. These experimental data clearly support the current position on An(VI) solubility under WIPP-relevant conditions. In the broader consideration of a high level waste repository, uranium chemistry has a bigger importance. Consequently, these experimental data could support the disposal of radioactive waste present in a uranium dioxide-like matrix in underground saline formations similar to the Salado and Castile formations.

REFERENCES

1. U.S. Environmental Protection Agency (EPA). Teleconference with U.S. Department of Energy (DOE), Sandia National Laboratories (SNL), and Los Alamos National Laboratory (LANL) re: Change in U(VI) Solubility Assumption to a Concentration to 1 mM. 2 March 2005.

2. LUCCHINI, J.-F., et al.. "Uranium(VI) Solubility in carbonate-free WIPP Brine." *Radiochimica Acta,* to be published (currently at preprint stage) (2013).

3. LUCCHINI, J.F., et al. "Influence of Carbonate on Uranium Solubility in the WIPP". *Actinides and Nuclear Energy Materials*, Material Research Society Symposium Proceedings, **1444**: 217-22 (2012).

Long-Term Plutonium Speciation in Fe-Dominated High Ionic-Strength Brines

D.T. Reed, J.F. Lucchini, M.K. Richmann and M. Borkowski

Earth and Environmental Sciences Division, Los Alamos National Laboratory, 1400 University Drive, Carlsbad NM, USA
dreed@lanl.gov

INTRODUCTION

The role and importance of iron chemistry in the redox reactions of multivalent metals, including actinides, is well established. There are also important links between the subsurface microbiology and this iron chemistry and this chemistry is a key pathway by which microbial processes influence metal speciation. In a salt-based repository, the presence and reactivity of zero-valent iron is critical to the long-term performance of the repository should brine saturation occur as the result of low-probability intrusion events [1]. Once self-sealing occurs, this iron reactivity will remove oxygen, produce hydrogen, and further react to reduce higher-valent metals and actinides to establish strongly reducing conditions. For these reasons we have investigated the short and long-term speciation of plutonium in iron-rich systems as well as the degree of association with the iron colloids that are invariably formed in near-neutral pH systems.

In the absence of iron, plutonium can exist in high ionic-strength systems for long times (at least several years) [2, 3]. The addition of reduced iron (as Fe coupons, Fe powder, and magnetite) leads to the rapid reduction of Pu(V/VI) to form reduced Pu(III/IV) species that lowered the overall solubility of plutonium by orders of magnitude. For this reason, under the expected conditions in the WIPP, plutonium is predicted to exist predominantly as Pu(III) and Pu(IV) species.

The shorter-term iron reduction study was extended for an additional 6 years to help establish the long-term speciation and, in particular, evaluate the colloidal fraction and relative Pu(III/IV) oxidation state distribution of the aqueous and solid plutonium species present in an iron-rich anoxic brine system. The analyses of these experiments are not yet complete. The results for experiments where the iron was added as a pure Fe coupon, and iron corrosion is the predominant source of iron colloids, are summarized herein.

DESCRIPTION OF THE WORK

Plutonium-spiked brines were prepared by adding Pu(VI), as the Pu-242 isotope, to WIPP-specific GWB and ERDA-6 brine as a function of pH. Plutonium was oxidized to Pu(VI) by fuming in two drops of perchloric acid, dissolved in ~ pH 3 sodium chloride, and analyzed using absorption spectrometry to establish and verify oxidation state. This stock solution was added directly to the brine at the desired pH. Plutonium (VI) stability was established for each brine by letting each experiment equilibrate for a few months and confirming that no reduction and/or loss of plutonium from solution had occurred.

These redox experiments were left to sit unperturbed in a nitrogen glovebox for almost six years and selected experiments were re-analyzed to establish oxidation state and colloidal fraction of the plutonium and iron. Iron was analyzed by the Ferrozene® method [3], and plutonium was analyzed by ICP-MS. The size distribution was determined by sequential filtration under anoxic conditions using sequential filtration with Fisher Amicon® ultrafilters down to 3 kDa (~ 2.5 nm).

RESULTS

A description of the experiments analyzed is given in Table 1. In all of these experiments, the iron underwent anoxic corrosion and generated some colloidal iron in solution. In this context, information on both the association of plutonium with the iron and the potential formation of plutonium intrinsic colloids was obtained.

Experiment	Description	[a] Oxidation State of Pu Solid	[b] [Fe]$_{total}$ in mM (%Fe^{2+} in solution)	[c] E$_h$ Measured (± 3 mV)
	Table 1 Redox Indicators for Iron Interactions with Plutonium under Anoxic Conditions			
PuFeCE8	ERDA-6 brine at pC$_{H+}$ = 8.34 with Fe coupon	~100 % Pu(III)	ND	ND
PuFeCE10	ERDA-6 brine at pC$_{H+}$ = 9.54 with Fe coupon	~100% Pu(III)	0.27 (100%)	ND
PuFeC	ERDA-6 brine at pC$_{H+}$ = 9.11 with Fe coupon	~90% Pu(III), rest Pu(IV)	0.18 (58%)	-110 mV
PuFeG7	GWB brine at pC$_{H+}$ = 7.71 with Fe coupon	~ 100% Pu(III)	12.62 (97%)	-210 mV

a. Pu(III) content established by XANES analysis of solids
b. Fe(II) content established by analysis using FerroZene®
c. E$_h$ measurement made using an Orion combination ORP electrode
ND – not determined

Oxidation state analyses of the sorbed and dissolved aqueous plutonium showed that mostly Pu(III) was present in this system given the strongly reducing conditions established by the iron. These results are also summarized in Table 1. A plot of the concentration of plutonium as a function of pC$_{H+}$ and filtration size is shown in Figure 1.

In the presence of reduced iron, we have shown that reduction occurs under all anoxic conditions that have been investigated. Measured E$_h$ values between -100 mV

and -250 mV are observed. Plutonium (IV) and Pu(III) are initially observed in the solids present (XANES) with a predominance of Pu(IV).
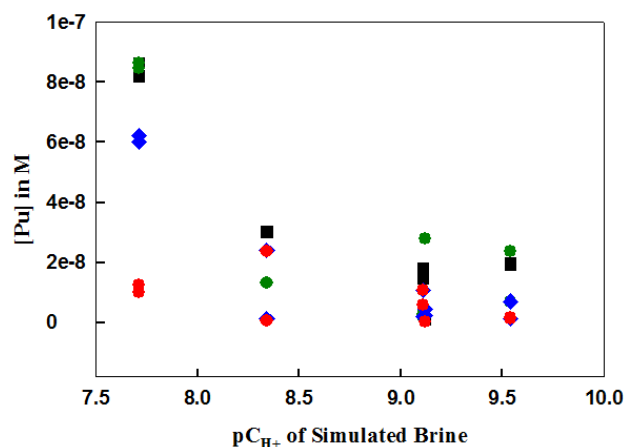

Fig. 1 Effect of filtration on the measured concentration of plutonium as a function of pC_{H+}. Data shown are 0.45 µ (black squares), 0.22µ (green circles), 20 nm (blue diamonds) and 10 nm (red circles) filtrations. Uncertainty in the filtration data, based on ICP-MS analyses, is estimated to be ±20%.

The predominant plutonium oxidation state in the long-term studies was Pu(III). This was established by XANES analysis (see Fig. 2) for the solids and TTA extraction for the aqueous species. Overall plutonium concentrations were measured by ICP-MS as a function of filtration, brine composition and pH. These are in the range of 10^{-8} M to 10^{-10} M across the pH range and are factors of 10 to 100 lower than the Nd(III) and Th(IV) oxidation state analogs used in our more general brine studies. In the unfiltered samples, there is strong correlation with the iron concentrations and reflects the fact that there are Fe fines in these system that is readily suspended. The 0.2µ-filtered concentration, however, does not track with the iron concentration in solution and we as yet do not have structural data on this species. The 30K-filtered results correlate well with expected solubility trends there is a qualitative correlation between the Pu(III/IV) fraction and the Fe(II/III) fraction measured.

Collectively, these data show that we are seeing fairly low plutonium concentrations across the pH range investigated (7-10) but some mineral and intrinsic "colloidal" solubilization was also evident due to the iron present. Work is ongoing to further establish the nature of the colloidal fraction observed and investigate the long-term stability of Pu(III) phases in these brine systems..
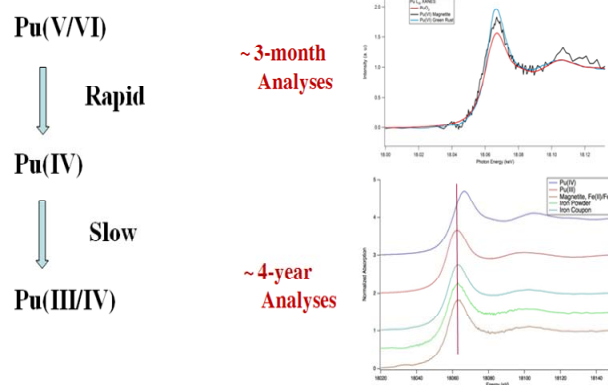
Fig. 2 Plutonium XANES showing the oxidation state of the iron-associated plutonium at short and long times. Initially Pu(IV) is predominant, but at long time almost all the plutonium converted to the Pu(III) oxidation state.

ACKNOWLEDGMENT

REFERENCES

[1] Title 40 CFR Part 1991 Subparts B and C Compliance Recertification Application 2009, Appendix PA, Attachment SOTERM, U.S. Department of Energy Carlsbad Field Office, Carlsbad, NM (2009).

[2] Reed, D. T., J. F. Lucchini, M. Borkowski, and M. K. Richmann. "Reduction of Higher-Valent Plutonium by Iron Under Waste Isolation Pilot Plant (WIPP)-Relevant Conditions: Data Summary and Recommendation," Los Alamos report LCO-ACP-09, 2010.

[3] Reed, D. T., J. F. Lucchini, S. B. Aase and A. J. Kropf. Radiochim. Acta., 94 (2006) 591-597.

[4] Pepper, S.E., M. Borkowski, M.K. Richmann and D.T. Reed. "Determination of Ferrous and Ferric Iron in Aqueous Biological Solutions," Anal. Chim. Acta,, 663(2) (2010) 172-177.

Redox Chemistry and Solubility of ^{99}Tc in Saline NaCl and MgCl$_2$ Solutions

E. Yalcintas[1], X. Gaona[1], T. Kobayashi[2], M. Altmaier[1], H. Geckeis[1]

[1]*Karlsruhe Institute of Technology, Institute for Nuclear Waste Disposal, P.O. Box 3640, 76021 Karlsruhe, Germany*
[2]*Department of Nuclear Engineering, Kyoto University, 615-8530, Kyoto, Japan*
ezgi.yalcintas@kit.edu, marcus.altmaier@kit.edu

INTRODUCTION

Reliable predictions of radionuclide chemistry are necessary for the long-term safety analysis of nuclear waste repositories. Knowledge of redox state distribution, complex formation and solubility limits provides the basis to assess the potential mobilization of a radionuclide from the repository into the biosphere. ^{99}Tc is a highly relevant radionuclide due to its abundance in radioactive waste, long half-life (t$_{1/2}$ ~211.000 a) and redox sensitivity. Tc can exist in several oxidation states (+III to +VII), although only Tc(VII) and Tc(IV) are long-time stable in relevant aqueous systems under non reducing and reducing conditions. Tc(VII) exists as the highly soluble and potentially mobile TcO$_4^-$ anion, whereas Tc(IV) forms sparingly soluble hydrous oxides (TcO$_2$·xH$_2$O(s)). The review on thermodynamic data for technetium conducted within the NEA–TDB project provided a compilation of data for redox processes, hydrolysis reactions and other solubility phenomena [1]. However, the current selection is limited to dilute systems, with SIT ion interaction parameters lacking for even the most relevant Tc(IV) aqueous species. Recently Hess et al. (2004) investigated the solubility of TcO$_2$·xH$_2$O(s) in dilute to concentrated NaCl solutions under acidic to near-neutral pH conditions and derived thermodynamic data and activity models following the Pitzer approach [2]. Investigations focussing on repository-relevant alkaline conditions in brine systems are so far lacking although much needed in view of waste disposal concepts in rock salt. In the present study, redox transformations of Tc(VII)/Tc(IV) and Tc(IV) solubility were investigated in diluted to concentrated NaCl and MgCl$_2$ solutions from acidic to hyperalkaline pH conditions.

DESCRIPTION OF THE WORK

Redox experiments were performed in 0.5–5.0 M NaCl and 0.25–4.5M MgCl$_2$ solutions in the presence of homogenous (Na$_2$S$_2$O$_4$, SnCl$_2$, Fe(II)/Fe(III), Fe powder) and heterogeneous (magnetite, mackinawite and siderite) reducing systems. pH$_c$ was adjusted with HCl–NaCl/MgCl$_2$ and NaOH–NaCl/Mg(OH)$_2$–MgCl$_2$ solutions at the respective constant ionic strength. Initial Tc(VII) concentrations were set to [TcO$_4^-$] = 10^{-5} M by spiking a NaTcO$_4$ stock solution to the pre-equilibrated background electrolyte solutions. The values of pH$_c$ = pH$_{exp}$ + A$_c$ were calculated from the operational "measured" pH$_{exp}$ using empirical corrections factors (A$_c$) reported elsewhere [3]. No corrections factors were used for E_h values. Experimentally determined pH$_c$ and E_h values are plotted in Tc *Pourbaix* diagrams where the redox borderline for TcO$_4^-$ + 4H$^+$ +3e$^-$ $\Leftrightarrow$ TcO$_2$·xH$_2$O(s) + (2−x) H$_2$O was calculated following NEA–TDB [1]. Tc concentrations after 10 kD ultrafiltration were determined by liquid scintillation counting (LSC). The decrease of the Tc concentration in the aqueous phase is interpreted as a reduction of Tc(VII) and formation of TcO$_2$·xH$_2$O(s) solids. The redox state of Tc was further confirmed by solvent extraction [4].

The solubility of Tc(IV) was studied in 0.5–5.0 M NaCl and 0.25–4.5 M MgCl$_2$ solutions. A Tc(VII) stock solution was electrochemically reduced and precipitated as TcO$_2$·xH$_2$O(s) in a strongly reducing Na$_2$S$_2$O$_4$ solution at pH$_c$ ~12. About 5 mg of the resulting solid phase were added to each independent batch experiment. Pre-equilibrated matrix solutions were used at $2 \leq$ pH$_c \leq 14$ and Na$_2$S$_2$O$_4$, SnCl$_2$ or Fe powder (depending upon target pH) added to maintain reducing conditions. Tc concentration, pH$_c$ and E_h values were monitored at regular time intervals.

RESULTS

Redox Studies of Tc(VII)/Tc(IV) couple

Fig. 1 shows the *Pourbaix* diagram of Tc(VII)/Tc(IV) in 5.0 M NaCl solution. Analogous diagrams are obtained in 0.5 M NaCl and 0.25–4.5M MgCl$_2$ solutions. In all cases, the reduction of Tc(VII) to Tc(IV) is observed for E_h values below the thermodynamically calculated Tc(VII)/Tc(IV) borderline, independent of the reducing system, background electrolyte and ionic strength. No reduction of Tc(VII) occurs in those systems with redox potentials above the borderline. This indicates that E_h and pH are robust and reliable parameters for the prediction of Tc redox behaviour in the investigated dilute to concentrated NaCl and MgCl$_2$ solutions. Significantly higher E_h values are observed for samples in 4.5 M MgCl$_2$ regardless of the reducing system. This was found to influence Tc redox chemistry as expected from the calculated Tc(VII)/Tc(IV) redox borderline.
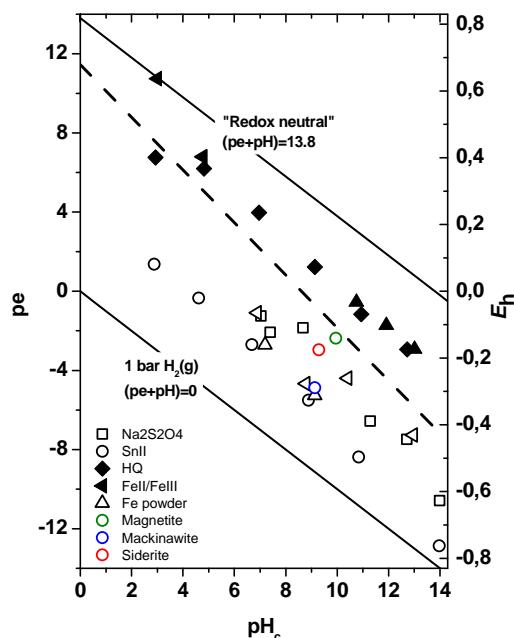
Fig. 1: Redox behavior of Tc(VII)/Tc(IV) in 5.0 M NaCl. Open symbols indicate reduction to Tc(IV); solid symbols correspond to samples without reduction of Tc(VII). The dashed line indicates the Tc(VII)/Tc(IV) borderline calculated from NEA–TDB.

Solubility Studies of Tc(IV)

Tc(IV) solubility data obtained in 0.5 M and 5.0 M NaCl solutions are shown in Fig 2. Experimental data in 0.5 M NaCl agree very well with previous solubility data reported by Meyer et al. (1991) [5] and Eriksen et al. (1992) [6] in diluted systems, as well as with thermodynamic calculations performed considering the current hydrolysis scheme and log $*K_{s,0}(TcO_2 \cdot xH_2O(s))$ selected in the NEA–TDB [1]. Our solubility data is in disagreement with data reported in Warwick et al. (2007) [7], likely indicating significant differences in the solid phase controlling the solubility of Tc(IV).

In agreement with the Tc(IV) chemical model selected in the NEA–TDB, the increase in solubility observed at $pH_c \leq 4$ and $pH_c \geq 10$ indicates the formation of $TcOOH^+$ and $TcO(OH)_3^-$ hydrolysis species, respectively. Furthermore, the pH–independent solubility reaction $TcO_2 \cdot xH_2O(s) \Leftrightarrow TcO(OH)_2(aq) + (1-x) H_2O$ controls the solubility of Tc(IV) within $4 \leq pH_c \leq 10$. In the more acidic pH range, the increase of solubility observed with increasing ionic strength is consistent with previous experimental evidences reported by Hess et al. (2004). Note that these authors only reported the formation of Tc(IV)–Cl aqueous species under very acidic and high [Cl⁻]. Similar species might be expected to form at low pH values in

concentrated $MgCl_2$ solutions. Solid and aqueous phase characterisation (XRD, SEM–EDS, XAFS, chemical analysis) are scheduled after completion of the solubility experiments. A complete thermodynamic description (SIT, Pitzer) for the system $Tc^{IV}–H^+–Na^+–Mg^{2+}–OH^-–Cl^-$ valid over the entire pH_c range will include the new solubility data and is expected for the near future.
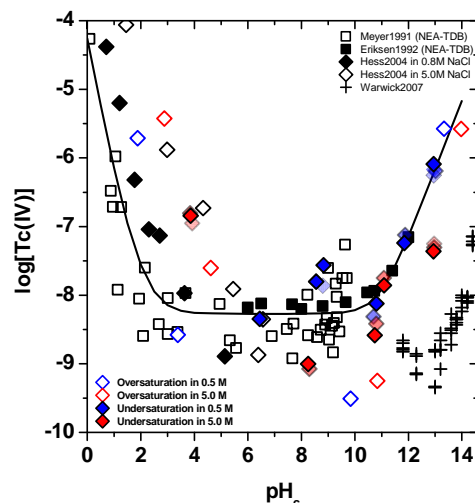
Fig. 2: Solubility of Tc(IV) in 0.5 M and 5.0 M NaCl. Solid line corresponds to $TcO_2 \cdot xH_2O(s)$ solubility calculated with the current NEA–TDB selection at I = 0.

References

[1] R. Guillaumont, et al., eds. *Chemical Thermodynamics 5. Update on the Chemical Thermodynamics of Uranium, Neptunium, Plutonium, Americium and Technetium.* ed. E. NEA OECD (2003).

[2] N. J. Hess, et al., *Thermodynamic model for the solubility of $TcO_2.xH_2O(am)$ in the aqueous $Tc(IV)-Na^+-Cl^--H^+-OH^--H_2O$ system.* Journal of Solution Chemistry, **33**, 199-226, (2004).

[3] M. Altmaier, et al., *Solid-liquid equilibria of $Mg(OH)_2(cr)$ and $Mg_2(OH)_3Cl.4H_2O(cr)$ in the system $Mg-Na-H-OH-O-Cl-H_2O$ at 25^oC.* GCA, **67**, 3595-3601, (2003).

[4] T. Omori, et al., *Solvent-Extraction Mechanism of Pertechnetate with Tetraphenylarsonium Chloride.* Journal of Radioanalytical and Nuclear Chemistry, **178**, 237-243, (1994).

[5] R. E. Meyer, et al., *Solubilities of Tc(IV) Oxides.* Radiochim. Acta, **55**, 11-18, (1991).

[6] T. E. Eriksen, et al., *The Solubility of $TcO_2 . nH_2o$ in Neutral to Alkaline-Solutions under Constant pCO_2.* Radiochim. Acta, **58-9**, 67-70, (1992).

[7] P. Warwick, et al., *The solubility of technetium(IV) at high pH.* Radiochim. Acta, **95**, 709-716, (2007).

Retention of trivalent Cm and Eu on Stable Solid Phases in the System Mg-Na-Cl-H$_2$O at Room Temperature

M. Wiedemann, V. Metz, T. Rabung, H. Geckeis

Karlsruhe Institute of Technology, Institute for Nuclear Waste Disposal (KIT–INE), Germany
martin.wiedemann@kit.edu

INTRODUCTION

Retention of actinides in the near field is critical for the long-term disposal and storage of radioactive waste in geological salt deposits. Under reducing conditions, which develop after closure of deep underground repositories for nuclear waste, actinides are expected to prevail in tri- and tetravalent redox states. There is currently a strong interest in developing backfill materials which provide favorable chemical conditions with respect to low actinide solubility and significant actinide retention capacities. For decades, a combination of Mg-oxychloride Mg$_2$(OH)$_3$Cl·4H$_2$O(s), so-called Sorel phase, and brucite Mg(OH)$_2$(s) is used as building material in conventional salt mines and currently discussed in concepts for sealing of radioactive waste repositories in rock salt [1,2].

At 25 °C brucite and Mg-oxychloride are the thermodynamically stable solid phases in the system Mg-Na-Cl-H$_2$O, besides halite NaCl(s) and bischofite MgCl$_2$·6H$_2$O(s) [2,3] (Fig. 1). For the Asse II salt mine (Lower Saxony, Germany) and the Waste Isolation Pilot Plant (New Mexico, USA), where low level and intermediate level radioactive waste products are emplaced, brucite / Sorel based materials and MgO are used as sealing material and engineered buffer, respectively. In contact with NaCl or MgCl$_2$ dominated salt brines, these materials buffer the pH at 8 – 9, and scavenges CO$_2$ potentially produced by microbial degradation of organic waste constituents [1].

The present study focus on the retention of a trivalent actinide (Cm(III)) and a trivalent lanthanide (Eu(III)) by brucite and Mg-oxychloride, at room temperature.

DESCRIPTION OF THE WORK

Various batch experiments were prepared with pure MgCl$_2$ and mixed NaCl–MgCl$_2$ solutions as background electrolytes. In the brucite experiments, the ionic strength was adjusted to 0.15, 1.2 and 5.2 mol·(kg(H$_2$O))$^{-1}$, and in the experiments with Mg-oxychloride it was adjusted to 9.9, 10.0 and 15.0 mol·(kg(H$_2$O))$^{-1}$, respectively. In presence of brucite and Mg-oxychloride, the specific pH$_m$ (pH$_m$ = -log(m(H$^+$))) values were fixed in a disposal relevant range of $8.7 \leq$ pH$_m$ ≤ 9.4 (Fig. 1). After a preequilibration of at least two weeks, the suspensions were doped with Eu(III). Brucite experiments were doped with $\leq 7 \cdot 10^{-9}$ mol·(kg(H$_2$O))$^{-1}$, Mg-oxychloride experiments

with $\leq 7 \cdot 10^{-7}$ mol·(kg(H$_2$O))$^{-1}$ per batch, to ensure Eu(III) concentrations considerably below the solubility of Eu(OH)$_3$(cr). For the different MgCl$_2$ an MgCl$_2$-NaCl solutions three sorption experiments and one blank experiment were prepared and sampled continuously for each V/m ratio (10-1000 mL·g^{-1}) and doping concentration. All experiments were prepared and stored in Ar gloveboxes under exclusion of oxygen and CO$_2$. To determine sorption species and the aqueous speciation of the studied systems, time-resolved laser fluorescence (TRLFS) measurements were performed with $1 \cdot 10^{-7}$ mol·L^{-1} Cm(III) per sample.
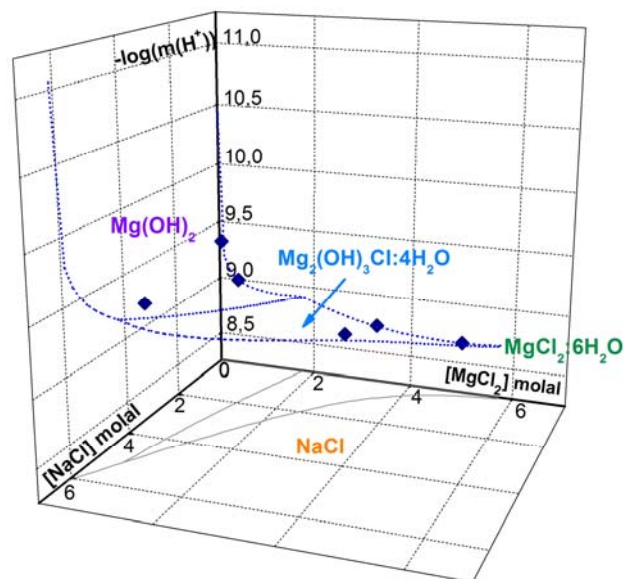
Fig. 1: Studied sorption systems, indicated by diamonds, in the stability fields of brucite Mg(OH)$_2$(s) and Mg-oxychloride Mg$_2$(OH)$_3$Cl·4H$_2$O(s) at 25° C.

Brucite (BioUltra $\geq$ 99%) was purchased from Fluka and Mg-oxychloride was synthesized by transformation of brucite in 5 mol·(kg(H$_2$O))$^{-1}$ MgCl$_2$ solution. Brucite and Mg-oxychloride were characterized using DTA-TG (Netzsch STA409C/CD), Raman spectroscopy (Bruker Senterra), SEM–EDX (Quanta 650 FEG, FEI), XPS (ULVAC-PHI) and XRD (D8 Advance diffractometer, Bruker AXS). The molar H$^+$ concentration (pH$_c$) of the suspensions was determined with combination pH electrodes (type Orion Ross, Thermo Scientific). To convert the operational measured "pH$_{exp}$" values, the approach of

Altmaier et al. [3] was applied. Eu(III) concentrations were determined by ICP–MS (X–Series II, Thermo Scientific). Cm(III) fluorescence spectra were collected using a Nd:YAG laser (Continuum Surelite II 10 Hz) pumping a dye laser (Narrowscan Dye Laser, Radiant Dyes).

RESULTS

In the macroscopic sorption experiments and in the TRFLS measurements a strong retention of Eu(III) and Cm(III) of $\geq 95.5\%$ ($R_s \gg 210$ ml·g^{-1}) and $\geq 99.5\%$ is determined, respectively. Since the Eu(III) concentration decreased to below the ICP-MS detection limit of $3 \cdot 10^{-10}$ mol·L^{-1} within less than a week, the reported R_s value represents a lower limit for the retention by brucite. A less pronounced retention of Eu(III) and Cm(III) is observed in the experiments with Mg-oxychloride (R_s = 24 - 30 ± 10 ml·g^{-1}). Laser fluorescence spectra of Cm(III) / brucite / brine suspensions show a significantly shifted emission band at 609 nm (Fig. 2). Fluorescence lifetime measurements show a biexponential decay with two species at 198 ± 25 μs and 67.4 ± 5.2 μs. Regarding to Kimuras equation [4] the longer-lived species corresponds to 2.3 - 2.5 H$_2$O or ~ 5 OH$^-$, considering the quenching by OH$^-$ to be half as efficient as quenching by H$_2$O. According to the results of H. Piepers [5] coprecipitation studies (two species at 176.8 ± 4.8 μs and 64.2 ± 2.7 μs) and the significant shifted emission band, this longer-lived component can be interpreted as an incorporated species. The shorted-lived species would correlate with a surface coordinated sorption. To confirm this assumption further investigation are needed. Measured spectra of Cm(III) / Mg-oxychloride / brine suspensions do not allow an unambiguous determination of Cm(III) sorption species.
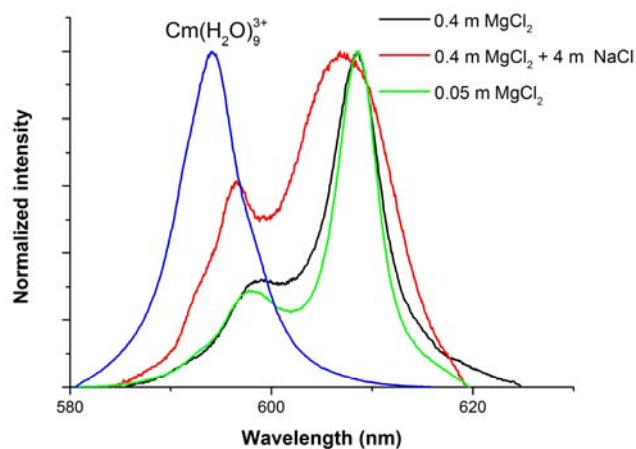
Fig. 2: Laser fluorescence spectra of Cm(III) / brucite / MgCl$_2$ and NaCl–MgCl$_2$ suspensions in comparison to the spectrum of the hydrated Cm^{3+} ion.

The observed retention of Cm(III) and Eu(III) by brucite at I = 0.15 to 5.2 mol·(kg(H$_2$O))$^{-1}$ and Mg-oxychloride at I = 9.9 to 15 mol·(kg(H$_2$O))$^{-1}$ demonstrates the suitability of brucite / Sorel based materials as engineered buffer with respect to retention of trivalent actinides under a wide range of saline conditions. In experimental studies in diluted solutions, an incorporation of Eu(III) and Am(III) into the octahedral brucite structure was determined by Finck et al. [6]. Ongoing TRFLS studies with Cm(III) / brucite / brine suspensions focus on the ionic strength effect of Cm(III) incorporation or surface sorption. Further investigations at low temperature and kinetic studies are planned.

REFERENCES

[1] Metz, V., Schüßler, W., Kienzler, B., Fanghänel, Th. (2004) Radiochim. Acta 92, 819-825
[2] Freyer, D. (2012) Sorel cement as geotechnical barrier in salt formations. Proceed. Int'l Workshops ABC-Salt(II) and HiTAC 2011. KIT Scientific Reports 7625, Karlsruhe, p. 29
[3] Altmaier, M., Metz, V., Neck, V., Müller, R., Fanghänel, T. (2003) Geochim. Cosmochim. Acta (2003), 67, 3595-3601.
[4] Kimura, T., Choppin, G. R. (1994) J. Alloy. Compd. 213, 313-317.
[5] Pieper, H. (2005) Kristallchemischer Einbau trivalenter f-Elemente in trioktaedrische Smectite. Dissertation, Forschungszentrum Karlsruhe, Institute of Nuclear Waste Disposal.
[6] Finck, N., Schlegel, M. L., Bosbach, D. (2008) J. Contam. Hydrol., 102, 253-262.

Solid-liquid Equilibria in the System Mg(OH)$_2$-MgCl$_2$-H$_2$O at Elevated Temperatures (60°C-100°C)

Melanie Pannach, Daniela Freyer and Wolfgang Voigt

Institute of Inorganic Chemistry, TU Bergakademie Freiberg, Leipziger Str. 29, 09596 Freiberg,
daniela.freyer@chemie.tu-freiberg.de

INTRODUCTION

The phases in the system Mg(OH)$_2$ - MgCl$_2$ - H$_2$O (x Mg(OH)$_2 \cdot$ y MgCl$_2 \cdot$ z H$_2$O) represent the binder phases of magnesia cement with a current importance as barrier construction material in final disposal concepts for radioactive wastes in salt formations [1]. The phase formations, existence and properties were subject to numerous investigations in science and applications since more than a century. Different hydrates with the composition x-y-z = 3-1-8, 5-1-8, 9-1-4 (formerly 9-1-5 corrected by [2]), 2-1-4 and 2-1-2 were characterized [3-23] related to magnesia cement research [24-33]. As known from long term solubility investigations the 3-1-8 phase is the thermodynamic stable phase in presence of Mg^{2+} containing as well as sodium chloride saturated salt solutions at ambient temperatures [34]. Now the investigations on solubility equilibria have been extended to elevated temperatures at 60°C, 80°C and 100°C. The results allow also the prediction of the pH buffer capacity of the material (brucite or x-y-z phase) in the range of elevated temperatures - an important aspect for solubility limitation of radionuclides in context of nuclear waste disposal in underground salt mines.

DESCRIPTION OF THE WORK

For determination of the phase equilibria in the system Mg(OH)$_2$-MgCl$_2$-H$_2$O the following reactants were used (phase purity was verified by X-ray powder diffraction): MgO of the company *Magnesia* and magnesium chloride solution at different concentrations prepared by dissolution of MgCl$_2 \cdot$ 6 H$_2$O (Fluka, p.a.) in deionized water (before use boiled to remove CO$_2$). The samples were prepared by mixing of MgO or brucite or 3-1-8 or 2-1-4 phase with MgCl$_2$ solutions, for higher concentrations MgCl$_2 \cdot$ 6 H$_2$O was added. 60°C-experiments: The suspensions of 0.1g -1g solid and 200 g solution were shaked in 250 mL PP-bottles at 60 ± 0.2°C in a closed water bath for at least 1.5 years. Afterwards the suspensions were filtered with a micro fibre glass filter (Munktell, graduation MGB = 1.0 µm). 80°C and 100°C-experiments: The reactants were placed in Teflon cups with a volume of 30 mL situated in TiPd autoclaves. The autoclaves were rotated around their own axis with alternating directions in a metal-block thermostat at constant temperature of 80 ± 0.5°C and 100 ± 0.5°C

respectively for 11 - 19 days. Due to the special construction of the autoclaves the subsequent separation of the solid phase from the solution took place after crossover from the thermostat in a special high temperature centrifuge at 80 ± 1°C and 100 ± 1°C respectively. The entire equipment is described in detail by Freyer *et al.* [35]. Afterwards the autoclaves were opened for sampling of the separated phases. The Mg^{2+} concentrations of the solutions were determined by complexometric titration, 0.05-M EDTA (Indicator: Erio T) with an uncertainty of ± 0.3%. By potentiometric titration with 0.1-M AgNO$_3$ the chloride content was quantified with an uncertainty of ± 0.1%. In the case of the very low hydroxide concentrations an appropriate part of the solution was directly, without further dilution, analyzed by potentiometric acid back titration. A defined volume of 0.1-M HCl was added to the solution sample. For determination of the not neutralized remaining acid, 0.1-M sodium hydroxide solution was used. The uncertainty can be estimated as within ± 0.5%.

The separated solids were washed several times with deionized cold water (T < 5°C) to remove the adherent magnesium chloride (bischofite crystallized from adherent mother liquor). The adherent water was finally eliminated by washing with cold ethanol (T < 5°C). All solid phases were identified by X-ray powder diffraction in Bragg-Brentano geometry (D8, Bruker).

RESULTS

The system Mg(OH)$_2$ - MgCl$_2$ - H$_2$O was equilibrated at 60°C, 80°C and 100°C. The results are illustrated in **Figure 1** together with the literature data of Nakayama at 50°C [36] and 100°C [37]. According to that there are four thermodynamic stable phases in the system between 50°C and 100°C. Brucite occurs at low concentrated MgCl$_2$ solutions. With increasing temperature the invariant point brucit – 3-1-8 phase shifts to higher MgCl$_2$ concentrations (from about 2.5 molal at 50°C to 3.5-4.0 molal at 100°C). The branch of the 3-1-8 phase (with the highest solubility at 100°C) becomes smaller with increasing temperature. At 100°C the invariant point 3-1-8 / 2-1-4 phase is found between 5.0 and 5.5 molal MgCl$_2$ and is shifted with decreasing temperature to higher MgCl$_2$ concentrations. The experimental data of the 3-1-8 phase at 60°C finish at 5.3 molal MgCl$_2$. Whether a small field of the 2-1-4 is enclosed or not up to the saturation of

bischofite ($MgCl_2 \cdot 6\ H_2O$) still had to be investigated. The invariant point of 2-1-4 phase and bischofite shifts with increasing temperature corresponding to the increased solubility of bischofite to higher $MgCl_2$ concentrations. Thus, an enlarged existence field of the 2-1-4 phase is found at 100°C.

The high temperature phase 2-1-4 was isolated from equilibrium solution for detailed characterization beside the 2-1-2 phase (found above 100°C) by our previous research [38].

According the data of Nakayama at 100°C [37] the occurring phases are brucite and the 2-1-4 phase (as 2-1-6 phase indicated - probably due to difficulties to determine the stoichiometry). He give the invariant point of both at 5.409 mol $MgCl_2$/kg H_2O and 0.127 mol $Mg(OH)_2$/kg H_2O. From our experience the equilibrium was not reached. The formation of the 3-1-8 phase from the metastable brucite branch (from supersaturation) is controlled kinetically and can be extremely slow. Nakayama found the extended solubility isotherm of brucite and analysed the metastable invariant point of brucite and the 2-1-4 phase with significant higher solubilitiy than we found for the 3-1-8 phase in this region after long term equilibration. In this context, we observed an intermediate occurrence of the 9-1-4 phase at 100°C with higher solubility in the field of the later 3-1-8 phase formation.

The presented results should be considered as preliminary because the studies are currently still continued to check whether the phase equilibrium were achieved.
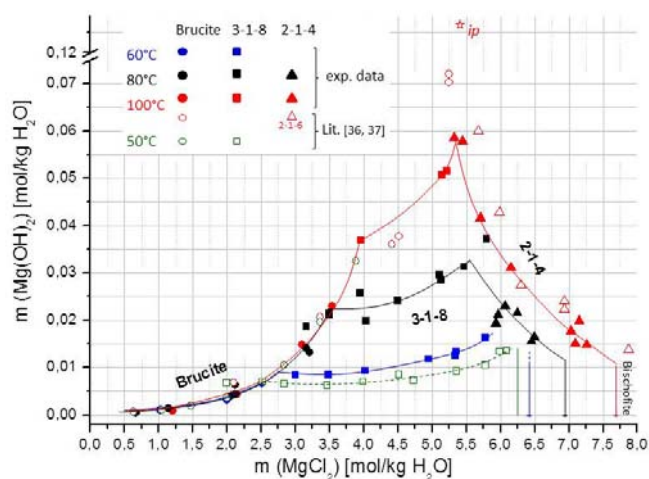

Fig. 1: Solubility equilibria in the system $Mg(OH)_2$-$MgCl_2$-H_2O at elevated temperatures

REFERENCES

1. N. Müller-Hoeppe, M. Breustedt, J. Wolf, O. Czaikowski, K. Wieczorek, *VSG-Abschlussbericht* "Vorläufige Sicherheits-analyse für den Standort Gorleben" AP 9.2, Integrität geo-technischer Barrieren, GRS Braunschweig, GRS 287 und GRS 288 (2013).
2. R. E. Dinnebier, D. Freyer, S. Bette, M. Oestreich, *Inorg. Chem.* **49**, 9770-9776 (2010).
3. W. Feitknecht, *Helv. Chim. Acta* **9**, 1018 (1926).
4. W. Feitknecht, F. Held, *Helv. Acta* **10**, 140 (1927).
5. W. Feitknecht, F. Held, *Helv. Acta* **13**, 1380 (1930).
6. W. Feitknecht, F. Held, *Helv. Acta* **27**, 1480 (1944).
7. H. S. Lukens, *J. Am. Ceram. Soc.* **54**, 2372 (1932).
8. C. R. Bury, E. R. H. Davies, *J. Chem. Soc. (London)* 2008 (1932).
9. L. Walter-Levy, P. M. de Wolff, *C. R. Acad. Sci. Paris* **229**, 1077 (1949)
10. L. Walter-Levy,; P. M. de Wolff, *C. R. Acad. Sci. Paris* **229**, 1232 (1949).
11. L. Walter-Levy,; Y. Bianco, *C. R. Acad. Sci. (Paris)* **232**, 730 (1951).
12. Y. Bianco, *C. R. Acad. Sci. Paris* **232**, 1108 (1951).
13. W. F. Cole, T. Demediuk, *Aust. J. Chem.* **8**(2), 243 (1999).
14. T. Demediuk, W. F. Cole, H. V. Hueber, *Aust. J. Chem.* **8**, 215 (1955).
15. J. D'Ans, W. Busse, H.-E. Freund, *Kali u. Steinsalz* **8**, 3 (1955).
16. Y. Bianco, *Ann. Chim. (Paris)* **3**, 370 (1958).
17. M. Ball, *Cement and Conc. Res.* **7**, 575 (1977).
18. S. Xia, P. Xing, S. Gao, *Thermochim. Acta* **183**, 349 (1991).
19. I. Kanesaka, S. Aoyama, *J. Raman Spectroscopy* **32**, 361 (2001).
20. I. Kanesaka, R. Shimizu, *Spectrochim. Acta* **A 59**, 569 (**2003**).
21. M. Altmaier, V. Metz, V. Neck, R. Müller, Th. Fanghänel, *Geochim. Cosmochim. Acta* **67** (19), 3595 (2003).
22. Y. Xiong, H. Deng, M. Nemer, S. Johnsen, *Geochim. Cosmochim. Acta* **74**, 4605 (2010).
23. R. E. Dinnebier, I. Halasz, D. Freyer, J. C. Hanson, *Z. Anorg. Allg. Ch.* **637**(11), 1458 (2011).
24. E. S. Newman, J. V. Gilfrich, L. S. Wells, *J. Res. Nat. Bur. Stand.* **49** (6), 377 (1952).
25. F. C. Harper, *J. Appl. Chem.* **17** (1), 5 (1967).
26. J. J. Beaudoin, V. S. Ramachandran, *Cem. Concr. Res.* **5** (6), 617 (1975).
27. C. A. Sorrell, C. R. Armstrong, *J. Am. Ceram. Soc.* **59** (1-2), 51 (1976).
28. E. I. Ved, E. F. Zharov, H. van Phong, *Zh. Prikl. Khim.* **49** (10), 2154 (1976).
29. B. Matkovic, S. Popovic, V. Rogic, T. B. Zunic, J. F. Young, *J. Am. Ceram. Soc.* **60** (11-12), 504 (1977).
30. L. Urwongse, C. A. Sorrell, *J. Am. Ceram. Soc.* **63** (9-10), 501 (1980).
31. C. Mazuranic, H. Bilinski, B. Matkovic, *J. Am. Ceram. Soc.* **65** (10), 523 (1982).
32. D. Deng, C. Zhang, *Cem. Concr. Res.* **29**, 1365 (1999).
33. Z. Li, C. K. Chau, *Journal of Materials in Civil Engineering* **20** (3)**, 239 (2008).
34. M. Pannach, D. Freyer, M. Altmaier, Ch. Bube, V. Metz, V. Neck, W. Voigt, prepared for publication in *Geochim. Cosmochim. Acta* (2013)
35. D. Freyer, W.Voigt, *Geochim. Cosmochim. Acta* **68**, 307 (2004).
36. M. Nakayama, *Bull. Agr. Chem. Soc. Japan* **24**, 362 (1960)
37. M. Nakayama, *Bull. Agr. Chem. Soc. Japan* **23**, 46 (1959)
38. R. E. Dinnebier, M. Oestreich, S. Bette, D. Freyer, *ZAAC* **638** (3-4),628 (2012).

Thermodynamic Interactions of Carbonate and Fe Ion Species in Brine Solutions

Sungtae Kim, Taya Olivas, Leslie Kirkes and Terry Westfall

Sandia National Laboratories, Defense Waste Management Programs,
4100 National Parks Highway, Carlsbad, NM 88220, USA
(email): *sunkim@sandia.gov*

INTRODUCTION

The Waste Isolation Pilot Plant (WIPP) repository uses steel in the waste containers and lead in shielded containers. These metals are expected to interact strongly with sulfide, and to compete with the transuranic species in complexation of the organic ligands such as citrate, EDTA and oxalate in the brine. To estimate the consequence of potential radionuclide releases from the repository to the environment after decommissioning, it is required to recognize the solubility of the radionuclides in the brine, which is chemically equilibrated by the above interactions. The solution chemistry for brines relevant to the WIPP repository are determined by using the Pitzer model [1,2] to evaluate the activity coefficients for the various components of the brine. To date, the WIPP thermodynamic database does not incorporate iron (II), lead, or sulfide species. As part of updating the thermodynamic database, the parameters necessary for more accurate modeling are being determined. As a result, we present here the interaction of carbonate (CO_3^{2-}) to iron species (Fe^{2+}, $FeOH^+$, and $Fe(OH)_3^-$)

EXPERIMENTAL WORK

To mimic an environment consistent with the expected anoxic WIPP conditions, experiments have been performed inside a glovebox, where oxygen levels were maintained below 3 ppm. Ferrous carbonate ($FeCO_3(s)$) was synthesized based on the following chemical reaction:
$FeCl_2 \cdot 4H_2O + NaHCO_3 \rightarrow FeCO_3(s) + Na^+ + 2Cl^-$

$+ H^+ + 4H_2O$. Production of $FeCO_3(s)$ was analyzed using an x-ray diffractometer (XRD). About 0.5 gram of $FeCO_3(s)$ was added into each brine solution (X molal Na_2CO_3 + 0.15 molal NaCl, where X = 0.01, 0.1, 0.5, 1.0, 1.5, and 2.0). These samples were named as FeCO3-XCO3-5 and FeCO3-XCO3-6 (here, 5 and 6 represent replicates) and have been aged under anoxic conditions for more than 6 months. Total iron (Fe) concentrations analyzed on an inductively coupled plasma atomic emission spectrometer (ICP-AES) shows that samples aged six months have reached equilibrium (Fig. 1).
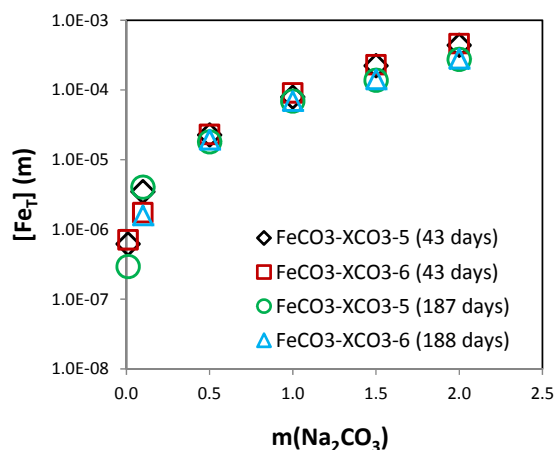

Fig. 1: Total Fe concentration in brine showing insignificant changes with the aging times

RESULTS

The +2 oxidation states of iron (Fe^{2+}) are stable over broad ranges of pH, and chemical reactions for $FeOH^+$ and $Fe(OH)_3^-$ at 25 °C are [3]:

$FeOH^+ + H^+ \rightarrow Fe^{2+} + H_2O$ logK=9.3148 (1)

$Fe(OH)_3^- + 3H^+ \rightarrow Fe^{2+} + 3H_2O$ logK=31.0   (2)
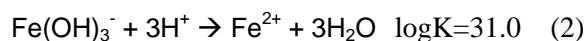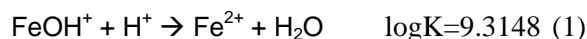
where logK is 10-based logarithm of the equilibrium constant K. For the reactions (1) and (2), due to K > 1 Fe^{2+} ion is more likely to exist than $FeOH^+$ and $Fe(OH)_3^-$. Subtraction of reaction (2) from reaction (1) leads:

$FeOH^+ + 2H_2O \rightarrow Fe(OH)_3^- + 2H^+$
$$logK = -21.6852 \ (3)$$
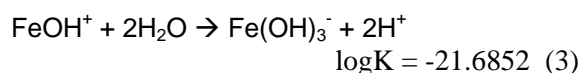
Reactions (1-3) indicate that the existence affinity becomes Fe^{2+} > $FeOH^+$ > $Fe(OH)_3^-$. However, each reaction contains H^+ ion, meaning that pH (or pmH) of solution influences the existence affinity of Fe(II) ion species. We have investigated the existence affinity of Fe(II) ion species as a function of pmH (Fig. 2). In our brine solutions, Fe^{2+} ion is a minor species, meaning that the interactions of $FeOH^+$ and $Fe(OH)_3^-$ ion species with CO_3^{2-} ion seem to be in chemical equilibrium.
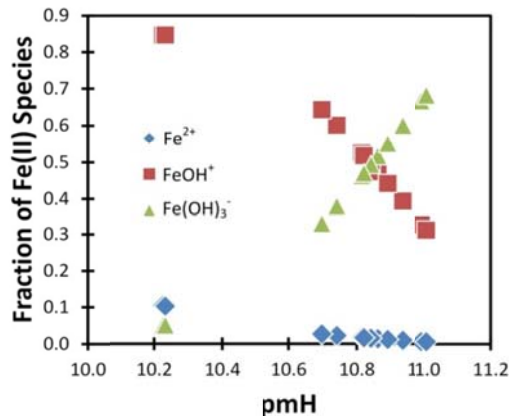
Fig. 2: Distribution of Fe(II) species with the changing pmH.

CO_3^{2-} ion interactions with Fe(II) ions in the forms of Fe^{2+}, $FeOH^+$ and $Fe(OH)_3^-$ in brine solutions, respectively, were investigated. EQ3NR packaged in EQ3/6 v.8.0a [4] and Python programming language, *EQ3CodeModule.py* [5], were implemented to calculate the aqueous speciation and saturation

indices for given EQ3NR input files (*.3i files) by referring known values of logK and Pitzer parameters. The calculation of aqueous speciation and saturation indices was repeated by adjusting these unknown Pitzer parameters until the sum of squared saturation indices (henceforth referred to as "residuals") reaches the smallest value for the given number of *.3i files.

REFERENCES

[1] PITZER, KS, "Thermodynamics of Electrolytes. I. Theoretical Basis and General Equations." Journal of Physical Chemistry, vol. 77 p. 268 (1973).

[2] PITZER, KS, "Thermodynamcis of Electrolytes. V. Effects of Higher-Order Electrostatic Terms." Journal of Solution Chemistry, vol. 4 p. 249 (1975).

[3] ymp database (**data0.ymp.R2**), one of the EQ3/6 databases that come with the installation package for EQ3/6 v.8.0a.

[4] WOLERY, TJ et al., "Verification and Validation Plan/Validation Document for EQ3/6 Version 8.0a for Actinide Chemistry, Document Ver. 8.10". Carlsbad, NM: Sandia National Laboratories, ERMS 550239 (2010); Xiong, Y-L, "WIPP Verification and Validation Plan/Validation Document for EQ3/6 Ver. 8.0a for Actinide Chemistry, Rev. 1" Carlsbad, NM: Sandia National Laboratories, ERMS 555358 (2011)

[5] KIRCHNER, TB., "User's manual for the EQ3CodeModule", Carlsbad, NM: Sandia National Laboratories, ERMS 557360 (2012).

_____

ABC-Salt III Workshop

Tuesday, April 16th
Presentation
Abstracts

This page intentionally left blank.

Microorganisms in Saline Environments

Andrea Geissler, Velina Bachvarova, Katrin Flemming, Sonja Selenska-Pobell

Helmholtz Center Dresden Rossendorf, Institute of Resource Ecology, Germany
email: a.geissler@hzdr.de

INTRODUCTION

The long-term safety of nuclear waste in deep geological repositories is an important issue in the German society. The migration of actinides and long-lived fission products within the respective host rock and the transport behaviour after a possible release from the repository should be well known. Presence of microorganisms was shown in the subsurface geologic layers, including salt formations, which are considered as potential host rocks /1/. This is of interest because microbes can affect physical and geochemical conditions (e.g. pH, Eh, release of gases) on site and they can also interact with actinides. Important interaction processes are biosorption, bioaccumulation, biotransformation, biomineralization and microbial enhanced chemisorption /2/.

Microbial communities were investigated in two different saline environments - the Arava desert in Israel and the salt formation near Gorleben in Germany.

DESCRIPTION OF THE WORK

Total DNA was recovered from the salt crust (7EY) and from 0 to 3cm depth (10EY) samples of the Arava desert and from one hydrocarbon rich sample C1 from the Gorleben site. Direct molecular analyses of prokaryotic communities were performed by using bacteria specific 16S rRNA gene primers 27F and 1513R /3/ and archaea specific 16S rRNA gene primers 21F and 968R /4/. Modified R2A medium was used for cultivation of halophilic microbial isolates as described in /5/.

RESULTS

It was demonstrated that the archaeal communities in both 7EY and 10EY samples were predominated by *Halobacteriaceae* /4/. The recently actualized affiliation of the 16S rRNA gene sequences demonstrated presence of representatives of the genera *Haloplanus, Natronomonas, Halobacterium* and *Halolamina*. Several archaeal isolates were cultivated from the salt crust sample 7EY and one of them was characterized as *Halobacterium* sp. UJ-EY-1 /5/.

As evident from the results presented in Fig. 1, on the bacterial phylum level, the samples 7EY and 10EY were predominated by *Bacteroidetes.* They were accompanied by *Firmicutes, Gamma-, Alpha-, and Deltaproteobacteria*

- all of them occurring in a sample-specific way. Additional differences were found on the species level.
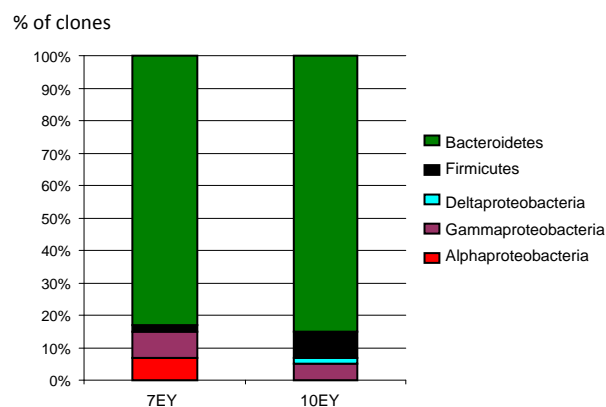
Fig. 1: Bacterial composition (phylum level) in the samples 7EY and 10EY from the Arava desert.

Preliminary results demonstrate that *Bacteroidetes* are predominant in the Gorleben sample C1 where, in addition, *Firmicutes* are rather abundant as well. Besides, different *Proteobacteria* are identified in this sample. Further investigations of microbial diversity in this and in other samples from the Gorleben site are in progress.

At this step of investigation characterization of microbial communities in salt formations, representative for potential nuclear waste disposals is ongoing. The next step will be to understand the microbe-actinide interactions of salt-specific microorganisms. This knowledge will be used to take the microbial activity into account in evaluating the long-term safety of the repositories hosted in salt formations.

REFERENCES

1. Vreeland, R.H. *et al.*: Distribution of halophilic bacteria in subsurface salt formations. Extremophiles 2, 321-31 (1998).
2. Lloyd, J. R., Macaskie, L. E.: Biochemical basis of microbe-radionuclide interactions. Interactions of Microorganisms with Radionuclides, eds. Keith-Roach, M. J., Livens, F. R. Elsevier Science Ltd., 313-342 (2002).
3. Geissler, A., Selenska-Pobell, S.: Addition of U(VI) to a uranium mining waste sample and resulting changes in the indigenous bacterial community. Geobiology 3, 275-285 (2005).
4. Buchvarova, V. *et al.*: Halophilic archaeal populations in Arava Desert (Israel) as examined by using direct molecular and cultivation methods FZR-Report 511, p. 34 (2008).
5. Jankowski, U. *et al.*: Characterization of a *Halobacterium* sp. isolate cultivated from samples collected from Arava Desert. FZR-Report 511, p. 35 (2008).

- 72 -

This page intentionally left blank.

Insights into the Biodiversity of salt sumps in the Asse II salt mine, Germany

Isabel Zirnstein[1], Thuro Arnold[1]

[1]*Helmholtz-Zentrum Dresden Rossendorf, Institute of Resource Ecology, Bautzner Landstr. 400, 01328 Dreden, Germanyy
email: i.zirnstein@hzdr.de*

INTRODUCTION

The former salt mine (1908-1964) Asse II, Germany is a final disposal site of radioactive waste. It is composed of salt rocks, which are approximately 250 million years old. The geology of the Asse salt mine is described in detail by Schwartz [1].

From 1967 to 1978, 125.787 barrels of low- and medium-grade radioactive waste produced by medicine and nuclear power plants were stored in the Asse II [2]. The waste is situated in 13 chambers in a depth of 750 and 511 meters, respectively with a total radioactivity of 2.900.000 GBq (in the year 2010). Radionuclides, which represent a large portion of the total radioactivity, are cobalt (60), nickel (63), strontium (90), cesium (137), and plutonium (241).

A number of salt sumps exist in the Asse II, which were so far not microbiologically characterized. In this study, microbiological methods, e.g. pyrosequencing, were applied to identify the microbial diversity in these unique salt sump habitats.

DESCRIPTION OF THE WORK

Samples from three salt sumps in 750m depth were taken on two sampling campaigns in December 2011 and July 2012. An example of a salt sump environment is shown in Fig. 1. Samples of 300 mL to 6 L salt solution were obtained from the Asse salt sumps.

The chemical composition of the salt solutions were analyzed for cations by inductively coupled plasma mass spectrometry (ICP-MS) and by atomic absorption spectrometry (AAS) for Na, K und Ca. Anions, i.e. chloride, nitrate, phosphate and sulfate were determined by ion chromatography.

The collected samples were examined by cultivation-independent methods. For molecular analyses the salt solutions were concentrated by centrifugation (4000×g, 30 min). After-DNA-extraction by NucleoSpinforSoil-Kit (Marchery-Nagel), DNA-amplification was performed with primers targeting the 16S rRNA gene. The forward primers were modified containing specific tags for pyrosequencing. The synthesis of the primers and the procedure of amplicon-sequencing were performed by Eurofins MWG Operon (Germany). The resulting community sequence data were analyzed by the software package MOTHUR 1.15.0 [3]. The obtained sequences were assigned into bacterial and archaeal taxonomy using the Bayesian approach and the SILVA database [4].

Fig. 1: Sampling from Asse II salt sumps in a depth of 750m.

RESULTS

Chemical Analyses

The geochemical conditions of the Asse II salt sumps in a depth of 750m was dominated by high concentration of cations e.g. Mg (108 g/L), Na (4 g/L), K (2.93 g/L), Br (3.63 g/L), Ca (24 mg/L), Mn (13 mg/L), and anions, e.g. Cl^- (274 g/L), SO_4^{2-} (28 g/L) and lower concentrations of Zn, Fe, As. The sumps in the underground Asse II galleries are characterized by a relatively constant on-site temperature ranging between 30-35°C and a pH of 4.7.

Microbial diversity

In this study, a total of 3.168 sequences, divided in 314 operational taxonomic units (OTUs), representing bacterial and archaeal groups from the underground Asse II salt mine. Fig. 2 summarizes the phylogenetic distribution of the 16S rRNA gene sequences of archaea. The class halobacteria (Euryarchaeota) dominates the archaeal community, representing 99.5% of all sequences. Halobacteria are described as the dominant microorganisms in extreme hypersaline (>20% NaCl) environments [5]. The least abundant sequences were

represented by Thermoprotei (0.34%; Crenarchaeota) and Methanobacteria (0.11%; Euryarchaeota). The halobacterial sequences are dominated by geni, e.g. *Halobacterium spp.* (~38%) and unclassified halobacteria (~41%). Other halobacteria, extracted from the salt sumps, are *Halolamina spp.* (9.34%), *Haloplanus spp.* (6.09%), *Halorhabdus spp.* (2.88%) and *Halorubrum spp.* (1.42%). Halobacteria, which were detected with <1% are *Haloarcula spp., Halomarina spp., Halomicrobium spp., Halonotius spp., Halosimplex spp., Natronomonas spp.* and *Salarchaeum spp.*. The halophilic *Methanobrevibacter spp.* and *Methanosphaera spp.* belonging to Methanobacteria were extracted with <1%.
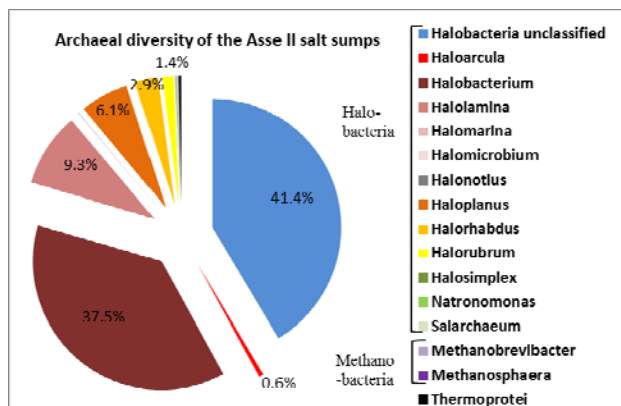

Fig. 2: Phylogenetic distribution of archaeal sequences observed in the Asse II salt sumps. The similarity of the above listed archaea with the SILVA database [4] is greater than 90 %.

In addition, halophilic bacteria have been detected in the salt sumps of the underground Asse II mine. A total of 8 phyla of bacteria were identified by 16S rRNA sequence analyzes. The dominating phylum are Firmicutes (e.g. Bacilli, Halocella, Filifactor, Veillonella) with ~51% of all detected bacterial sequences, followed by Proteobacteria (Marinobacter, Hyphomicrobium, Methylophilus, Pseudomonas, Sphingomonas) with ~19%. Similar to these results, other studies reporting on the bacterial diversity in hypersaline environments, also found that Bacteroidetes, Firmicutes, and/or Proteobacteria accounted for the majority of the bacterial taxa [6, 7]. A large proportion of the detected bacterial sequences from the Asse II salt sumps were affiliated with Bacteroidetes (8.3%), TM7 (10.4%) and Actinobacteria (7.3%). The bacterial phyla Verrucomicrobia (2%), Acidobacteria (1%) and Deinococcus-Thermus (1%) were only found in minor proportions.

Halophilic archaea and bacteria have been identified in underground salt environments, e.g. the WIPP site in New Mexico (USA) [8, 9].

This study identified for the first time extreme halophilic bacteria and archaea in the underground salt sumps of the Asse II environment. For generating a final

disposal site, not only geological, chemical or physical, but also microbiological aspects are important to consider. The microbiological influence in respect to transport of radionuclides, on barrier stability and on oxidation/corrosion of container materials in repositories in salt formations are still open questions which have to be addressed in future studies.

REFERENCES

[1] SCHWARTZ, M.O. "Modelling groundwater contamination above the Asse 2 medium-level nuclear waste repository, Germany." *Environmental Earth Sciences,* 59(2): 277-286 (2009).

[2] METZ *et al*. "Geochemically derived non-gaseous radionuclide source term for the Asse salt mine-assessment for the use of a Mg(OH)$_2$-based backfill material." *Radiochimica Acta* 92(9-11): 819-825 (2004).

[3] SCHLOSS, P.D. *et al.* "Introducing mothur: open source, platform-independent, community-supported software for describing and comparing microbial communities". *Applied and Environmental Microbiology* 75: 7537–7541 (2009).

[4] http://www.arbsilva.de

[5] BENLLOCH, S. *et al*. "Description of prokaryotic biodiversity along the salinity gradient of a multipond solar saltern by direct PCR amplification of 16S rDNA." *Hydrobiologia* 329: 19-31 (1996).

[6] MOUNÉ, S. *et al. "*Molecular sequence analysis of prokaryotic diversity in the anoxic sediments underlying cyanobacterial mats of two hypersaline ponds in Mediterranean salterns." *FEMSMicrobiol. Ecol.* 44: 117–130 (2003).

[7] HOLLISTER, E.B. "Shifts in microbial community structure along an ecological gradient of hypersaline soils and sediments." *ISME J.* 4: 829–838 (2010).

[8] FRANCIS A.J. *et al.* "Uranium association with halophilic and non-halophilic bacteria and archaea." *Radiochimica Acta,* 92(8): 481-488 (2004).

[9] SWANSON J.S. "Degradation of Organic Complexing Agents by Halophilic Microorganisms in Brines." *Geomicrobiology Journal* 30(3): 189-198 (2013).

Update on Microbiology Research at the Waste Isolation Pilot Plant

Juliet S. Swanson[1], Karen A. Simmons, David A. Ams, Jean-François Lucchini, Donald T. Reed

Los Alamos National Laboratory—Carlsbad Operations
1400 University Drive, Carlsbad, NM USA
email: jsswanson@lanl.gov

INTRODUCTION

This talk provides an update on the microbiology research conducted in support of the Waste Isolation Pilot Plant (WIPP). Topics discussed include microbial characterization, degradation of organic waste components, microbially enhanced reduction and/or precipitation of metals, and biosorption of actinides.

METHOD OVERVIEW

A description of the microbial characterization and biosorption studies can be found in other workshop presentations. Work on cellulose degradation was carried out with fungi isolated from WIPP halite and grown on solid media containing either carboxymethylcellulose or Kimwipes as the sole carbon source. Iron reduction studies were carried out using organisms isolated from groundwaters with differing ionic strengths. Organisms were inoculated into growth media with iron (III) as the terminal electron acceptor.

RESULTS

Characterization studies support the hypothesis that microorganisms within the repository will be less active than predicted by the performance model, and that far-field organisms will exhibit a higher metabolic diversity than those in the near-field. This is due to the thermodynamic constraints of survival in hypersaline environments, leading to a decrease in diversity as salinity increases, and has a profound impact on the adverse effects attributed to microbial activity in waste repositories. Various assumptions regarding microbial influence on the performance of nuclear waste repositories are reviewed in light of information obtained in the characterization studies [1, 2].

The WIPP near-field environment will be dominated by haloarchaea. These organisms are well adapted to the high ionic strength conditions of the repository brines and are capable of aerobic degradation of certain complexing agents, but they are unable to grow under anaerobic conditions [3]. The WIPP far-field environment, the Culebra aquifer, supports the existence of halophilic bacteria with diverse metabolic capability, including aerobic and anaerobic respiration and fermentation. Although these organisms are unlikely to survive in high ionic strength brines in the near-field, they may degrade complexing agents or reduce metals/actinides should those waste components reach the far-field.

Fungal isolates have also been obtained that are able to grow on cellulose as the sole carbon source [4]. However, they are obligately aerobic, suggesting that their role in cellulose hydrolysis will be limited to the repository's oxic phase.

Fig 1: Growth of fungus Cladosporium on Kimwipe.

Iron reduction was shown previously in incubations of groundwater organisms at both low (1.5 M) and high (3.7 M) ionic strength. Substrate fermentation caused a shift in redox potential, leading to the indirect reduction of iron in the 3.7 M incubation; whereas, direct reduction likely occurred in the 1.5 M incubation. Additionally, iron reduction was observed in abiotic (control) incubations. The fraction of reduced to total iron showed an apparent increase with increasing ionic strength, but this was due to a decrease in iron solubility. The rate of reduction appeared to be correlated with NaCl concentration, with faster rates of reduction observed at lower ionic strengths. Whether these findings extend to actinides in similar media is under investigation.
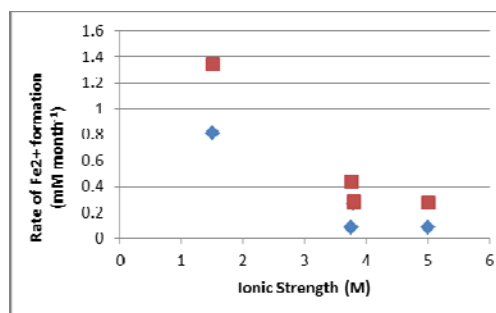
Fig 2: Rates of iron reduction as a function of [NaCl]

Biosorption of actinides onto microbial surfaces shows a dependence upon ionic strength, pC_{H+}, organism, and actinide [5]. The extent of sorption onto *Chromohalobacter* was higher at 4 M NaCl than 2 M. Sorption also increased with increasing pC_{H+}, until carbonate complexation competed with cell surface functional groups. *Chromohalobacter*, a bacterium, also exhibited more sorption than *Halobacterium noricense*, an archaeon. Finally, the extent of thorium sorption was less than that of neodymium, and both were reduced in the presence of EDTA.
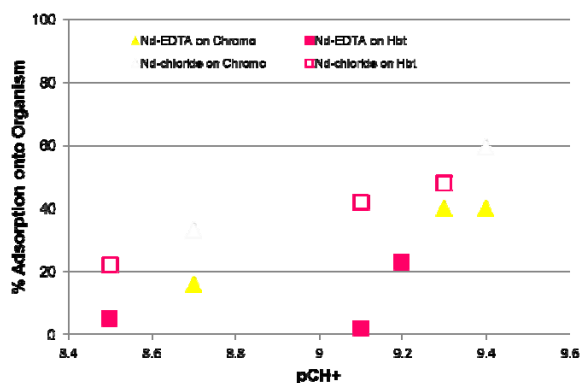
Fig. 3: Adsorption of neodymium onto Bacteria (*Chromohalobacter*) and Archaea (*Halobacterium*, Hbt) as a function of pC_{H+} and EDTA complexation.

REFERENCES

1. Compliance Recertification Application for the Waste Isolation Pilot Plant. 2009. Title 40 CFR Part 191; Subparts B and C; Appendix SOTERM-2009, Actinide Chemistry Source Term. United States Department of Energy—Carlsbad Field Office/Waste Isolation Pilot Plant; Carlsbad, NM.
2. OREN A. "Thermodynamic limits to microbial life at high salt concentrations" *Environmental Microbiology* **13**, 1908-1923 (2011).
3. SWANSON JS et al., "Degradation of organic complexing agents by halophilic microorganisms in brines" *Geomicrobiology Journal* 30, 189-198 (2013).
4. GUNDE-CIMERMAN N. et al., "Halotolerant and halophilic fungi" *Mycological Research*, **113**, 1231-1241 (2009).
5. AMS DA et al., "The effect of high ionic strength on neptunium (V) adsorption to a halophilic bacterium", *Geochimica et Cosmochimica Acta*, in press (2013).

Solubility of Thorium in WIPP Brine

Marian Borkowski, Mike Richmann, Jean-Francois Lucchini, Julie Swanson, Danielle Cleveland, Donald Reed.

Earth and Environmental Sciences, Los Alamos National Laboratory- Carlsbad Operations, 1400 University Drive, Carlsbad, NM 88220, USA
email: marian@lanl.gov

INTRODUCTION

The solubility of thorium oxide and/or its hydroxide forms have been studied at different ionic strengths for many years. Thorium has a very stable tetravalent oxidation state, and for this reason, the environmental chemistry of Th(IV) is understood from the perspective of the solubility and complexation of this species. This redox stability is the reason thorium is often used as an analog for other tetravalent actinides such as Pu(IV). Of the tetravalent actinides, plutonium (IV) is the most important species with respect to the potential for TRU release from the WIPP environment should dissolved brine (DBR) and transport release scenarios become important.

DESCRIPTION OF THE WORK

The experiments in carbonate-free and carbonate-containing Waste Isolated Pilot Plant (WIPP) simulated brine were conducted to establish the effects of carbonate, pC_{H+}, and time on thorium (IV) solubility. Ultracentifugation and sequential filtration were used to determine the colloidal contribution to the total dissolved thorium (IV) concentration. Total thorium concentration was measured using ICP-MS (Agilent model 7500 ce).

RESULTS

After 2 years of equilibration in carbonate-free brine the measured solubility of thorium was $6\text{-}7\times10^{-7}$ M and was essentially independent of pH and brine composition over the 6.5 to 11.5 pC_{H+} range investigated (see Figure 1). Sequential filtration to ~ 10 nm pore size had little effect on the measured concentration. Subsequent ultracentrifugation up to 1,000,000 g resulted in up to a 40% colloidal fraction indicating that there was relatively little intrinsic colloid formation. The steady-state thorium concentrations we measured are consistent with literature reports for simplified brine systems [1] but show a significantly lower extent of aggregation to form intrinsic colloids [2].

After an additional 2 years of equilibration the thorium concentrations in GWB brine carbonate-free significantly decreased (green points in the Figure 1). In the pC_{H+} range between 7.5 and 8.3 for some samples the thorium concentration was not changed, for others it decreased by over one order of magnitude and were very
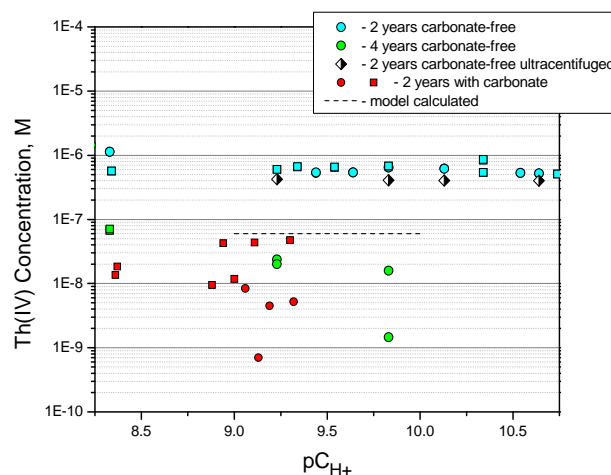
Fig. 1: The concentration of thorium measured in WIPP simulated brine as a function of time, filtration and the presence of carbonate. Although high, but metastable, concentrations were initially present, in time the measured concentrations decreased and are conservatively below the WIPP model-predicted values.

close to the thorium concentrations measured in GWB brine containing 10^{-2} and 10^{-3} M carbonate.

The presence of carbonate at concentration 10-fold greater than expected in WIPP had little/no effect on the measured thorium concentrations. After two years of equilibration the thorium concentrations measured from under- and oversaturation in GWB brine did not depend on carbonate concentration. Concentrations measured from oversaturation were 2.5 orders of magnitude greater than those measured from undersaturation indicating that metastable states can last a long period of time. The trend of oversaturation data is consisted with the literature data [3]. In the undersaturation experiments which are more relevant to the WIPP situation, the average thorium concentration was 2×10^{-8} M and continued to decrease at $pC_{H+} > 9$. The oversaturation experiments showed a

similar trend and at $pC_{H+} > 9$ the thorium concentrations decreased to below 10^{-8} M. These results reproduce, to some extent, the trends reported in the literature [3], but the much higher ionic strength solutions used in our experiments shift our data to a lower pC_{H+} value by approximately 1 pH unit.

At the expected WIPP repository pC_{H+} (~ 9.5), in the presence of carbonate, the thorium concentrations in GWB brine were 2×10^{-8} M or lower. This concentration trend suggests that at repository conditions the mixed thorium hydroxy-carbonato complexes do not play any role in the thorium solubility at $pC_{H+} > 9$.
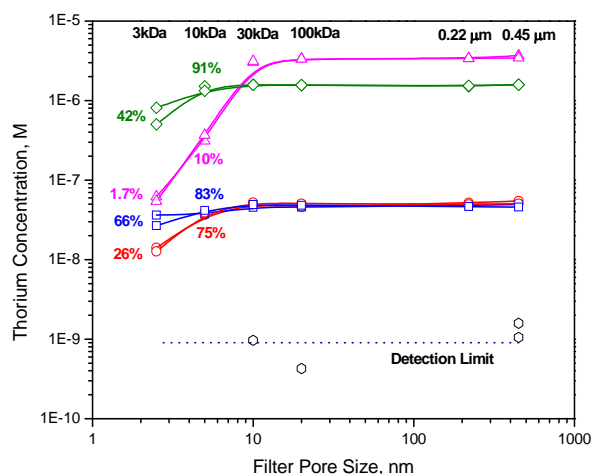
Fig. 2:   Distribution of thorium concentrations in simulated WIPP brine measured as a function of pore size.

The sequential filtration of thorium in the carbonate system, Figure 2, led to a dissolved thorium concentrations in GWB in the range of $2\text{-}6\times10^{-8}$ M. In ERDA-6 brines, however, the dissolved thorium concentration was about 10 fold greater and steady state thorium concentrations were not achieved. The colloidal thorium species appear to be very small, less than 10 kDa. Overall, the truly dissolved thorium concentration was $3(\pm2)\times10^{-8}$ M. The average total thorium concentration consists of 30 - 60% dissolved fraction and 40 - 70% colloidal fraction.

The thorium solubility results summarized in [2] support the ongoing WIPP recertification effort in three important ways: 1) they provide empirical solubilities over a broad range of conditions that improve the robustness of the WIPP PA model, 2) they resolve and address published literature data in simplified brine systems that appeared to disagree with the current WIPP PA approach, and 3) they provide an input that will help establish the intrinsic colloidal enhancement factors for

IV actinides. There is general agreement between our data and results reported in the literature for simplified brine systems, although we are seeing a far lower colloidal fraction in the total concentrations measured. After 4 years of equilibration our measured solubilities are slightly lower (by a factor of ~ 2) than the Performance Assessment, PA, calculated solubilities but are well within the order of magnitude agreement typically observed between calculated and measured solubilities in complex brine systems.

These solubility data support the current WIPP PA assumptions on An(IV) solubility and extend past project data to a broader range of pH and carbonate levels. These results also note that Ca-enhanced hydroxyl complexation can greatly increase the solubility of actinides (IV) [4], something that has only been understood in the last couple of years; however this complexation requires relatively high pH in combination with very high Ca levels, something that is not expected in the WIPP. The expected pH and dissolved Ca levels in WIPP predict no effect on An(IV) dissolved concentration due to formation of this complex.

REFERENCES

1. ALTMAIER M., et al., "Solubility and Colloid Formation of Th(IV) in Concentrated NaCl and MgCl$_2$ Solution" *Radiochimica Acta* **92**, 537-543 (2004).

2. BORKOWSKI M., et al., "Solubility of An(IV) in WIPP Brine: Thorium Analog Studies in WIPP Simulated Brine" LCO-ACP-17 Report (2013)

3. ALTMAIER M., et al., "Solubility of ThO$_2$.xH$_2$O(am) and Formation Ternary Th(IV) Hydroxide-Carbonate Complexes" *Radiochimica Acta* **93**, 83-92 (2005).

4. ALTMAIER M., et al., "Solubility of Zr(IV), Th(IV) and Pu(IV) Hydrous Oxides in CaCl$_2$ Solutions and the Formation of Ternary Ca-M-OH Complexes" *Radiochimica Acta* **94**, 495-500 (2006).

Actinide Chemistry in Alkaline High Ionic-Strength Solutions

D.T. Hobbs, L.N. Oji, K.M.L. Taylor-Pashow, W.R. Wilmarth
Savannah River National Laboratory
Aiken, SC 29808

The production of nuclear materials for defense began at the Savannah River Site (SRS) in the 1950s. Chemical residues from the production processes were released to underground carbon steel tanks after the addition of concentrated sodium hydroxide solution. The highly alkaline conditions precipitated the bulk of the metallic elements as metal hydroxides and hydrous metal oxides, which gravity settle in the storage tanks into a concentrated solids layer referred to as sludge. To conserve tank space, the supernatant liquids were evaporated and cooled to produce crystalline salts. Thus, the high level waste (HLW) at SRS presently consists of sludge, saltcake and supernatant.

The hydroxide concentration in the supernatant can range from about 1.0 M to 17 M. Other major components include nitrate, nitrite, aluminate, carbonate, and sulfate. Disposition of the HLW will separate the radioactivity from the HLW supernatant, which will be combined with the sludge, and incorporated into a borosilicate glass wasteform in the Defense Waste Processing Facility (DWPF). Two separation processes are used at SRS, (1) ^{90}Sr and alpha-emitting radionuclides of uranium, neptunium, plutonium and americium are removed by adsorption onto monosodium titanate (MST) and (2) $^{134/137}$Cs is removed by liquid/liquid extraction using a calixarene extractant.

Monosodium titanate, $NaHTi_2O_5 \cdot xH_2O$, is an effective ion exchanger in weakly acidic, neutral and alkaline solutions including high ionic strength solutions. The actinide removal performance of MST is influenced by ionic strength. However, laboratory and operating experience has shown that MST will meet processing requirements for waste solutions with sodium ion concentrations as high as 8.0 M. Since 2008, MST has been used at SRS in the Actinide Removal Process (ARP) facility to treat more than 4 million gallons of HLW. In the ARP operation, MST is added as a fine powder and contacted with the waste solution for 12 hours before separating by ultrafiltration. A peroxide-modified sodium titanate, referred to a modified MST or mMST, has recently been developed that features much faster removal of strontium and plutonium. Figure 1 shows a plot of plutonium concentration versus time upon contact of a 5.6 M sodium salt solution with MST and mMST.

The DWPF returns a relatively dilute wastewater stream to the HLW tank farm. Upon startup of the DWPF in 1996, this recycle water was discharged to Tank 43H where it was mixed with typical fuel reprocessing wastes and evaporated using the 242-16H (2H) evaporator. Problems with chemical incompatibility between the silicon-containing DWPF recycle and the aluminum containing fuel reprocessing waste initially manifested as an aluminosilicate deposit in the concentrate line from the evaporator in July 1997. These aluminosilicate deposits were removed with high-pressure water. Frequent video inspections showed improved evaporator operation occurred during 1998. However, significant aluminosilicate scale build-up was subsequently observed in the evaporator vessel in October 1999. Figure 2 shows a photograph of the interior of the evaporator vessel with the scale deposits.

These aluminosilicate solids also included significant quantities of enriched uranium. This uranium accumulation mechanism had not been previously identified nor analyzed for criticality safety. Thus, a significant research effort was undertaken to understand reaction thermodynamics and kinetics, use of inhibiting agents for deposition and particle growth, role of hydrodynamics in deposition location and rate of growth, and thermodynamic modeling for use as a predictive process control strategy for continued operation of the SRS evaporators. Based on this work, controls were developed to limit the concentrations of silicon in high-aluminum bearing waste solutions.

The presence of the enriched uranium in the evaporator scale deposits presents a criticality safety concern during removal of the deposits and subsequent processing for return to the HLW tank farm. Dissolution of the scale in nitric acid, isotopic dilution of the enriched uranium with depleted uranium followed by the addition of concentrated sodium hydroxide was selected to successfully clean the evaporator vessel and return the uranium to the HLW tank farm. Furthermore, an isotopic dilution method was developed and successfully deployed in Tank 43H to reduce the ^{235}U enrichment in the supernatant from 3.1 wt % to <0.96 wt %. This process featured the measured addition of an alkaline carbonate solution of depleted uranium to the mixing zone of a Flygt mixed installed in Tank 43H.
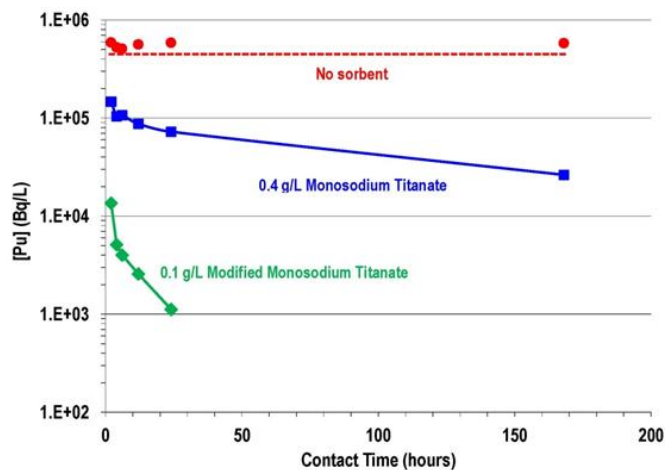
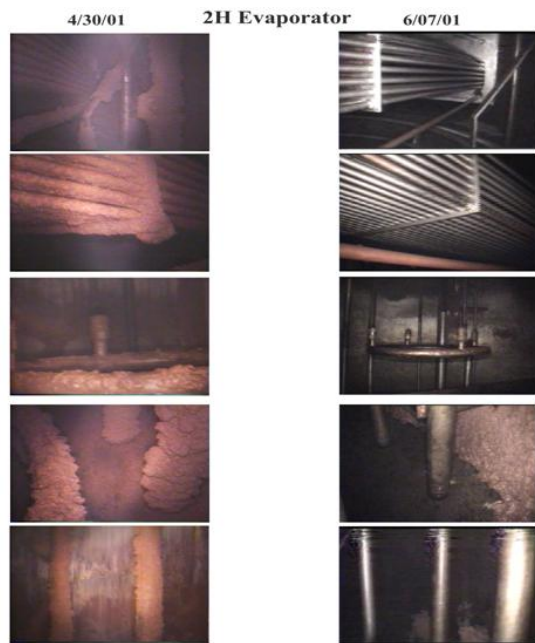**Figure 1. Plot of Plutonium Activity (Bq/L) versus Time upon contact of a 5.6 M sodium salt solution with MST and mMST**

Figure 2. Photographs of the interior of 2H-evaporator with and without scale deposits

Re-assessment of the WIPP Actinide Colloid Model

D.T. Reed, J.S. Swanson, J.F. Lucchini, M.K. Richmann and M. Borkowski

Earth and Environmental Sciences Division, Los Alamos National Laboratory, 1400 University Drive, Carlsbad NM, USA
dreed@lanl.gov

INTRODUCTION

The Waste Isolation Pilot Plant (WIPP), located in South-Eastern New Mexico, has operated for over ten years as the only working TRU repository in the United States. It is the continuing success of this repository that is the basis of discussions to evaluate salt-based repository concepts for the permanent disposal of high level and spent fuel nuclear waste. In the WIPP safety case, colloidal actinide species are considered because they can contribute to the source term in the unlikely scenario of brine inundation.

The current WIPP colloid model [1] was based on an extensive literature review, some WIPP-specific experimental data, and some conservative simplifications that were extensively peer reviewed prior to the first license application. In this model, four types of colloids that could contribute to the actinide source term are identified: mineral, intrinsic, humic and microbial:

1. *Mineral fragment colloids: hydrophobic, hard-sphere particles that are kinetically stabilized or destabilized by electrostatic forces, and may consist of crystalline or amorphous solids that act as substrates for sorption of actinides.*

2. *Actinide intrinsic colloids: hydrophilic macromolecules of actinides (e.g., true colloids, nanoclusters, polymers)*

3. *Humic colloids: hydrophilic, soft-sphere organic particles that are stabilized by solvation forces.*

4. *Microbial colloids: microbes that may act as substrates for extracellular actinide sorption or they may actively bioaccumulate actinides intracellularly.*

There has been essentially no change in this model and the associated model parameters since the initial certification of the WIPP by the EPA in 1998. The model parameters, however, were reevaluated in light of more recently published results and our current understanding of the nature and structure of actinide colloids. Additionally, analyses to re-examine the mineral, intrinsic and microbial contribution to the WIPP mobile colloidal actinide source term were also performed [2]. These data were used to update the colloid model parameters. A revision of the overall model itself, given the many new insights to the colloid issue over the past ~ 20 years, is identified as a likely future need to strengthen the safety case for a nuclear waste repository in salt.

DESCRIPTION OF THE WORK

The intrinsic and to a lesser extent the mineral colloidal actinide fraction was evaluated by examining size distribution of actinide/analog species in our WIPP-specific long-term solubility studies through sequential ultrafiltration and, in some cases, ultracentrifugation. Actinide/analog samples were consecutively filtered through different pore size filters (Fisher Amicon® ultrafilters). The following pore size filters were used: 0.45µm, 0.22µm, ~20nm (100kDa), ~10nm (30kDa), ~5nm (10kDa), and ~2.5nm (3kDa). That this approach did not impact the apparent actinide/analog concentrations was established by filtration of species known to be non-colloidal (see Fig. 1).
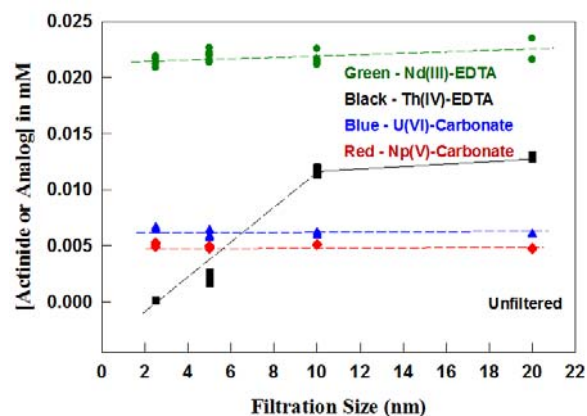
Fig. 1 Effect of the sequential filtration approach on dissolved actinide species in GWB brine at pC_{H+} ~ 9. For the Nd-EDTA, U-carbonate, and Np(V)-carbonate systems essentially full recovery of the actinide/analog was obtained. A significant filtration effect is noted for Th-EDTA in an analogous brine system where truly dissolved species were not expected.

The biosorption of An(III) and An(IV) actinides, in the presence and absence of EDTA, was also determined experimentally in WIPP brine using redox-invariant analogs (Nd^{3+} and Th^{4+}). The WIPP-indigenous microorganisms investigated were *Halobacterium noricense* (archaea) and *Chromohalobacter sp.* (bacteria). These were rinsed three times with 4M NaCl, weighed, and re-suspended in pC_{H+}-specific brines to obtain a concentration of 20g/L. The biosorption experiments were initiated when same-pH solutions of the actinide/analog species and the microorganism suspensions were mixed together. The experiments were slowly agitated for ~2

hours to ensure homogenization of the mixture and to reach equilibrium. The filtered supernatants were analyzed using ICP-MS. The extent of sorption is defined as the amount of the actinide/analog that became associated with the biomass (difference between initial concentration and concentration in the filtrate).

RESULTS

In the actinide/analog brine solubility studies that were analyzed by sequential filtration, we observed <10 nm species in all cases investigated – specifically for the Nd(III), Pu(III), Th(IV) and U(VI) systems (see Table 1). The proposed changes make the current parameter set consistent with the supporting recertification documentation that intrinsic colloids are correlated with the oxidation state of the actinide. This also addresses the several observations in the literature that actinides other than plutonium can also form intrinsic colloids. These changes, taken together, continue to show that the intrinsic colloidal contributions do not significantly impact calculated actinide concentrations and increase the robustness of the current WIPP PA position on all actinides that contribute to the potential for actinide release from the WIPP.

Table 1. Summary of Observed Intrinsic Colloidal Fraction and Comparison to Existing WIPP Parameters			
Actinide/Analog	% Intrinsic Colloidal Fraction (<10 nm)	Equivalent [Actinide/analog] in M and % of WIPP PA calculated or assumed actinide/analog solubility*	Current CRA-2009 Intrinsic colloid enhancement parameter (M)
Nd(III)	~ 33%	~4 x 10^{-9} M (0.2%)	0
Pu(III)	~ 79%	~ 4 x 10^{-9} M (0.2%)	1 x 10^{-9} M
Th(IV)	~ 33%	~2 x 10^{-8} M (34%)	0
U(VI)	~ 2.5%	~1 x 10^{-8}M (0.1%)	0
*Solubilities used were those calculated for the CRA-2009 PABC			

The initial conclusions and observations that led to the current mineral colloid enhancement parameters were that only iron oxides, specifically goethite and magnetite, formed actinide mineral colloids in the systems investigated. There were no colloidal enhancements noted that could be attributed to the presence of Mg phases in our long-term studies. The plutonium experiments performed included iron and showed that the iron oxides generated due to anoxic corrosion in WIPP brine led to some mineral colloid formation. At the most repository-relevant pH (~ 9.5), a significant amount of Pu^{3+} was associated with the iron in solution corresponding to additional plutonium concentrations of 8.6 x 10^{-9} M to 2.3 x 10^{-8} M respectively. This is consistent with the 2.6 x 10^{-8} M that is currently in the WIPP model.

The biosorption experiments, performed at pC_{H+} ~ 9-10 were difficult to interpret because of the coupling of

sorption and precipitation (see Fig. 2). The biosorption of actinides towards microorganisms should correlate with their aqueous speciation. For this reason, it would be expected that similar oxidation states would exhibit similar biosorption behavior, at least to the extent that their aqueous speciation is similar.
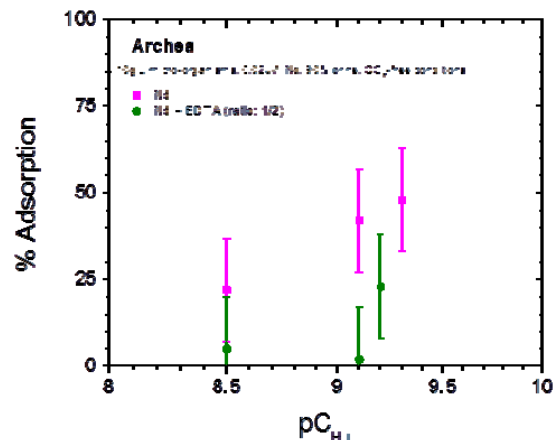
Fig. 2 Adsorption of neodymium (in %) measured in carbonate-free brines (90% saturated composition) at different pC_{H+} values, in the presence (green symbols) or the absence (pink symbols) of EDTA.

A notable observation is that the extent of biosorption is different for *Bacteria* and *Archaea*. In both +3 and +4 cases and in both Francis et al. [3] and our current work, the biosorption values obtained for *Archaea* are less than those for *Bacteria*. Changes proposed include relying on *Archaeal* data since these microorganisms are likely to predominate in the WIPP repository. The maximum biosorption parameters are also now based on the estimated amount of bio-associated actinide/analog with conservatively high esitmates of the achievable biomass concentrations - rather than estimated from toxicity data. These changes lead to decreased, but still conservative, microbial colloid enhancement parameters and lower biocolloid formation.

REFERENCES

1. Compliance Certification Application for the Waste Isolation Pilot Plant, Appendix SOTERM. Title 40 CFR Part 191, Subparts B and C. Actinide Chemistry Source Term. 1996. United States Department of Energy/Waste Isolation Pilot Plant. Carlsbad Field Office; Carlsbad, NM.

2. Reed, D.T., J.S. Swanson, J.F. Lucchini, and M.K. Richmann, "Intrinsic, Mineral and Microbial Colloid Enhancement Parameters for the WIPP Actinide Source Term", LANL report LCO-ACP-18, 2013.

3. Francis A.J., J.B. Gillow, C.J. Dodge, M. Dunn, K. Mantione, B.A. Strietelmeier, M.E. Pansoy-Hjelvik, H.W. Papenguth. 1998. "Role of Bacteria as Biocolloids in the Transport of Actinides from a Deep Underground Radioactive Waste Repository." *Radiochimica Acta,* vol. 82: 347-354.

Actinide Materials: Uranyl Peroxide Cage Clusters

Ginger E. Sigmon[1], Christine M. Wallace[1], Ernest M. Wylie[1], Kristi L. Pellegrini[1], Brendan McGrail[1], Peter C. Burns[1,2]

[1]*Department of Civil & Environmental Engineering and Earth Sciences, 156 Fitzpatrick Hall, University of Notre Dame, 46556, USA*
email: gsigmon@nd.edu
[2]*Department of Chemistry and Biochemistry, University of Notre Dame, 46556, USA*

INTRODUCTION

Uranyl peroxide cage clusters were discovered in 2005 and over 40 different clusters have been published and structurally characterized [1]. All clusters contain uranyl ions bridged by bidentate peroxide ligands and other ligands such as two hydroxide groups, pyrophosphate, or oxalate.

Crystals of the uranyl cage clusters are synthesized in aqueous solution at ambient temperatures by combining uranyl ions with peroxide at elevated pH. Clusters form in as little time of 1 hour confirmed by small-angle X-ray scattering (SAXS) and others crystallize in as little time of 15 minutes. A typical synthesis of U60 (a uranyl cage cluster containing 60 uranyl peroxide polyhedra) crystallizes by slow evaporation in air within seven days in a pH range of 8.5 to 9.5 [2]. Single crystal X-ray diffraction was used to determine the structure of the known cage clusters and current studies are examining clusters in solution.

DESCRIPTION OF THE WORK

Our research is currently focused on the aqueous behaviour of uranyl peroxide cage clusters in solution. The syntheses of U60 and U24P have been optimized and are the most heavily studied. Once crystallized, the clusters are dissolved in ultrapure water to yield a mono-dispersed solution (Fig. 1). Techniques such as small angle X-ray scattering (SAXS) and dynamic light scattering (DLS) are used to determine the size and shape of clusters in solution. Assembly mechanisms of the clusters are investigated using Raman spectroscopy and electro-spray ionization mass spectrometry (ESI-MS).

RESULTS

ESI-MS spectra show that U60 is persistent in solution for a period of close to one year and thermodynamic studies have shown that U60 clusters are stable relative to the oxides [3]. Counter-cations associated with the clusters can be exchanged in solution and a mass shift is observed. The addition of cations in solution causes the cage clusters to aggregate. The aggregation behavior is closely monitored using SAXS and DLS showing particles in the size range of 30-50 nm.
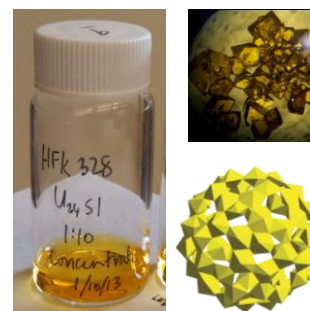
Fig. 1: Solution of U60, crystals of U60 and the U60 cage cluster.

Raman spectroscopy demonstrates cluster formation from the starting materials of dissolved uranyl ions, peroxide, and base. Over a period of a few hours, all free peroxide in the synthesis is bound to the uranyl ion in solution forming clusters (Fig. 2).
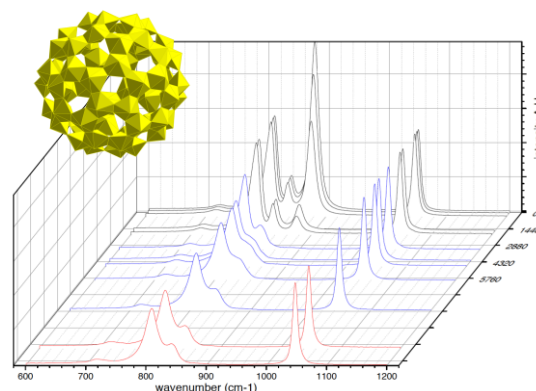
Fig. 2: Raman spectra of U60 clusters in solution overtime.

Applications of this research are found in the nuclear energy cycle. Separations of uranium from used fuel would allow for a closed fuel cycle. This separation technique is based on mass filtration. Forming uranyl peroxide cage clusters in solution from uranium oxide allows for a one step conversion from U(IV) to U(VI). Several methods have been tested to complete the

separations by mass such as centrifugation through filters and stir cell filters. We are further examining stirred cell filtration where gas pressure is used to push solutions across various membranes. This process allows us to have more control over the pore size of the filter and speed of filtration. Currently these separations show we are capable of removing uranyl clusters from ultrapure water, but dissolved cations remain with the clusters instead of passing through the membranes. Future studies will look at separating the clusters from cations of interest.

REFERENCES

1. Qiu, J. and Burns, P.C. "Clusters of Actinides with Oxide, Peroxide, or Hydroxide Bridges" Chemical Reviews, 113, 1097-1120 (2013).

2. Sigmon, G.E. et al. "Symmetry versus Minimal Pentagonal Adjacencies in Uranium-Based Polyoxometalate Fullerene Topologies" Angewandte Chem., Int. Ed, 48, 2737-2740 (2009).

3. Armstrong, C.R. et al. "Uranyl peroxide enhanced nuclear fuel corrosion in seawater" PNAS, 109, 1874-1877 (2012).

Recent Activities on HLW and Spent Nuclear Fuel Related Research at KIT-INE

B. Kienzler, V. Metz, E. González-Robles, E. Bohnert, A. Loida, N. Müller

Karlsruhe Institute of Technology, Institute for Nuclear Waste Disposal, P.O. Box 3640, 76021 Karlsruhe, Germany

bernhard.kienzler@kit.edu; volker.metz@kit.edu

RESEARCH ON SPENT NUCLEAR FUEL

Since 1990, the corrosion of used (spent) nuclear fuel (SNF) and the scientific description of radionuclide mobilization from HLW (SNF, glass) are investigated under disposal relevant conditions. The specific approach adopted in recent SNF studies includes:

- The atmosphere of the experiments range from anaerobic conditions (Ar atmosphere or Ar with radiolytically produced hydrogen) as well as strongly reducing atmospheric conditions with up to 8 bar H_2 partial pressure and/or in the presence of corroding iron.
- The corroding solutions include distilled water, concentrated NaCl solutions, a typical Gorleben $MgCl_2$ brine, and artificial cement pore waters. The pH in solution was ranging from $-\log m_{H_+} = 4.9$ in the Gorleben brine, 6.5 in DIW, 7.0 – 8.0 in NaCl solutions and > 12.5 in the cement pore water.
- The SNF used in all experiments is a UO_2 fuel, produced by AREVA by the "NIKUSI" two steps low temperature sintering process at 1100 to 1200°C in CO_2 atmosphere with subsequent reduction in hydrogen atmosphere. The fuel did not contain any additives. The fuel had an initial enrichment of 3.8 wt.% [235]U and was irradiated in the Gösgen PWR to a burn-up of 50.4 GWd/t_{HM}.
- Most of the experiments are performed with complete SNF pellets including the zircaloy cladding.

In some experiments, the impact of near-field materials on the SNF corrosion rates has been analysed. The investigated materials were iron, magnetite, hydroxyapatite and bentonite. Under reducing conditions in the presence of molecular hydrogen the corrosion rate of the SNF decreased significantly. This effect was explained by hydrogen impeding the radiolytic decomposition of the solution and subsequent inhibition of the corrosion of the $UO_2(s)$ matrix. However, solutions found in German rocksalt formations contain up to 1 mmol Br^-. This anion interferes with the radiolytic scheme by preventing the recombination of oxidizing species. It was found that in the presence of Br^-, the SNF corrosion rate was not reduced, even under partial pressure of 8 bar H_2.

Fig. 1: *HLW material is investigated at the Institute for Nuclear Waste Disposal (INE) at KIT. Above: SNF leaching experiments. Below: hot-cell facility at KIT-INE.*

FIRST NUCLDES PROJECT

Since 2011, KIT-INE is the coordinator of the Collaborative Project (CP) Fast / Instant Release of Safety Relevant Radionuclides from Spent Nuclear Fuel (FIRST-Nuclides). This project is funded by the European Commission (by 50% of total costs) within the 7th Framework Programme Topic Fission-2011-1.1.1 "research activities in support of implementation of geological disposal". The CP started in January 2012 and has duration of 36 month. The objectives of the project are in line with the Vision Report and the Strategic Research Agenda (SRA) of the "Implementing Geological Disposal – Technology Platform (IGD-TP)". Six experimental facilities having specialized installations and equipment for work with highly radioactive materials and four organizations having specific knowledge enter into an Inter-European collaboration. The experimental facilities perform studies using high burn-up spent nuclear fuels in combination with advanced analytical methods. Several organisations from France (Commissariat à l'énergie atomique et aux énergies alternatives, CEA), USA (Los Alamos Natonal Laboratory, SANDIA

National Laboratories), UK (Nuclear Decommissioning Authority (NDA), National Nuclear Laboratory (NNL) and a consortium coordinated by the University Cambridge), Finland (Posiva Oy, Teollisuuden Voima (TVO)) and Germany (Gesellschaft für Anlagen- und Reaktorsicherheit (GRS) mbH) contribute to the project as *Associated Groups (AG)* in view of their particular interest in exchange of information without receiving any funding from the First Nuclides project. A group of six implementation and regulatory oriented organizations, SKB (Sweden), NAGRA (Switzerland), ANDRA (France), ONDRAF/NIRAS (Belgium), BfS (Germany) and ENRESA (Spain) are participating as an *"End-User Group (EUG)"*. This group ensures that end-user interests are reflected in the project work, and reviews the project work and the scientific-technical outcome.

The outcome of the project is documented by Scientific/Technical Contributions to be published in the Annual Workshop Proceedings. During the first 10 months of the project, most of the efforts were dedicated to selection, characterization and preparation of materials and set-up of tools for handling and transportation of the highly radioactive material, including licensing issues. Nevertheless, 20 S&T contributions have been submitted for the 1st Annual Workshop Proceedings. The report KIT-SR 7639 can be downloaded from http://dx.doi.org/10.5445/KSP/1000032486.

Fig. 1: *The First Nuclides web page offers comprehensive information on the project (visit www.firstnuclides.eu).*

New results from the First Nuclides project described in the above mentioned report cover:

- Gas release + rim and grain boundary diffusion
  - Determination of FGR of a 50.4 GWd/tHM fuel rod: 5.3% (Kr), 6.3% (Xe)
  - Preparation of the 18O-labelled water diffusion study and shielded SIMS
  - Microstructure analysis of high burn-up fuel
  - Determination of the internal free volume of fuel rods

- Dissolution based release
  - Experiments started using the harmonized specified water composition under different redox regimes, oxidizing / anaerobic / reducing
  - Samples: pellet-sized cladded segment, decladded SNF fragments, fuel powder.
- Modelling
  - Semi-empirical IRF modelling of high burn-up SNF leaching experiments
  - Boundary / initial conditions for up-scaling (inventories, temperature history, properties of the rim zone, Xe concentrations and rim porosity.
  - Model for water penetration into the inner parts of fuel pellets required for duration of experiments.
- Knowledge, reporting and training
  - Exchange of scientists, lab meeting (03/2013), Annual Workshop Proceedings: KIT-SR 7639.

PRELIMINARY SAFETY ASSESSMENT FOR GORLEBEN (VSG)

The expertise at KIT-INE on HLW topics has been integrated into the Preliminary Safety Assessment (VSG) for the potential German waste disposal site Gorleben performed during the past three years. VSG was funded by the German Federal Ministry for the Environment, Nature Conservation and Nuclear Safety (BMU) and coordinated by the Gesellschaft für Reaktorsicherheit (GRS). Within this large collaborative project, several institutions were contributing expertise and addressing key questions related to Gorleben salt dome as potential nuclear waste disposal site for high level radioactive waste. One activity of KIT-INE was focused on deriving radionuclide source terms for different classes of radioactive waste. Two recently publicly available reports on the radionuclide source term estimations by KIT-INE within the VSG project have been published at KIT Scientific Publishing [1,2]. They are available from the authors or can be downloaded at http://www.ksp.kit.edu.

REFERENCES

[1] B. Kienzler, M. Altmaier, Ch. Bube and V. Metz, Radionuclide Source Term for HLW Glass, Spent Nuclear Fuel, and Compacted Hulls and End Pieces (CSD-C Waste), KIT Scientific Reports 7624, (2012), KIT Scientific Publishing, Karlsruhe, Germany.

[2] B. Kienzler, M. Altmaier, Ch. Bube and V. Metz, Radionuclide Source Term for Irradiated Fuel from Prototype, Research and Education Reactors, for Waste Forms with Negligible Heat Generation and for Uranium Tails, KIT Scientific Reports 7635, (2013), KIT Scientific Publishing, Karlsruhe, Germany.

Aquatic Chemistry of Actinides at Elevated Temperatures: Solubility and Spectroscopic Studies at KIT–INE

X. Gaona[1], A. Skerencak-Frech[1], M. Marques[2], D. R. Fröhlich[3], J. Rothe[1], K. Dardenne[1], P. J. Panak[1,3], M. Altmaier[1]

[1] *Karlsruhe Institute of Technology, Institute for Nuclear Waste Disposal (KIT–INE), Germany*
xavier.gaona@kit.edu; andrej.skerencak@kit.edu
[2] *Paul Scherrer Institut, Laboratory for Waste Disposal (PSI–LES), Switzerland*
[3] *Ruprecht-Karls-Universität Heidelberg, Physikalisch-Chemisches Institut, Heidelberg, Germany*

INTRODUCTION

Temperature is one of the parameters that will vary during the different phases of operation of a high level radioactive waste (HLW) repository. Elevated temperature conditions (up to 200°C depending on host rock system and repository concept) will affect actinide chemistry in the near-field of a HLW repository.

The hydrolysis of U(VI) has been thoroughly studied at 25°C. The thermodynamic data selection resulting from the NEA–TDB reviews [1] is thus very complete (with log K^0, $\Delta_r G^0_m$ or $\Delta_f G^0_m$ being reported) and includes most of the hydrolysis species expected to form from acidic to hyperalkaline pH conditions. On the contrary, a very limited number of studies is dedicated to assess the effect of temperature on the aquatic chemistry of U(VI). This is especially critical for neutral and anionic U(VI) hydrolysis species and solid compounds prevailing in pH neutral to alkaline, repository-relevant conditions.

Under the reducing conditions expected after the closure of deep underground repositories for the disposal of nuclear waste, tri– and tetravalent actinide oxidation states are expected to dominate. Chloride is present in high concentrations in brines of deep salt formations as well as in the pore water of certain clay rocks. Although Cl^- is a weak ligand for complexation of trivalent actinides at ambient temperature, complexation studies with lanthanides have shown a strong increase of the log $\beta^0_{(1,n)}$ values (n = 1, 2) at T > 100°C.

This contribution summarizes on-going activities at KIT–INE focusing on the aquatic chemistry of actinides at elevated temperatures. The systems U(VI) hydrolysis/solubility and An(III)–Cl complexation are highlighted as dedicated research studies with particular emphasis on repository-relevant conditions.

SOLUBILITY OF U(VI) AT ELEVATED T

Experimental details

Undersaturation solubility experiments were conducted with $UO_3 \cdot 2H_2O(cr)$ and $Na_2U_2O_7 \cdot H_2O(cr)$ solid phases synthesized and characterized in a previous solubility study at 25°C [2]. All samples were prepared in an inert gas (N_2) glovebox under exclusion of O_2 and CO_2. U(VI) solid phases were distributed in several independent batch experiments (5–15 mg solid per

sample), arranged in two series of 0.5 M NaCl–NaOH solutions with $4 \leq pH_m \leq 7$ ($UO_3 \cdot 2H_2O(cr)$) and $8 \leq pH_m \leq 12$ ($Na_2U_2O_7 \cdot H_2O(cr)$) and stored in an oven at 80°C (in a N_2 glovebox). Samples were equilibrated for ~6 months and monitored at regular time intervals for dissolved uranyl, [U], and pH_m. Triplicate aliquots (supernatant, 0.1 μm filtration and 10 kD ultrafiltration) were taken for the quantification of [U] by ICP–MS using standard protocols. Solid phase characterization of selected samples (XRD, SEM–EDS, quantitative chemical analysis) is performed after the completion of the solubility experiment.

Results and discussion

The solubility of $UO_3 \cdot 2H_2O(cr)$ slightly decreases (~0.5 log–units) at 80°C compared to similar solubility experiments at 25°C (Figure 1). The species UO_2^{2+} is expected to prevail within $4 \leq pH_m \leq 6$ in 0.5 M NaCl, and this observation therefore can be related to the effect of temperature on log $*K_{s,0}(UO_3 \cdot 2H_2O(cr))$.
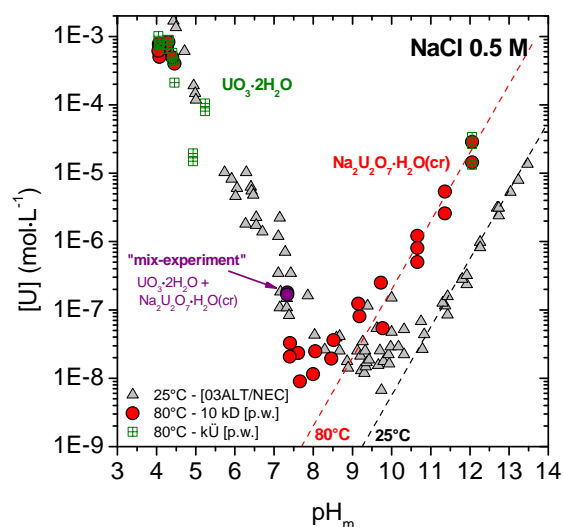
Fig. 1: Solubility of $UO_3 \cdot 2H_2O(cr)$ and $Na_2U_2O_7 \cdot H_2O(cr)$ in 0.5 M NaCl at 80°C. Data at 25°C reported in [2] under analogous I_m and pH_m values added for comparison.

On the contrary, a significant increase in solubility (~1.5 log units) is observed at 80°C for $Na_2U_2O_7 \cdot H_2O(cr)$.

Similar to 25°C, the solubility of U(VI) as a function of pH shows a well defined slope of +1 at pH_m 9–12, likely corresponding to the equilibrium $0.5\ Na_2U_2O_7 \cdot H_2O(cr) + 2\ H_2O \Leftrightarrow Na^+ + UO_2(OH)_4^{2-} + H^+$. This observation is consistent with the expected increase of hydrolysis of metal ions with increasing temperature as a result of the increase of the ion-product of water (K_w). The combination of slope analysis with detailed solid phase characterization allows the development of a thermodynamic model for the system UO_2^{2+}–H^+–Na^+–OH^-–Cl^- at 80°C valid within $4 \le pH_m \le 12$.

COMPLEXATION OF Cm(III) AND Am(III) WITH CHLORIDE AT ELEVATED T

Experimental details

The complexation of Cm(III) and Am(III) with Cl^- was studied at T = 25–200°C by means of TRLFS and EXAFS. For the TRLFS measurements a set of samples was prepared at: $[Cm(III)] = 10^{-7}$ m, $[H^+] = 8.9 \cdot 10^{-2}$ m, $[Cl^-] = (0.51, 1.01, 2.02, 2.52, 3.03, 3.50, 4.00)$ m.

Am-L_{III}-EXAFS spectra were collected at the INE–Beamline for Actinide Research at ANKA [3]. For this purpose, one sample with $[Am(III)] = 10^{-3}$ m, $[H^+] = 8.9 \cdot 10^{-2}$ m, $[Cl^-] = 3.03$ m was prepared and experiments were performed in a custom build high pressure cell for spectroscopic studies within 25–200°C.

TRLFS results

A comparison of the emission spectra of Cm(III) in NaClO$_4$ and NaCl solutions (0.51 m; 4.0 m) is displayed in figure 2. Perchlorate is a very weak ligand towards trivalent actinides and does not form complexes with Cm(III) up to $[ClO_4^-] = 7.0$ m and $T \le 200$°C [4]. In the chloride solutions, the emission band is shifted distinctly stronger to longer wavelengths with increasing temperature. This effect is attributed to a strong increase of the fractions of the $CmCl_n^{3-n}$ complexes at increased temperatures.

The TRLFS spectra are analysed by peak deconvolution and the speciation is determined as f(T). However, due to the small shift of the band of the $CmCl^{2+}$ complex ($\Delta\lambda \sim 1$ nm), this species cannot be quantified at increased temperatures. Furthermore, the $CmCl_3$ complex starts to form only at T > 180°C and remains below 5%. Thus, the $\log \beta^0_1(T)$ and $\log \beta^0_3(T)$ values cannot be determined with acceptable accuracy. The fraction of the $CmCl_2^+$ complex increases considerably in the studied temperature range, showing that this species plays an important role at T > 100°C.

The conditional stability constants $\log \beta'_2(T)$ are determined as f(T) and extrapolated to $I_m = 0$ with the SIT approach [1]. The results show a linear increase of $\log \beta^0_2(25°C) = -0.81 \pm 0.20$ to $\log \beta^0_2(200°C) = 2.83 \pm 0.09$. This is in excellent agreement with the literature data for the analogous Ln(III) chloride complexes [5]. The

temperature dependency is very well fitted by the integrated van't Hoff equation with:

$$\Delta_r H^0_m = 54.9 \pm 4.5 \text{ kJ/mol,}$$
$$\Delta_r S^0_m = 168.8 \pm 5.5 \text{ J/mol·K.}$$
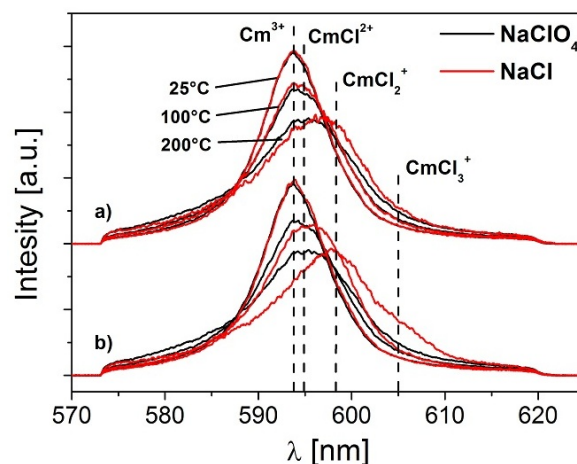
Fig. 2: Emission spectra of Cm(III) in aqueous NaCl and NaClO$_4$ at T = 25, 100 and 200°C. **a)** $[Cl^-] = [ClO_4^-] = 0.51$ m, **b)** $[Cl^-] = [ClO_4^-] = 4.00$ m

EXAFS results

The spectra recorded at 25 and 90°C are almost identical. They are well described by 9 to 10 oxygen neighbours at a distance of 2.45 to 2.48 Å. This is in good agreement with the literature [6]. At 200°C about 2.5 Cl^- ligands must be included into the fit to describe the experimental data.

The debye-waller factor of the Am–O shell increases continuously with increasing temperature. The Am-O and Am–Cl distances obtained at 200°C are significantly shorter compared to the results at 25 and 90°C. Also, they are significantly shorter than the literature values at 25°C [6]. This is attributed to an asymmetric (non-Gaussian) distribution of distances which is known to occur at high temperature [7]. These results are in excellent agreement with the TRLFS data summarized above.

REFERENCES

[1] Guillaumont, R. et al., Chemical Thermodynamics Vol. 5. NEA OECD, Elsevier (2003).
[2] Altmaier, M. et al. (2003). Migration Conference 2003, Gyeongju (Korea).
[3] Rothe, J. et al., *Rev Sci Instrum* **83**, 043105 (2012).
[4] Lindqvist-Reis, P. et al., *J. Phys. Chem. B*, **109**, 3077-3083 (2005).
[5] Gammons, C.H. et al., *Geochim. et Cosmochim. Acta*, **23**, 4615-4630 (1996).
[6] Allen, P.G. et al, *Inorg. Chem.*, **39**, 595-601 (2000).
[7] Dalba, G. et al., *J. Synchrotron. Rad.*, **4**, 243-255 (1997).

Complexation of Actinides with Oxalate at High Temperature and Ionic Strength

P. Thakur

Calrsbad Environmental Monitoring & Research Center, NM, 88220, USA
email: pthakur@cemrc.org

INTRODUCTION

One of the strategies for the safe management of high level nuclear waste (HLW) is to dispose of it in deep geological repositories. In this context, studies of actinides complexation at elevated temperatures, and potentially at high ionic strengths, provide the scientific basis for assessments of repository safety. High ionic strength groundwater may be encountered at repository depth in several types of geologic host rock formations. If the selected host rock is salt, the only water present will be saturated brines. This means there is a need to understand and quantify the complexation of actinides, in particular, since they are the longest lived radionuclides in HLW, with organic and inorganic ligands at elevated temperature and at high ionic strength. The temperature of the HLW in the repository could rise to as high as $200\text{-}300^{\circ}\mathrm{C}$, decrease gradually with time, and remain significantly higher than the ambient temperature even thousands of years after the closure of the repository [1]. If some scenario brings waste into contact with brine, estimating the potential migration behavior of actinides needs to take into consideration the effect of temperature on the complexation.

The composition of US defense waste is extremely diverse. A number of carboxylic acids such as acetic acids, oxalic acids, citric acid, EDTA, etc., are known to be present in significant amounts even in the transuranic (TRU) wastes currently being emplaced in the Waste Isolation Pilot Plant (WIPP) in New Mexico. The total amount of sodium oxalate and oxalic acid in the WIPP inventory is expected to be close to 50 tons, more than the total amounts of acetate/acetic acids and citrate/citric acids [2]. In addition, oxalate is also present in relatively high concentrations in several natural environments such as soil solutions, oil field sedimentary basin brines, and deposits from thermal degradation of complex organic matter [3]. As a result, complexation of actinides with oxalic acid could play an important role in determining the transport of actinides in the repository. While providing support to the WIPP performance assessment, the ion interaction parameters applicable to high temperatures and high ionic strengths generated could improve the predictability of actinide transport behavior in HLW repositories where temperature and ionic strength could be high.

The scarcity of fundamental thermodynamic data at $25^{\circ}\mathrm{C}$ and the absence of data at elevated temperatures and high ionic strength make it difficult to predict the chemical behavior of actinides for a wide range of applications that are of interest to radioactive waste disposal programs proposing to use locations with high ionic strength ground waters. Therefore, reliable experimental data on the complexation of actinides at elevated temperatures are still needed.

DESCRIPTION OF THE WORK

Based on the interests at both the practical and fundamental levels, we have studied the thermodynamics of the complexation of actinides with a number of organic ligands at elevated temperatures. This work reports the dissociation constants of oxalate and their stability constants with actinides (UO_2^{2+}, NpO_2^+, Pu^{4+}, Am^{3+} and Cm^{3+}) as a function of temperature and ionic strength were measured using potentiometric titration and an extraction technique, respectively. The complexation thermodynamics were determined by the temperature dependence of the stability constants at $I=5.0$ M $NaClO_4$.

RESULTS AND DISCUSSION

The formation of only the 1:1 complex was observed for NpO_2^+, while both 1:1 and 1:2 complexes were observed for UO_2^{2+}, Pu^{4+}, Am^{3+} and Cm^{3+} with oxalate. The stability constant values calculated as a function of temperature are summarized in Table 1. The results show that the complexation of actinides with oxalate is moderate to very strong and becomes stronger at higher temperature. For the 1:1 complexation, the values of the stability constants increased in the order: $NpO_2^+ < Am^{3+} < UO_2^{2+} < Pu^{4+}$ in accordance with the metal charge density, reflecting strong ionic bonding.

Table 1. Stability constants of actinides with oxalate at I= 5.0 M (NaClO$_4$)

Reactions	Temp.(^{o}C)	log β_{101}	log β_{102}	ΔH_{101} (kJ/mol)	ΔS_{101} (J/K/mol)
NpO$_2^+$ + ox^{2-} = NpO$_2$ox$^-$	25	3.91±0.05	-	11.3±2.7	113±9
	35	3.98±0.04	-		
	45	4.05±0.05	-		
	60	4.12±0.03	-		
UO$_2^{2+}$ + jox^{2-} = UO$_{2}$(ox)$_j^{2-2j}$ (j = 1, 2)	10	6.18±0.07	11.49±0.09	8.2±3.4	148±11
	25	6.28±0.06	11.66±0.08		
	45	6.35±0.07	11.78±0.10		
	60	6.42±0.08	11.94±0.10		
Pu^{4+} + jox^{2-} = Pu(ox)$_j^{4-2j}$ (j = 1, 2)	0	8.91±0.05	16.46±0.08	12.2±2.7	215±10
	10	8.96±0.03	16.53±0.07		
	25	9.10±0.05	16.35±0.07		
	35	9.15±0.04	16.35±0.10		

The stability constants of actinide -oxalate complexes are plotted against 1/T in Fig. 1. It appears that the data could be approximately fitted with straight lines. From the slopes of the linear fits (weighted by the uncertainties), the "average" enthalpies of actinide-oxalate complexation in the temperature range (0-60°C) were calculated. The positive enthalpy and entropy terms indicate entropy-driven complexation between actinides and oxalate at high ionic strength.
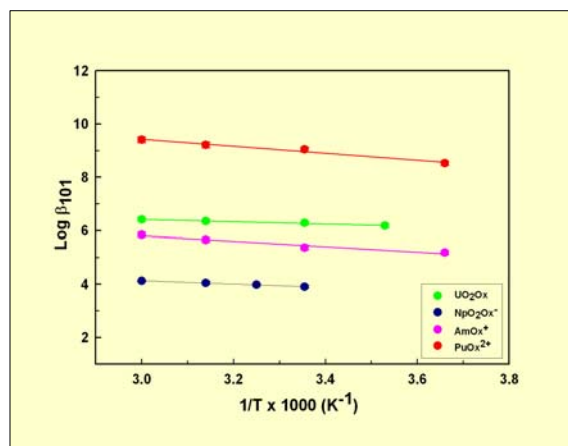

Fig. 1. log β_{101} vs. 1/T for the complexation of actinides with oxalate.

FUTURE DIRECTION

The stability constant values measured as a function of ionic strength will be used for the Pitzer model interaction parameters. The thermodynamic data obtained in NaClO$_4$ media from this study will be compared to similar data in NaCl solutions to assess the role of Cl$^-$ complexation. Since there are two important brines in the WIPP repository, i.e., GWB, a Na-Mg-Cl dominated brine [4] and ERDA-6, a Na-Cl dominated brine [5], our goal will be to develop a consistent thermodynamic model that can reliably predict the solubilities of actinides in the WIPP brines. The usefulness of this work extends beyond WIPP, however, the demonstrated methodology, and to an extent the measured stability constants ought to be useful in evaluations for other high ionic strength solutions and other temperatures.

REFERENCES

[1] DOE, *The 1995 Baseline Environmental Management Report*, DOE/EM/0232, USA Department of Energy, Washington,DC, USA1995.
[2] Crawford, B.A., Lott, S.A., Sparks, L.D., Van Soest, G., B. McInroy, B. "*The Road to Recertification*: *WIPP TRU Waste Inventory*", in *Proceedings of Waste Management Conference*, Feb.26-Mar 2, 2006, Tucson, Arizona
[3] Gammons C.H and Wood, S.A. *Chem. Geol.*, **166**, 103-124 (2000).
[4] U.S. DOE, (2004) *Title 40 CFR Part 191 Compliance Recertification Application for the Waste Isolation Pilot Plant, Vol. 1-8*. DOE/WIPP 2004-3231. Carlsbad, NM: U.S. DOE Carlsbad Field Office.

[5] Popielak, R.S., Beauheim, R.L., Black, S.R., Coons, W.E., Ellingson, C.T., and Olsen, R.L. (1983) Brine Reservoirs in the Castile Formation, Waste Isolation Pilot Plant Project, Southeastern New Mexico. TME 3153. Carlsbad, NM: U.S. Department of Energy WIPP Project Office.

Np(V) Interactions and Speciation at High Ionic Strength

M.K. Richmann, M. Borkowski, J.S. Swanson, D.A. Ams, J-F., Lucchini, K. Simmons, D. Cleveland and D.T. Reed

Earth and Environmental Sciences Division, Los Alamos National Laboratory, 1400 University Drive, Carlsbad NM, USA
richmann@lanl.gov

INTRODUCTION

Neptunium primarily exists in the environment in the Np(IV) and Np(V) oxidation state, although there are some high-pH (pH >12) conditions where Np(VI) is also stabilized. Under oxic conditions in near-neutral pH, $Np(V)O_2^+$ is the predominant species and is relatively mobile in the environment due to its high solubility and low tendency toward hydrolysis and complexation. Anaerobic microbial processes [1] and iron(0, II) will reduce neptunium to the Np(IV) oxidation state, which has an analogous environmental chemistry to Pu(IV), e.g., very strong hydrolysis, very strong tendency towards polymer/colloid formation, and low solubility. For this reason, Np(IV) will likely predominate under most anoxic conditions in brine or low ionic-strength groundwater.

In a long-term geologic repository setting, Np(V) can become an important contributor to release at long times (> 10, 000 years) under mildly oxidizing conditions. This increased importance is because it is very long-lived, its inventory builds up in time due to the decay of Am-241 in the wasteform, and it has a relatively high solubility and mobility over a wide pH range. In the USA, this potential release issue is mainly linked to repository concepts for the long-term disposal of high level waste (HLW) and spent fuel (SF) and not TRU nuclear waste disposal (e.g., the WIPP). In the WIPP, neptunium is not a key contributor to release due to its very low overall inventory in TRU waste (~ 10 Kg predicted for the entire waste inventory), the Am-241 inventory is also relatively low, and the timeframe for repository performance is only 10,000 years.

In this context, we are investigating the effects of temperature and ionic strength on the speciation of Np(V), and eventually Np(IV), to support the development of the safety case for an HLW/SF repository in salt should the low-probability event of brine inundation occur. This will also be supported in time with micro-calorimetric studies. Neptunium, for a number of reasons, is a model system to study and this will help form a strategy that will be extended to other multivalent actinides. Herein we report the progress we have made along this research path and present some initial data on the effects of temperature and ionic strength on the Np(V) aquo species, the complexation of Np(V) with borate, the complexation of Np(V) with carbonate and the modelling of the bio-associated of Np(V) with halophilic bacteria.

DESCRIPTION OF THE WORK

Neptunium-237 (~ 98% by mass) was purified by oxidation to Np(VI) in fuming perchloric acid, reduced to Np(V) by the addition of a few drops of 30% hydrogen peroxide, and precipitated as a carbonate solid by titration with sodium carbonate to ~ pH 7-8. This was then re-dissolved in the desired media (perchlorate, sodium chloride, or 0.1 M HCl) to make up the stock solutions.

The initial approach was to use absorption spectrometry to establish the speciation of neptunium. A Varian CARY 5000 spectrometer, equipped with a circulating water bath for temperature control (0 to 90°C) was used to obtain temperature-specific spectra. These spectra were obtained in gas-tight cuvettes by temperature-equilibrating the reference and sample cuvette prior to obtaining a baseline correction and then spiking in the neptunium (typically 5-40 μL) to obtain the spectrum as function of complexation, ionic strength and temperature. Liquid scintillation counting (Beckman-Coulter LS6500 multipurpose scintillation counter) of the neptunium was done for each sample to correct for minor differences in neptunium concentration due to the pipetting. Lorentzian and gaussian fitting was done to model the absorption peaks and de-convolute the peaks and calculate λ_{max} and the half-height width of the spectra obtained. EQ3/6 and modified FITEQL approach was used to fit the biosorption data.

RESULTS

Data from four sets of experiments are reported: 1) the effect of ionic strength on the Np(V) aquo peak, 2) the effect of temperature on the Np(V) aquo peak, 3) Np(V)-borate complexation, and 4) Np(V) biosorption towards *Choromohalobacter sp*. (bacteria).

Effect of high ionic strength on the Np(V) aquo peak

The Np(V) spectrum was obtained in perchloric and NaCl media up to ionic strengths of ~ 5 M. The effect of ionic strength in the perchlorate media is shown in Figure 1. Here a small blue shift was observed (~ 1.5 nm) as the ionic strength was increased. There was no significant change in the half-height peak width. In contrast, a red shift of ~ 2 nm was observed when spectra were obtained in NaCl media. This was interpreted as due to the formation of an Np(V)-Cl complex peak at 983 nm, that grows in with ionic strength.
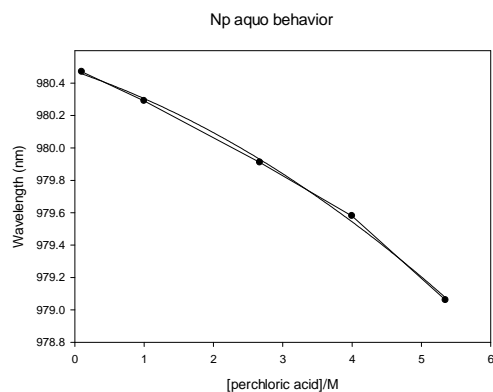
Fig. 1. Peak shift in the Np(V) aquo absorption band as a function of ionic strength in perchlorate media.

Np(V) complexation with borate and carbonate

The complexation of Np(V) with borate and carbonate led to new band formation that can be de-convoluted to determine the complex formation constants. Borate formed a 1:1 complex with Np(V) with a peak maximum at 985 nm (see Figure 2). Isobestic behavior was observed at fixed pH with variable borate concentration and at fixed borate concentration and variable pH indicating that a single species was being formed. The apparent formation constant for this complex was Log K_{app} = 2.11 ± 0.08.

The carbonate peak initially formed is at 991 nm ($NpO_2CO_3^-$) and a second species forms at 997 nm ($NpO_2(CO_3)_2^{3-}$). These two processes compete with each other and it is critical to maintain low concentrations of carbonate to investigate the borate complexation. In all cases, no evidence of hydrolysis was obtained until pH ~ 10 or higher [2].
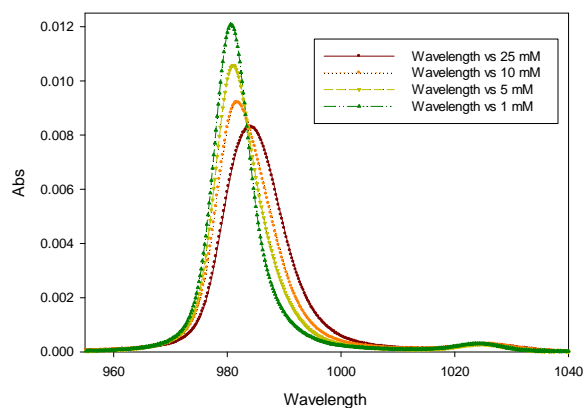

Fig. 2. Np(V) spectrum in the presence of varying concentrations of borate and pH ~ 8 showing an isobestic point.

Effect of temperature on the Np(V) aquo spectrum

The effect of temperature (20 – 90 ^{o}C) was established for Np(V) in 0.1 M HCl (no uncertainty in the speciation). The increase in temperature resulted in a steady blue shift in the absorption maximum (~ 2 nm – see Figure 3) and a corresponding decrease in the line width. These changes, although small, are significant when de-convoluting the neptunium spectra at variable temperature given the very small spectral shifts observed in the complexes formed (e.g., chloride and borate). These data provide baseline spectra that are needed to evaluate the effects of temperature on complexation.
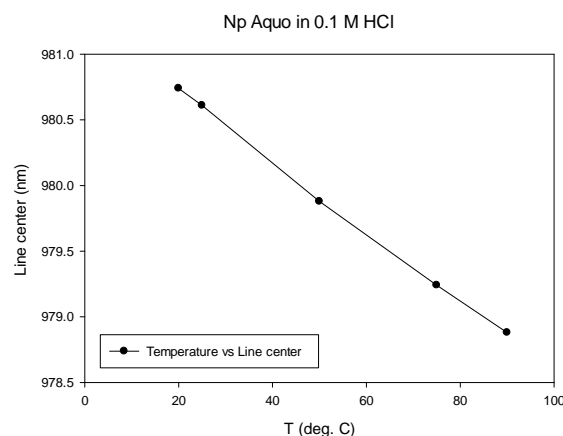
Fig 3. Effect of temperature on the peak position of the Np (V) aquo spectrum in 0.1 M HCl.

Modeling of biosorption data

The modeling of biosorption data, Np(V) sorption onto *Chromohalobacter sp.*, was attempted and is problematic due to the limited availability of Pitzer data and a fitting program that incorporates the Pitzer formulation (FITEQL). This is identified as something that needs further development and improvement to fully address the high ionic strength interactions of neptunium.

REFERENCES

[1] Banaszak, J. E., S. M. Webb, B. E. Rittmann, J.-F. Gaillard, and D. T. Reed, "Fate of Neptunium in Anaerobic, Methanogenic Microcosm," Scientific Basis for Nuclear Waste Management XXII", 556 (1999) 1141-1149.

[2] Rao, L., T.G. Srinivasan, A.Y. Garnov, P. Zanonato, P.D. Bernardo and A. Bismondo, "Hydrolysis of Neptunium(V) at Variable Temperatures (10–85°C)", Geochimica et Cosmochimica Acta, Vol. 68, No. 23, pp. 4821–4830, 2004

[3] Ams, D.A., J. S. Swanson, J. E. S. Szymanowski, J. B. Fein, M. Richmann, and D.T. Reed, " The Effect of High Ionic Strength on Neptunium (V)Adsorption to a Halophilic Bacterium" accepted for publication in Geochimica et Cosmochimica Acta, 2013.

Investigations of Actinide and Lanthanide Sorption on Clay Minerals under Saline Conditions

A. Schnurr, R. Marsac, Th. Rabung, J. Lützenkirchen, H. Geckeis

Institute for Nuclear Waste Disposal (KIT-INE), Karlsruhe Institute of Technology, P.O. Box 3640, D-76021 Karlsruhe, Germany
thomas.rabung@kit.edu

INTRODUCTION

The final disposal in deep geological formations is considered as the safest way to keep high level radioactive waste isolated from the biosphere. Due to their high sorption capacity, their swelling properties and their low water permeability, clay minerals are of great interest as suitable components of geotechnical and geological barriers. Therefore, several countries have selected clay formations for their deep geological disposal projects e.g. Opalinus clay (Switzerland), Callovo-Oxfordian (France) or Boom clay (Belgium). In other concepts compacted clays have been proposed as backfill and sealing materials. For the safety assessment of nuclear waste concepts, the potential contact of waste forms with groundwater has to be considered. Sedimentary clay formations in Germany (lower and middle Jurassic and lower Cretaceous) discussed as potential repository host rocks can be in contact with highly saline (up to 5 molal) groundwater [1]. Only a few studies so far addressed radionuclide sorption under high ionic strength conditions [2]. The non-electrostatic 2SPNE SC/CE sorption model developed by Bradbury and Baeyens to describe metal ion sorption onto two main components of natural clay stones (illite and smectite) is only valid/calibrated for relatively low ionic strength systems ($I < 1$ M) [3]. The present work focuses therefore on the sorption of trivalent metal cations (Eu(III)/Cm(III)) and hexavalent uranium onto different natural relevant clay minerals (illite, smectite and kaolinite) under saline conditions and exclusion of CO_2.

DESCRIPTION OF THE WORK

Batch sorption edge experiments were carried out with three different background electrolytes (NaCl, $CaCl_2$ and $MgCl_2$) at different ionic strengths ([NaCl] up to 4 M, [$CaCl_2$] and [$MgCl_2$] up to 2 M), at fixed metal concentration ([Eu]$_{total}$ = 2 E-7 M labeled with ^{152}Eu for γ-counting or [U(VI)]$_{total}$ = 4 E-7 M, measured with ICP-MS) and at constant solid to liquid ratios (S:L = 2 g/L) over a wide pH$_c$ range (3-12).

RESULTS

The extent of metal ion adsorption onto the different clay minerals approaches 100% at pH$_c$ > 7 for all investigated electrolyte solutions. In general, sorption edges slightly shift to higher pH$_c$-values with increasing ionic strength (confirmed for Eu(III), first hints for U(VI)). In presence of divalent cations, however, actinide/lanthanide sorption is much stronger suppressed than observed for NaCl solutions. This is explained by the stronger competition of divalent cations with actinide/lanthanide sorption to cation exchange sites (dominating metal ion sorption at lower pH$_c$-values) but also to inner sphere sorption sites at the edge planes of the clay particles.

The applicability of the 2SPNE SC/CE model [3] was tested to describe Eu(III) sorption at high ionic strength. A good agreement of experimental data and model prediction was achieved in the NaCl systems at pH$_c$ < 7 where metal ion activities were calculated using the Pitzer approach. However, the existing model under-estimates sorption at higher pH$_c$. The agreement for Ca/MgCl$_2$ systems is much better. Deviations might be due to uncertainties in the Pitzer parameter data set for An(III) in NaCl solutions.

Time resolved laser fluorescence spectroscopy (TRLFS) studies confirm the existence of three distinguished Cm(III) surface complexes which have been described already earlier for low ionic strength conditions [4] also at high salinity. This finding demonstrates that the coordination of adsorbed actinide species does not change noticeably under highly saline conditions and validates speciation assumptions underlying the 2SPNE SC/CE model. However, with an improved detection system, an additional fourth inner-sphere surface species could be identified at higher wavelengths (λ ~ 610 nm) being comparable to the findings of a previous study on curium interaction with kaolinite. This species was interpreted as a clay/curium/silicate/hydroxide ternary/quarternary complex [5].

First experiments using U(VI) show a significant decrease of sorption at pH$_c$ > 10 which was not observed for Eu(III). This finding can be explained by the formation of a twofold negatively charged U(VI) species ($UO_2(OH)_4^{2-}$) which dominates U(VI) aqueous speciation

in the alkaline pH region and which reduces U(VI) sorption.

The present work clearly demonstrates that clay minerals represent strong retardation barriers for tri- and hexavalent metal ions even under highly saline conditions.
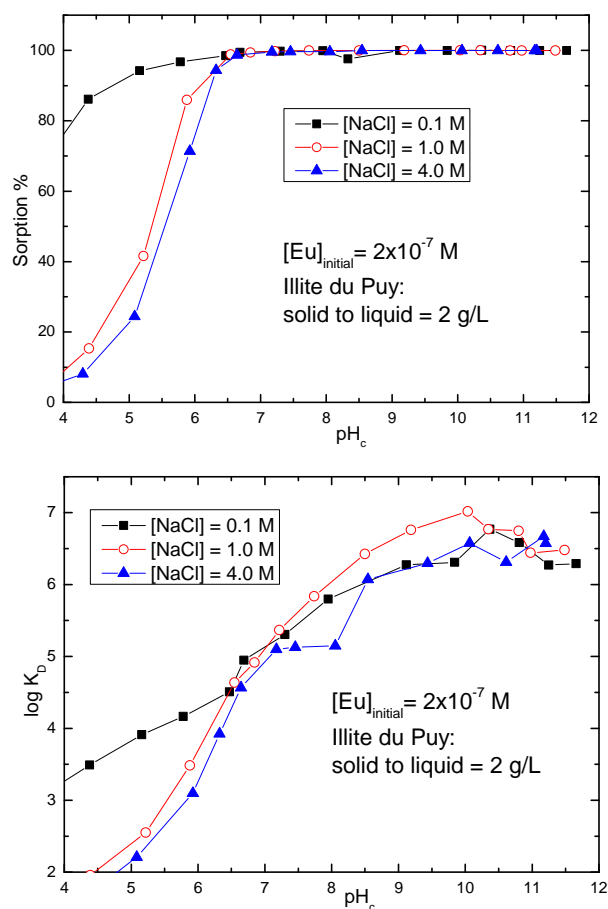
Fig. 1: Eu(III) sorption onto illite in percentage uptake (above) and as the logarithm of the distribution coefficient (below) vs. pH_c at different ionic strengths.

REFERENCES

1. Brewitz, W.: Eignungsprüfung der Schachtanlage Konrad für die Endlagerung radioaktiver Abfälle. GSF-T136, Neuherberg (1982).

2. Vilks, P.: Sorption of Selected Radionuclides on Sedimentary Rocks in Saline Conditions – Literature Review. Nuclear Waste Management Organization, Toronto, Ontario, Technical Report NWMO TR-2011-12 (2011).

3. Bradbury, M.H., Baeyens, B.: Sorption of Eu on Na- and Ca-montmorillonites: Experimental investigations and modeling with cation exchange and surface complexation, Geochim. Cosmochim. Acta, 66, 2325-2334 (2002).

4. Rabung, Th., Pierret, M.C., Bauer, A., Geckeis, H., Bradbury, M.H., Baeyens, B.: Sorption of Eu(III)/Cm(III) on Ca-montmorillonite and Na-illite. Part 1: Batch sorption and time-resolved laser fluorescence spectroscopy experiments, Geochim. Cosmochim. Acta, 69, 5393-5402 (2005).

5. Huittinen, N., Rabung, Th., Schnurr, A., Hakanen, M., Lehto, J., Geckeis, H.: New insight into Cm(III) interaction with kaolinite – Influence of mineral dissolution, Geochim. Cosmochim. Acta, 99, 100-109 (2012).

Acknowledgement

Uranium(VI) Sorption on Montmorillonite in High Ionic Strength Media

Katharina Fritsch, Katja Schmeide

Helmholtz-Zentrum Dresden-Rossendorf, Institute of Resource Ecology, P.O. Box 510119, 01314 Dresden, Germany
email: k.fritsch@hzdr.de

INTRODUCTION

Of the three main choices for radioactive waste repository host rock—salt dome, argillaceous rock and crystalline rock—Germany has deposits of two eligible rock types. Salt dome, present in Northern Germany, has long been investigated as host rock and in recent years argillaceous rock has come to attention. There are two areas in Germany with sizable clay deposits: In the more populated south of Germany there is a deposit of the already well-researched Opalinus clay (OPA) and in the north of Germany there are clay deposits whose pore waters have a salt concentration of up to 4 mol L^{-1}, ten times that of OPA [1-2].

Montmorillonite is a bentonite. Bentonites are smectites (2:1 clays) that have excellent swelling properties and that are thixotropic when suspended in aqueous solutions. These properties make bentonites the preferred sealing materials in radioactive waste repositories. Bentonites are furthermore a component of OPA and other argillaceous rocks. Montmorillonite is used as model clay for the class of bentonites [3].

The aim of this work is to determine the sorption and diffusion properties of uranium(VI) on/in model clays and OPA at increased salinities in NaCl, KCl, $CaCl_2$ and $MgCl_2$. The basis for this work is formed by sorption experiments with Wyoming montmorillonite (SWy-2) in several strong electrolyte solutions. This also includes leaching experiments.

DESCRIPTION OF THE WORK

The montmorillonite was cleaned according to the procedures of Poinssot [4] and Bradbury and Baeyens [5]. Subsequent analysis showed that the clay composition is in excellent agreement with the literature [6-8]. Furthermore, the cation exchange capacity (CEC) and the specific surface area were determined and gave values of 85.0 ± 22.4 mmol$_c$ $(100\ g)^{-1}$ and 41.1 ± 0.8 m² g^{-1} (N_2-BET) respectively.

The sorption experiments were carried out under the following conditions:
- S/L = 4.00 ± 0.01 g L^{-1}
- background electrolytes NaCl and $CaCl_2$ with $b_{cation} = 1 \cdots 3$ mol kg^{-1}
- pH = $4 \cdots 10$
- room temperature, atmospheric conditions
- $c_{U(VI)} = 1 \times 10^{-6}$ mol kg^{-1}

- sorption time: 5 days.

The leaching experiments were carried out without the addition of uranium; additionally, there was a control series without clay to detect any impurities introduced by the chemicals used.

RESULTS

The sorption results in NaCl and $CaCl_2$ show a clear pH dependency, but they differ very much from each other.

In NaCl, sorption is negligible at the pH values of 9 and 10 and sorption is rather low at pH 4. At pH 6 and 7, uranium has practically completely sorbed onto the clay. From pH 6 to 10, there is no difference in sorption between the different electrolyte concentrations. The sorption data at pH 4 and 5 show a difference between $b \approx 1$ mol kg^{-1} (which for montmorillonite is a low sodium concentration) and the two higher concentrations. This means that as soon as the concentration in acidic media goes above a certain concentration threshold that lies between 1 and 2 mol kg^{-1}, the sorption remains basically the same, while there is no discernible difference in neutral and alkaline media anyway.
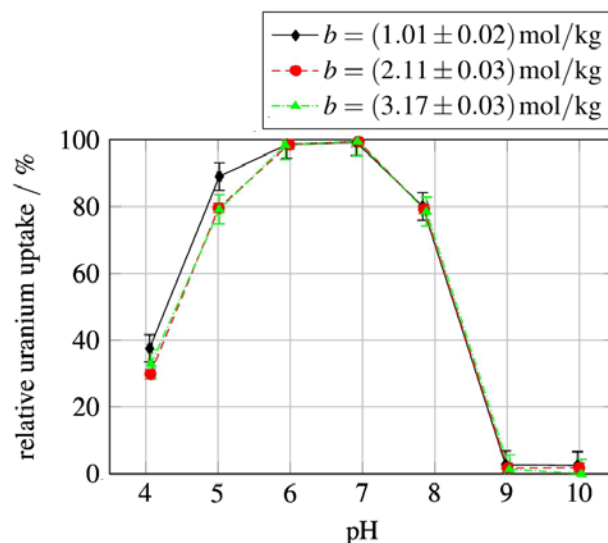

Fig. 1: Uranium sorption on montmorillonite in NaCl.

In $CaCl_2$, matters look decidedly different. There are no pH values where the uranium uptake equals zero. At pH 4, sorption is about 60 % and while there are differences in the sorption values at different calcium concentrations, there is no clear trend to be found. At pH

5 and 6, almost all uranium has sorbed onto montmorillonite. The most interesting pH range lies between pH 6 and 9: uranium sorption decreases and there is a clear distinction in the uranium uptake for the different concentration series—the higher the $CaCl_2$ concentration, the higher the sorption (and thus the more immobile the uranium). At pH 9 and 10, there is again almost complete sorption of the uranium, presumably onto calcite that has precipitated; further experiments will clear this matter up.
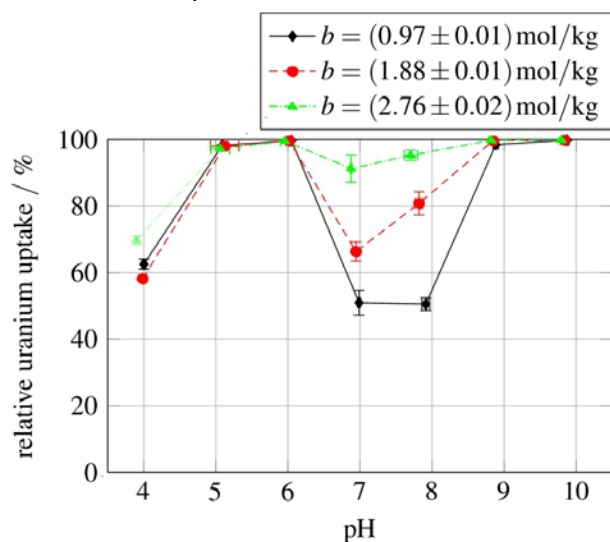

Fig. 2: Uranium sorption on montmorillonite in $CaCl_2$.

What makes the calcium chloride system stay out are the many interdependencies of various parts of the system: firstly, the calcium exchanges against residual sodium in the clay—in a sodium system, sodium migrates into the clay as well, but with Wyoming montmorillonite being a sodium clay, this does not change the properties of the clay, while an exchange against calcium ion does (visible as a decrease in swelling). Furthermore, calcium is able to form a complex with uranium, namely the $Ca_2UO_2(CO_3)_3(aq)$ complex [9-10]. In fact, this mobile complex is usually reported in the pH range where less sorption can be observed in the $CaCl_2$ series. In the alkaline pH range $CaCO_3$, which is part of the carbonate balance, is prone to form, and indeed it does form from pH 8 upwards. Since a change in one of the mentioned subsystems affects the equilibria in the other subsystems, the calcium chloride system as a whole is very difficult to predict and noticeably less stable (though still controllable in the laboratory) than the sodium chloride system.

The present experiments have shown that increased salinities (NaCl, $CaCl_2$) influence the uranium(VI) sorption on montmorillonite in certain pH ranges. Further experiments in KCl and $MgCl_2$ are under way and will complete the overview of the different salt systems.

REFERENCES

1. "Endlagerung radioaktiver Abfälle in Deutschland", BGR (2007).
2. BREWITZ, W., "Eignungsprüfung der Schachtanlage Konrad für die Endlagerung radioaktiver Abfälle. Abschlussbericht.", Gesellschaft für Strahlen- und Umweltforschung *GSF-T 136* (1982).
3. LAGALY, G. et al., "Colloid chemistry of clay minerals: the coagulation of montmorillonite dispersions" *Adv. Colloid Interface Sci.*, **100**, 105-128 (2003).
4. POINSSOT, C. et al. "Experimental studies of Cs, Sr, Ni, and Eu sorption on Na-illite and the modelling of Cs sorption", *Nagra Technical Report 99-04* (1999).
5. BRADBURY, M. et al., "Sorption modelling on illite Part I: Titration measurements and the sorption of Ni, Co, Eu and Sn" *Geochim. Cosmochim. Acta*, **73**, 990-1003 (2009).
6. OLPHEN, H. V. et al., "Data handbook for clay materials and other non-metallic minerals", Pergamon Press, Oxford (1979).
7. MERMUT, A. et al., "Baseline studies of the clay minerals society source clays: Chemical analyses of major elements" *Clays Clay Miner.*, **49**, 381-386 (2001).
8. VOGT, K. et al., "Zur Mineralogie, Kristallchemie und Geochemie einiger Montmorillonite aus Bentoniten" *Clay Minerals*, **13**, 25-43 (1978).
9. BERNHARD, G. et al., "Uranyl(VI) carbonate complex formation: Validation of the $Ca_2UO_2(CO_3)_3$ (aq.) species" *Radiochim. Acta*, **89**, 511-518 (2001).
10. JOSEPH, C. et al., "Sorption of uranium(VI) onto Opalinus Clay in the absence and presence of humic acid in Opalinus Clay pore water" *Chem. Geol.*, **284**, 240-250 (2011).

Complexation of An(III/IV) with Borate in Dilute to Concentrated Alkaline NaCl, CaCl$_2$ and MgCl$_2$ Solutions

K. Hinz[1], M. Altmaier[1], Th. Rabung[1], M. Richmann[2], H. Geckeis[1]

[1] *Karlsruhe Institute of Technology, Institute for Nuclear Waste Disposal, P.O. Box 3640, 76021 Karlsruhe, Germany*
[2] *Los Alamos National Laboratories, Carlsbad Office, 1400 University Drive, Carlsbad NM 88220, N.M., USA*
katja.hinz@kit.edu, marcus.altmaier@kit.edu

INTRODUCTION

For the long-term performance assessment of a nuclear waste repository it is necessary to predict the chemical behavior of actinides in aqueous solutions. Waste disposal in deep underground facilities located in rock salt formations are currently operative or under consideration in the USA and Germany, respectively. In the unlikely scenario of water intrusion, concentrated salt brine solutions are expected to occur. Scientific research on aqueous actinide chemistry in brine systems is therefore a highly relevant research topic.

Under the reducing conditions expected after the closure of a deep underground nuclear waste repository, An(III) and An(IV) are characteristic for the chemistry of the most relevant actinides (Pu, Am, Np, U, Th) in the disposed waste. Boron can be present in the repository as part of the emplaced waste inventory or as a component of the respective aqueous solutions themselves. Hence, the interaction of actinides with borate rich solutions has to be understood in order to assess potential mobilization paths of the actinides into the environment. A previous study has shown that the solubility of Nd(OH)$_3$(am) can be slightly increased by the presence of borate at pH$_c$ ~8.6 [1]. No studies are available so far assessing the interaction of An(IV) with borate. In this framework, the complexation of borate with Nd(III), Cm(III) and Th(IV) (studied as representative analogues for An(III) and An(IV) systems) has been investigated by solubility and TRLFS experiments at an extended pH$_c$ range in dilute to concentrated NaCl, CaCl$_2$ and MgCl$_2$ solutions.

EXPERIMENTAL

All experiments were prepared and carried out in Ar-gloveboxes. Solubility experiments of Nd(III)/Th(IV) were performed with Nd(OH)$_3$(am)/Th(OH)$_4$(am) as solid phase. Samples were prepared in 0.1/5.0 M NaCl, 0.25/3.5 M CaCl$_2$ and 0.25/3.5 M MgCl$_2$ as background electrolytes, with 4 mM $\leq$ [B]$_{tot}$ $\leq$ 400 mM and 7 $\leq$ pH$_c$ $\leq$ 13. The Concentration of Nd and Th was determined by ICP-MS (Perkin Elmer) after phase separation by 10 kd (2-3 nm) ultrafiltration.

TRLFS measurements were performed with ~10^{-7} M Cm(III) per sample, with 0.1/5.0M NaCl and 0.25/3.5M CaCl$_2$/MgCl$_2$ as background electrolytes and 4 mM $\leq$ [B]$_{tot}$ $\leq$ 400 mM. In all systems pH$_c$ 8 and in the CaCl$_2$ system additional pH$_c$ 12 conditions were investigated. Single emission spectra and fluorescence lifetimes were collected.

RESULTS

Nd(OH)$_3$(am) solubility in NaCl/CaCl$_2$ and MgCl$_2$ solutions with borate

No significant increase in the solubility of Nd(OH)$_3$(am) was observed in NaCl, CaCl$_2$ and MgCl$_2$ systems in the presence of borate, compared with the borate-free reference system [2]. On the contrary, a significant decrease in Nd(III) solubility can be observed in NaCl and MgCl$_2$ solutions with pH$_c$ < 9 and [B]$_{tot}$ $\geq$ 40 mM.
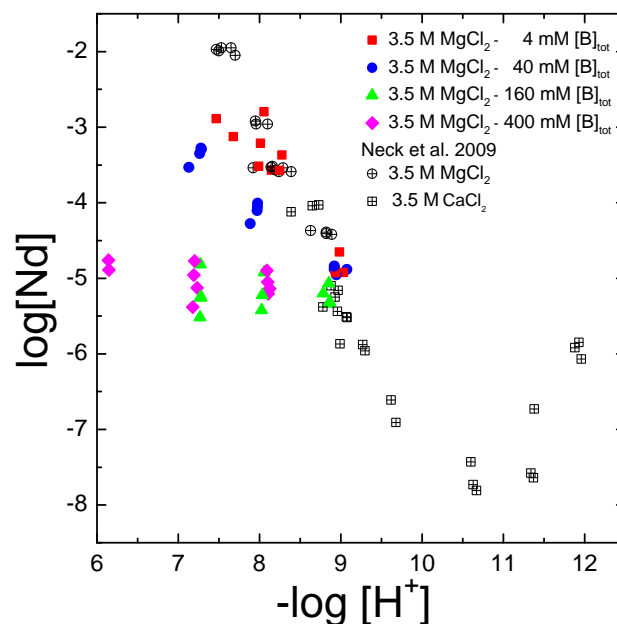

Fig. 1: Solubility of Nd(OH)$_3$(am) in 3.5 M MgCl$_2$ and 4 mM $\leq$ [B]$_{tot}$ $\leq$ 400 mM as function of pH$_c$. Solubility in borate-free systems reported in [2] has been included in the figure for comparison purposes.

This unexpected significant decrease in solubility cannot be explained by changes in aqueous Nd speciation, but rather indicates a transformation of the initial $Nd(OH)_3$(am) solid and the formation of a new secondary Nd(III)-borate phase controlling solubility in borate rich media. This effect would constitute a potential mechanism for actinide retention in a nuclear waste repository not considered in the context of solubility studies and An(III) source term estimations before. Further XRD, SEM-EDX and Raman studies are presently on-going at KIT-INE aiming at a detailed identification and characterization of the newly formed solubility controlling alteration phase.

TRLFS of Cm(III) in NaCl, CaCl$_2$ and MgCl$_2$ solutions and presence of borate

TRLFS spectra collected in the presence of increasing $[B]_{tot}$ at pH_c ~8 show a clear red shift of the Cm(III) fluorescence thus indicating the formation of Cm(III)-borate complexes (see Fig. 2). The number of Cm(III)-borate species and their stoichiometry cannot be resolved from the collected spectra, also due to the expectedly complex and largely unclear boron speciation. At higher pH_c conditions (pH_c ~12), borate complexation is clearly out-competed by the strong hydrolysis of Cm(III). The Cm(III) emission spectra are in good agreement with the borate free system at pH_c ~12 [3].
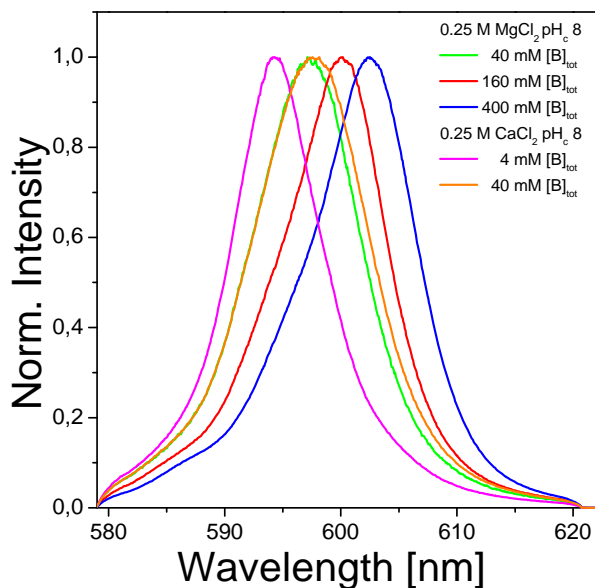

Fig. 3: Emission spectra of Cm(III) at four boron concentrations (4, 40, 160 and 400 mM) and 0.25 M CaCl$_2$ and MgCl$_2$ as background electrolyte. (pH_c = 8 fixed in all cases).

The fluorescence spectra in NaCl, CaCl$_2$ and MgCl$_2$ systems show Cm-borate complexation at pH_c 8-9 but no complexation at higher pH_c where hydroxide is present in high concentrations. The results from Cm-TRLFS are in agreement with the Nd(III) solubility data.

Th(OH)$_4$(am) solubility in NaCl and MgCl$_2$ solutions with borate

First experiments indicate that the solubility of Th(OH)$_4$(am) seem to remain largely unaffected by borate within $7 \leq pH_c \leq 11$ in dilute to concentrated NaCl and MgCl$_2$ solutions in view of large overall uncertainties. The observed large scattering of the measured data may be attributed to the presence of colloids in solution due to insufficient phase separation.

Despite the large scattering, experimental data obtained up to 160 mM $[B]_{tot}$ indicate that even high borate concentrations do not significantly enhance Th(IV) solubility. In contrast to An(III), no solubility decrease for higher boron concentrations is observed at pHc 7-8, probably owing to the much lower total concentration level of solubility data and large scatter of data. The Th(IV) system is currently under further investigation at KIT-INE.

REFERENCES

[1] M. Borkowski et al., "Complexation of Nd(III) with tetraborate ion and its effect on actinide (III) solubility in WIPP brine" *Radiochimica Acta*, **98**, 577 (2010).

[2] V. Neck et al., "Thermodynamics of trivalent actinides and neodymium in NaCl, MgCl$_2$, and CaCl$_2$ solutions: Solubility, hydrolysis and ternary Ca-M(III)-OH complexes", *Pure and Applied Chemistry*, **81**, 1555-1568 (2009).

[3] Th. Rabung et al., "A TRLFS study of Cm(III) hydroxide complexes in alkaline CaCl$_2$ solutions", *Radiochimica Acta*, **96**, 551-559 (2008).

Investigations to the Eu(III)-B(OH)₃-Organic System at Increased Salt Concentrations

J. Schott[1], M. Acker[2], J. Kretzschmar[1], A. Barkleit[1,3], S. Taut[2], V. Brendler[1], G. Bernhard[3]

[1]*Helmholtz-Zentrum Dresden-Rossendorf, Institute of Resource Ecology, P.O. Box 510119, 01314 Dresden, Germany*
email: j.schott@hzdr.de
[2]*Dresden University of Technology, Central Radionuclide Laboratory, 01062 Dresden, Germany*
[3]*Dresden University of Technology, Departm. of Chemistry and Food Chemistry, Radiochemistry, 01062 Dresden, Germany*

INTRODUCTION

Actinides, such as Am, Cm and Pu, will define the long-term radiotoxicity of spent nuclear fuel in nuclear waste repositories. Due to water ingress into a repository, these actinides could be dissolved and might become accessible to subsequent reactions like complexation with organic and inorganic ligands or formation of solid phases. For the safety and risk assessment of a nuclear repository, these physicochemical reactions have to be understood.

Boric acid ($B(OH)_3$) and (poly)borates are of great interest regarding the mobilization of trivalent actinides in nuclear waste repositories, particularly in salt deposits [1]. There, borates can appear in increased amounts due to naturally occurring deposits and anthropogenic sources (waste containers, borosilicate glasses).

The aqueous chemistry of boric acid/borates is very complex. Up to a critical boric acid concentration of 25 mM, only the dissociation of $B(OH)_3$ is observed, whereas at higher concentrations also polymerization of $B(OH)_3$ to tri-, tetra-, pentaborate and higher structured species occur. In the past, some investigations were carried out to clarify the borate speciation in aqueous solution (e.g. by Raman or NMR [2, 3]).

The complexation properties of $B(OH)_3/B(OH)_4^-$ and polyborates concerning radionuclides, especially trivalent actinides, are still hardly investigated. A first work was carried out by Borkowski et al. regarding the complexation between Nd(III) and tetraborate [1]. They found a moderate complexation (log β = 3…4), which could compete with the carbonate complexation.

Furthermore, different polyborates of trivalent actinides and lanthanides were synthesized via hydrothermal syntheses, e.g. [4]. The obtained borate structures are very complex and the solid structure depends on the metal ion.

This work describes the complex formation between a borate ester of salicylate (Fig. 1) and Eu(III).
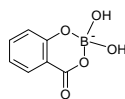

Fig. 1: salicylate borate ester

The motivation was to use this borate ester structure (which occur in the acidic pH range) as analog structure for the monoborate ion $B(OH)_4^-$, which only exists in adequate amounts for complexation studies in the alkaline pH range. To avoid the strong hydroxide complexation or precipitation of Eu(III) this detour due to the borate ester was tested as strategy to determine the formation constant between Eu(III) and $B(OH)_4^-$. In preliminary experiments (TRLFS, ^{11}B-NMR) an influence of $B(OH)_3$ on the Eu(III) salicylate complexation due to the borate ester formation could be observed.

Furthermore, a solid Eu(III) borate species can be reported, which already occurs under ambient conditions in slightly acidic (pH 6) salt solutions (0.1 - 3 M NaClO₄/ NaCl) in presence of polyborates. This could be an interesting possibility for the immobilization of trivalent actinides in a nuclear waste repository.

DESCRIPTION OF THE WORK

Complex formation between Eu(III) and borate ester of salicylate

The formation constant of the salicylate borate ester was obtained from potentiometric titration (Metrohm).
For the determination of the stability constant of the Eu(III) borate ester a spectrophotometric TRLFS (time-resolved laser-induced fluorescence spectroscopy) titration was carried out. A Eu(III) solution (8×10^{-6} M) was titrated with a stock solution of 0.02 M salicylate and 0.6 M $B(OH)_3$ at pH 5. After each titration step a static fluorescence spectrum was measured with a Nd:YAG-OPO laser system (Continuum).

Eu(III) borate solid formation

Samples of different $B(OH)_3$ concentrations (0.2 - 0.7 M) and c(NaClO₄) = 0.1 M were prepared at pH 5 and pH 6 under ambient conditions (22°C, $p_{CO2} = 10^{-3.5}$ atm). Eu(III) (3×10^{-5} M) and NaClO₄/NaCl (0.1 - 3 M salt concentration) were added to aliquots of the prepared $B(OH)_3$ stock solutions. The samples were investigated by membrane filtration (0.2 μm pore size) and TRLFS over time. Static and time-resolved spectra were recorded. The same samples without Eu(III) were investigated with ^{11}B-NMR spectroscopy (Varian Unity Inova 400) to determine the (poly)borate speciation at pH 5 and pH 6.

RESULTS

Complex formation between Eu(III) and borate ester of salicylate

The stability constant of the salicylate borate ester (Fig. 1) was determined to be log β = 1.20 ± 0.04, which is in good agreement with literature data [5, 6].
A stability constant of the Eu(III) borate ester was determined to be log β = 3.35 ± 0.06, which is in good agreement with the stability constant between Nd(III) and borate determined by Borkowski et al. [1]. The stability constant is under validation.

Eu(III) borate solid formation

Due to filtration experiments, the formation of a solid Eu(III) borate species at pH 6 can be established which was not observed at pH 5 after 71 days observation time of the samples [7]. This shows the involvement of polyborate species in the solid formation. Using ^{11}B-NMR spectroscopy polyborate species (tri-, pentaborate) at pH 6 and above 0.4 M $B(OH)_3$ can be detected and at pH 5 in marginal (detection limit) amounts at higher concentrations (> 0.6 M $B(OH)_3$) [8]. Furthermore, only in presence of Eu(III) a solid formation is observable.

The solid formation at pH 6 was investigated by TRLFS (Fig. 2). After a start-up phase, the solid formation begins, which is reflected in a characteristic band splitting of the $^5D_0{\rightarrow}^7F_1$ and $^5D_0{\rightarrow}^7F_2$ transition of the Eu luminescence and an extensive increase of the Eu luminescence lifetime τ. This can be used as a marker for the solid formation progress. From this result, a mechanism of the solid formation can be postulated. Starting from a soluble weak Eu polyborate complex (τ ~ 150 μs), a clustering of this species occurs followed by a nucleation and precipitation of the solid Eu borate species (τ ~ 650 μs).

The solid formation depends on the polyborate concentration (Fig. 3). The smaller the initial $B(OH)_3$ (polyborate) concentration the slower the formation of the solid species. The solid formation (in $NaClO_4$ medium) can be detected for $B(OH)_3$ concentrations ≥ 0.4 M which is consistent with the borate speciation at pH 6 [8].

Furthermore, the solid formation depends on the salt ($NaClO_4$/NaCl) concentration and shows a dependence on the salt type. This was not expected, because the borate speciation at pH 6 is independent from the salt concentration. In the $NaClO_4$ medium a minimum of the formation rate at ~ 0.5 M $NaClO_4$ can be detected. Very high salt concentrations (~ 3 M $NaClO_4$) lead to a rapid solid formation. For the NaCl medium, the formation rate decreases with increasing salt concentration. This could be explained by the complexation of Eu(III) with chloride as a competition reaction to the solid formation.
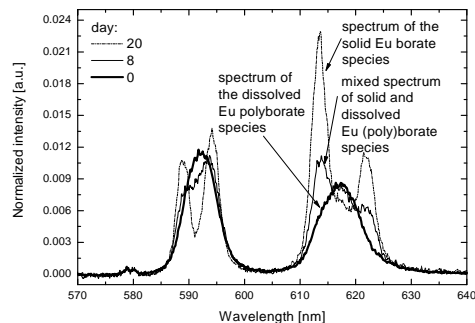

Fig. 2:   Eu luminescence spectra of the dissolved and solid Eu borate
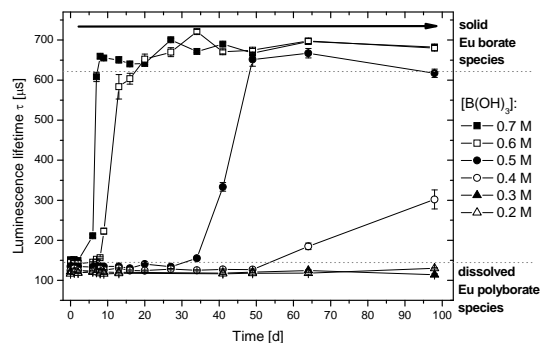
Fig. 3:   Eu luminescence lifetime τ with time in dependence on initial $[B(OH)_3]$; 0.1 M $NaClO_4$, pH 6

REFERENCES

1. M. Borkowski et al., "Complexation of Nd(III) with tetraborate ion and its effect on actinide(III) solubility in WIPP brine" *Radiochim. Acta,* **98**, 577-582 (2010).
2. T. Hirao et al., "Raman spectra of polyborate ions in aqueous solution" *J. Inorg. Nucl. Chem.,* **41**, 1217-1220 (1979).
3. A. Hertam, Thesis, Freiberg University of Mining and Technology (2011).
4. M. J. Polinski et al., "Differentiating between trivalent lanthanides and actinides"*J. Am. Chem. Soc.,* **134**, 10682-10692 (2012).
5. O. Lukkari et al., "Equilibria of nitrosalicylic acids. Complex formation between boric acid and salicylic and nitrosalicylic acid" *Fin. Chem. Let.*, **15**, 13-17 (1988).
6. R. Larsson et al., "An infrared spectroscopic investigation on the complexes formed between boric acid and salicylate ions" *Acta Chem. Scan.*, **26**, 1503-1509 (1972).
7. J. Schott et al., "The formation of an Eu(III) borate solid species in aqueous solution", Annual Report HZDR-030, 57 (2013).
8. J. Schott et al., "Borate speciation at pH 5 and pH 6 determined by ^{11}B-NMR spectroscopy", Annual Report HZDR-030, 56 (2013).

Preliminary High Temperature Experiments Bearing on Pu Solubility Using Nd Analogs

Jonathan P. Icenhower[1], David K. Shuh[2], and Donald T. Reed[3]

[1]*Lawrence Berkeley National Laboratory, Earth Sciences Division, One Cyclotron Road, Berkeley CA 94720, USA*
email: *jpicenhower@lbl.gov*
[2]*Lawrence Berkeley National Laboratory, Chemical Sciences Division, One Cyclotron Road, Berkeley CA 94720, USA*
[3]*Los Alamos National Laboratory, 1400 University Drive/Carlsbad, NM 88220, USA*

INTRODUCTION

Of the actinide elements present in the WIPP repository, plutonium has garnered the most attention due to its abundance in the waste, its radiotoxicity, the long half-lives of its principal isotopes, and because of the many redox states that it can manifest under burial conditions. A number of investigators have recently concluded that Pu(III), rather than Pu(IV), may be the dominant redox state in WIPP brines [1, 2]. Geochemical modeling indicates that the solubility of Pu(III) is ~100× higher than that of Pu(IV) ($1.7 - 3.1 \times 10^{-7}$ M versus $0.58 - 2.5 \times 10^{-8}$ M, respectively, at $T = 25°C$) and plutonium may thus be more mobile than expected [1] . The objective of this work is to obtain high temperature (50 – 200°C) solubility measurements of $Nd(OH)_3$, an analog of $Pu(OH)_3$. Part of our motivation stems from a need to understand the behavior of Pu in near-field environments, in which temperatures may exceed 150°C, and to validate thermodynamic properties of plutonium solids by taking measurements over a temperature interval. We herein report our strategy for quantifying the solubility of Pu, which begins by first obtaining data on Nd(III), a non-radiological analog element whose solubility at ambient conditions mimics that of Pu(III) closely.

DESCRIPTION OF THE WORK

Solubility data will be obtained using a titanium Parr reactor system at Lawrence Berkeley National Laboratory. The primary virtue of this system is that reagents can be mixed in a non-reactive vessel at constant temperature and pressure conditions up to 500°C and 1000 bars pressure. The system is pressurized by Xe gas in the headspace of the reactor. Xe is non-reactive with the reagents and has low solubility in the aqueous solution. Sampling is conducted periodically through a valve connected to a backpressure regulator the gas pressure maintains constant pressure while solution is removed.

Experiments will be conducted at 50, 100, 150, and 200°C. Solutions containing NaCl or $MgCl_2$ (0.0, 0.001, 0.005 and 0.010 m) will serve as the aqueous "matrix" at pH = 8 (the likely pH in WIPP vaults). More concentrated brines will used in later experiments. We will mainly rely on Nd(III) for the initial experiments before moving to

Pu-239. As the chemical analog of Pu(III), Nd(III) is useful because it is not redox-insensitive and possesses a nearly identical ionic radius to Pu(III) (111 vs. 112 pm at C.N. = 8; [3]). In all experiments, we will use solutions that are free of CO_2. Experiments using Nd(III) are divided into "direct" and "indirect" and are discussed separately below.

1. "Indirect" experiments with Nd(III). "Indirect" refers to experiments in which a solid is partially dissolved in solution at a temperature above that of the target, and then subsequently cooled to the target temperature in an attempt to get new crystal growth formation on the residual solids. The newly precipitated material "armors" the residual solid and equilibrium is established between the surface and the solution. In these experiments, Nd(III) will be added as $Nd_2O_3(s)$, which is unstable in the presence of aqueous solution [3]. Examination of the post-run solids will be performed using an electron microprobe equipped with wave-length dispersive spectrometry, transmission electron microscopy (TEM), as well as micro-nanobeam syncrohtron radiation methods including x-ray absorption near-edge structure, elemental mapping, scanning transmission x-ray microscopy, and diffraction (c.f., [4, 5]). The presence of new growth will be confirmed by the observation of overgrowths characterized by sharp terminations, rather than rounded and scalloped features on dissolved surfaces.

2. "Direct" experiments with Nd(III). With "direct" experiments, the temperature will be raised to the value of interest and held at constant temperature until equilibrium between the solid and solution has been established. As in the "indirect" experiments, $Nd_2O_3(s)$ will be added and the $Nd_2O_3(s)$ will partially dissolve into solution until equilibrium (as defined as constant concentration of dissolved Nd in the sampled solutions) is reached. Alternatively, the Nd(III)

will be added as $Nd(OH)_3$, which can be synthesized using the procedure outlined in [6].

Because the experiments will be conducted over a temperature interval, it may be possible to extract thermodynamic values from a plot of R ln K versus inverse temperature (van't Hoff equation) (c.f., [6]). However, the typical non-linearity of systems over a significant temperature interval usually requires a different strategy for retrieving thermodynamic properties. A successful strategy has been outlined by Clarke and Glew [7] and will be used if the van't Hoff-style regression fails.

REFERENCES

1. LUCCHINI, J-F et al., "Solubility of Nd^{3+} and UO_2^{2+} in WIPP brine as oxidation-state invariant analogs for plutonium," *J. Alloys Comp*. **444-445**, 506-511(2007).

2. REED, DT et al., "Reduction of plutonium(VI) in brine under subsurface conditions." *Radiochim. Acta* **94**, 591-597 (2006).

3. NECK, V. et al., "Thermodynamics of trivalent actinides and neodymium in NaCl, $MgCl_2$, and $CaCl_2$ solutions: Solubility, hydrolysis, and ternary Ca—M(III)—OH complexes." *Pure Appl. Chem*. **81**, 1555-1568 (2009).

4. DÄHN, R et al., "Soft X-ray Spectromicroscopy of Cobalt Uptake by Cement." *Environ. Sci. Technol*. **45**, 2021-2027 (2011).

5. KUNZ, M. et al., "A dedicated superbend X-ray microdiffraction beamline for materials; Geo- and environmental sciences at the Advanced Light Source." *Rev. Sci. Instru*. **80**, 035108 (2009).

6. RAO, L, RAI, D, and FELMY, AR, "Solubility of $Nd(OH)_3$[c] in 0.1 M NaCl aqueous solution at 25°C and 90°C." *Radiochim. Acta* **72**, 151-155 (1996).

7. KNAUSS, KG and COPENHAVER, SA, "The solubility of p-xylene in water as a function of temperature and pressure and calculated thermodynamic quantities." *Geochim Cosmochim. Acta* **59**, 2443-2448 (1995).

8. CLARKE, EC and GLEW, DN, "Evaluation of thermodynamic functions from equilibrium constants." *Trans. Faraday Soc*. **62**, 539-547 (1966).

The Effect of Nitrate on Trivalent Actinide and Lanthanide Solubility in Dilute to Concentrated Brine Solutions

M. Herm[1], X. Gaona[1], Th. Rabung[1], C. Crepin[2], V. Metz[1], M. Altmaier[1], H. Geckeis[1]

[1] *Karlsruhe Institute of Technology, Institute for Nuclear Waste Disposal (KIT–INE), Germany*
michel.herm@kit.edu
[2] *Ecole National Supérieure de Chimie de Montpellier (ENSCM), France*

INTRODUCTION

A reliable prediction of the chemical behavior of actinides in aqueous solutions is necessary in performance assessment studies for deep geological nuclear waste repositories. Though, to some extent, geological or geotechnical barrier systems may prevent formation water from contacting the waste, intrusion of aqueous solutions into a repository has to be taken into account within the long–term. In salt rock repositories, intruding water as well as fluid inclusions and brine pockets are characterized by high ionic strengths, mostly dominated by high $[Na^+]$, $[Mg^{2+}]$ and $[Cl^-]$. Formation waters with elevated ionic strength are also expected to occur in certain sedimentary bedrocks and argillites.

Under reducing conditions, which develop after closure of deep underground repositories for nuclear waste, actinides are expected to prevail in tri– and tetravalent redox states. In repositories with waste from nuclear fuel reprocessing, high concentrations of nitrate (≥ 1 M) and slow nitrate reduction kinetics have to be taken into account.

Nitrate complexes of actinides are reported to be weak, though clearly more stable than the chloride complexes [1]. Accounting for An(III)–NO_3 complexes, the last NEA–TDB update [2] selected only thermodynamic data for the complex $AmNO_3^{2+}$, whereas no thermodynamic data was made available for the system Pu(III)–NO_3. Recent Cm(III)–TRLFS studies with nitrate concentrations up to 4.0 M proposed the formation of $CmNO_3^{2+}$ and $Cm(NO_3)_2^+$ complexes and provided both log $\beta°$ and $\Delta_r H°$ data [3–4]. So far all these studies focused on acidic conditions, leaving aside the assessment of nitrate effects under neutral to alkaline, repository–relevant pH conditions.

In this study, the solubility and speciation of trivalent actinides and lanthanides in dilute to concentrated mixed NaCl–$NaNO_3$ and MgCl$_2$–Mg(NO_3)$_2$ solutions are investigated at an extended pH$_c$ range (7.5–13) at 22 ± 2°C.

DESCRIPTION OF THE WORK

All samples were prepared and stored in Ar gloveboxes under exclusion of oxygen. Solubility experiments of Nd(III) were conducted with Nd(OH)$_3$(am) as solid phase. Samples were prepared with NaCl–$NaNO_3$ (0.1, 0.5, 1.0, 2.5 and 5.0 M) and MgCl$_2$–Mg(NO_3)$_2$ (0.25, 1.0, 2.5, 3.5 and 4.5 M) as background electrolytes. Nitrate concentration ranged between 0.0 and 7.0 M per batch solubility experiment. The pH$_c$ values, determined with combination glass electrodes (Orion Ross, Thermo Scientific), were controlled by the addition of organic buffers, brucite/Mg–oxychloride, HCl and NaOH. [Nd(III)] was determined by ICP–MS (X–Series II, Thermo Scientific) after 10 kD ultrafiltration (Pall Life Science). Solid phases were characterized using XRD (D8 Advance diffractometer, Bruker AXS) and SEM–EDX (Quanta 650 FEG, FEI).

TRLFS measurements were performed with ~10^{-7} M Cm(III) per sample, with 0.25/3.5 M MgCl$_2$–Mg(NO_3)$_2$ as background electrolyte, containing 0.0 to 7.0 M NO_3^- and $1 \leq pH_c \leq 9$. Cm(III) fluorescence spectra were collected using a Nd:YAG (Surelite II Laser, Continuum) pumping a dye laser (Narrowscan Dye Laser, Radiant Dyes).

RESULTS

Nd(OH)$_3$(am) solubility in MgCl$_2$–Mg(NO_3)$_2$ and NaCl–$NaNO_3$ solutions

The comparison of Nd(III) solubility concentrations in MgCl$_2$–Mg(NO_3)$_2$ systems with nitrate–free MgCl$_2$ solutions [5] shows a clear increase of [Nd(III)] for $[Mg^{2+}] \geq 2.5$ M, $[NO_3^-] \geq 1.0$ M and pH$_c$ 8–9 (Figure 1). In contrast to Mg–bearing systems, no effect of nitrate on Nd(III) solubility is observed in dilute to concentrated NaCl–$NaNO_3$ solutions, even in 5.0 M $NaNO_3$.

XRD and SEM–EDX results confirm that Nd(OH)$_3$(am) is the solubility controlling solid phase in all systems with $[Cl^-] \leq 5.0$ M.

Cm(III)–TRLFS in MgCl$_2$–Mg(NO_3)$_2$ solutions

TRLFS studies in 3.5 M MgCl$_2$–Mg(NO_3)$_2$ with $0 \leq [NO_3^-] \leq 7$ solutions indicate the formation of $CmNO_3^{2+}$ (1,1) and $Cm(NO_3)_2^+$ (1,2) complexes in acidic to near neutral pH conditions, as previously described in [3]. Peak deconvolution of the complete set of fluorescence spectra further reveals the formation of

ternary Cm–OH–NO$_3$ species under weakly alkaline pH conditions, likely CmOHNO$_3^+$ and Cm(OH)$_2$NO$_3$(aq) (Figure 2). These results confirm that the observed increase in solubility for Nd(OH)$_3$(am) is not a simple matrix effect (ion–interaction effect) but is clearly related to a genuine complexation reaction of Cm with nitrate.
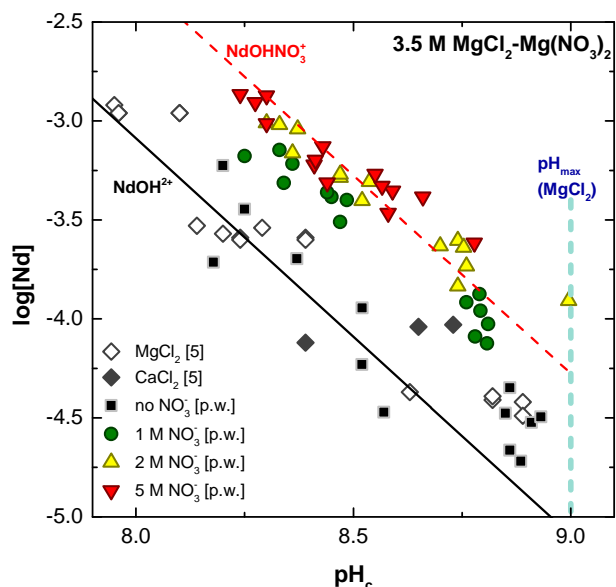

Fig. 1: Solubility of Nd(OH)$_3$(am) in 3.5 M MgCl$_2$–Mg(NO$_3$)$_2$ mixtures. Dashed red line is the solubility curve in the respective system for 5.0 M NO$_3^-$. Solid black line corresponds to calculated Nd(III) aqueous speciation in nitrate–free systems according with [5].

Chemical and thermodynamic model

The parallel slopes of the Nd(III) solubility curves (log[Nd] *vs.* pH$_c$) in presence and absence of nitrate clearly indicate that the number of OH–ligands involved in the complex formation is the same in both cases. Note that Neck et al. [5] reported the predominance of NdOH^{2+} under virtually the same pH$_c$ and absence of NO$_3^-$. TRLFS further indicates that only one nitrate ligand is complexing with Cm(III). Both observations hint towards the predominance of the species An^{III}OHNO$_3^+$ in the aqueous phase. The lack of any effect of nitrate in NaCl–NaNO$_3$ solutions indicates the relevant role of ionic strength in enhancing the stability of this species.

Further considering Nd(OH)$_3$(am) as solubility controlling solid phase (XRD, SEM–EDX), the chemical model of An(III) as proposed in [5] must be extended in the presence of nitrate with the chemical reaction:

$$Nd(OH)_3(am) + 2H^+ + NO_3^- \Leftrightarrow NdOHNO_3^+ + 2H_2O$$
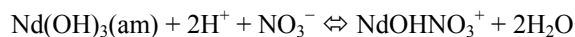
where

$$\log {}^*K'_{s,(1,1,1)} = \log[Nd] - \log[NO_3^-] + 2\,pH_c$$

Thermodynamic modelling of the An(III)–NO$_3$ system in MgCl$_2$–Mg(NO$_3$)$_2$ solutions will include both SIT and Pitzer approaches.
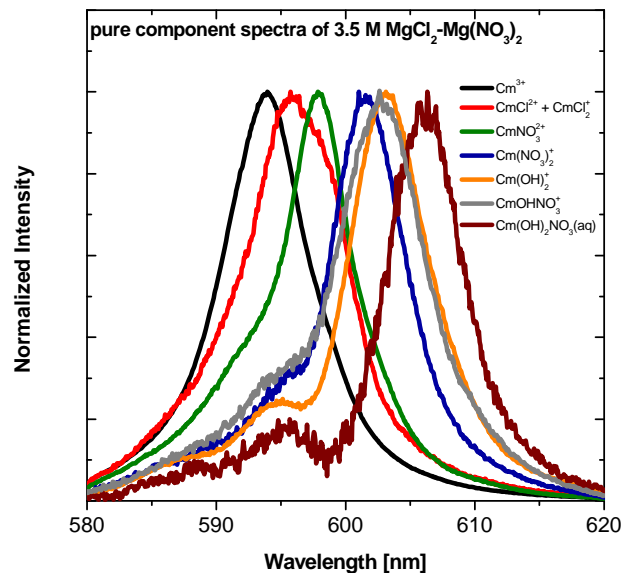

Fig. 2: Deconvoluted spectra of pure components in the Cm(III)–H$_2$O–Cl–NO$_3$ system.

REFERENCES

[1] Altmaier, M. et al., "Recent advances in aqueous actinide chemistry and thermodynamics" *Chemical Reviews*, **113**, 901–943 (2013).

[2] Guillaumont, R. et al., "Chemical Thermodynamics 5. Update on the Chemical Thermodynamics of Uranium, Neptunium, Plutonium, Americium and Technetium" Elsevier, Amsterdam (2003).

[3] Skerencak, A. et al., "TRLFS study on the complexation of Cm(III) with nitrate in the temperature range from 5 to 200°C" *Radiochimica Acta*, **97**, 385–393 (2009).

[4] Rao, L. et al., "The effect of temperature on the complexation of Cm(III) with nitrate in aqueous solutions" *Dalton Transaction*, **40**, 914–918 (2011).

[5] Neck, V. et al., "Thermodynamics of trivalent actinides and neodymium in NaCl, MgCl$_2$, and CaCl$_2$ solutions: Solubility, hydrolysis, and ternary Ca–M(III)–OH complexes" *Pure and Applied Chemistry*, **81**, 1555–1568 (2009).

ABC-Salt III Workshop

Wednesday, April 17th
Presentation
Abstracts

This page intentionally left blank.

Geochemical Process Modeling for the Waste Isolation Pilot Plant (WIPP)
2014 Compliance Recertification Application (CRA-2014) Performance Assessment (PA) Calculations[A]

L. H. Brush[1] and P. S. Domski[2]

[1]Nuclear Waste Disposal Research and Analysis Dept. 6222, Sandia National Laboratories,[B] Albuquerque, NM 87108 USA
lhbrush@sandia.gov
[2]S. M. Stoller Corporation, 400-2 Cascades Ave., Suite 202, Carlsbad NM 88220 USA

INTRODUCTION

The Waste Isolation Pilot Plant (WIPP) is a U.S. Department of Energy (DOE) repository in southeast New Mexico for defense-related transuranic (TRU) waste. The repository, which opened in March 1999, is located at a subsurface depth of 655 m in the Salado Fm., a Permian bedded-salt formation. After filling the repository with TRU waste and installation of panel closures, creep closure of the salt will crush the steel waste containers in most cases and encapsulate the waste.

We use Generic Weep Brine (GWB)[1, 2] to simulate intergranular brines from the Salado Fm. at the stratigraphic horizon of the repository and Energy Research and Development Administration (WIPP Well) 6 (ERDA-6)[3] to represent fluids in brine reservoirs in the underlying Castile Fm. ERDA-6 is mainly an NaCl brine; GWB is a high-Mg brine.

Anoxic corrosion of Fe-, Pb-, and Al-base metals in the waste containers and/or TRU waste; and microbial consumption of cellulosic, plastic, and rubber (CPR) materials in the waste containers and/or TRU waste could produce significant quantities of gas (H_2, CO_2, H_2S, and CH_4) in the WIPP. The DOE is emplacing MgO in the repository to decrease the solubilities of the actinide elements in TRU waste in any brine present in the postclosure repository. MgO will decrease actinide solubilities by consuming essentially all of the CO_2 produced by microbial consumption of CPR materials (even if microbes consume all of the CPR materials in the TRU waste and/or waste containers), thereby maintaining the f_{CO_2} and pH within ranges favorable from the standpoint of actinide solubilities.

We assume that equilibria among these brines and the solids halite (NaCl), anhydrite ($CaSO_4$), brucite ($Mg(OH)_2$), and hydromagnesite ($Mg_5(CO_3)_4(OH)_2 \cdot 4H_2O$) will control near-field chemical conditions.

_____

We expect that the brucite-hydromagnesite carbonation reaction will buffer f_{CO_2} in the repository during the first several hundred to a few thousand years, but that the brucite-magnesite ($MgCO_3$) reaction might buffer f_{CO_2} thereafter.

Calculations with EQ3/6, version 8.0a[4, 5, 6, 7] and the thermodynamic database (DB) DATA0.FM1[8] predicted an f_{CO_2} of 3.14×10^{-6} atm[9] in the repository for both GWB and ERDA-6, based on the brucite-hydromagnesite buffer. This value of the f_{CO_2}, along with the predicted values of pH provided in the next paragraph and the predicted actinide solubilities for the CRA-2014 PA (see Table 1 on the next page), are our predictions for the minimum volume of brine required for a release from the repository to the surface. Compositions for larger volumes (2 ×, 3 ×, 4 ×, and 5 × the minimum brine volume) are not shown in this abstract, may vary from those predicted for the minimum brine volume, and will be provided on request.

The brucite dissolution-precipitation reaction will increase the "Pitzer pH" of GWB or ERDA-6 from their mildly acidic in situ values to predicted values of 8.82 in GWB[9] and 8.99 in ERDA-6[9]. The Pitzer pH scale is an unofficial scale consistent with pH values calculated using single-ion activity coefficients based on the Pitzer activity-coefficient model and the Harvie-Møller-Weare (HMW) DB,[10] expanded to include Th(IV), Np(V), and Am(III). T. J. Wolery of Lawrence Livermore National Laboratory (LLNL) in Livermore, CA, proposed the term "Pitzer scale" unofficially.

Our predictions of actinide speciation and solubilities under the long-term chemical conditions expected in the WIPP include: (1) solubility models based on the Pitzer activity-coefficient model and the HMW DB,[10] extended to include Th(IV), Np(V), and Am(III); (2) inclusion of the effects of acetate, citrate, EDTA, and oxalate (the organic ligands in TRU waste) on Th(IV), Np(V), and Am(III) speciation and solubilities; (3) redox speciation of Th, U, Np, Pu, and Am entirely as Th(IV), U(IV), Np(IV), Pu(III), and Am(III); or Th(IV), U(VI), Np(V), Pu(IV), and Am(III); (4) use of EQ3/6 to calculate the speciation and solubilities of Th(IV), Np(V), and Am(III) in GWB and ERDA-6; (5) use of the oxidation-state analogy[11] to apply the solubilities calculated for Th(IV) to U(IV), Np(IV), and Pu(IV); and to apply those calculated for Am(III) to Pu(III) (the model developed for

Np(V) has been used only for Np(V) because Np is the only actinide expected to speciate in the +V oxidation state under expected WIPP conditions); and (6) use of a solubility estimate of 1×10^{-3} M for U(VI)[12].

Table 1 (see below) compares the "baseline" or "nominal" solubilities[9] (to which deviations sampled from the uncertainty ranges are added or subtracted) predicted for the 1997 Performance Assessment Validation Test (PAVT), the Compliance Recertification Application-2004 (CRA-2004) Performance Assessment Baseline Calculation (PABC), the CRA-2009 PABC, and the CRA-2014 PA.

Table 1. Comparison of the Baseline Solubilities[9] Predicted for the 1997 PAVT, the CRA-2004 PABC, the CRA-2009 PABC, and the CRA-2014 PA (M).

	PAVT	CRA-2004 PABC
An(III), GWB	1.2×10^{-7}	3.87×10^{-7}
An(III), ERDA-6	1.3×10^{-8}	2.88×10^{-7}
An(IV), GWB	1.3×10^{-8}	5.64×10^{-8}
An(IV) ERDA-6	4.1×10^{-8}	6.79×10^{-8}
An(V), GWB	2.4×10^{-7}	3.55×10^{-7}
An(V), ERDA-6	4.8×10^{-7}	8.24×10^{-7}

	CRA-2009 PABC	CRA-2014 PA
An(III), GWB	1.66×10^{-6}	2.59×10^{-6}
An(III), ERDA-6	1.51×10^{-6}	1.48×10^{-6}
An(IV), GWB	5.63×10^{-8}	6.05×10^{-8}
An(IV) ERDA-6	6.98×10^{-8}	7.02×10^{-8}
An(V), GWB	3.90×10^{-7}	2.77×10^{-7}
An(V), ERDA-6	8.75×10^{-7}	8.76×10^{-7}

We established uncertainty factors for the Th(IV) and Am(III) solubility models by comparing laboratory measurements of solubilities from the literature with EQ3/6 predictions made for the same conditions. We constructed separate cumulative distribution functions (CDFs) of the logs of the differences between measured and predicted solubilities for the Th(IV) and Am(III) models. No uncertainty analysis was carried out for Np (this element has essentially no effect on WIPP PA).

WIPP PA uses Th(IV) and Am(III) solubilities obtained by multiplying the baseline solubilities for GWB or ERDA-6 by uncertainty factors sampled from the CCDFs for Th(IV) or Am(III).

REFERENCES

1. Krumhansl, J.L., K.M. Kimball, and C.L. Stein. 1991. *Intergranular Fluid Compositions from the Waste Isolation Pilot Plant (WIPP), Southeastern New Mexico*. SAND90-0584. Albuquerque, NM: Sandia National Laboratories.
2. Snider, A.C. 2003. "Verification of the Definition of Generic Weep Brine and the Development of a Recipe for This Brine." ERMS 527505. Carlsbad, NM: Sandia National Laboratories.
3. Popielak, R.S., R.L. Beauheim, S.R. Black, W.E. Coons, C.T. Ellingson and R.L. Olsen. 1983. *Brine Reservoirs in the Castile Formation, Waste Isolation Pilot Plant Project, Southeastern New Mexico*. TME 3153. Carlsbad, NM: U.S. Department of Energy WIPP Project Office.
4. Wolery, T.J., and R.L. Jarek. 2003. "Software User's Manual: EQ3/6, Ver. 8.0." Doc. No. 10813 UM-8.0-00. Albuquerque, NM: Sandia National Laboratories.
5. Wolery, T.J. 2008. "Analysis Plan for EQ3/6 Analytical Studies." ERMS 548930. Carlsbad, NM: Sandia National Laboratories.
6. Wolery, T.J., Y.-L. Xiong, and J.J. Long. 2010. "Verification and Validation Plan/Validation Document for EQ3/6 Version 8.0a for Actinide Chemistry, Document Ver. 8.10." . ERMS 550239. Carlsbad, NM: Sandia National laboratories.
7. Xiong, Y.-L., 2011. "WIPP Verification and Validation Plan/Validation Document for EQ3/6 Ver. 8.0a for Actinide Chemistry, Rev. 1." ERMS 555358. Carlsbad, NM. Sandia National Laboratories.
8. Xiong, Y.-L. 2011. "Release of EQ3/6 Database DATA0.FM1." ERMS 555152. Carlsbad, NM: Sandia National Laboratories.
9. Brush, L.H., and P.S. Domski. 2013. "Prediction of Baseline Actinide Solubilities for the WIPP CRA-2014 PA." ERMS 559138. Carlsbad, NM: Sandia National Laboratories.
10. Harvie, C.E., N. Møller, and J.H. Weare. 1984. "The Prediction of Mineral Solubilities in Natural Waters: The Na-K-Mg-Ca-H-Cl-SO$_4$-OH-HCO$_3$-CO$_3$-CO$_2$-H$_2$O System to High Ionic Strengths at 25 °C," *Geochimica et Cosmochimica Acta*. Vol. 48, no. 4, 723-751.
11. Choppin, G.R. 1999. "Utility of Oxidation State Analogs in the Study of Plutonium Behavior," *Radiochimica Acta*, Vol. 85, 89–95.
12. U.S. EPA. 2006. "Technical Support Document for Section 194.24: Evaluation of the Compliance Recertification – Actinide Source Term and Culebra Dolomite Distribution Coefficient Values," EPA Air Docket A 98-49, Item II B1-3, U.S. Environmental Protection Agency Office of Air and Radiation, Washington, DC.

The Role of Laboratory Data and Screening Criteria on the WIPP Actinide Solubility Uncertainty Analysis[i]

P. S. Domski[1] and L. H. Brush[2]

[1]*S.M. Stoller Corporation 400-2 Cascades Ave., Suite 202 Carlsbad NM 88220 USA*
psdomsk@sandia.gov
[2]*Nuclear Waste Disposal Research and Analysis Dept. 6222, Sandia National Laboratories[ii], Albuquerque, NM 87108 USA*
lhbrush@sandia.gov

INTRODUCTION

The Waste Isolation Pilot Plant (WIPP) is a U.S. Department of Energy (DOE) repository in southeast New Mexico for defense-related transuranic (TRU) waste. The repository, which opened in March 1999, is located at a subsurface depth of 655 m in the Salado Fm., a Permian bedded-salt formation. After filling the repository with TRU waste and installation of panel closures, creep closure of the salt will crush the steel waste containers in most cases and encapsulate the waste.

The WIPP repository must be recertified by the U.S. Environmental Protection Agency (EPA) every five years after first receipt of waste in order to continue receiving waste. For the first recertification, the EPA requested that the DOE update the actinide-solubility uncertainty analysis to include new experimental data unavailable at the time of the original WIPP Compliance Certification Application (CCA). Beginning in 2004, each compliance recertification application (CRA) has included updated actinide-solubility uncertainty analyses. In addition to new experimental data, subsequent uncertainty analyses have also updated the screening criteria used in deciding which data to include.

The method by which the actinide solubility uncertainty analysis is updated is a four-step process:
1) Literature searches and screening
2) Simulate laboratory studies
3) Compare experimental and simulated results
4) Derive cumulative distribution functions

For the CRA-2014 Performance Assessment (PA), a new screening criterion, G11, was implemented to include only experimental data obtained under experimental conditions at — or close to − the buffered values of pcH, ionic strength, and total inorganic carbon (TIC) content expected at WIPP.

This paper documents each WIPP actinide-solubility uncertainty analyses and how the addition of new experimental data has changed the uncertainty distributions for each CRA, for both Th(IV) and Am(III). Particular attention is given to the CRA-2014 PA uncertainty analysis and how the addition of the new screening criterion affected the uncertainties distributions.

RESULTS

Figure 1 shows the CRA-2014 PA Th(IV) distribution before criterion G11 was applied (green), and the data that did not meet the pcH subcriterion (blue). Neither the ionic strength nor TIC subcriteria applied to Th(IV) because of prior prescreening for ionic strength and because none of the experiments included bicarbonate or carbonate.

Table 1 provides the statistical parameters of Brush and Domski (2013a &b) and the previous two PABCs.

Table 1. Results of Th(IV) Uncertainty Analyses.

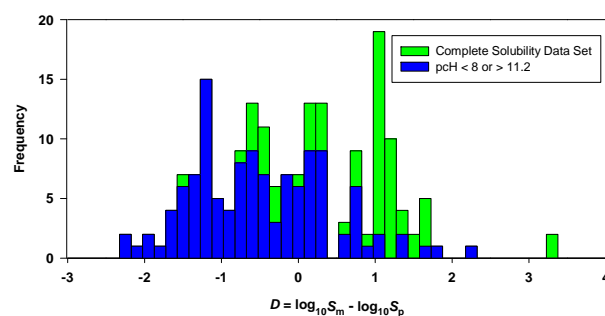|	CRA-2004 PABC	CRA-2009 PABC	Complete Solubility Data Set	G11 Data Set
Maximum	2.40	3.30	3.19	3.19
Minimum	−1.80	−2.25	−2.28	−1.52
Mean	0.108	−0.346	−0.136	0.676
Median	0.075	−0.520	−0.189	1.029
Std. Dev.	0.837	0.995	1.061	0.869
n	45	140	185	64

Figure 1. Th(IV) uncertainty distributions showing data retained and screened out by the pcH criterion (blue).
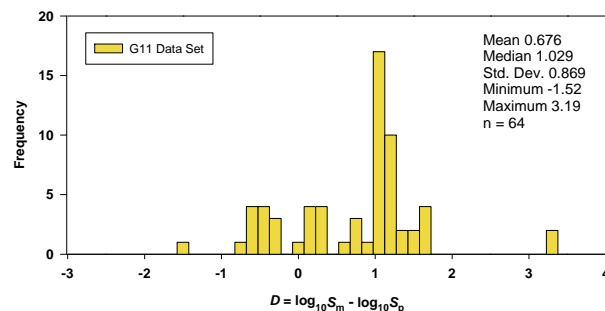

Figure 2. Th(IV) uncertainty distribution Brush and Domski (2013b).

Figure 2 shows the final Th(IV) distribution that resulted from subtracting the blue from the green in Figure 1. Application of criterion G11 moved the

distribution to the right; increased the mean from -0.136 to 0.676; and decreased the number of comparisons from 185 to 64 (Table 1).

Figures 3, 4, and 5 show the full Am(III) dataset in green, and the data screened out by the G11 criteria in blue for ionic strength, pcH, and TIC, respectively. The final dataset used in the CRA-2014 PA is shown in yellow in Figure 6. For Am(III), criterion G11 moved the distribution to the left; decreased the mean from 0.441 to −0.678 (Table 1); and decreased the number of comparisons from 647 to 172.

Table 2. Results of Am(III) Uncertainty Analyses.

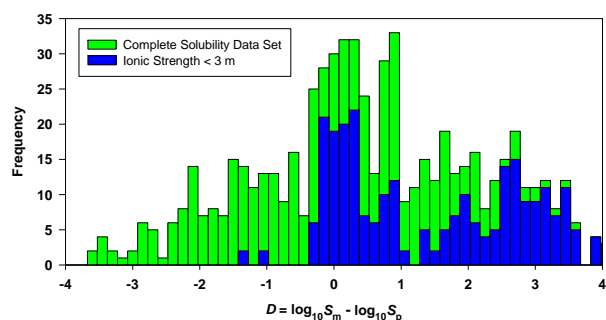|	CRA-2004 PABC	CRA-2009 PABC	Complete Solubility Data Set	G11 Data Set
Maximum	2.85	2.70	3.95	2.97
Minimum	−3.00	−4.20	−3.67	−3.55
Mean	0.035	−0.142	0.441	−0.678
Median	−0.031	0.072	1.17	−0.866
Std. Dev.	0.900	1.17	1.67	1.57
n	243	441	647	172

Figure 3. Am(III) uncertainty distributions showing data retained and screened out by the ionic-strength subcriterion (blue).
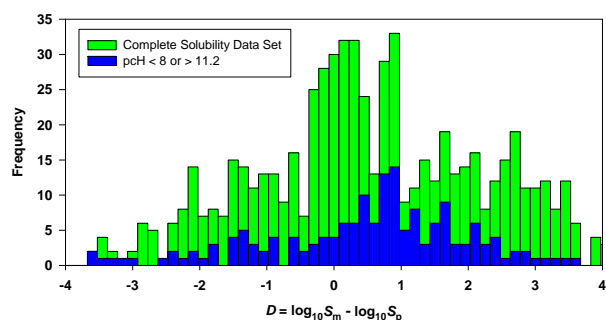

Figure 4. Am(III) uncertainty distributions showing data retained and screened out by the pcH subcriterion (blue).

Implementation of the WIPP-specific screening criterion G11 restricted the results of experimental studies used in the uncertainty analysis to those which are representative of expected WIPP near-field conditions. Each subsequent recertification results in more experimental studies screened for inclusion in the uncertainty analyses, and also provides the opportunity to improve the methods used in these analyses.
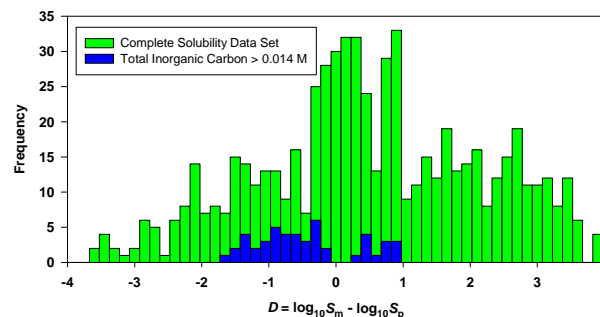

Figure 5. Amercium(III) uncertainty distributions showing data retained and screened out by the TIC subcriterion (blue).
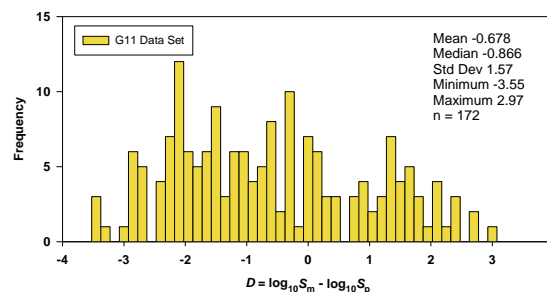

Figure 6. Am(III) uncertainty distribution used for the CRA-2014 PA.

REFERENCES

Brush, L.H., and P.S. Domski. 2013a. "Uncertainty Analysis of Actinide Solubilities for the WIPP CRA-2014 PA". Carlsbad, NM: Sandia National Laboratories. ERMS 559278.

Brush, L.H., and P.S. Domski. 2013b. "Uncertainty Analysis of Actinide Solubilities for the WIPP CRA-2014 PA, Rev.1, Supersedes ERMS 559278". Carlsbad, NM: Sandia National Laboratories. ERMS 559712.

Xiong, Y.L., L.H. Brush, P.S. Domski, and J.J. Long. 2011. "Uncertainty Analysis of Actinide Solubilities for the WIPP CRA-2009 PABC, Rev. 1, Supersedes ERMS 552500. Carlsbad, NM: Sandia National Laboratories. ERMS 554875.

Xiong, Y.L., L.H. Brush, A.E. Ismail, and J.J. Long. 2009. "Uncertainty Analysis of Actinide Solubilities for the WIPP CRA-2009 PABC. Carlsbad, NM: Sandia National Laboratories. ERMS 552500.

Geochemical Modeling in Highly Saline Conditions

L. Duro[1], D. García[1], E. Colàs[1], V. Montoya[2, 1]

[1]Amphos 21, Passeig de Garcia i Fària, 49-51, 1-1, 08019 Barcelona (Spain)
[2]Karlsruhe Institute of Technology (KIT), Institute for Nuclear Waste Disposal (INE), Hermann-von-Helmholtz-Platz 1, 76344 Eggenstein-Leopoldshafen (Germany)

INTRODUCTION

Solubility assessment of radionuclides is a fundamental process in the performance assessment exercises of repositories for high level nuclear waste management. Most of the work done up to date refers to the conditions existing in the groundwaters likely to contact the wastes in the eventuality of the failure of the container. Saline groundwaters are of special concerns for some of the disposal concepts in Europe and especially the USA. The treatment of salinity and how it affects the chemical behavior of radionuclides is a yet non-resolved issue. Several activity correction methods have been developed to account for the calculation of activity coefficients under saline groundwaters. The most widely used is the Pitzer approach, which considers different long-range ion interactions. Although much advance has been done in the last years in the determination of Pitzer coefficients, the current state of knowledge is far from ideal. This is why alternative approaches for activity corrections are normally used in solubility assessment exercises, such as the Specific Ion-Interaction Theory (SIT), which accounts for shorter-range interactions but provides in many cases a good estimation of salinity effects over its usual range of application (I<0.3m). This work shows the comparison between both approaches (SIT and Pitzer) in reproducing the chemistry of some radionuclides of interest under the conditions of the Canadian generic repository for high level nuclear wastes.

We present the solubility of 19 radionuclides (Am, As, Bi, C, Cu, Mo, Nb, Np, Pa, Pb, Pd, Pu, Ra, Se, Sn, Tc, Th, U and Zr) calculated by using two different thermodynamic databases, mainly activity correction approaches: i) The Yucca Mountain Pitzer (YMP) database [1], which uses Pitzer ionic strength corrections, and, ii) ThermoChimie [2], the thermodynamic database of ANDRA (The French National Radioactive Waste Management Agency). ThermoChimie uses SIT (Specific Ion Interaction Theory) for ionic strength corrections and its most update version is released as sit.dat with the PhreeqC code [3]. Solubility limits for several radionuclides of interest for Canada were calculated 15-20 years ago based on a range of water chemistries from Canadian Shield crystalline rock data and using thermodynamic data available at that time [4]. The calculations have been conducted with the PhreeqC, geochemical code.

DESCRIPTION OF WORK

Two different groundwater compositions representative of groundwaters expected in the geological formation likely to host a future Canadian geological repository have been chosen in this study: the saline crystalline groundwater (CR-10) and the highly saline sedimentary groundwater (SR-270) provided by NWMO (Nuclear Waste Management Organization) [5].

Solubility calculations have been carried out with groundwaters equilibrated with minerals present at repository depth (*CR-10 eq* and *SR-270 eq*) and groundwaters equilibrated with the bentonite buffer and the carbon steel insert of the copper container (*CR-10 NF* and *SR-270 NF*). Main assumptions in these calculations are: i) the system temperature is fixed at 25ºC, ii) neither sulfate to sulfide reduction nor sulfide to sulfate oxidation is considered, iii) reduction of carbonate to methane and reduction of nitrate to ammonium or $N_2(g)$ are neglected, and iv) the basic Ostwald's principle [6], i.e. the less crystalline phases are kinetically favored to precipitate, is assumed.

The Yucca Mountain Pitzer (YMP) database has been used in the solubility assessment of Am, C, Cu, Np, Mo, Pu, Tc, Th, U and Zr. ThermoChimie has been used to compare the results obtained with the Yucca Mountain Pitzer database. The SIT database has also been used for the solubility assessment of the elements not included in the Yucca Mountain Pitzer database (As, Bi, Nb, Pa, Pb, Pd, Ra, Se, Sn and Zr). Fig.1 shows an example of the work done in the comparison exercise.
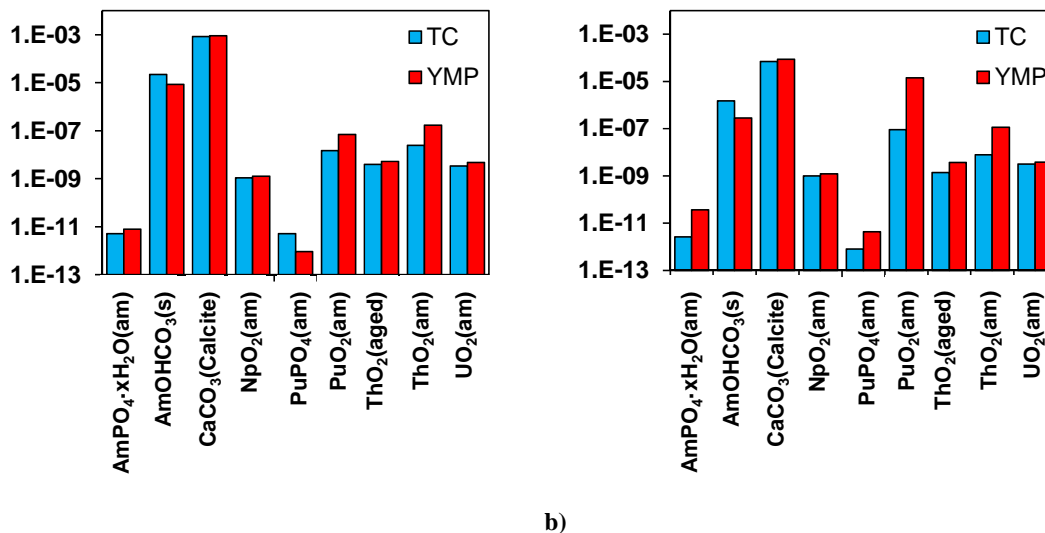
a)　　　　　　　　　　　　　　　　**b)**

Fig. 1. Calculated solubility limits for Am, C, Np, Pu, Th and U. Calculations done by using the ThermoChimie (TC, blue bars) and Yucca Mountain Pitzer (YMP, red bars) databases. Solubilities are calculated for two groundwaters: a) CR-10 eq, and b) CR-10 NF.

Sensitivity analyses, studying the influence of some key parameters (pH, Eh, iron, carbonate, calcium, chloride, phosphate concentrations, sulfate reduction to sulfide, and carbonate reduction to methane) on the solubility of radionuclides, and qualitative uncertainty analysis, describing the conceptual uncertainties that may affect the solubility limits of a radionuclide, are also provided.

CONCLUSIONS

The solubility assessment done for the elements in both databases led, except in few cases, to differences in the solubility values below ± 1 logarithmic unit for all elements. Main differences obtained in the assessment are due to: i) lack of thermodynamic data in the database, ii) difference in activity coefficients calculated with each approximation, and/or, iii) inconsistencies in the thermodynamic data selection.

ACKNOWLEDGEMENTS

REFERENCES

[1] C. Jove-Colon, T. Wolery, J. Rard, A. Wijesinghe, R. Jareck, K. Helan. *Pitzer database development: Description of the Pitzer geochemical thermodynamic database data0.ypf.R2. Appendix I. In In-Drift Precipitates/Salts Model*. Report ANL-EBS-MD-000045 REV 03 (2007)
[2] L. Duro, M. Grivé, E. Giffaut. *ThermoChimie, the ANDRA Thermodynamic Database.* MRS Proceedings, 1475 (2012)
[3] D. Parkhurts and T. Appelo. *User's guide to PHREEQC*. USGS Report 99-4259 (1999)
[4] R.J. Lemire and F. Garisto. *The Solubility of U, Np, Pu, Th and Tc in a Geological Disposal Vault for Used Nuclear Fuel.* Report AECL-10009. (1989)
[5] L. Duro, V. Montoya, E. Colàs, D. García. *Groundwater equilibration and radionuclide solubility calculations.* NWMO TR-2010-02 (2010)
[6] W. Ostwald. *Studien über die Bildung und Umwandlung fester Körper.* Zeitschrift für Physikalische Chemie, 22, 289–330 (1897)

Pitzer Equations and Alternative Methods of Modelling Multicomponent Electrolyte Solutions

Darren Rowland and Peter May.

Chemical and Analytical Sciences, Murdoch University, South St, Murdoch 6150, Australia
email: d.rowland@murdoch.edu.au

INTRODUCTION

The Pitzer equations have been applied to a large number of electrolyte solutions under ambient and non-ambient conditions. This has resulted in the appearance in the literature of many sets of parameters. Unfortunately, the various parameters are frequently incompatible, restricted to limited ranges of conditions and constantly at risk of being superseded. In order to meet the demands of different modelling contexts and make the most of available data, automated methods of generating reliable Pitzer models are needed.

While binary solutions of environmentally-significant electrolytes have generally been characterised experimentally over large ranges of temperature, pressure and concentration, sometimes by independent investigators, the coverage of experimental results for ternary electrolyte solutions is far less satisfactory. Data for ternary systems are rarely consistent enough to obtain meaningful ternary parameter values [1]. As such, subjective judgements are common, for example, opting to set all of the ternary interaction parameters to zero [1]. Due to this fact, finding a complete set of parameters to model multicomponent systems is problematic [2].

Against this background, mixing rules like Young's rule [3] and Zdanovskii's rule [4] can serve a useful role in modelling mixed electrolyte solutions. One of the key advantages of mixing rules is that mixture properties can be predicted even in the absence of experimental measurements on ternary electrolyte solutions.

DESCRIPTION OF THE WORK

A facility has been developed for obtaining Pitzer parameters that describe binary strong electrolyte solutions under ambient conditions and an appropriate upper concentration limit for their validity. In addition, this allows Pitzer model parameters to be optimised over ranges of temperature, pressure and concentration.

Given the difficulties of applying the Pitzer equations to electrolyte solutions for which there are few available data, the mixing rules of Young and Zdanovskii, which do not require ternary interaction parameters, have been investigated for their ability to estimate the physicochemical properties of multicomponent electrolyte solutions in a robust manner.

RESULTS

The equations of the Pitzer theoretical framework are general and flexible. For aqueous binary electrolyte solutions that are experimentally well-characterised, the Pitzer equations provide an excellent way to harmonise data from various literature sources and to represent the data up to high concentrations. Of 180 binary electrolyte solutions investigated, more than 80% were satisfactorily represented at 25 °C to the limit of available data or to concentrations greater than 6 mol kg^{-1} [5].

However, in some cases physicochemical properties are not so well characterised. When the Pitzer equations are used to describe data having gaps or larger-than-normal errors they are prone to diverge from realistic/theoretical trends (Fig. 1). Having insufficient data to constrain the Pitzer parameters is especially problematic under superambient conditions. To overcome the lack of robustness and excessive flexibility of the Pitzer equations, subjective judgements must be made regarding how many parameters are best-suited to describe the available data.
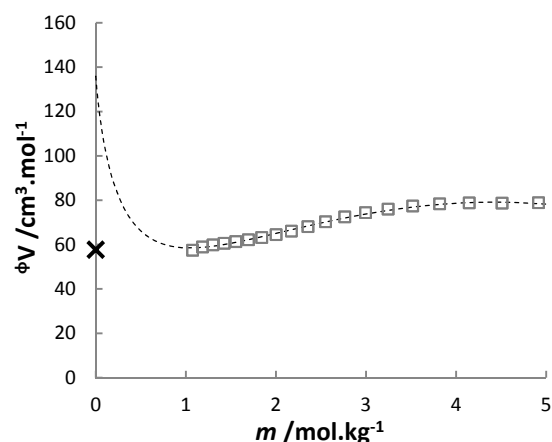
Fig. 1: Calculated values of the apparent molar volume of CsSO$_4$(aq) at T = 298.15 K. The Pitzer model (dashed line) has been fitted to data from [6] (squares). The approximate standard state apparent molar volume based on additivity is shown (cross).

In contrast, when dealing with multicomponent electrolyte solutions, mixing rules provide a robust alternative to the Pitzer equations. For example, although Young's rule has typically been employed using binary solutions at the same ionic strength as the mixture, other

conditions can be employed without altering the mathematical form of the mixing rule. A key finding of this work is that many predictions derived from different mixing rules only differ insignificantly, i.e., within the estimated experimental uncertainty based on measurements from different investigators (see Fig. 2).
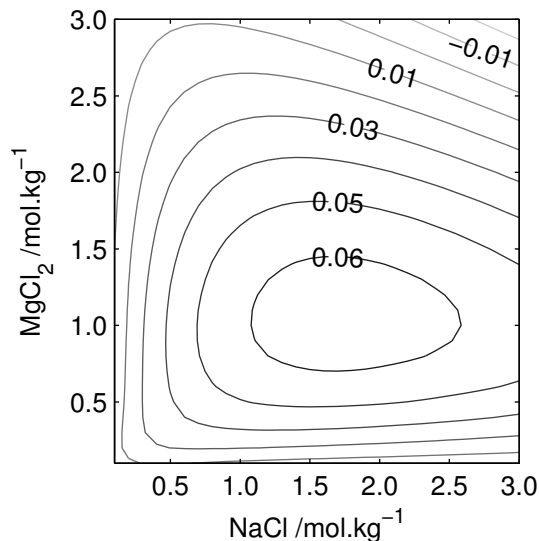

Fig. 2: Apparent molar volume (cm^3 mol^{-1}) difference contours calculated from Young's rule. Values are the difference between predictions based on binary solutions having equal ionic strength and the predictions based on binary solutions having equal water activity. This is to be compared with a probable uncertainty of (0.1 to 0.2) cm^3 mol^{-1} between independent experimentalists.

Mixing rules also offer modellers other benefits. Practically all properties of multicomponent solutions can be predicted based on the known behaviour of the binary electrolyte sub-systems. This is true even under superambient conditions. Accordingly, the need for experimental data is greatly reduced.

On the other hand, there are some evident drawbacks to using mixing rules to predict mixture properties. First, as is well known, the binary properties must be well-characterised to high concentrations – sometimes greater than the aqueous solubility limit of the electrolyte. Second, the predictions assume that the net interactions between the solutes are negligible, which is obviously not always the case, e.g., when complexes are known to form. Finally, due to numerical difficulties mixing rules are best suited to predicting the properties of major solution components rather than minor components, i.e., water activity is predicted more reliably than trace activity coefficients [7].

REFERENCES

[1] MONNIN, C, "An Ion Interaction Model for the Volumetric Properties of Natural Waters: Density of the Solution and Partial Molal Volumes of Electrolytes to High Concentrations at 25 °C" *Geochim. Cosmochim. Acta,* **53**, 1177-1188 (1989).

[2] KRUMGALZ, BS et al., "Ion Interaction Approach for Volumetric Calculations for Solutions of Single Electrolytes at 25 °C" *J. Solution Chem.,* **23**, 849-875 (1994).

[3] YOUNG, TF et al., "Thermodynamic Properties of Mixtures of Electrolytes in Aqueous Solutions" *J. Phys. Chem.,* **58**, 716-724 (1954).

[4] CHEN, H et al., "A General Method of Predicting the Water Activity of Ternary Aqueous Solutions from Binary Data" *Can. J. Chem. Eng.,* **51**, 234-241 (1973).

[5] MAY, PM et al., "A Generic and Updatable Pitzer Characterization of Aqueous Binary Electrolyte Solutions at 1 bar and 25 °C" *J. Chem. Eng. Data,* **56**, 5066-5077 (2011).

[6] ASEYEV, GG et al., "Estimation Methods and Experimental Data" Begell House Inc., N.Y., U.S.A. (1996).

[7] ROWLAND, D et al., "An Investigation of Zdanovskii's Rule for Predicting the Water Activity of Multicomponent Aqueous Strong Electrolyte Solutions" *J. Chem. Eng. Data,* **57**, 2589-2602 (2012).

Advanced Simulation Capability for Environmental Management – Current Status and Phase II Demonstration

Paul Dixon[1], Mark D. Freshley[2], Susan S. Hubbard[3], Tim Scheibe[2], Stefan Finsterle[3], J. David Moulton[1], Carl I. Steefel[3], Roger R. Seitz[4], and Justin Marble[5]

[1]Los Alamos National Laboratory, MS B284, P.O. Box 1663, Los Alamos, NM 87544
[2]Pacific Northwest National Laboratory, MSIN K9-33, P.O. Box 999, Richland, WA 99352
[3]Lawrence Berkeley National Laboratory, 1 Cyclotron Road, MS 50B-4230, Berkeley, CA 94720
[4]Savannah River National Laboratory, Savannah River Site, Bldg 773-43A, Aiken, SC 29808
[5]Department of Energy, 19901 Germantown Road, Germantown, MD 20874-1290

Introduction

Advanced Simulation Capability for Environmental Management (ASCEM) is developing a state-of-the-art scientific tool and approach for understanding and predicting contaminant fate and transport in natural and engineered systems. ASCEM is combining supercomputing capabilities, with new and open-source high performance computing modeling application platforms, data analysis and integration approaches, and evolving understanding of subsurface hydrological-biogeochemical processes in order to improve subsurface contaminant fate and transport simulations as needed to support risk-informed environmental remediation and waste management decisions. ASCEM will also provide other DOE programs, such as WIPP, and the scientific community with a powerful open-source code and approach that should be applicable to a variety of subsurface flow and transport problems, as well as performance and risk assessments. ASCEM will be updated and augmented as new insights and approaches are developed through research and testing.

ASCEM Technical Work Flow

ASCEM initiative is organized into three Thrust Areas (Figure
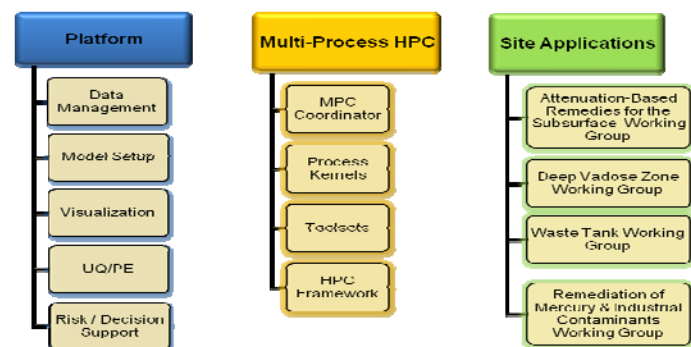
Figure 1: ASCEM Technical Organization

➢ Multi-Process High Performance Computing (HPC), **Amazi** [1] provides a flexible and extensible simulation capability and supports a wide range of process complexity in flow and reactive transport models [2] and

supports the graded and iterative approach to performance and risk assessment.

➢ Platform and Integrated Toolsets—The **Akuna** Toolset is a collection of Java-based desktop graphical user interfaces (GUIs) to support a complete modeling workflow, from model setup to simulation execution and analysis. It is designed to perform basic model setup, Sensitivity Analysis (SA), inverse modeling, Parameter Estimation (PE) and Uncertainty Quantification (UQ), launching and monitoring simulations, and visualization of both model setup and simulation results. **Agni** software—located on the computer server—takes modeling requests from the Akuna client, executes them, and reports information back to the user interface.

➢ Site Applications provides the field test bed for testing and vetting ASCEM capabilities and working the EM enduser interface.
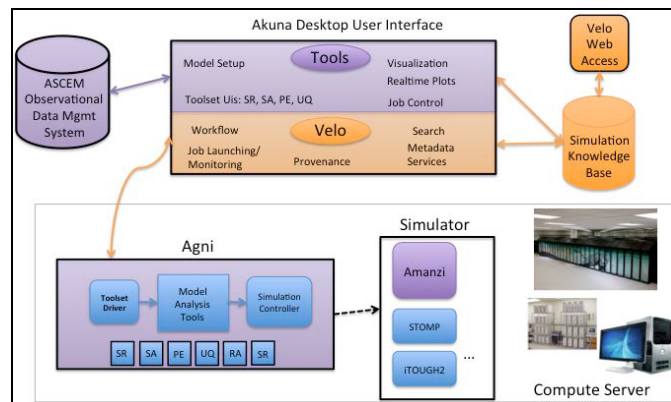
Figure 2: ASCEM Technical Work Flow

ASCEM Program Status

As part of the development process, demonstrations are planned to test and highlight ASCEM components, engage end users in applications, and provide feedback to developers. The **Phase I** demonstration report focused on illustrating individual (stand-alone) ASCEM capabilities. **Phase I** demonstration was conducted at the Savannah River Site (SRS) F Area and provided an early snapshot of advances associated with four specific components of ASCEM: Data Management; Visualization; UQ; and High Performance Computing (HPC).

1) and the work flow between these thrusts is illustrated in Figure 2:

The **Phase II** demonstration [4] followed a major development phase and relied on the Site Applications Thrust Working Group for testing developing capabilities, providing feedback to developers on the relative priority and implementation of new capabilities in association with the demonstrations. The Phase II Demonstration report built upon Phase I, and the future demonstrations will focus on integrating all of ASCEM capabilities, on continuing to develop ASCEM components, and on illustrating how the ASCEM toolsets can be used to address DOE-EM problems. The Phase II demonstration was the Hanford Site deep vadose zone (BC Cribs). This site and it served as an application site for a start to finish demonstration of capabilities, with emphasis on integration and linkages between the Platform and HPC components. Other Phase II demonstrations included addressing attenuation-based remedies at the Savannah River Site F Area to exercise linked ASCEM components under data dense and complex geochemical conditions.

The **Phase III** demonstration will build upon past successes though developing capabilities. For instance at SRS, Phase III demonstration will be used to create a 'living model' for the F-Area, which can in turn be used with F-Area operations staff to assess existing and consider new remediation strategies.   In conjunction with Phase III activities, an "ASCEM Tutorial and User Testing Sessions" is planned for the purpose of introducing the EM community to ASCEM and getting feedback for the project.   In addition, modules could be developed in ASCEM to represent the Thermal-Mechanical and Thermal-Hydrological-Chemical processes necessary for accurate analysis of various in-drift emplacement concepts.
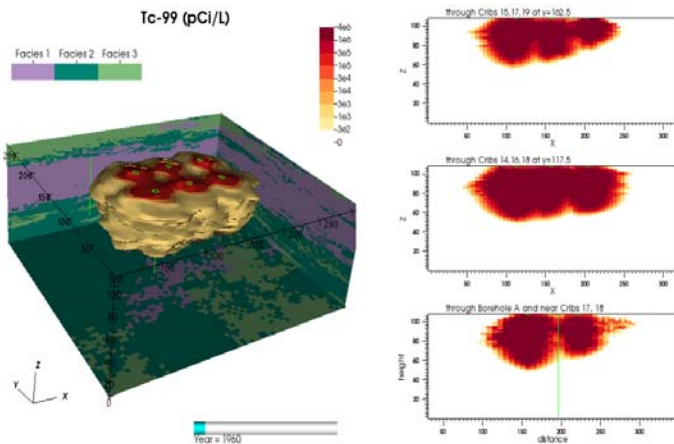

Figure 2. Spatial Distribution of ^{99}Tc after the releases from the Hanford B-C cribs using VisIt software.
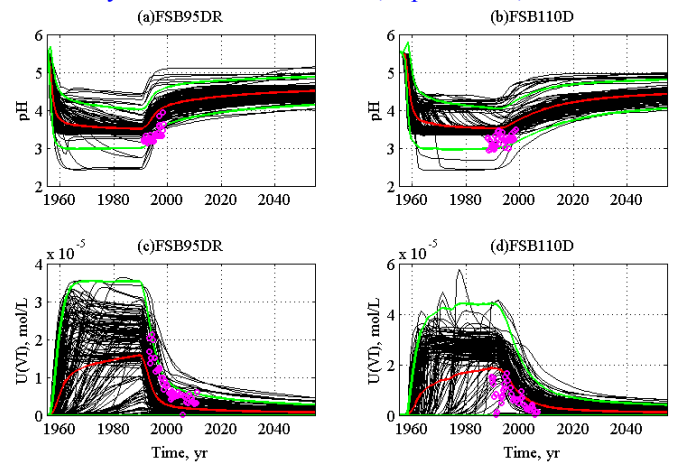

Figure 3. Monte Carlo simulation results: breakthrough curves and uncertainty ranges. The black lines are the predicted breakthrough curves, red lines are the mean predicted curves, green lines are the mean +/- 2 standard deviations, and the magenta dots are observations.

References

[1] Moulton D, et al., 2011, *High-Level Design of Amanzi, the Multi-Process High Performance Computing Simulator*, ASCEM-HPC-2011-03-1, U.S. Department of Energy, Washington, D.C.

[2] Steefel C, et al., 2011, *Mathematical Formulation Requirements and Specifications for the Process Models*. ASCEM-HPC-2011- 1-0a, U.S. Department of Energy, Washington, D.C.

[3] Gorton I, et al., 2010, *System Requirements for ASCEM Platform and Integrated Toolsets,* ASCEM-PIT-102610-Rev. 3, U.S. Department of Energy, Washington, D.C.

[4] Freshley et al., 2012, *Phase II Demonstration*, ASCEM-SITE-2012-01, U.S. Department of Energy, Washington, DC, OSTI ID is 1055500.

THEREDA Database Project

Helge C. Moog

Global Research for Safety, GRSmbH, Theodor-Heuss-Str. 4, 38122 Braunschweig, Germany.

ABSTRACT

Part of the process to ensure the safety of radioactive waste disposal is the possibility to give good estimates of the solubility of toxic elements in aqueous solutions. In Germany the prospective disposal in rock salt sparked the interest in the modeling of dissolution reactions in brine solutions. Usually the Pitzer and the SIT approach were used to calculate aqueous phase activity coefficients.

To ensure the reliability of such calculations and to facilitate the comparability of the results, it was decided by several institutions in Germany to create a common database with mutually accepted thermodynamic data - THEREDA.

From a technical point of view THEREDA can be thought of as a suite of programs to enter, manipulate, and export thermodynamic data, thereby maintaining internal consistency and to assist the editors with the usually necessary debugging of a database of increasing complexity.

As the question about the nature of host rock for the disposal of radioactive waste in Germany is still a matter of debate, THEREDA was designed as flexible as possible, to enable it to also meet future demands. It is therefore not restrained to the Pitzer model nor to any other specific model for the calculation of activity coefficients. It is also possible to handle other non-ideal mixed phases as the aqueous one.

The principal outputs of the project are ready-to-use parameter files for four supported codes:

- PHREEQC
- EQ3/6
- Geochemist's Workbench (GWB)
- CHEMAPP

Each released parameter file is accompanied by a document in which a number of benchmark calculations are presented along with the result. As the database gradually evolves, these benchmark calculations are repeated to ensure that by the addition of new data (and possibly by the manipulation of data in the meantime) earlier achievements are not compromised.

The following benchmarks have been releases so far:

- R01: Polythermal solubilities in selected ternary solutions with regard to the system of oceanic salts
- R02:
  - Am(III), Cm(III), Nd(III) in $MgCl_2$ and $CaCl_2$ solutions at 298.15K
  - Am(III), Cm(III), Nd(III) in NaCl solutions at 298.15K
- R03: Solubility in selected ternary salt solutions with regard to the system of oceanic salts in presence of CO_2 and carbonates
- R04: Solubility and hydrolysis of Np(V) in NaCl solutions at 298.15K
- R05: Activities and solubilities in solutions of Cs, Na, K, Mg, Ca, Cl and SO_4 at 298.15 K

The further development of THEREDA is closely related to the ongoing work on the data. At present the technical foundation is laid to save and export surface complexation data. For the modeling of CO_2-solubility in brines we have adopted the gas model by Spycher and Reed [1]. We are also considering the addition of a fifth supported code (GEMS [2]), but a final decision on this has not been made yet.

REFERENCES

1. NICHOLAS F. SPYCHER, MARK H. REED: Fugacity coefficients of H_2, CO_2, CH_4, H_2O and of H_2O-CO_2-CH_4 mixtures: A virial equation treatment for moderate pressures and temperatures applicable to calculations of hydrothermal boiling. *Geochim. Cosmochim. Acta* **52,** 739-749 (1988).

2. D. A. KULIK, T. WAGNER, S. V. DMYTRIEVA, G. KOSAKOWSKI, F. F. HINGERL, K. V. CHUDNENKO, U. BERNER: GEM-Selektor geochemical modeling package: revised algorithm and GEMS3K numerical kernel for coupled simulation codes. Computational Geosciences **17**, 1-24 (2013).

This page intentionally left blank.

A Brief Comparison of Pitzer Databases for Nuclear Waste Disposal Modeling

Frank Bok[1], Wolfgang Voigt[2], Christiane Bube[3], Stefan Wilhelm[4] and Helge Moog[5]

[1]Helmholtz-Zentrum Dresden-Rossendorf e.V., Institute of Resource Ecology, P.O. Box 510119, 01314 Dresden, Germany
Email: F.Bok@hzdr.de
[2]TU Bergakademie Freiberg, Institute of Inorganic Chemistry, Leipziger Strasse 29, 09596 Freiberg, Germany
[3]Karlsruhe Institute of Technology (KIT), Institute for Nuclear Waste Disposal (INE), Hermann-von-Helmholtz-Platz 1, 76344 Eggenstein-Leopoldshafen, Germany
[4]AF-Consult Switzerland Ltd, Groundwater Protection and Waste Disposal, Taefernstrasse 26, CH-5405 Baden, Switzerland
[5]Gesellschaft fuer Anlagen- und Reaktorsicherheit (GRS) mbH, Waste Management Research Division, Theodor-Heuss-Strasse 4, 38122 Braunschweig, Germany

INTRODUCTION

For the modeling of different chemical aspects of a salt repository for nuclear waste, the Pitzer formalism is necessary. Therefore, a comprehensive database with the relevant aqueous and mineral species, the corresponding reaction constants and associated ion-ion interaction parameters are required.

A number of different Pitzer databases are available for, or even delivered with various geochemical speciation codes such as EQ3/6, PHREEQC, Geochemist's Workbench® (GWB) or ChemApp. In this work we performed comparative calculations for well-defined chemical systems on the base of these Pitzer databases. In Addition, for a more comprehensive view experimentally measured values from the literature were included in the comparisons.

DESCRIPTION OF THE WORK

The following Pitzer datasets were used in this study:

– thermo_hmw.dat (Log K values and virial coefficients for the Harvie-Møller-Weare activity model as delivered with Geochemist's Workbench®) [1]
– data0.hmw.R2 (Log K values and virial coefficients for the Harvie-Møller-Weare activity model as delivered with EQ3/6; not identical to thermo_hmw.dat)
– pitzer.dat (Pitzer dataset as delivered with PHREEQC, mostly identical with thermo_phrqpitz.dat) [2]
– thermo_phrqpitz.dat (The Harvie-Møller-Weare activity model, as implemented in the USGS program PHRQPITZ including borate species and some temperature dependencies, as delivered with Geochemist's Workbench®) [1]
– data0.ypf.R0–2 (Yucca Mountain Pitzer File: R0, R1, and R2 version) [3]
– THEREDA Release 1–6 [4]

These databases are available in the formats of different geochemical speciation codes only. For a direct database comparison the influences of the different codes had to be excluded. Therefore the databases were transformed into the GWB format because only the transformations into this format were possible without the loss of information namely concerning the functions describing the temperature dependence of various parameters. The database transformations were checked using example calculations from the corresponding literature [5, 6].

To compare the different databases, solubility curves and invariant points were calculated within the following chemical systems:

– Oceanic salt system at 25 and 100 °C
– Oceanic salt system including Carbonate/CO_2 at 25 °C
– Nd/Cm/Am(III) in chloride system at 25 °C
– Np(V) hydrolysis in NaCl solution at 25 °C
– Cs in Oceanic salt system at 25 °C
– Cement phases in Oceanic salt system at 25 °C

RESULTS

Oceanic salt system (Na,K,Mg,Ca/Cl,S – $H_2O(l)$)
Most ternary subsystems of the oceanic salt system can be modeled with good agreement at a temperature of 25 °C.

If the modeling is carried out for higher temperatures, the results of the calculations with the different databases sometimes differ widely e.g. in the System K^+,Mg^{2+}/SO_4^{2-} – $H_2O(l)$ at 100 °C (Fig. 1).
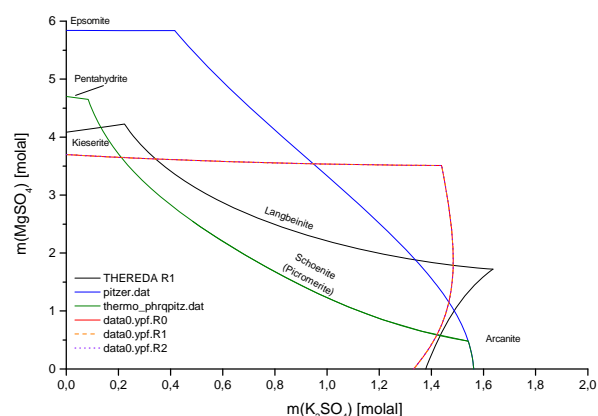
Fig. 1: Calculated solubility curves in the ternary system K^+,Mg^{2+}/SO_4^{2-} – $H_2O(l)$ at 100 °C.

These very different results occur because of the absence of solubility constants (log K) of some minerals, the lack of temperature-dependent log K values of other minerals (data for 25 °C only), or illicit use of log K values not valid for these temperature ranges.

Np(V) hydrolysis in NaCl solution

The solubility of freshly precipitated $NpO_2(OH)(am)$ in 1.0 m NaCl solution was calculated using the THEREDA R4 and the data0.ypf.R1/2 databases (Fig. 2).

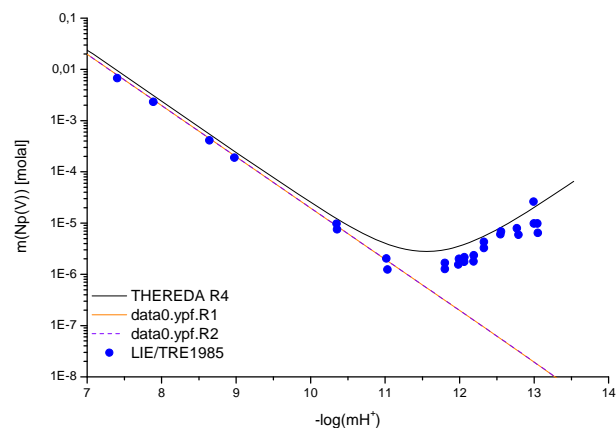**Fig. 2:** Solubility of fresh amorphous $NpO_2(OH)$ in 1.0 m NaCl solution (lines: databases used in calculations, dots: measured values from literature [7]).

In the weakly alkaline range, the Np(V) solubility can be equally reproduced using all Np-containing databases. However, the increase of Np(V) solubility in higher alkaline range $(-\log(mH^+) > 10)$ does not appear with some databases. This might be caused by strongly different $\log K$ values of anionic Np hydrolysis species $(\Delta \log K_{NpO2(OH)2-} = 8.85)$.

Nd/Cm/Am(III) in Na,Mg,Ca/Cl system

The solubility of amorphous or crystalline $Nd(OH)_3$ in 3.86 m $CaCl_2$ solution was calculated using the data0.ypf.R1/2 and the THEREDA R2 databases (Fig. 3).
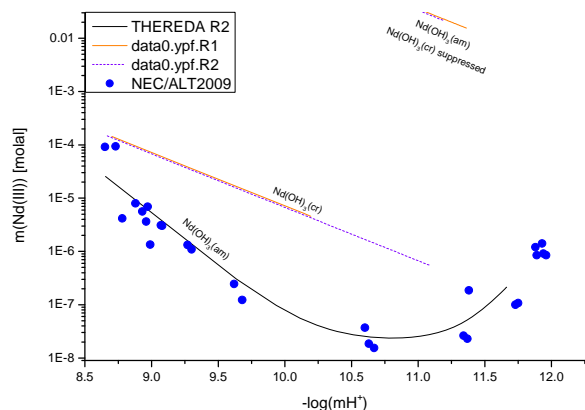

Fig. 3: Solubility of amorphous/crystalline $Nd(OH)_3$ in 3.86 m $CaCl_2$ solution (lines: databases used in calculations, dots: measured values from literature [8]).

The results of the calculations differ in numerical results and trend. Differences in the weak alkaline range might be caused by the differences in the solubility constants of the Nd hydroxides $(\Delta \log K_{Nd(OH)3(am)} \approx 3.3)$. The missing of the increase of Nd(III) solubility in higher alkaline range $(-\log(mH^+) > 10)$ using the data0.ypf.R1/2 databases might be caused by different aqueous species, especially for anionic and ternary $Ca-Nd-(OH)_x$ complexes. A detailed analysis of the differences in speciation and thermodynamic data for the actinides is not part of this study.

SUMMARY

Currently several Pitzer databases with different amounts of mineral and aquatic species and Pitzer parameters are available. Also the quality of the contained data is very different. Thus, each of these databases has strengths but also weaknesses.

To improve the quality of Pitzer databases, data gaps need to be identified and closed. Therefore mutual benchmark calculations using different speciation codes and involving comparisons with a wide base experimentally measured values from the literature seems to be an effective way with benefit for all participants and should be discussed.

REFERENCES

1. Aqueous Solutions LLC's Homepage (Database download section http://www.gwb.com/thermo.htm)
2. USGS's PHREEQC Homepage (http://wwwbrr.cr.usgs.gov/projects/GWC_coupled/phreeqc/)
3. WOLERY, TJ, Personal communication (2012-09-26)
4. THEREDA Homepage (http://www.thereda.de)
5. PARKHUST, DL et al., "Water-Resources Investigations Report 99-4259" (PHREEQC manual), Page 203 (1999).
6. LEIGH, CD et al., "WIPP Verification and Validation Document for EQ3/6 Version 8.0a for Actinide Chemistry" Document Version 8.10 ERMS #550239, Page 37 (2010).
7. LIERSE, C et al., "Hydrolysis Reactions of Neptunium(V)", *Radiochimica Acta*, **38**, Page 27–28 (1985).
8. NECK, V et al., "Thermodynamics of trivalent actinides and neodymium in NaCl, $MgCl_2$, and $CaCl_2$ solutions: Solubility, hydrolysis, and ternary Ca-M(III)-OH complexes" *Pure Appl. Chem.*, **81**, Page 1555–1568 (2009).

THEREDA Database Project: Extensions of the Pitzer Database with Respect to Phosphate, Alkaline Earth Metal Sulfates, Heavy Metals, and Fission Products – First Results

Helge C. Moog

Global Research for Safety, GRSmbH, Theodor-Heuss-Str. 4, 38122 Braunschweig, Germany.

ABSTRACT

In an effort to extend the database for fission products, an extensive screening of the literature was done for Cs, Rb, and Sr. The data for Cs were amended by own isopiestic measurements in the GRS, leading to an almost complete set of Pitzer parameters for interactions with Na, K, Mg, Ca – Cl, SO4 for 298.15 K and 1 atm [1, 2]. For Sr and (to a lesser extent) for Rb data gaps remain.

As a first step to model the solubility of low soluble phosphates in brines, the literature was screened for suitable data, essentially water vapor pressures and solubilities. Missing data were amended by own isopiestic measurements [3, 4].

For the solubility of alkaline earth sulfates at elevated temperatures, data sets were prepared specifically with regard to mixed NaCl-CaCl2-solutions. For Sr and Ba credit was taken from Monnin (1999) [5]. Experimental solubilities can be reproduced up 100°C. For higher temperatures considerable deviations occur. It is hypothesized that this is due to the limited temperature up to which the Pitzer parameters in THEREDA for the systems of oceanic salts is valid (about 100-120°C). As the extension of the database for these Pitzer parameters up to 200°C is presently underway, these results may change in the near future.

For binary RaCl2 interactions at 298.15K we adopted Pitzer parameters as estimated in Rosenberg 2011 [6]. The temperature dependence of BaCl2-interactions as given in [5] was projected on top so as to give the well founded values at 298.15K as given by Rosenberg et al. [6]. Temperature dependent RaSO4 interactions were adopted from Paige et al (1998) [7]. It was further assumed that BaSO4 and RaSO4 form an ideal solid solution at low values for x(RaSO4) [6].

For lead we adopted a set of internally consistent Pitzer parameters, solubility constants, and formations constants of chloro- and sulfato-complexes from Hagemann [8]. Temperature functions for the formation of chloro-complexes [9] were projected on top such as to yield the values from Hagemann at 298.15K.

No solubility data for Anglesite at elevated temperature were found. Thus, standard enthalpy of formation, standard entropy and heat capacity data were used to calculate a Gibbs energy function of temperature, which was subsequently adjusted to give the precisely known solubilities at 298.15K.

The presentation gives an account on intermediate results.

REFERENCES

1. T. Scharge, A. G. Munoz, and H. C. Moog: Activity Coefficients of Fission Products in Highly Salinary Solutions of Na^+, K^+, Mg^{2+}, Ca^{2+}, Cl, and SO_4^{2-}: Cs^+. *J. Chem. Eng. Data* **57**, 1637-1647 (2012). dx.doi.org/10.1021/je200970v.

2. T. Scharge, A. G. Munoz, and H. C. Moog: Addition to "Activity Coefficients of Fission Products in Highly Salinary Solutions of Na^+, K^+, Mg^{2+}, Ca^{2+}, Cl, and SO_4^{2-}: Cs^+". *J. Chem. Eng. Data* **57(6)**, 1637-1647 (2012). 10.1021/je200970v.

3. T. Scharge, A.G. Muñoz and H.C. Moog: Thermodynamic Modeling of High Salinary Phosphate Solutions I. Binary Systems. *J. Chem. Thermodynamics* (submitted paper).

4. T. Scharge, A.G. Muñoz and H.C. Moog: Thermodynamic Modelling of High Salinary Phosphate Solutions. II. The HxPO4-Na-K-Mg-Ca-Cl-SO4 System. *J. Chem. Thermodynamics* (in preparation).

5. Christophe Monnin: A thermodynamic model for the solubility of barite and celestite in electrolyte solutions and seawater to 200 8C and to 1 kbar. *Chemical Geology* **153**, 187–209 (1999).

6. Yoav O. Rosenberg, Volker Metz, Jiwchar Ganor: Co-precipitation of radium in high ionic strength systems: 1. Thermodynamic properties of the Na–Ra–Cl–SO4–H2O system – Estimating Pitzer parameters for RaCl2. Geochimica et Cosmochimica Acta 75 (2011) 5389–5402.

7. C. R. PAIGE, W. A. KORNICKER, O. E. HILEMAN JR., and W. J. SNODGRASS: Solution equilibria for uranium processing - The BaSO4-H2SO4-H2O system and the RaSO4-H2SO4-H2O system. Geochimica et Cosmochimica Acta, Vol. 62, No. 1, pp. 15–23, 1998.

8. S. Hagemann: Thermodynamische Eigenschaften des Bleis in Lösungen der ozeanischen Salze. PhD-thesis, 1999.

9. J. O. Nriagu, G. M. Anderson: Stability of the lead (II) chloride complexes at elevated temperatures. Chemical Geology 7 (1971) 171-183.

8. Ihsan Barin: Thermochemical Data of Pure Substances, VCH, ISBN 3-527-27812-5 (1989).

- 122 -

This page intentionally left blank.

List of Attendees: ABC-Salt III Workshop

Marcus Altmaier	*Karlsruhe Institute of Technology/Institute for Nuclear Waste Disposal (KIT/INE), Germany* *marcus.altmaier@kit.edu*
Thuro Arnold	*Helmholtz-Zentrum Dresden Rossendorf, Institute of Resource Ecology, Germany* *t.arnold@hzdr.de*
Jean Bahr	*NWTRB, University of Wisconsin, USA* *jmbahr@geology.wisc.edu*
Rebecca Beard	*Nuclear Decommissioning Authority Radioactive Waste Management Directorate, Harwell, UK* *rebecca.beard@nda.gov.uk*
Frank Bok	*Helmholtz-Zentrum Dresden Rossendorf, Institute of Resource Ecology, Germany* *f.bok@hzdr.de*
Marian Borkowski	*Los Alamos National Laboratory – Carlsbad, USA* *marian@lanl.gov*
Ingo Böttcher	*Department of Safety of Nuclear Waste Management, Federal Office for Radiation Protection, Germany* *iboettcher@bfs.de*
Hakim Boukhalfa	*Los Alamos National Laboratory, USA* *hakim@lanl.gov*
Guido Bracke	*Gesellschaft für Anlagen- und Reaktorsicherheit (GRS) mbH, Germany* *Guido.Bracke@grs.de*
Larry Brush	*Sandia National Laboratories – Albuquerque, USA* *lhbrush@sandia.gov*
Florie Caporuscio	*Los Alamos National Laboratory, USA* *floriec@lanl.gov*
David Clark	*Los Alamos National Laboratory, USA* *dlclark@lanl.gov*
Danielle Cleveland	*Los Alamos National Laboratory – Carlsbad, USA* *danielle.cleveland@gmail.com*
Paul Dixon	*Los Alamos National Laboratory, USA* *P_Dixon@lanl.gov*
Paul Domski	*S.M. Stoller Corporation, Sandia National Laboratories, USA* *psdomsk@sandia.gov*
Joe Franco	*Department of Energy, Carlsbad Field Office, Carlsbad, USA* *Joe.Franco@wipp.ws*
Daniela Freyer	*University Freiberg, Germany* *Daniela.Freyer@chemie.tu-freiberg.de*
Katharina Fritsch	*Helmholtz-Zentrum Dresden Rossendorf, Institute of Resource Ecology, Germany* *katha.fritsch@googlemail.com*
Xavier Gaona	*Karlsruhe Institute of Technology/Institute for Nuclear Waste Disposal (KIT/INE), Germany* *Xavier.Gaona@kit.edu*
David García	*Amphos 21, Barcelona, Spain* *david.garcia@amphos21.com*

Horst Geckeis	*Karlsruhe Institute of Technology/Institute for Nuclear Waste Disposal (KIT/INE), Germany* *horst.geckeis@kit.edu*
Andrea Geissler	*Helmholtz-Zentrum Dresden Rossendorf, Institute of Resource Ecology, Germany* *a.geissler@hzdr.de*
Jack Gwo	*Nuclear Regulatory Commission, USA* *Jin-Ping.Gwo@nrc.gov*
David Hobbs	*Savanah River National Laboratory, USA* *david.hobbs@srnl.doe.gov*
Jonathan Icenhower	*Lawrence Berkeley National Laboratory, USA* *Currently: jpicenh@sandia.gov*
Je-Hun Jang	*Sandia National Laboratories - Carlsbad, USA* *djang@sandia.gov*
Carlos Jove-Colon	*Sandia National Laboratories, Albuquerque, USA* *cfjovec@sandia.gov*
Sungtae Kim	*Sandia National Laboratories – Carlsbad, USA* *sunkim@sandia.gov*
Christi Leigh	*Sandia National Laboratories – Carlsbad, USA* *cdleigh@sandia.gov*
Jean-Francois Lucchini	*Los Alamos National Laboratory – Carlsbad, USA* *lucchini@lanl.gov*
Paul Mariner	*Sandia National Laboratories, Albuquerque, USA* *pmarine@sandia.gov*
Dave Martin	*New Mexico Environmental Department, NMED, USA* *Unknown*
Albert Martínez-Torrents	*UPC Barcelona, Tech, Spain* *albert.martinez@ctm.com.es*
Helge Moog	*Gesellschaft für Anlagen- und Reaktorsicherheit (GRS) mbH, Germany* *helge.moog@grs.de*
Andrés Muñoz	*Gesellschaft für Anlagen- und Reaktorsicherheit (GRS) mbH, Germany* *Andres.Munoz@grs.de*
Russ Patterson	*Department of Energy, Carlsbad Field Office, Carlsbad, USA* *Russ.Patterson@wipp.ws*
Thomas Rabung	*Karlsruhe Institute of Technology/Institute for Nuclear Waste Disposal (KIT/INE), Germany* *thomas.rabung@kit.edu*
Don Reed	*Los Alamos National Laboratory – Carlsbad, USA* *dreed@lanl.gov*
Michael Richmann	*Los Alamos National Laboratory – Carlsbad, USA* *Richmann@lanl.gov*
Bob Roback	*Los Alamos National Laboratory, USA* *roback@lanl.gov*
Bruce Robinson	*Los Alamos National Laboratory, USA* *robinson@lanl.gov*

Greg Roselle	*Sandia National Laboratories – Carlsbad, USA* *gtrosel@sandia.gov*
Darren Rowland	*Chemical and Analytical Sciences, Murdoch University, Australia* *d.rowland@murdoch.edu.au*
Wolfgang Runde	*Los Alamos National Laboratory, USA* *runde@lanl.gov*
Nan Sauer	*Los Alamos National Laboratory, USA* *nsauer@lanl.gov*
Juliane Schott	*Helmholtz-Zentrum Dresden Rossendorf, Institute of Resource Ecology, Germany* *j.schott@hzdr.de*
Michael Schramm	*Federal Institute for Geosciences and Natural Resources (BGR),Germany* *michael.schramm@bgr.de*
Michael Siemann	*Nuclear Energy Agency, OECD/NEA, France* *Michael.SIEMANN@oecd.org*
Ginger Sigmon	*Notre Dame University, USA* *gsigmon@gmail.com*
Karen Simmons	*Los Alamos National Laboratory – Carlsbad, USA* *ktorczyn@gmail.com*
Julie Swanson	*Los Alamos National Laboratory – Carlsbad, USA* *jsswanson@lanl.gov*
Punam Thakur	*New Mexico State University – Carlsbad, USA* *pthakur@cemrc.org*
Abe Van Luik	*Department of Energy, Carlsbad Field Office, Carlsbad, USA* *abraham.vanluik@wipp.ws*
Yong-Liang Xiong	*Sandia National Laboratories – Carlsbad, USA* *yxiong@sandia.gov*
Hongwu Xu	*Los Alamos National Laboratory, USA* *hxu@lanl.gov*
Tammy Yang	*Nuclear Waste Management Organization (NWMO), Canada* *TYang@nwmo.ca*
Mavrik Zavarin	*Lawrence Livermore National Laboratory, USA* *zavarin1@llnl.gov*